



Assiut University
Faculty of Engineering
Department of Architecture

Sustainable Design for Built Environment of New Residential Complexes

--Integration of evaporative cooling technique with solar chimney-- (New Assiut City-Egypt)

By

Arch: Amr Sayed Hassan Abdallah

Assistant Lecturer, Dept. of Architecture,
Faculty of Eng., Assiut University
Member of channel system scholarship, Tohoku University, Japan

A thesis

Submitted in partial fulfillment of the requirements for the degree of
doctorate of philosophy in Architectural

Supervised by:

- Prof. Dr. \ Magdy Mohamed Radwan**
Professor of Architecture, Department of
Architecture, Assiut University - Assiut -
Egypt
- Prof. Dr. \ Mohamed Abdelsamee Eid**
Professor of Architecture, Department of
Architecture, Assiut University - Assiut -
Egypt
- Prof. Dr. \ Hiroshi YOSHINO**
Emeritus Professor, Department of
Architecture and Building Science,
Laboratory of Building Environmental
Engineering, Tohoku University, Japan

Examined by

- Prof. Dr. \ Morad Abdelkader
Abdelmohsen**
Professor of Architecture,
Department of Architecture, Ain-
Shames University - Egypt
- Prof. Dr. \ Mohamed Moemen Afify**
Professor of Architecture,
Department of Architecture, Cairo
University - Egypt
- Prof. Dr. \ Magdy Mohamed Radwan
Mohamed Abdelsamee Eid**
Professor of Architecture,
Department of Architecture,
Assiut University - Assiut - Egypt

2014

Table of content

Table of content	I
List of figures	V
List of tables	XIV
Abstract	XVI
Acknowledgment	XIX

Chapter 1: Research context, background, problem and aims

1.1 Research geographical and climatic context.....	1
1.2 Research background.....	4
1.3 Research problem.....	7
1.4 Research aim and objectives.....	7
1.5 Research questions.....	8
1.6 Research methodology.....	8
1.7 Research Scope.....	9
1.8 Research structure.....	10

Chapter 2: Case study building measurement & evaluation for indoor environment (New Assiut city)

Introduction.....	12
2.1 Location of New Assiut city.....	14
2.2 Case study location & description.....	14
2.3 Climatic analysis of outdoor condition for new Assiut city (one year data).....	18
2.3.1 Air temperature.....	18
2.3.2 Relative humidity.....	20
2.3.3 Wind speed & direction.....	21
2.3.4 Solar radiation.....	23
2.4 Methodology.....	23
2.5 Monitoring of indoor temperature & humidity in May.....	25
2.6 Evaluation of June measurement.....	28
2.6.1 Temperature, humidity & absolute humidity profiles for one month measurements-June 2012.....	29

2.6.2	Temperature, humidity & absolute humidity for 3 days data (June 1 st ~ June 4 th).....	31
2.6.3	Temperature & humidity distribution of 3 cases in June 2012.....	33
2.6.4	Evaluation of humidity environment according to ASHRAE 55, 2004 in June 2012.....	35
2.6.5	The relationship between indoor and outdoor air temperatures (June 1 st ~June 4 th ,2012).....	37
2.7	Evaluation of July measurement.....	39
2.7.1	Temperature, humidity & absolute humidity profiles for one month measurements.....	39
2.7.2	Temperature, humidity & absolute humidity for 3 days data.....	42
2.7.3	Temperature & humidity distribution of the 3 cases.....	45
2.7.4	Evaluation of humidity environment according to ASHRAE 55, 2004 in July 2012.....	47
2.7.5	Relationship between indoor and outdoor air temperature (16July~18 July 2012).....	49
2.8	Monitoring of indoor carbon dioxide concentration	51
2.9	Research for the suitable strategy for climate of New Assiut city.....	54
	Conclusion	57

Chapter 3: Solutions and strategies for indoor environmental problems

	Introduction.....	59
3.1	The effect of traditional strategies for achieving indoor thermal comfort.....	60
3.1.1	Natural ventilation.....	60
	a. Wind pressure.....	60
	b. Stack effect (thermal buoyancy).....	61
3.1.2	Evaporative cooling.....	62
3.1.3	Wind tower.....	64
3.2	Search for solutions & strategies for providing thermal comfort.....	65
3.2.1	Wind tower concept for providing thermal comfort.....	65
3.2.2	The solar chimney concept for providing thermal comfort.....	70
3.2.3	Integration of the solar chimney with an evaporative cooling concept for providing thermal comfort.....	73

3.3 Comfort ventilation.....	76
Conclusion.....	76

Chapter 4: Integration of solar chimney with new cooling tower as a passive ventilation technique

Introduction.....	78
4.1 Developing and description of the system.....	79
4.2 TRNSYS and COMIS simulation programs.....	81
a. COMIS program.....	81
b. TRNSYS program.....	82
c. Couple concept of TRNSYS & COMIS programs.....	82
4.3 Multi-zone thermal ventilation model.....	83
4.4 System mechanism.....	85
4.5 Mathematical modeling of the integrated system.....	87
4.5.1 Pressure calculation and mass flow rate through openings (COMIS model).....	87
4.5.2 Temperature prediction in solar chimney.....	89
4.5.3 Temperature predictions in evaporative cooling wind tower.....	91
4.6 Air flow network & building thermal model of the integrated system in COMIS-TRNSYS programs.....	94
4.6.1 Building thermal model (TRNSYS model).....	94
4.6.2 Air flow network (COMIS model).....	96
4.6.3 Mathematical calculation of building thermal model.....	97
4.7 The impact of the integrated system on indoor environment.....	99
4.7.1 Indoor temperature investigation.....	99
4.7.1.1 The steady state condition.....	100
4.7.1.2 Actual weather data.....	102
4.7.2 Evaluation of the humidity environment.....	105
4.7.3 Evaluation of CO ₂ concentration in the room.....	106
Conclusion.....	107

Chapter 5: Optimization and parametric investigation of the new proposed system

Introduction.....	109
-------------------	-----

5.1 Optimization methodology.....	111
5.2 Parametric studies and optimization.....	113
5.2.1 Investigation of solar chimney parameters only under steady state.....	113
a. Effect of solar chimney inclination angle on indoor ventilation rate.....	113
b. Effect of chimney air gap dimension on ventilation rate.....	116
c. Effect of chimney area on ventilation rate.....	117
5.2.2 Investigation of tower parameters only under steady state.....	119
5.2.3 Selection for important optimization parameters.....	120
a. Width of the chimney.....	120
b. Air gap thickness.....	121
c. Wind tower dimension.....	122
5.3 Optimization of solar chimney and wind tower using real weather data.....	122
5.3.1 Indoor temperature and air flow rate investigation.....	123
5.3.2 Evaluation of the humidity environment after optimization.....	127
5.3.3 Evaluation of CO ₂ concentration in the room.....	129
5.4 The performance of the integrated system.....	130
Conclusion	131

Chapter 6: Conclusions and further work

6.1 Conclusion.....	133
6.1.1 Concerning understand indoor environment.....	133
6.1.2 Concerning search for the suitable strategy for that climate.....	133
6.1.3 Concerning investigating for the possibility of achieving indoor comfort using natural ventilation and evaporative cooling	134
6.2 Guideline for efficient optimization process.....	136
6.3 Further work.....	138

References	140
-------------------	-----

Appendix (A): Thermal comfort standard.	153
--	-----

Appendix (B): COMIS and TRNSYS input.	156
--	-----

Appendix (C): Nomenclature	173
-----------------------------------	-----

Appendix (D): Abstract of published papers	176
---	-----

List of Figures

Chapter 1

Figure (1-1):	The location of Egypt and its classification.	1
Figure (1-2):	The climate classification in Egypt.	2
Figure (1-3):	The structure for thesis organization.	11

Chapter 2

Figure (2-1):	Classification of climatic zones in Egypt and position of Assiut city.	14
Figure (2-2):	The satellite image of New Assiut city with the location of family housing and youth housing sector.	15
Figure (2-3):	The location of the case study in the family housing and youth housing sector.	16
Figure (2-4):	The plan and the floor of the building and the detailed plan of case1 (Author).	17
Figure (2-5):	The plan for the second floor of the house, case 2 (Author).	17
Figure (2-6):	The plan for the top floor level of the house, case 3 (Author).	18
Figure (2-7):	Temperature ranges for New Assiut city during one year weather data.	19
Figure (2-8):	Outdoor temperature percentage distribution between sunrise and sunset for one year.	20
Figure (2-9):	Outdoor average relative humidity data profile for one year data.	20
Figure (2-10):	Outdoor relative humidity percentage distribution (between sunrise and sunset) data for one year.	21

Figure (2-11):	Wind velocity range for new Assiut city during one year data.	21
Figure (2-12):	Outdoor wind speed percentage distribution between sunrise and sunset for one year.	22
Figure (2-13):	Outdoor average wind direction in all months of the year.	22
Figure (2-14):	Radiation profile and the mean dry bulb temperature for one year weather data.	23
Figure (2-15):	Temperature and humidity patterns for indoor environment of the last four days of May in case 1.	27
Figure (2-16):	Temperature and humidity patterns for indoor environment of the last four days of May in case 2.	27
Figure (2-17):	Temperature and humidity patterns for indoor environment of the last four days of May in case 3.	28
Figure (2-18):	Temperature, humidity and absolute humidity patterns for indoor environment of June in case 1.	29
Figure (2-19):	Temperature, humidity and absolute humidity patterns for indoor environment of June in case 2.	29
Figure (2-20):	Temperature, humidity and absolute humidity patterns for indoor environment of June in case 3.	30
Figure (2-21):	Temperature and humidity patterns for indoor environment from June 1st~June 4th in case 1.	32
Figure (2-22):	Temperature and humidity patterns for indoor environment from June 1st~June 4th in case 2.	32
Figure (2-23):	Temperature and humidity pattern for indoor environment from June 1st~June 4st in case 3.	33
Figure (2-24):	Temperature and humidity distribution during daytime for the three cases with outdoor condition for June	34

	2012.	
Figure (2-25):	Temperature and humidity distribution during nighttime for the three cases with outdoor condition for June 2012.	34
Figure (2-26):	Temperature and humidity conditions in case 1 during daytime & nighttime.	35
Figure (2-27):	Temperature and humidity conditions in case 1 during daytime & nighttime with and without air conditioning.	36
Figure (2-28):	Temperature and humidity conditions in case 2 during daytime & nighttime.	36
Figure (2-29):	Temperature and humidity conditions in case 3 during daytime & nighttime.	37
Figure (2-30):	The regression lines between the daily outdoor temperature and indoor temperature in the three different zones; living room, master bedroom, and bedroom June 2012; (a) the regression line in case 1, (b) the regression line in case 2, (c) the regression line in case 3.	38
Figure (2-31):	Temperature, humidity and absolute humidity patterns for indoor environment of July 2012 in case 1.	40
Figure (2-32):	Temperature, humidity and absolute environment patterns for indoor environment of July 2012 in case 2.	41
Figure (2-33):	Temperature, humidity and absolute environment patterns for indoor environment of July 2012 in case 3.	41
Figure (2-34):	Temperature and humidity patterns for indoor environment on the hottest days of July 2012 in case 1.	43
Figure (2-35):	Temperature and humidity patterns for indoor environment in the hottest days of July 2012 in case 2.	43
Figure (2-36):	Temperature and humidity patterns for indoor	44

	environment from July 16th ~18th , 2012 in case 3.	
Figure (2-37):	Temperature and humidity distribution during daytime for the three cases and outdoor condition for July 2012.	46
Figure (2-38):	Temperature and humidity distribution during nighttime for the three cases and outdoor condition for July 2012.	46
Figure (2-39):	Temperature and humidity conditions in case 1 during daytime & nighttime of July, 2012.	47
Figure (2-40):	Temperature and humidity conditions in case 1 during daytime & nighttime with and without air condition (AC) of July, 2012.	47
Figure (2-41):	Temperature and humidity conditions in case 2 during daytime & nighttime of July, 2012.	48
Figure (2-42):	Temperature and humidity conditions in case 3 during daytime & nighttime of July, 2012.	48
Figure (2-43):	The regression line between the daily outdoor temperature and indoor temperature in the three different zones; living room, master bedroom & bedroom from July 16 th to July 18 th , 2012; (a) the regression line in case 1, (b) the regression line in case 2, (c) the regression line in case 3.	50
Figure (2-44):	CO ₂ concentration in the living room of cases 1 & 2 during June, 2012.	52
Figure (2-45):	Three days measurements of CO ₂ concentration in June, 2012.	53
Figure (2-46):	CO ₂ concentration profiles for indoor environment during July 16th~19th, 2012.	53
Figure (2-47):	CO ₂ concentration profiles for indoor environment during August 16th~19th, 2012.	54
Figure (2-48):	The bioclimatic chart for building design strategies with	55

the measurement data for (May, June & July), 2012.

- Figure (2-49): The outdoor DBT and WBT of the outdoor measurement data. 56
- Figure (2-50): The feasibility index pattern based on the outdoor measurement data. 57

Chapter 3

- Figure (3-1): Schematic distribution of wind pressure around & inside a building exposed to perpendicular wind flow. 61
- Figure (3-2): Natural driving mechanisms of stack pressure. 61
- Figure (3-3): The mechanism of stack ventilation in a room & an atrium. 62
- Figure (3-4): Direct evaporative cooling process shown psychrometrically. 64
- Figure (3-5): Wind tower with wetted baffles, design by Hassan Fathy. 65
- Figure (3-6): The problems of the conventional system integration. 75

Chapter 4

- Figure (4-1): Schematic diagram of the new proposed system and the reference system. 79
- Figure (4-2): The location of the room with the new proposed system according to north-south orientation and its location in the building block as a pilot base case. 81
- Figure (4-3): The concept of the couple project between TRNSYS & COMIS programs. 82
- Figure (4-4): Flow chart solving procedure of TRNSYS-COMIS. 84
- Figure (4-5): The mechanism of the system during daytime. 86

Figure (4-6):	Evaporative cooling with constant water flow.	86
Figure (4-7):	The location of different pressure points taking into account base pressure on the ground.	87
Figure (4-8):	Thermal network for solar chimney with air flow.	89
Figure (4-9):	Evaporative cooler schematic.	93
Figure(4-10):	The building thermal model with the heat flows in the ECWT, Room & the solar chimney with the combination of ventilation rate in the TRNSYS model	95
Figure (4-11):	The air flow network of the integrated model with a description of the internal node, external node & airflow component	97
Figure (4-12):	The variation of indoor ACH with different solar radiation.	100
Figure (4-13):	The variation of the absorber & chimney temperature with different solar radiation and with/without wind.	101
Figure (4-14):	Indoor temperature of single room without any cooling system.	103
Figure (4-15):	The influence of the integrated system on indoor temperature.	103
Figure (4-16):	The general concept of the system performance.	104
Figure (4-17):	The performance of the system during the three months of summer (21 May until 21August).	104
Figure (4-18):	The performance of the system for the hottest day of the summer season (20 June).	105
Figure (4-19):	The temperature and humidity condition of the system on 20 June.	105
Figure (4-20):	Indoor carbon dioxide concentration relative indoor air change rate in the room between May 21 th to August	107

Chapter 5

Figure (5-1):	Schematic diagram of the solar chimney with evaporative cooler wind tower.	111
Figure (5-2):	Flow chart of the optimization procedure.	112
Figure (5-3):	Optimization structure of the inclination angle.	114
Figure (5-4):	Figure (5-4): The result of ACH according to different inclination angle: (a) wide range of inclination angle in the first stage; (b) angle estimation in the second stage.	115
Figure (5-5):	The effect of different inclination angles on indoor ACH and chimney solar absorption.	116
Figure (5-6):	The optimization structure of the air gap of the solar chimney.	116
Figure (5-7):	The effects of different air gap on indoor air change rate and chimney air temperature.	117
Figure (5-8):	The relation between the convective heat transfer coefficient and the chimney air gap.	117
Figure (5-9):	The optimization structure of the chimney area.	118
Figure (5-10):	The change in ACH under the effect of Chimney width and air gap.	118
Figure (5-11):	The change of indoor temperature under the effect of Chimney width and air gap.	119
Figure (5-12):	The optimization structure of the tower dimension.	119
Figure (5-13):	The change of ACH & chimney air temperature under the effect of wind tower width and depth.	120
Figure (5-14):	The criteria for choosing chimney width parameters.	121
Figure (5-15):	The criteria for choosing air gap parameters.	121

Figure (5-16):	The criteria for choosing wind tower parameters.	122
Figure (5-17):	The optimization structure for group A & B.	123
Figure (5-18):	Indoor air temperature for the system before optimization and the optimum case after optimization with relation to other 10 cases.	124
Figure (5-19):	Indoor air temperature for the system before and after optimization on 20 June.	125
Figure (5-20):	The performance of the system in the hot hour during daytime.	126
Figure (5-21):	The effective ventilation rate in the system after optimization.	127
Figure (5-22):	Indoor air temperature pattern for the proposed system after optimization between May 21 th ~ August 21 th	127
Figure (5-23):	The temperature and humidity conditions for the system before and after optimization.	128
Figure (5-24):	Temperature and humidity levels for the system after optimization between May 21 st ~August 21 st .	128
Figure (5-25):	The CO ₂ concentration pattern and indoor ACH between 21 st May~ August 21 st .	129
Figure (5-26):	The CO ₂ concentration and ACH of the proposed system before and after optimization between 19 June until end of 23 June with the percentage difference.	130
Figure (5-27):	The performance of the system under the effect of solar radiation only.	131

Appendix

Figure (A-1):	ASHRAE psychrometric chart.	155
Figure (B-1):	Flow chart of solving procedure.	156

Figure (B-2):	The schematic of the system with the description of COMIS parameters.	156
Figure (B-3):	The parameters used for the cooling duct.	157
Figure (B-4):	The parameters used for chimney duct.	158
Figure (B-5):	The description for the opening in the north façade of the tower.	159
Figure (B-6):	Wind velocity profile: relations at Meteo and on building site.	163
Figure (B-7):	The base point of the building and the name of the façade according to the FORTRAN data set.	166
Figure (B-8):	The location of Cp points and the location of the living room with the surrounding obstacles.	167
Figure (B-9):	The TRNSYS file program façade.	169

List of Tables

Chapter 1

Table (1-1):	The Egyptian climatic design regions classification and properties	3
Table (1-2):	Comparison between the traditional old Islamic building and the new buildings in the new cites	5

Chapter 2

Table (2-1):	The description of the measurement device.	24
--------------	--	----

Chapter 3

Table (3-1):	Important researches that studied the wind tower concept.	66
Table (3-2):	The limitations for the conventional wind tower.	69
Table (3-3):	Important researches that studied the solar chimney concept.	70
Table (3-4):	Important researches that studied the integration concept.	73

Chapter 4

Table (4-1):	Description of building material used in the calculation.	95
Table (4-2):	Material properties in the model.	96
Table (4-3):	The parameters used in the solar chimney calculation.	96
Table (4-4):	The results of the steady state condition with different combination of solar radiation, temperature & relative humidity.	102

Chapter 5

Table (5-1):	The optimization cases of the first and the second stage.	113
--------------	---	-----

Table (5-2):	The optimum angle estimation during different months according to Morcos equation.	114
--------------	--	-----

Appendix

Table (B-1):	The results of the Cp values.	167
--------------	-------------------------------	-----

Abstract

Houses in Egypt are often designed without sufficiently taking the climate into account. Factors; such as the urban environment, site characteristics, orientation, architectural design of the building, and choice of building materials, etc.; are not emphasized.

Many researches have been involved in studying thermal comfort in Egyptian housing, especially in the New Assiut City and conducted small and wide scale measurements so far. The results showed that serious problems of discomfort generally exist in the new housing projects with poor indoor air quality. Based on the measurements conducted, the strategies that may be appropriate for the building in such climate are evaporative cooling and natural ventilation; according to the bioclimatic chart for building strategies and other indices. Therefore, there is a great expansion in using air conditioning to cool buildings. But high energy consumption is not affordable, especially for low income people, as low income people have limited, insufficient financial resources to use AC. Therefore, these conditions encourage such a concept to enhance using the natural passive cooling strategy for the New Assiut City with zero energy consumption for cooling.

To achieve this aim; the research adopts four methods: the descriptive method (chapter 1), the analytical method (chapter 2), the deductive method (chapter 3), and the applied method (chapters 4, 5). Finally, the research is concluded (chapter 6) with the results and guidelines for the system performance.

Chapter One: Research context, background, problem and aims

It is the introductory chapter that gives an overview of the whole research contents. In it, the overview of the whole research project, the research geographical & climatic context, the research background, the research problem, the research scope, the research structure, the research objectives and its main aim are all presented. Finally, the research general methodology is outlined.

Chapter Two: Case study building measurements & evaluation for indoor environment (New Assiut City)

The aim of this chapter is to investigate indoor environment for the new housing in New Assiut city, through monitoring indoor air temperature, humidity and CO₂ concentration in the summer season, in order to understand the real situation in some houses in New Assiut city and search for new suitable passive strategies to solve the problem of occupants' thermal comfort and search for the new suitable passive strategy. New Assiut city is chosen as a case study. Also, a

detailed analysis of the chosen case study is conducted through highlighting indoor CO₂ concentration, thermal comfort and its effect on indoor air quality (IAQ) with different ventilation scenarios.

Chapter Three: Solutions and strategies for indoor environmental problems

This chapter presents science related to natural ventilation (Stack effect & wind pressure) and evaporative cooling. Also, it presents a critical review of literature on different passive techniques (Wind tower, solar chimney, and integration of solar chimney with an evaporative cooler concept) in order to understand the limitations of the current system and search for a new system. In general, this chapter aims to understand the techniques for natural ventilation, evaporative cooling and search for new passive strategies based on the limitations of the conventional systems inside/outside Egypt to achieve compact and high advantage of integration.

Chapter Four: Integration of the solar chimney with the new cooling tower as a passive ventilation technique

In general, this chapter aims to investigate the possibility of using natural ventilation with an evaporative cooling strategy using numerical modeling (simulation), in order to achieve zero energy consumption for cooling and indoor thermal comfort according to ACS and ASHRAE under the steady state condition & the weather data of the New Assiut City. First, mathematical modeling of the integrated system is developed. Then, the proposed model is built into COMIS & TRNSYS simulation softwares. Finally, indoor temperature, humidity environment, and CO₂ concentration are evaluated.

Chapter Five: Optimization and parametric investigation for the new proposed system

This chapter focused on optimization of the important parameters of the system on indoor environment to achieve compact design and high advantage of integration. Investigation is done under the steady state condition & weather data of the New Assiut City based on the optimization methodology. As a result, indoor temperature, humidity environment, and air flow rate for the proposed system – after optimization – were analyzed and compared with the system before optimization. Important conclusions for the performance of the integrated system were drawn; highlighting the system limitation.

Chapter 6: Conclusions and further work

The research reached a conclusion for the case study in the New Assiut city through monitoring indoor environment, search for the suitable strategy for that climate, and the system performance based on the numerical modeling. Then, guidelines for the efficient optimization process were presented to apply the integrated system on different living rooms with different circumstances. Finally, the further work is proposed.

At the end of the thesis the appendices and the publications are presented.

Acknowledgment

This thesis is based on research work carried out at the Department of Architecture and Building Science, Laboratory of Building Environmental Engineering, Tohoku University, Japan under the supervision of Prof. Hiroshi YOSHINO and research advisor Associate Professor GOTO Tomonobu. This research was supported by the Ministry of Higher Education in Egypt (Assiut University) for the PhD degree with Joint supervision program (JSP) with Tohoku University, Japan.

I wish to thank my supervisors Professor M. Radwan for his invaluable advices and support throughout the study, Prof. M.Abdelsamee Eid for his valuable comments and Professor Yoshino for his invaluable comments and encouragement.

The author wishes to extend his sincere thanks to:

1. Mr. Hans C. Phaff (TNO, The Netherlands) one of the COMIS developers for his scientific help in the simulation software, and Mr. David Bradley one of the developers of TRNSYS software, Thermal Energy Systems Specialists, Madison, USA.
2. Dr. Napoleon Enteria Postdoctoral researcher, Tohoku University and specialist of renewable energy, energy conservation and energy efficiency for his strong effort and encourage in this research.
3. Eng. Ahmad Abo-Elmakarem for his help in installing measurement devices and collecting measurement data during the summer periods of 2012.

There are no words to express how grateful I am to my wife, two beautiful daughters and my dear parents for their continuous encouragement and prayers. Finally, and before all, I would like to thank Allah for everything and ask Him the reconciliation

Amr Sayed

Special appreciation to members of Laboratory of Building Environmental Engineering of Tohoku University for making my stay in Japan easy, memorable and full of Joy. Also, Thanks for research advisor Prof. Goto for his kind and valuable knowledge.



TOHOKU
UNIVERSITY

بِسْمِ اللَّهِ الرَّحْمَنِ الرَّحِيمِ

In the Name of Allāh, the Most Gracious, the Most Merciful



صدق الله العظيم



Chapter 1

**Research context, background, problem
and aims**

1.1 Research geographical and climatic context

Egypt is located in the northeastern corner of the African continent and the Sahara desert. It is located between the northern latitudes of 22° and 32°. It has a total area of million m² [1]. It is located in a hot arid desert climatic zone according to Köppen Geiger climate classification [2] as shown in figure (1-1).

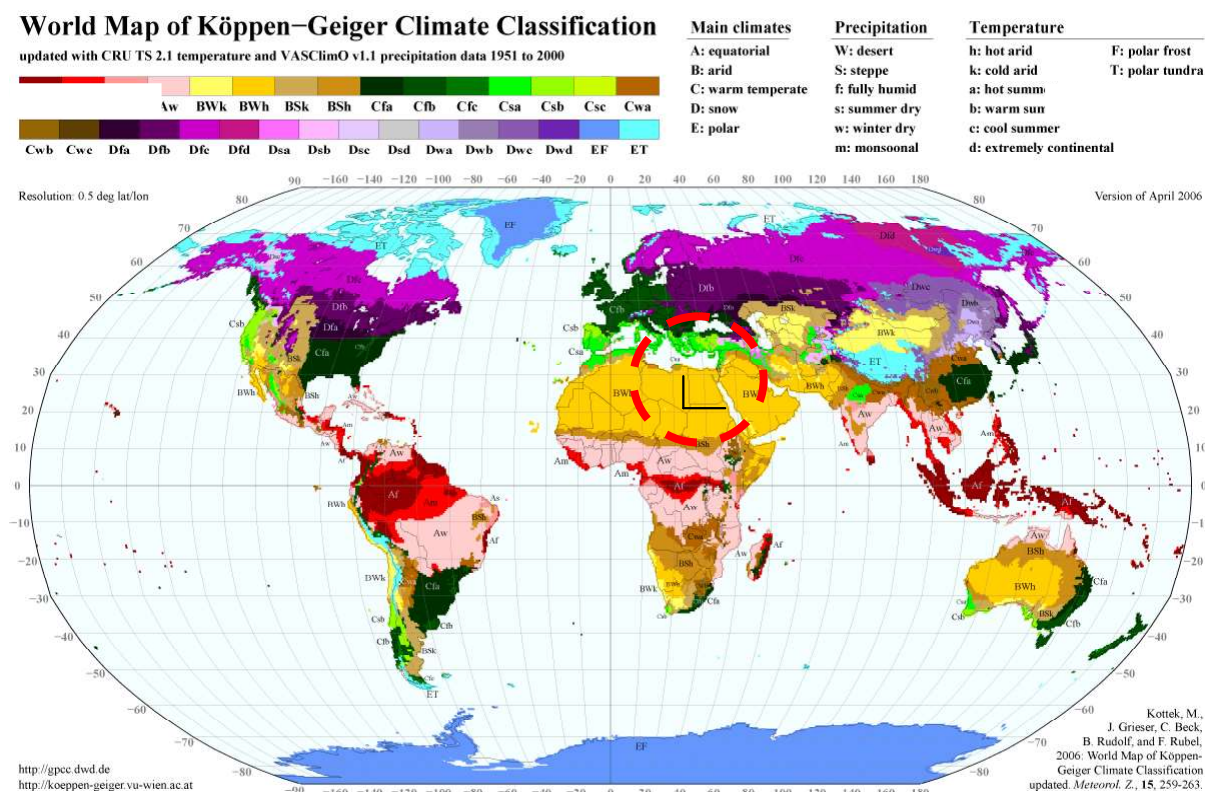


Figure (1-1): The location of Egypt and its classification [2].

In terms of climate, Egypt has a significant variation in climatic conditions; it is divided by the Egyptian organization for Energy Conservation and planning (EOECP) into seven different climatic design regions based on analyzing the climatic data observed at 45 meteorological stations across the country. Those seven climatic design regions are: the Mediterranean Sea coastal region, the Red Sea coastal region, the Semi-moderate region, the Semi-desert region, the Desert region, the Very dry desert region and the Mountain region. These regions vary significantly in the climatic conditions [3].

Another additional climate classification was developed by housing and building research center (HBRC) in Egypt [4]. The classification divided Egypt

into eight climatic zones: Northern Coast zone, Delta and Cairo zone, Northern Upper Egypt zone, Southern Upper Egypt zone, East Coast zone, Highlands zone, Desert zone and Southern Egypt zone [4]. This classification depends on operating temperature, humidity, rainfall, wind speed, altitude and solar radiation, as well as the physical topography of the country [5]. However, this research will use the HBRC classification because it has collected more details than EOECF. Figure (1-2) shows the classification of the climatic zone in Egypt according to HBRC classification. Table (1-1) illustrates the main aspects of different climatic design regions and their borders according to HBRC classification.

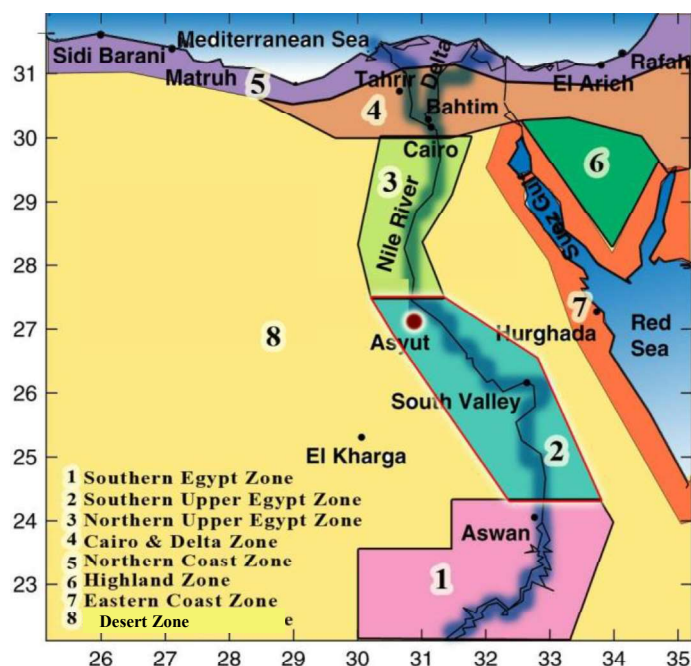


Figure (1-2): The climate classification in Egypt [4].

Table (1-1): The Egyptian climatic design regions classification and properties [4, 5]

Climatic regions	Border	Region description
Southern Egypt zone	It extends from the Sudanese borders (latitude 22° N to latitude 24°5'N).	The operating temperature varies from 43°C to 48°C as the maximum and from 18°C to 2°C as the minimum during the summer months. The global radiation ranges from 1100 to 1210W/m ² in summer.
Southern upper Egypt zone	It extends along the River Nile from latitude 24°5' N to 27° 42'N.	The operating temperature varies from 41°C to 46°C as the maximum and from 16°C to 21°C as the minimum during the summer months. The global radiation ranges from 950 to 1160W/m ² in summer.
Northern upper Egypt zone	It extends northern Nile Valley from latitude 27° 42'N to latitude 30° N.	The operating temperature varies from 40°C to 47°C as the maximum and from 10°C to 22°C as the minimum during the summer months. The global radiation ranges from 950 to 1160W/m ² in summer.
Cairo and Delta zone	It lies between latitude 30°N to 31°N.	The operating temperature varies from 37°C to 46°C as the maximum and from 13°C to 21°C as the minimum during the summer months. The global radiation ranges from 940 to 1050W/m ² in summer.
Northern coast zone	It occupies a narrow belt of 10 km width parallel to the Mediterranean coastline.	The operating temperature varies from 33°C to 37°C as the maximum and from 18°C to 23°C as the minimum during the summer months. The global radiation ranges from 800 to 890W/m ² in summer.
Highlands zone	It occupies the southern part of the Sinai Peninsula	The operating temperature varies from 37°C to 39°C as the maximum and from 12°C to 16 °C as the minimum during the summer months. The global radiation ranges from 840 to 930W/m ² in summer.
Eastern coast zone	It occupies a narrow strip of the coastal areas parallel to the Red Sea	The operating temperature varies from 39°C to 42°C as the maximum and from 19°C to 22°C as the minimum during the summer months. The global radiation ranges from 950 to 1000W/m ² in summer.
Desert zone	This zone covers the entire Western Desert area except for the northern part.	The operating temperature varies from 42°C to 48°C as the maximum and from 19°C to 22°C as the minimum during the summer months. The global radiation ranges from 1030 to 1200W/m ² in summer .

Also, according to the National Oceanic and Atmospheric Administration [6], temperature and humidity level of cities in Egypt were provided by the World Meteorological Organization [WMO]. The mean average relative humidity for Cairo, Alexandria, Aswan and Assiut are 55.75%, 67.92%, 26.17% and 38.33% respectively. Therefore, this great variation in climate between different regions creates a different requirement of climatic response in building design in existing and new cities.

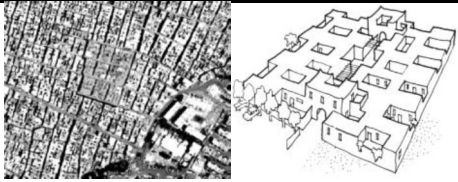
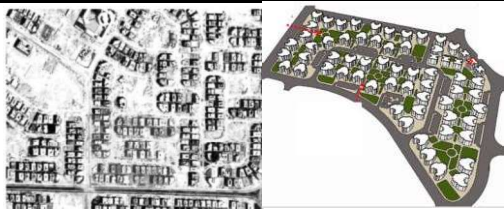
The New Assiut City is one of the Egyptian new cities built in the desert of the east of Assiut city. It's located in the north of the southern Upper Egypt zone. It was chosen to be the specific research geographical context for this research.

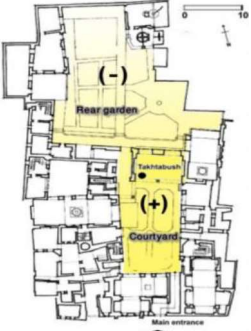



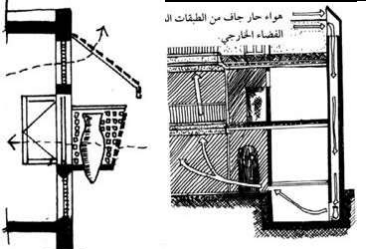

1.2 Research background

The climate problem in Egypt began to be more evident after the war in 1973, when the Egyptian government adopted different strategies to resolve housing problems for overpopulated cities of the Nile valley, particularly for low income people. The government developed a number of new communities in the desert surrounding existing cities without considering the importance of the climate conditions and comfort of occupants [7, 3]. The government established twenty-two new cities in three phases from 1977 to 2000 and another forty cities are planned to be built in the future with different flat area of 63, 73, and 100m² [8]. In October 2005, the Egyptian government adopted a massive project “*The National housing project*” to produce 500,000 dwellings (8500 units/year) for low income people in both old and new cities within a time period of six years [9]. The public housing projects (Youth housing project, Future housing project, Family housing project and National housing project) were designed as a fixed prototype that is being built all over the country regardless of climatic conditions [3]. Factors such as the urban environment, site characteristics, orientation and architectural design of the building, choice of building materials, etc. are not emphasized. Consequently, buildings often have a poor indoor climate which affects comfort, health and building efficiency [10, 11, 3].

One reason why buildings are poorly adapted to the climate is the lack of knowledge among architects, planners and engineers [3]. Also, the knowledge of traditional construction in old housing, which was quite well adapted to the climate, is often lost or difficult to apply to modern building techniques and society. Instead, people try to use mechanical ventilation and air conditioning which are energy consuming and environmentally damaging [12, 13]. Low-income people cannot afford the costs of such methods. Table (1-2) shows the comparison between the traditional and the new buildings according to urban form, unit, courtyard & cooling strategy and influence on the indoor environment.

Table (1-2): Comparison between the traditional old building and the new buildings in the new cites [14, 15, 16, 17, 3]

Item	Traditional building	New building
Urban form	 <p>The urban form of tradition buildings controls the access of the sun and wind to the buildings. This is done by providing more shading in the footpaths and the building due to compact design of these buildings</p>	 <p>The urban form of new building especially in new cities increases indoor and outdoor temperature. This is due to the reflection of solar radiation from street, building & desert, without providing any shade for the building. Also, the distance between the buildings is very wide.</p>

<p>Unit (plan)</p>	 <p>Al Suhaymai house Most of the houses are built based on creating a passive ventilation technique taking into account building orientation in order to ameliorate the microclimate. i.e; the air flows from the north prevailing wind directions during most hours of the day; with wind speed 1.3m/s.</p>	 <p>National housing project Family house project Most of the units are built as a fixed unit, without considering the creation of any passive ventilation or the building orientation.</p>
<p>Courtyard</p>	 <p>Most of the courtyards are inside the buildings with a fountain and a small landscape; creating a strong influence on the indoor environment.</p>	 <p>Most of the open spaces are outside the buildings, as a place for public social activity without considering inner courtyards.</p>
<p>Cooling strategies</p>	 <p>Pottery Wind tower Evaporative cooling strategy inside the wind tower and the pottery in front of the windows are used as a passive technique in these houses for providing good indoor comfort.</p>	 <p>Active strategies like mechanical fan and air conditioning are used in some houses for providing indoor comfort with high energy consumption due to poor indoor environment.</p>

1.3 Research problem

Based on past researches, concerning indoor climate and new housing projects;

- The new housing was designed as a fixed prototype regardless of climatic conditions.
- Many researchers conducted indoor measurements; in which there were high heat gains inside houses that caused discomfort for occupants [10, 11, 3].
- There is a lack of concern for indoor carbon dioxide concentration and indoor air quality in the Egyptian houses in past literature.
- Opening the windows, (for achieving comfort), will increase the indoor temperature especially during daytime.
- Lack of financial resources to use air conditioning (AC) for maintaining the comfort temperature in the new housing especially for low income (as low income people in Egypt represent nearly 50% [7]).

Therefore, the harsh climatic conditions of hot arid desert climatic zone, particularly in Egypt, raise the necessity of designing climatic responsive housing and search for passive solutions, in order to achieve thermal comfort for occupants and make a significant improvement in energy conservation.

1.4 Research aim and objectives

The main aim of this research is to achieve indoor thermal comfort and zero energy consumption for cooling by new natural passive cooling strategy for the New Assiut City.

In order to achieve the aim of the research, the objectives are:

1. To investigate indoor environment inside three houses in the New Assiut city by monitoring air temperature, relative humidity and carbon dioxide concentration.
2. To understand natural ventilation & the evaporative cooling technique in the traditional residential building.

3. To search for new suitable passive cooling strategies that use natural ventilation with cooling techniques, in order to achieve low energy consumption.
4. To investigate the possibility of using natural ventilation with evaporative cooling strategy in the New Assiut city using typical weather data.

1.5 Research questions

How can we find an alternative for achieving indoor thermal comfort & nearly zero energy consumption for cooling compared to the conventional passive cooling system in the housing of the New Assiut city, Egypt?

This will be done by answering the following questions:-

1. What is the performance of summer indoor environment in the New Assiut City, Egypt?
2. What is the performance of the conventional passive systems that use natural ventilation and cooling strategies? And what are their limitations?
3. What is the new technique that can use natural ventilation & evaporating cooling techniques to achieve indoor thermal comfort?
4. How can we achieve indoor thermal comfort by new compact and high performance passive cooling systems?

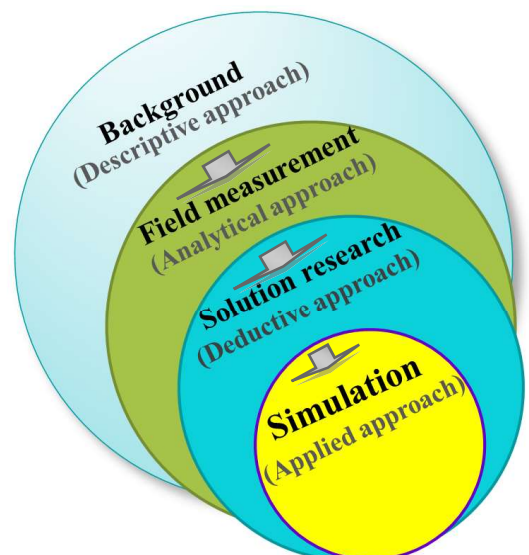
Research

1.6 Research methodology

The research depends on four steps;

- **The Descriptive approach** (chapter 1);

This chapter focused on studying the research background of indoor environment in the Egyptian new housing projects, compared to the traditional buildings.



- **The Analytical approach** (chapter 2);

This chapter focused on field measurements for indoor environments of three cases with different ventilation scenarios. Then, the results were analyzed in order to investigate the real situation of indoor environments and search for new suitable passive strategies.

- **The Deductive approach** (chapter 3);

Based on the results of indoor measurements, search for the suitable strategy for the building of that climate is conducted in order to provide indoor thermal comfort. The concept of the new system is discussed based on the limitation of the conventional passive technique.

- **The Applied approach** (chapters 4 & 5);

A new proposed system of inclined solar chimney with short wind tower is investigated by numerical modeling (COMIS-TRNSYS simulation software). Typical weather data of the New Assiut City are applied to the system. Then, the impact of the proposed system on Assiut climate is analyzed with the optimization investigation to achieve compact and high performance design.

1.7 Research Scope;

The research focuses on applying the new proposed system for the living room. The living room of the top floor is chosen as a pilot base case, where all the family members spend much time doing different activities and without any air exchange with other rooms. Simulation is done for the living room as a single zone located in a block of buildings with the same circumstances for the layout as Family housing sector in the New Assiut City.

1.8 Research structure;

The research is divided into six chapters in order to achieve the aim;

Chapter one; The introduction of the research: A brief background on issues related to indoor environments; discussion of the research objective, methodologies and structure is studied.

Chapter two; Investigates indoor environments through monitoring indoor air temperature, relative humidity and carbon dioxide concentration with different ventilation scenario in three cases. Also, it aims at understanding the suitable strategy for that climate based on three important indices.

Chapter three; Studies the limitations of the conventional passive systems that use natural ventilation and evaporative cooling for indoor thermal comfort. Also, a search is conducted for the new passive strategy that use zero energy consumption based on the conventional system limitation.

Chapter four; In this chapter, a new proposed system is investigated in order to achieve indoor thermal comfort and zero energy consumption for cooling based on simulation modeling using COMIS-TRNSYS software. Typical weather data for the New Assiut city is investigated in the model.

Chapter Five; This chapter addresses the parametric investigation and optimization of the important parameters of the system (solar chimney and wind tower) on indoor temperature and the air flow rate in order to achieve a new compact design with high performance (nearly 80% acceptable comfort range) and high advantage of integration of the two techniques.

Chapter six; Presents the critical discussion of the important findings in chapter 2, 3, 4 & 5 with the final achievement for indoor thermal

environment. Also, a guideline for the system is studied to be integrated on different cases with different area and different number of occupants. Finally, future research is considered based on the limitations of the system.

References This section includes scientific references on which the study is based.

Appendix This section includes the appendices which the study may need

Figure (1-3) shows the sequence of the thesis organization to achieve the aim.

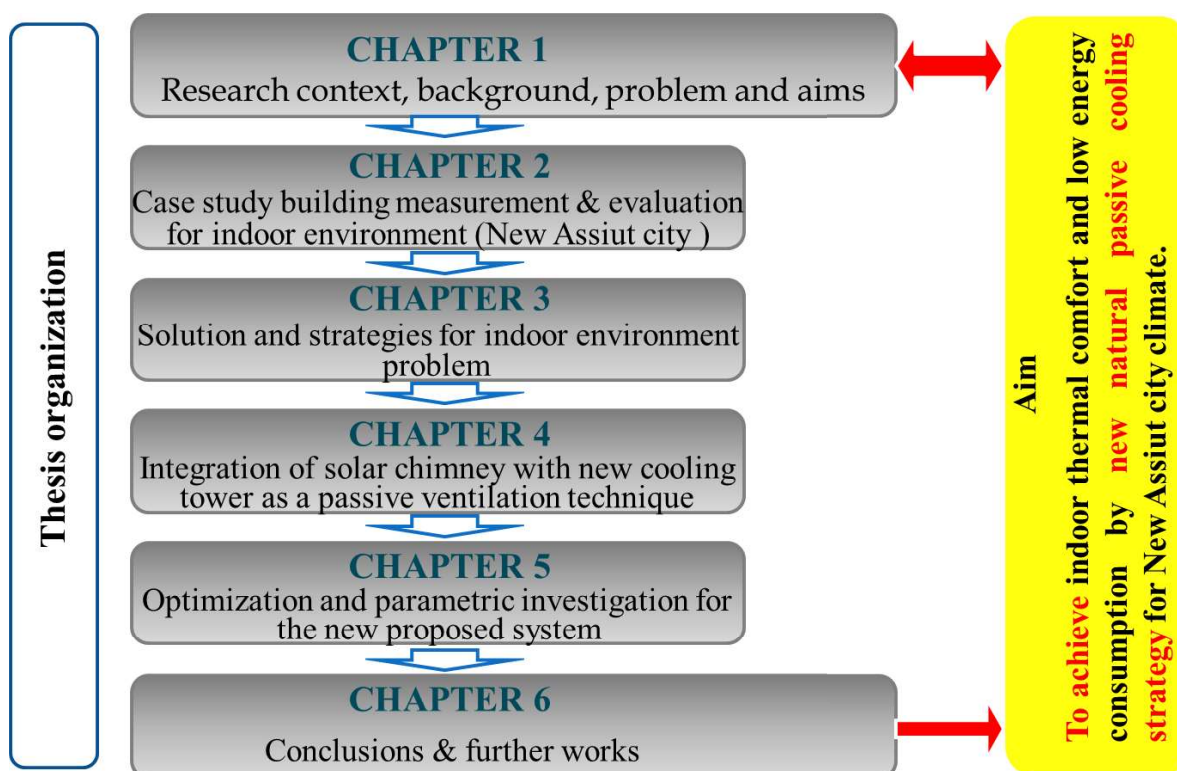


Figure (1-3): The structure for thesis organization



Chapter 2

**Case study building measurement &
evaluation for indoor environment
(New Assiut City)**

Introduction

The environment, building and energy are issues facing the building profession on a global scale. Buildings consume large amounts of energy for their operation [18]. Heating, ventilation and air conditioning (HVAC) systems are responsible for about one half of the energy used in buildings [19]. In order to achieve thermal comfort inside a housing block in Egypt and to choose the best design ventilation strategies for a building, it is very important to know the actual situation of the indoor environment concerning temperature and relative humidity. Many researchers have studied thermal comfort in housing and conducted small and wide scale measurements so far: S.M. Robaa investigated thermal comfort in buildings of Egypt based on a meteorological station database [20]. Riyadh verified and examined climatic conditions in the residential areas of Egyptian cities –New Assiut city. He made field measurements for indoor environment of Youth & Future housing project, pedestrian pathways between buildings and streets around these buildings in three months of the summer season and one month of the cold period with an interval of two hours in 12 days only with no internal load in order to take climatic conditions into account when designing new buildings [10]. Wael and Steve investigated thermal characteristics of the building in the hot season of new Cairo housing to enable appropriate solutions to be chosen at the early stages of design and to achieve low energy thermal comfort in dwellings. They investigated temperature & humidity during two and half months from June to the middle of August with 15 minute intervals in the living room & bedroom of one house without internal load [11]. Medhat investigated the possibility of enhancing the use of natural ventilation as a passive cooling strategy in public housing blocks in the arid deserts of Egypt. He investigated the temperature during four days of July at two hour intervals with all windows are open and all windows are closed [3]. However, there is little information available for the actual humidity and temperature for different ventilation scenarios in 15-minute

intervals of the summer season especially in New Assiut city. In addition, no studies were conducted to examine indoor CO₂ concentration and its effect on indoor air quality (IAQ).

Therefore, this research was conducted to investigate indoor environment for the new housing in New Assiut city, through monitoring indoor air temperature, humidity and CO₂ concentration in the summer season, in order to understand the real situation in some houses of New Assiut city and search for new suitable passive strategies to solve occupant thermal comfort. The New Assiut city is chosen.

2.1 Location of New Assiut city

New Assiut city is located on the east side of the River Nile with a latitude of $27^{\circ}3'N$ and a longitude of $31^{\circ}15'E$. New Assiut city is located northeast of the Southern Upper Egypt zone. This zone is located along the River Nile from $24^{\circ}50'N$ to $27^{\circ}42'N$ according to the HBRC classification [4]. It has a maximum operating temperature that range from $41^{\circ}C$ to $46^{\circ}C$ and minimum temperature that range from $16^{\circ}C$ to $21^{\circ}C$ in the summer months. In the winter months the minimum temperature ranges from $2^{\circ}C$ to $4^{\circ}C$. Figure (2-1 & 2) show the location of New Assiut city according to HBRC classification and its satellite image.

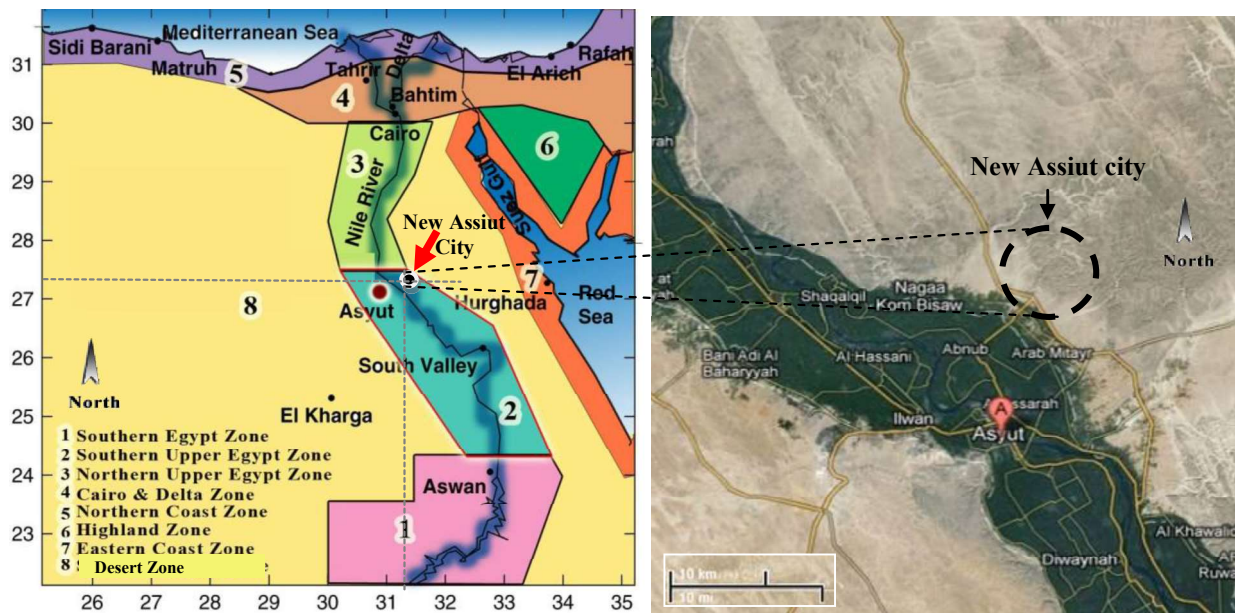


Figure (2-1): Classification of climatic zones in Egypt [4, 5] and position of Assiut city [21].

2.2 Case study location & description

Most of the houses in the New Assiut city were built as a fixed prototype without taking into account building orientation, indoor comfort, air quality or passive ventilation strategies [3]. Therefore, they were built without considering response to climatic conditions. Three cases are investigated and monitored: 2 cases in the family sector project and one case in the youth housing sector. Figure (2-2) shows the location of the two sectors within New Assiut city map.

The reason for selecting these cases, was that the selected houses were occupied by low income people and built in different periods from 1995 until 2004. Different ventilation scenarios needed to be investigated for knowing their effect of different floor levels. The researcher investigated many houses in order to choose these cases.

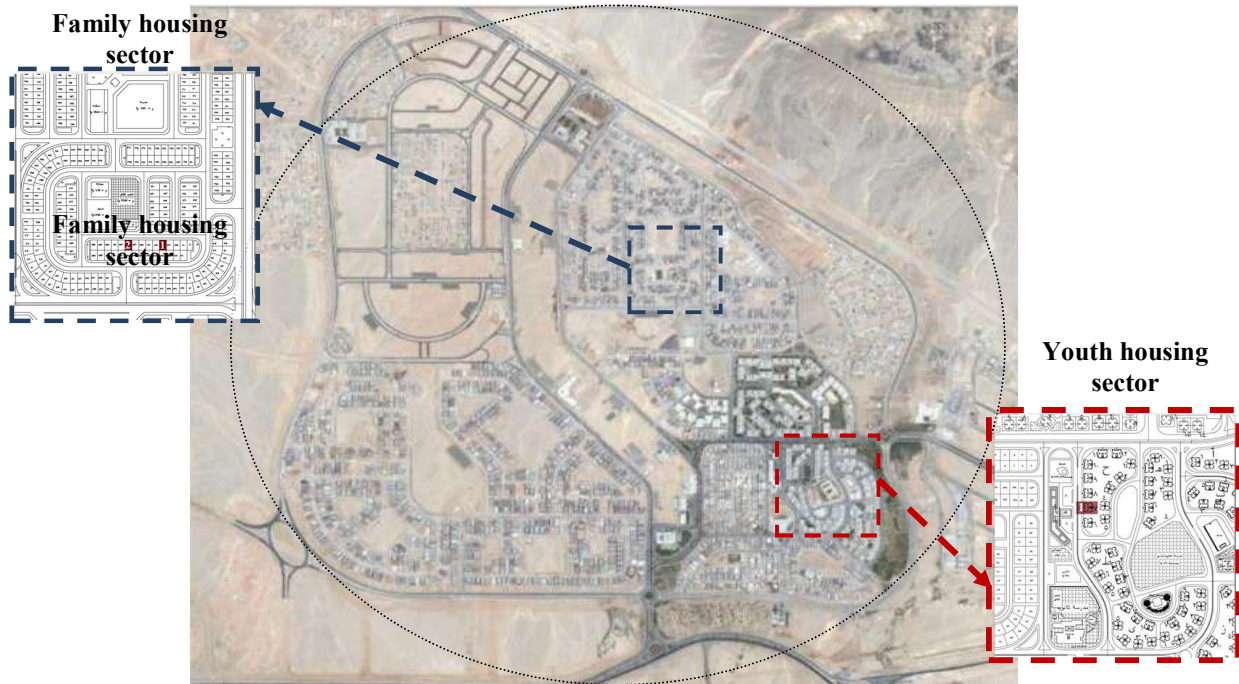


Figure (2-2): The satellite image of New Assiut city with the location of family housing and youth housing sector [21, 22].

Family housing project is one of the urban community projects for government housing project. It is located in the north east of New Assiut city. This project offers areas ranging from 150m^2 to 350m^2 , with a fixed plan [7]. The project was implemented in three phases: the first phase in 2003, and offers land areas ranging from 230m^2 to 350m^2 ; and the second and third phase at the end of 2004 offer land areas ranging from 150m^2 to 250m^2 .

Figure (2-3) shows the location of the three cases in youth housing & family housing sectors.

The researcher had to make much effort in installing the measurement device because of the privacy of the Egyptian.

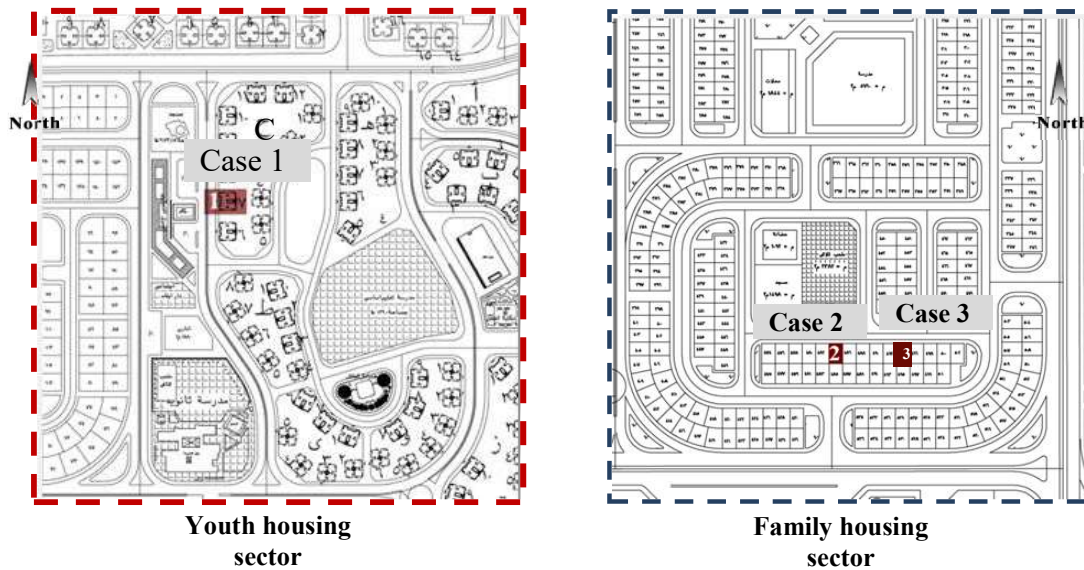


Figure (2-3): The location of the case study in the family housing and youth housing sector [22].

Case 1: It is located in block number 7 (C) of the youth housing project. The apartment used for measurement is located on the third floor level with two floors above it. The outside façade for this apartment faces the north and west. The kitchen and the bathroom open to on an outside space facing the north orientation. Natural ventilation with single side ventilation strategy is used in this unit with a mechanical fan. Also, one air conditioner (window cassette) is installed in the master bedroom. Figure (2-4) shows the plan of case 1 with its dimensions and the location of the measurement device in each room.

Case 2: It is located in the second family housing sector (block number 484). The apartment is located on the second floor level with one floor above it. The outer façade of the building faces a street with north orientation. While the inner façade of the building faces the back courtyard with south orientation. The living room and the bedroom face the north orientation. The master bedroom, the bathroom, and kitchen face back courtyards on the leeward side. Natural ventilation with cross ventilation strategy is monitored in this unit with a mechanical fan. Figure (2-5) shows the plan of case 2 with the location of measurement device on it.

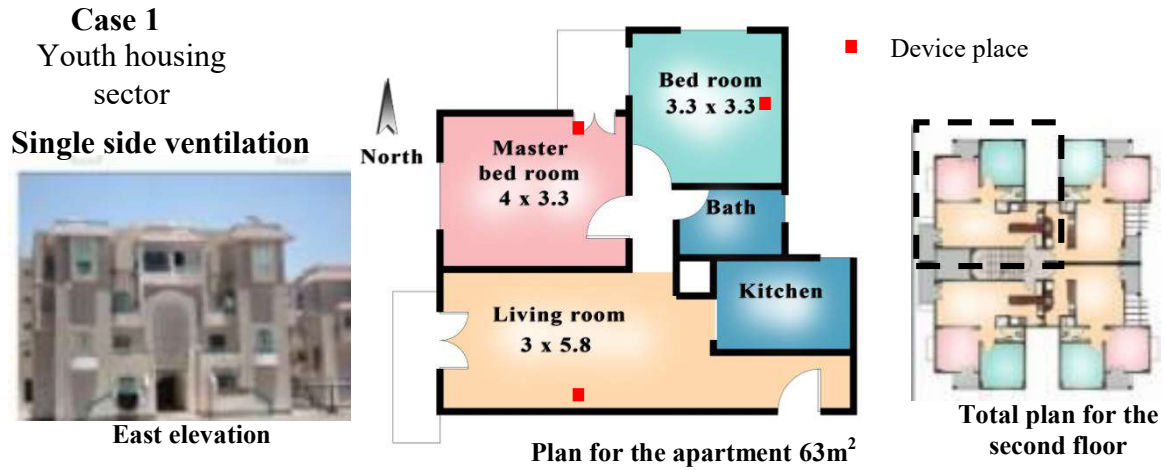


Figure (2-4): The plan and the floor of the building and the detailed plan of case1 [22, Author].

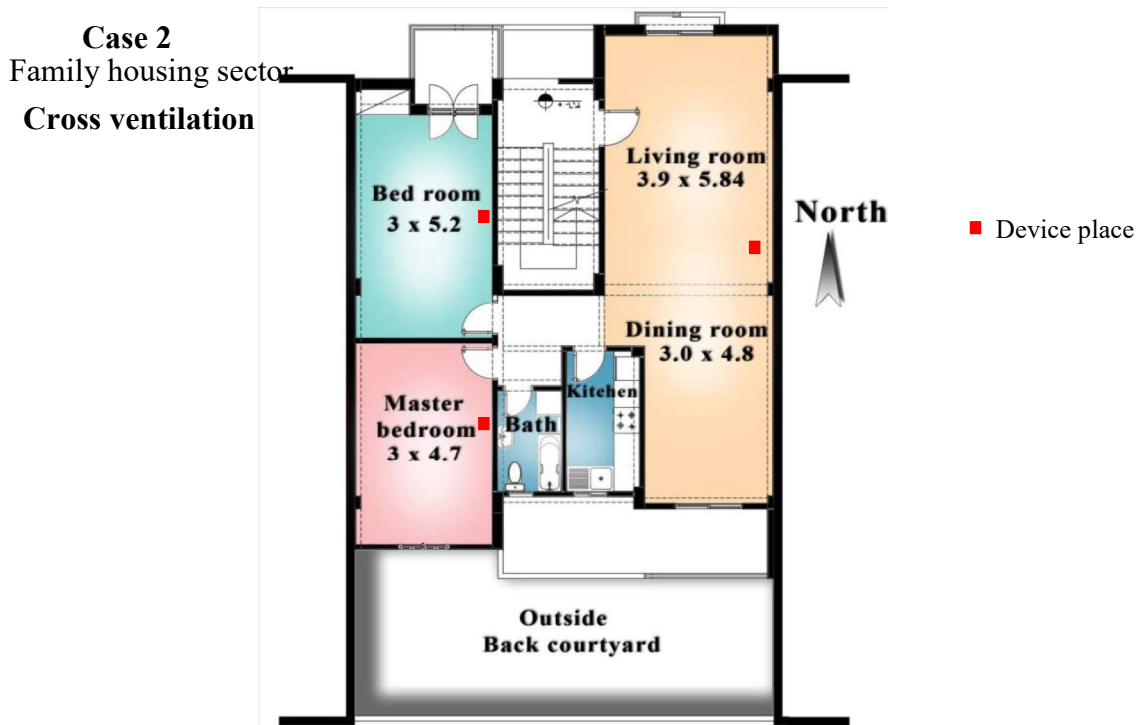


Figure (2-5): The plan for the second floor of the house, case 2 [22, Author].

Case 3: It is located in the second family housing project (block number 494), in the top floor level. Its orientation takes the same orientation of case 2. Natural ventilation with single side ventilation strategy is used with a mechanical fan. Figure (2-6) shows the plan of case 3 with the location of the measurement device on it.

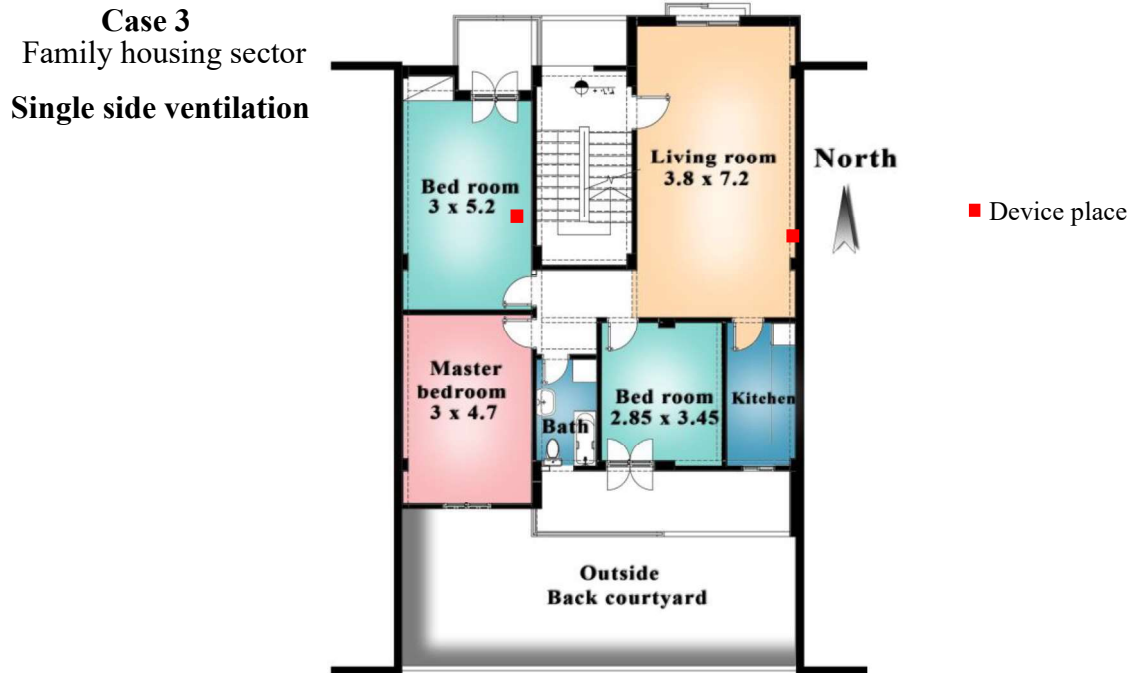


Figure (2-6): The plan for the top floor level of the house, case 3 [22, Author].

2.3 Climatic analysis of outdoor condition for New Assiut city (one year data)

Outdoor climate analysis for New Assiut city is done based on real weather data. It was derived from Egyptian Typical Meteorological Year (ETMY) of Egyptian Meteorological Authority for periods of 12 years from 1991 until 2003¹ [23]. The researcher used ETMY file (Asyut 623930 (ETMY)) in Energy Plus/ESP-r Weather (EPW) format using Building Energy Software Tools –Climate consultant to analyze standard one year data. This helps to understand the climate of New Assiut city in order to be used for input in simulation software.

2.3.1 Air temperature;

Figure (2-7) shows the average temperature for one year data in relation to adaptive comfort standard (ACS)². It shows that the average high temperature for the summer season (June, July & August) is 37°C, and the minimum average temperature is 22.5°C in July. The average comfort temperature is 25°C with (± 3.5) acceptability 80% limit according to ACS. Also, the maximum average

¹It is developed by U.S. National Climatic Data Center, California, USA

² Appendix A.

temperature during the winter (December, January & February) is 22°C, and the minimum average temperature is 8°C in January; with a comfort temperature of 22.5°C.

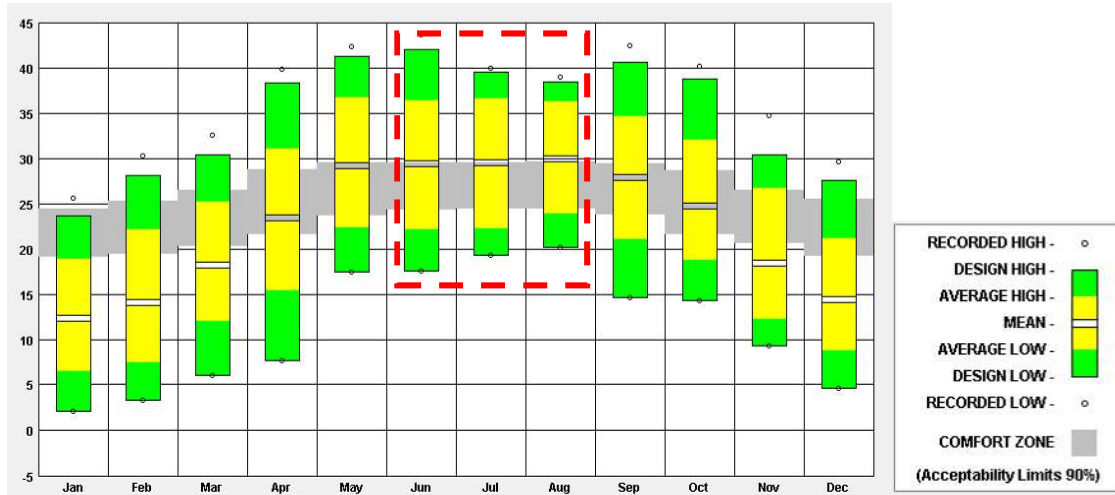


Figure (2-7): Temperature ranges for New Assiut city during one year weather data.

Figure (2-8) shows the temperature percentage distribution during the period of sunrise and sunset. It is important to understand the temperature range during daytime and nighttime; especially for the hot season in order to search for the best strategy for that climate. This model assumes occupants adapt their clothing to thermal conditions, and are sedentary (1.0 to 1.3 met) according to ACS of ASHRAE 2004. It is concluded that the average temperature ranges from 27 to 38°C from 9 am after sunrise until 12 pm after sunset in the summer season except in August it extends until 1am. This indicates high outdoor temperature during daytime and even at nighttime. This has a strong effect on indoor and outdoor thermal comfort.

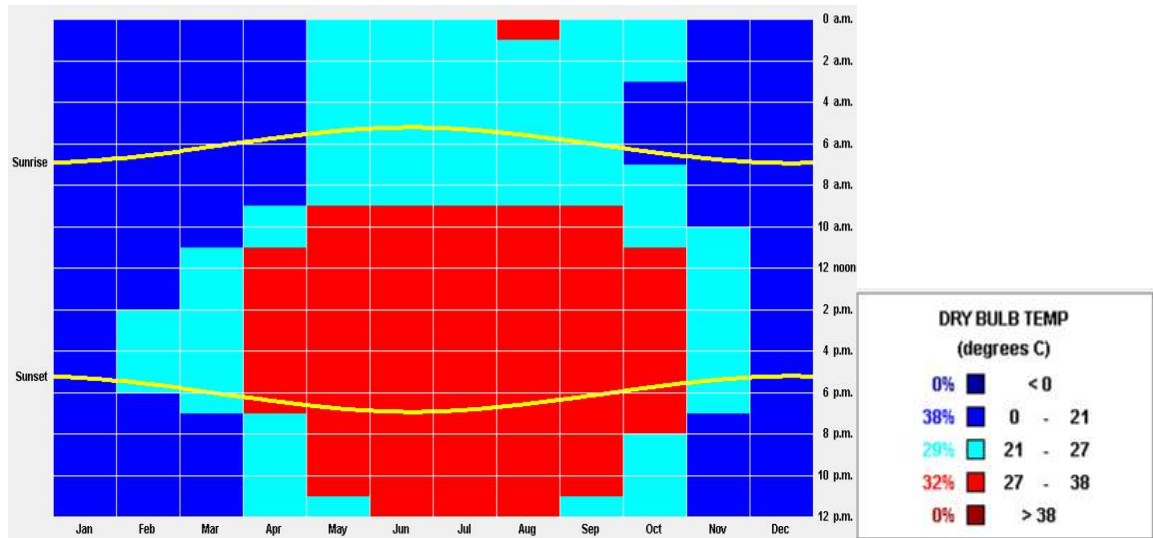


Figure (2-8): Outdoor temperature percentage distribution between sunrise and sunset for one year.

2.3.2 Relative humidity;

Figure (2-9) shows the average relative humidity percentage for every month in the real weather data. It is concluded that the average relative humidity percentage in the summer season ranges from 30% to 35%. It increases to 52%~57% during the winter season.

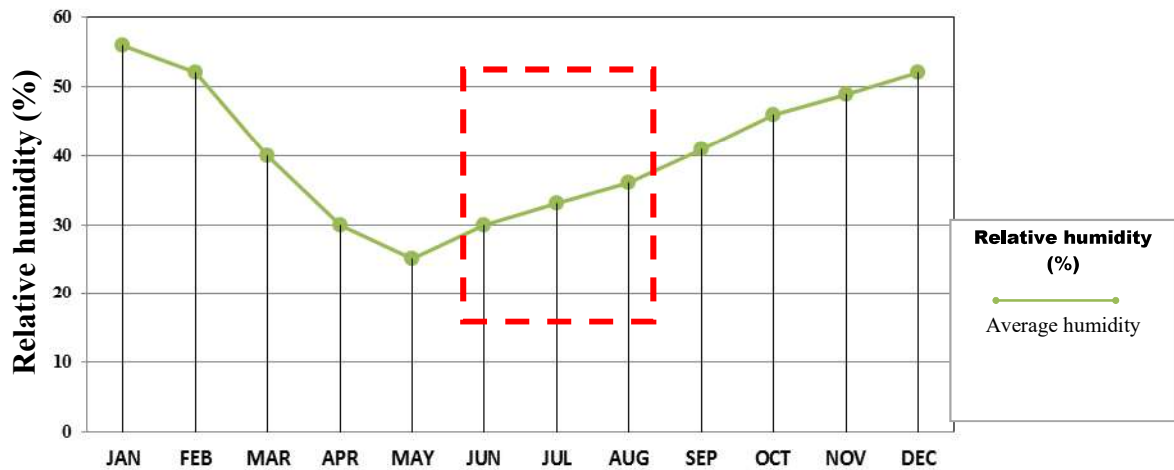


Figure (2-9): Outdoor average relative humidity data profile for one year data.

Figure (2-10) shows the relative humidity percentage distribution during sunrise and sunset. It is clear that the relative humidity percentage ranges from 20%~40% from 9am to 4am in June (except between 2pm to 6pm), 10am to 2am in

July (except between 4pm to 5pm), and 10 am to 1 am in August. Then, the relative humidity increases from 40~60% from 4am until 9am in June, 2am until 10am in July, and 1 am until 10 am in August.

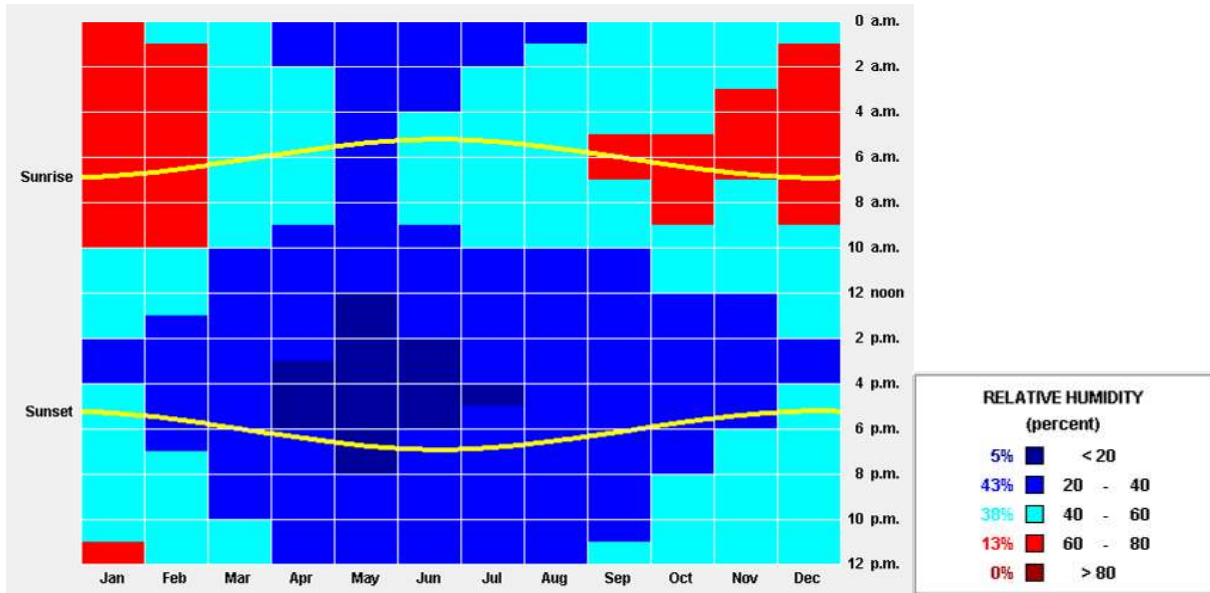


Figure (2-10): Outdoor relative humidity percentage distribution (between sunrise and sunset) data for one year.

2.3.3 Wind speed & direction

Figure (2-11) shows the average wind speed for all months of the year. It is concluded that the average maximum outdoor wind speed during the summer period is 7.8m/s in June, and the minimum average wind speed is 1.3m/s in August¹.

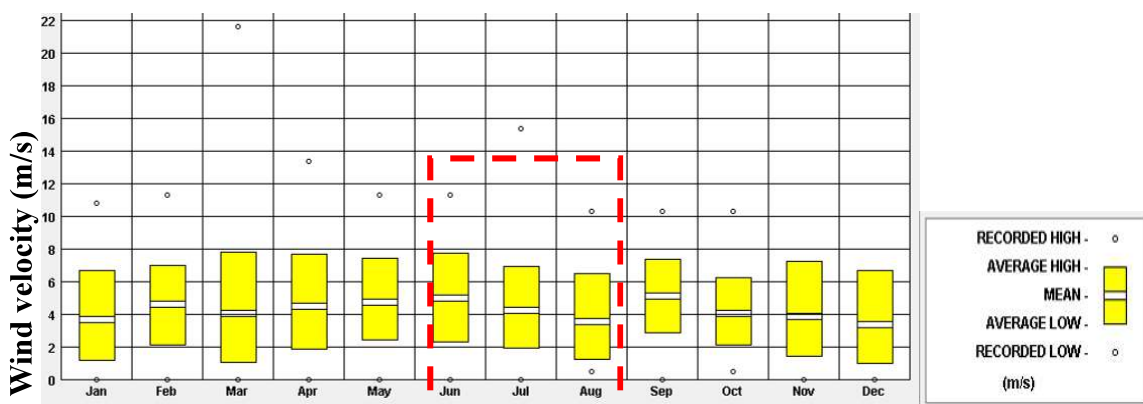


Figure (2-11): Wind velocity range for new Assiut city during one year data.

¹The measurement of the wind speed in the meteorological station.

Figure (2-12) show the wind speed distribution during the sunrise and sunset. It is clear that the wind speed distribution increases during daytime; especially from 10 am to 11 pm, 11am to 8am, 11am to 7pm in June, July, and August respectively. Besides, the wind speed is less than 2m/s in August between 1 am to 5am. This low wind speed affects indoor air flow rate during nighttime (night ventilation).

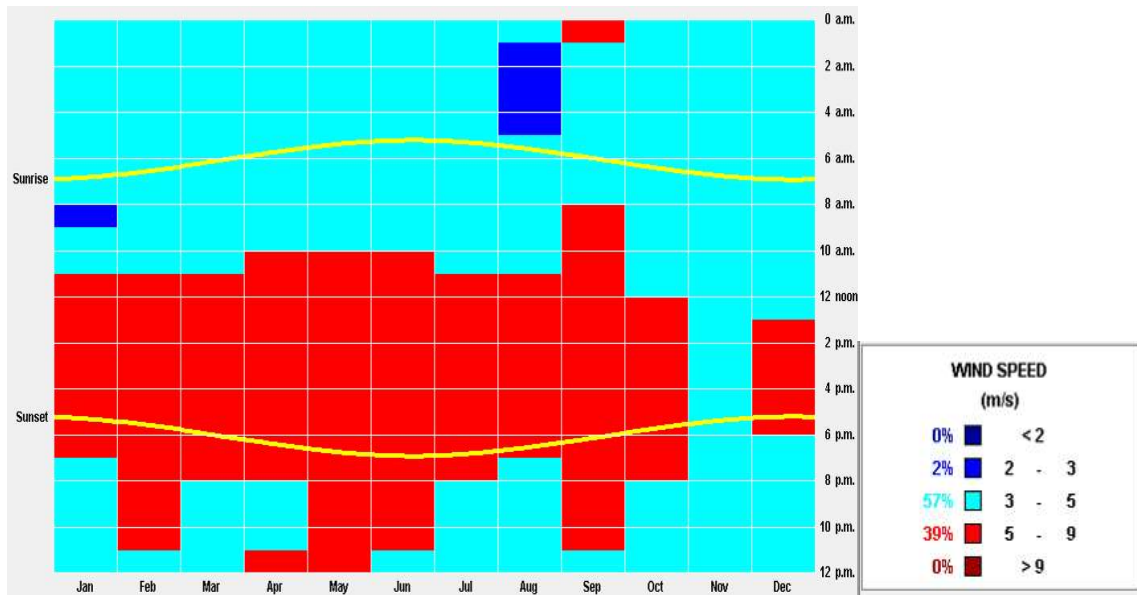


Figure (2-12): Outdoor wind speed percentage distribution between sunrise and sunset for one year.

Figure (2-13) shows average wind direction in all months of the year.

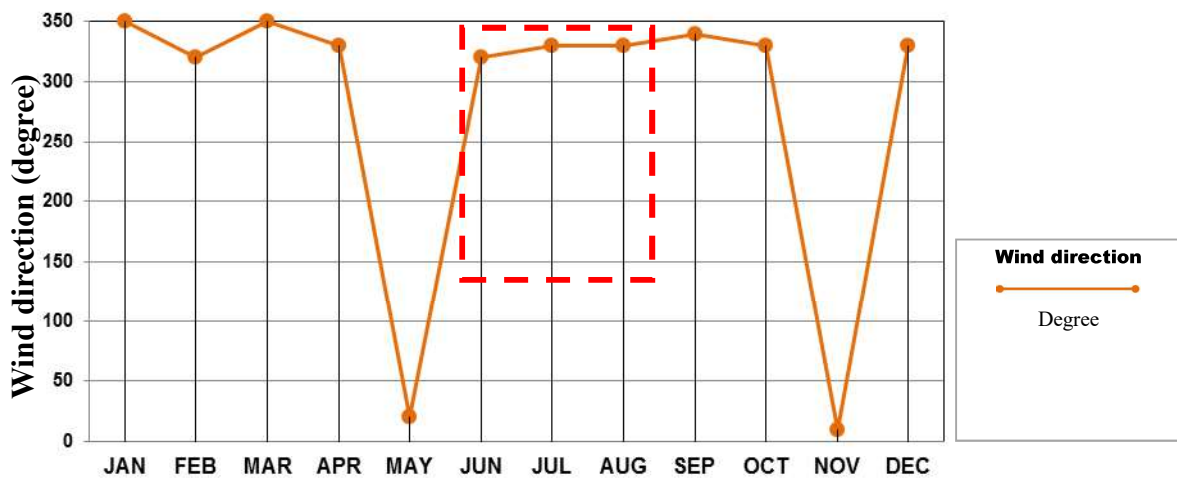


Figure (2-13): Outdoor average wind direction in all months of the year.

The graph shows that the average wind direction is from northwest with an angle range between 320° to 350° (measured from the north clockwise) in all months of the year except in May and November. But the wind changes its direction to northeast in May and November with an angle range between 10° to 20° (measured from the north clockwise). Therefore, the prevailing wind comes from the northwest most of the year except in early of May & November.

2.3.4 Solar radiation

Solar radiation is considered an important factors that influences indoor temperature. It is concluded from figure (2-14) that the maximum direct normal radiation in the summer season (June, July & August) is 1025W/m² in June with maximum global horizontal radiation 1125W/m². Then, it decreases to 850W/m² for direct normal radiation in July and a global radiation of 1025W/m².

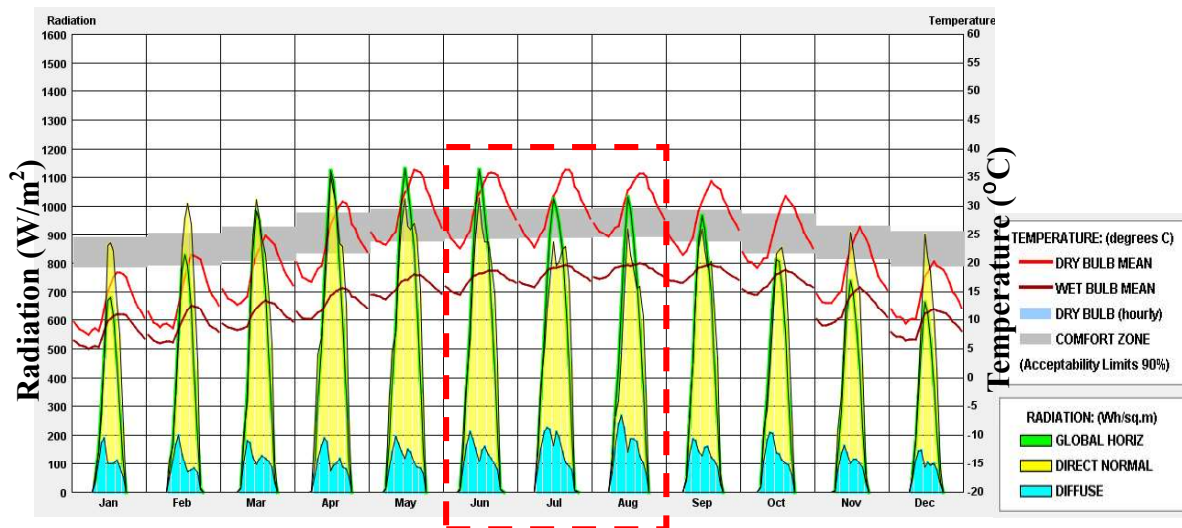




Figure (2-14): Radiation profile and the mean dry bulb temperature for one year weather data.

2.4 Methodology

In this measurement, 10 units of the thermo recorder TR-72Ui were used. Three units of the thermo recorder were placed in each house and one unit was placed outside the house under the porch, inside an aluminum duct to protect it from extreme solar radiation. In each house, one unit of thermo recorder was placed in the living room, bedroom, and master bedroom. When the measurement

started, one of the thermo recorders in the master bedroom of case 3 couldn't be setup and did not function correctly. Measurement of temperature and humidity was conducted in the end of May as a pilot study and to check the measurement devices and their locations. Then, measurement of carbon dioxide concentration was conducted. Two units of CO₂ sensor (JMS-301) were used. Each device was placed in the living room of cases 1 & 2. Each TR recorder could log more than 8000 data logs for full storage capacity and the CO₂ sensor capacity was 87000 data logs. One colleague was assigned to collect the data at the end of every month. Table (2-1) shows the description of the measurement devices.

Table (2-1): The description of the measurement device.

Equipment		Description
Ventilation rate data reader (JMS-301)		<ul style="list-style-type: none"> • Data range~ 4000 ppm) • Measuring accuracy: ±5% ppm, ±50 ppm.
Thermo Recorder model TR72Ui		<ul style="list-style-type: none"> • Humidity measurement range: 10 to 95%RH, • Temperature measurement range: 0 to 50°C, • Sensor durability Range: -10 to 55°C. • Humidity measuring accuracy: ±1%RH (at 25°C and 50%RH), ±0.1°C • Materials: temperature/humidity sensor polypropylene resin vinyl coated electrical

Company: T&D CorporationTECPEL Co. wire.

Standardization of the measurements was assigned as follows:

- Each unit was placed in a strategic place away from any thermal heat device or children; 1.0 to 1.5 m above the ground.
- The TR recorder was set to measure at 15 minute intervals and the CO₂ sensor was set to measure at 20 minutes interval to apply detail measurement

and investigate the little change in indoor environment .

- The measurement of temperature and humidity was started in 28 May~31 July 2012 for daytime and nighttime.
- The CO₂ sensor was placed in the living room of the two houses (cases 1&2), where all family members spend much time doing different activities.
- The measurements of CO₂ started in June for one month, three days in July, and three days of August.
- All the data were analyzed and compared according to Adaptive Comfort Standard (ACS)¹, ASHRAE thermal comfort standard [24] and ASHRAE acceptable CO₂ concentration [25, 26] in order to evaluate the measurement data based on comfort standard.

The researcher conducted measurements in three houses in order to understand the effects of different types of ventilation on occupant's thermal comfort; single side ventilation (with/without air conditioning in Master bedroom)² to study its effect on achieving indoor thermal comfort and cross ventilation in one occupied house.

2.5 Monitoring of indoor temperature & humidity in May.

Measurement started in the end of May from 28~31 for four days in order to monitor the difference scenarios (natural ventilation and air conditioning) in the three cases and check the device accuracy.

Figures (2-15, 16 & 17) show four days data during daytime and nighttime in the three cases. In case 1, the maximum temperature in the living, bedroom and master bedroom was 36°C, 36.5°C and 34.5°C respectively and the minimum temperature was 32°C, 30.5°C and 31°C respectively without air conditioning. It is clear that when the occupants used air conditioners during daytime; the

¹ ACS is the standard which determines the acceptable indoor operative temperature. This standard is based on the findings of surveys of thermal comfort conducted in the field.

² The air condition is operating by users of this case during the hot hours of daytime and nighttime.

temperature decreased to 27°C and became within the 80% acceptable comfort range. This indicates that occupants preferred to use air condition in the hot hour during daytime to achieve indoor comfort. But in case 2, the maximum indoor temperature in the living room, bedroom and master bedroom was 40.5°C, 40°C, and 39°C respectively and the minimum temperature was 26.5°C, 24.5°C, and 29°C respectively. The indoor temperature and humidity patterns follow the outdoor patterns. While during nighttime, the temperature decreases to be within the 80% acceptable comfort range in 30 & 31 May. In case 3, the maximum temperature in the living room and bedroom was 36.5°C and 36°C respectively, and the minimum temperature was 32°C and 28°C respectively. Also in case 3, the difference between the maximum and minimum temperature pattern was small due to high internal heat gain and thermal mass.

Then the absolute humidity¹ was calculated from the measured indoor relative humidity. This helps to understand the humidity level (sometimes) in each room with an occupant load. It is clear that the humidity level is more than the acceptable range (12g/kg') according to ASHRAE [24], especially in the living room and master bedroom of case 1 and the living room in case 3. This is because occupants were doing different activities in these zones.

¹**Absolute humidity** is an amount of water vapor per unit volume. Usually is given in (g/kg') or (kg/kg') water vapor per dry air. It is related to exchange by evaporation between person and environment.

Case 1

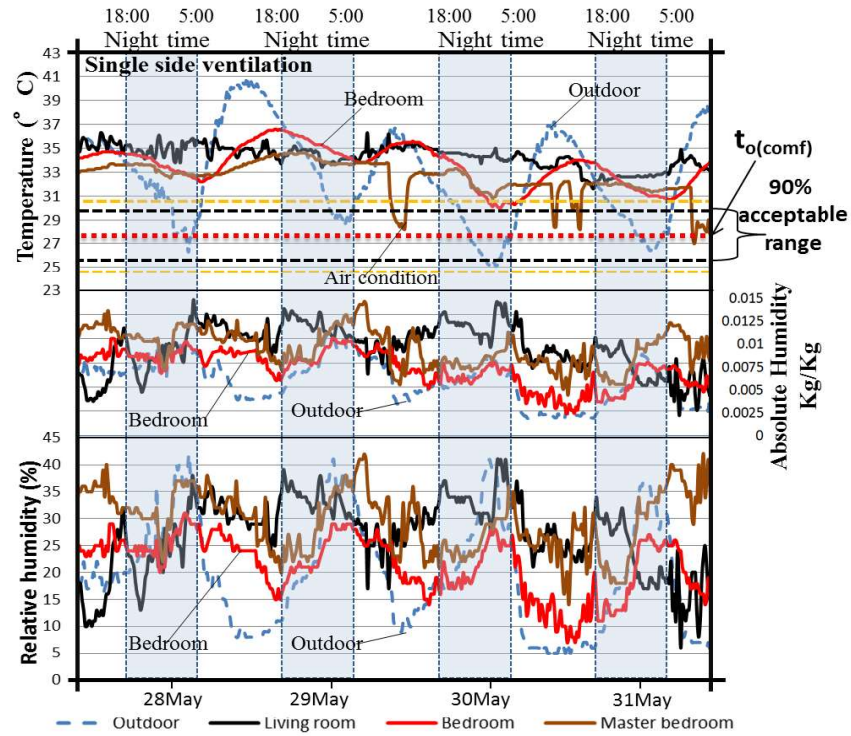


Figure (2-15): Temperature and humidity patterns for indoor environment of the last four days of May in case 1.

Case 2

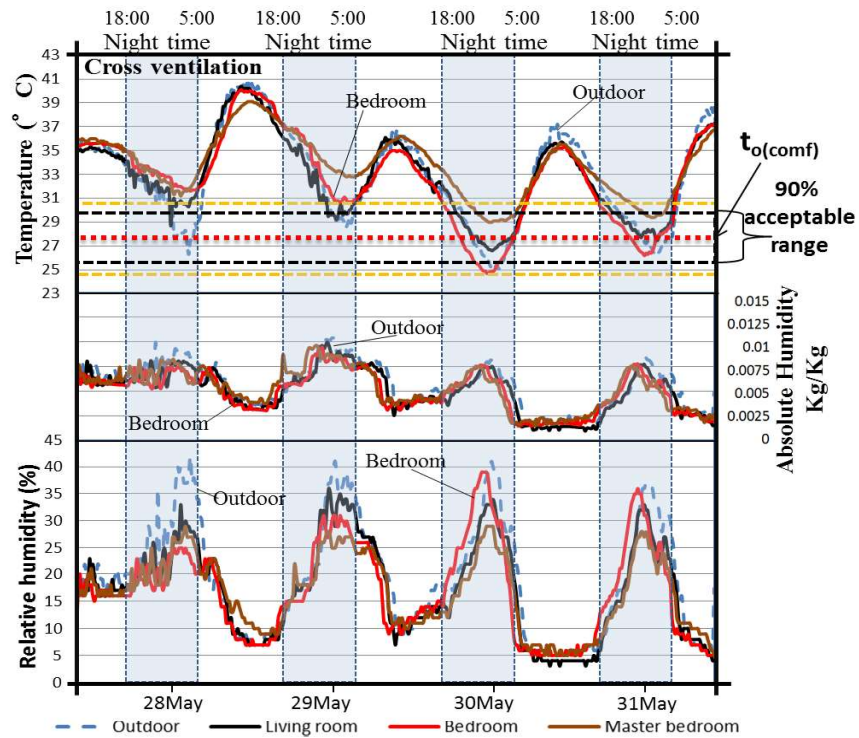


Figure (2-16): Temperature and humidity patterns for indoor environment of the last four days of May in case 2.

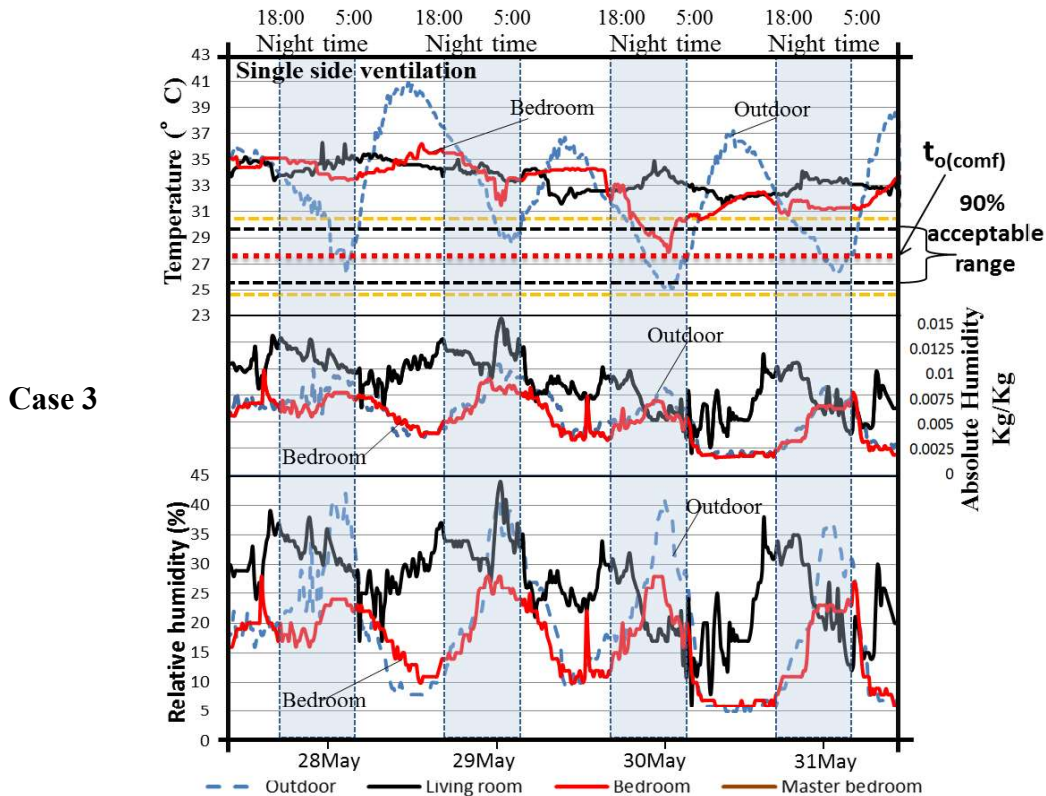


Figure (2-17): Temperature and humidity patterns for indoor environment of the last four days of May in case 3.

2.6 Evaluation of June measurement

2.6.1 Temperature, humidity & absolute humidity profiles for one month measurements-June 2012

Figures (2-18, 19 & 20) show the temperature and humidity levels for one month measurements for the three cases during June. By contacting the occupants in case 1, the occupants were out of the house for six days between June 21st~26th.

The results showed that, there is a great difference in the pattern of temperature and humidity in the three cases due to different ventilation strategies. In Case1, the orientation of living room & master bedroom towards the west affects indoor temperature. The fluctuation of temperature pattern in the bedroom is higher compared to other rooms. This is due to opening windows few times each day with high internal heat gain.

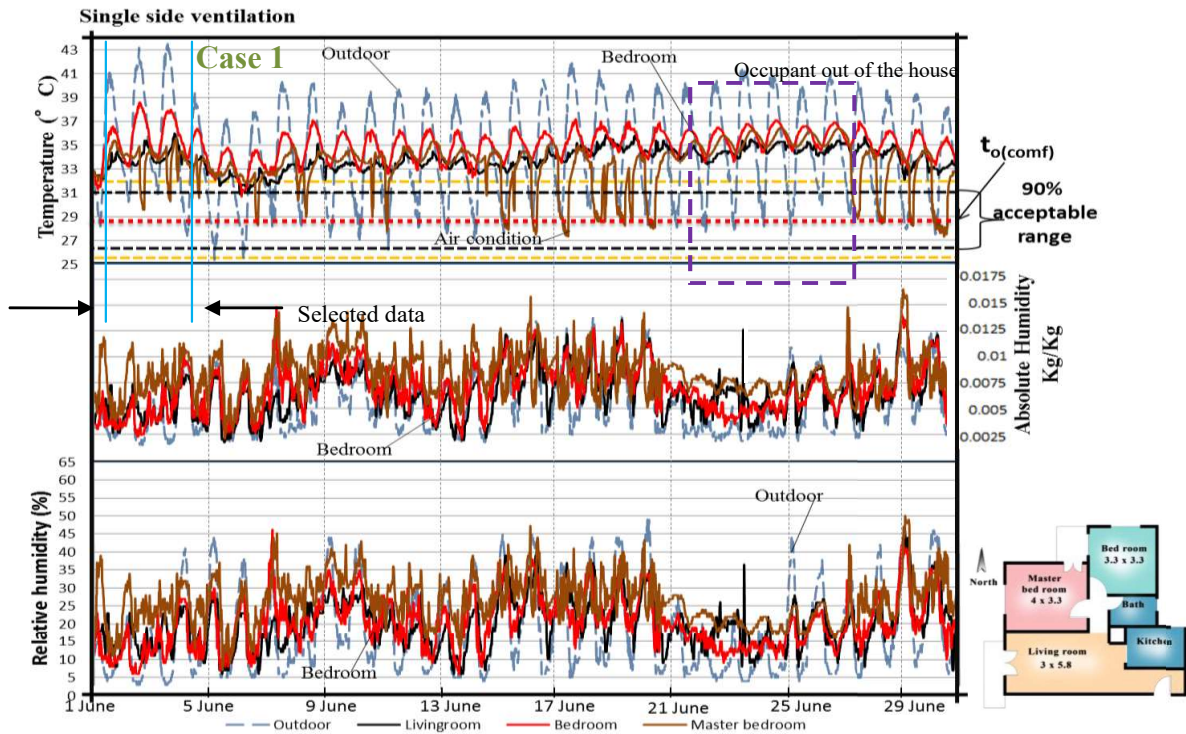


Figure (2-18): Temperature, humidity and absolute humidity patterns for indoor environment of June in case 1.

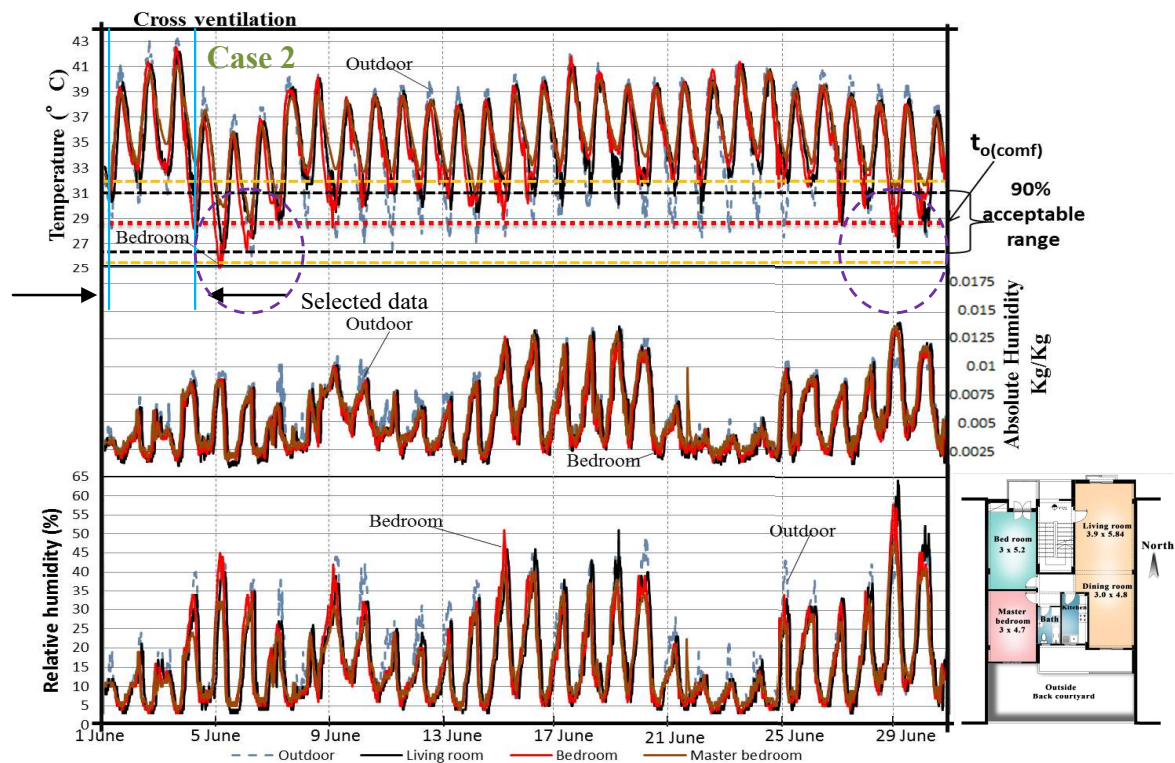


Figure (2-19): Temperature, humidity and absolute humidity patterns for indoor environment of June in case 2.

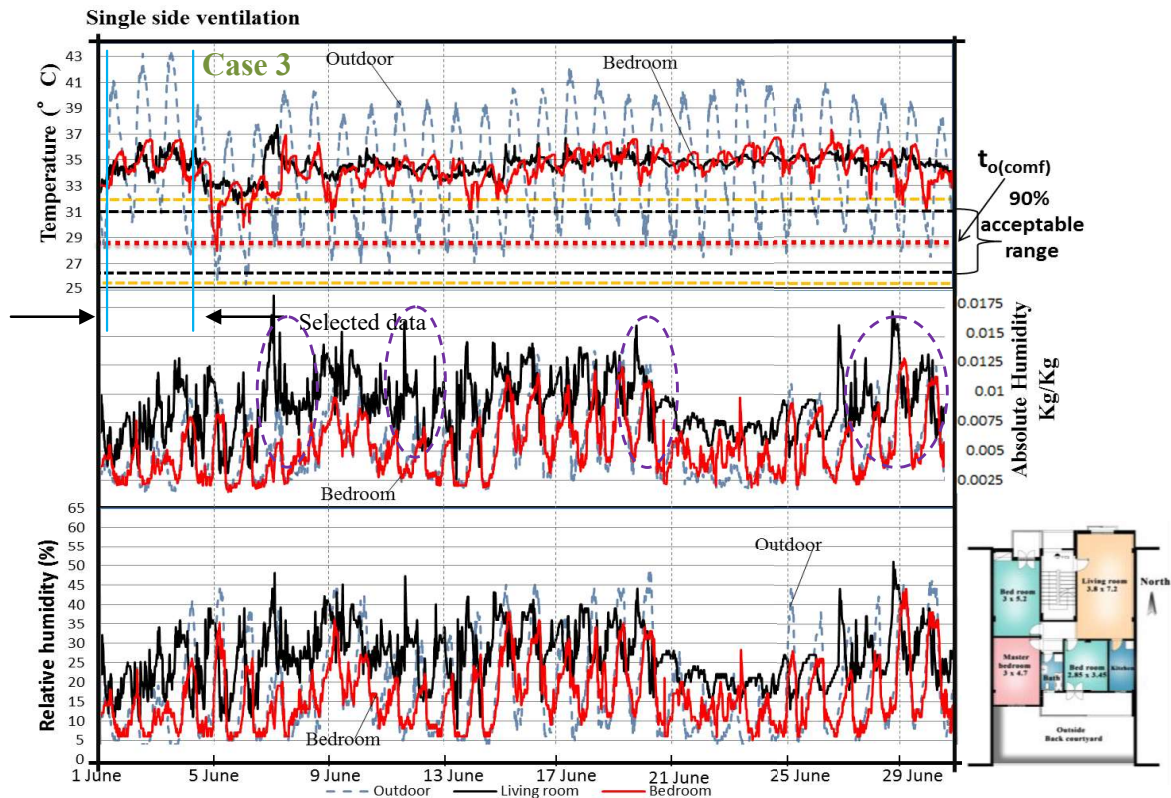


Figure (2-20): Temperature, humidity and absolute humidity patterns for indoor environment of June in case 3.

Also, the occupants sometimes used air conditioning in the master bedroom, in order to control indoor comfort temperature and reach 80% acceptable range. By focusing on the humidity pattern in the period of 21~26 June, there is no significant fluctuation in the absolute humidity. This is due to the absence of occupant's effect on indoor environment compared to other period.

In case 2, the pattern of indoor temperature follows the outdoor temperature. This causes an increase in indoor temperature due to opening the windows in daytime and nighttime. However, a few hours during the night and early morning dropped within the comfort 80% acceptable range most of the month. While in case 3, the fluctuation in indoor pattern was similar to case 1 with small differences between high and low temperature. It is clear from the absolute humidity pattern that occupants stayed most of time in the living room.

This caused an increase in indoor absolute humidity more than 12g/Kg' according to ASHRAE standards.

2.6.2 Temperature, humidity & absolute humidity for 3 days data (June 1st ~June 4th)

It is important to see the temperature pattern in details for indoor environments, three days were analyzed so that a clear pattern could be identified. It can be seen from figures (2-21, 22 & 23) that the differences in the indoor temperature profiles in the three cases depend on ventilation strategies and orientation. In case 1, when the outdoor temperature rose to more than 41°C in the daytime period the occupants tried to use air-conditioning in the master bedroom between 12pm~4pm and sometimes after the sunset. This helps to control indoor temperature to be within the 80% acceptable comfort range. Also, there was no large fluctuation in the living room. This is due to high internal gain stored in the building façade and increased by closing the windows most of the daytime. Also, the humidity ratio in the master bedroom was higher than outdoor and other zones.

In case 2, the indoor temperature profile in the living room, bedroom and master bedroom followed the outdoor profile. This is due to opening the windows and the internal door most of the daytime and nighttime. While in the living room the indoor temperature didn't completely follow the outdoor temperature pattern. This causes increase indoor temperature.

In case 3, there was no fluctuation either in the living room or the bedroom. This is because high thermal mass in this house affects indoor temperature. Also, the humidity ratio in the living room was higher than outdoor and bedroom.

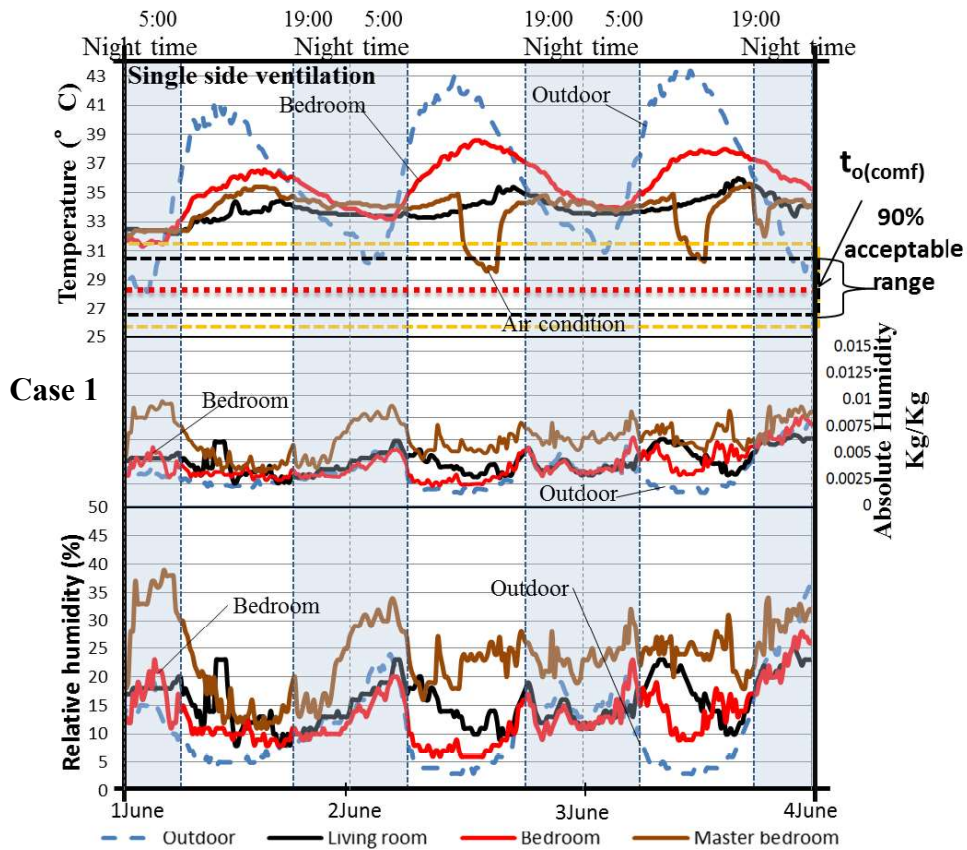


Figure (2-21): Temperature and humidity patterns for indoor environment from June 1st~June 4th in case 1.

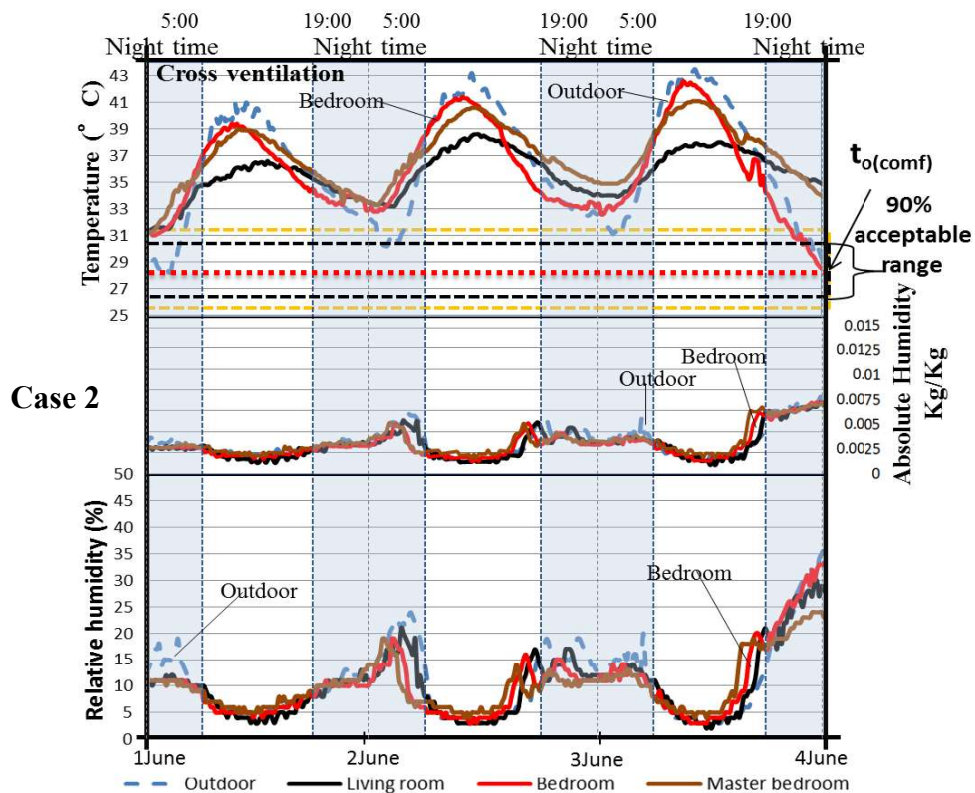


Figure (2-22): Temperature and humidity patterns for indoor environment from

June 1st~June 4th in case 2.

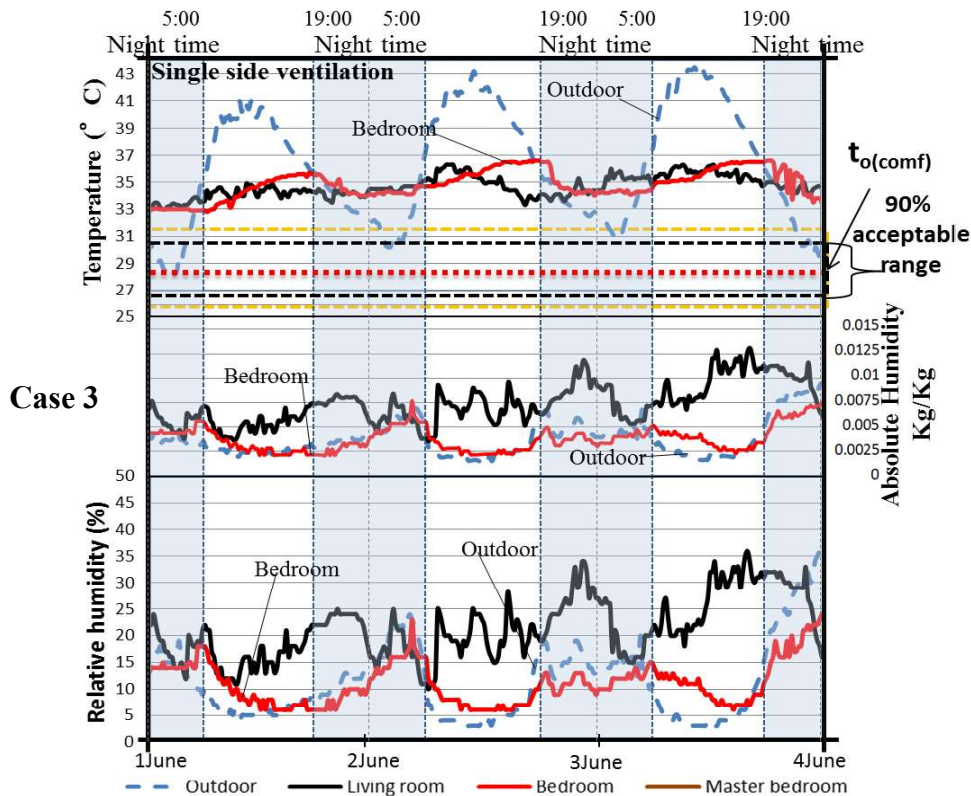


Figure (2-23): Temperature and humidity pattern for indoor environment from June 1st~June 4st in case 3.

2.6.3 Temperature & humidity distribution of 3 cases in June 2012.

Figures (2-24 & 25) show the temperature and humidity distribution during daytime and nighttime of June. It is concluded that;

Case 1: the maximum temperature ranges from 36°C to 39°C and the minimum temperature ranges from 30.5°C to 31.5°C with an average median equal 34°C during daytime and nighttime. However, the maximum relative humidity ranges from 44% to 49.5% with a minimum range of 6% to 10% with an average median equal to 21.5% during daytime and nighttime.

Case 2: the maximum temperature ranges from 38°C to 43°C and the minimum temperature ranges from 24.5°C to 31.2°C during daytime and nighttime with an average median equal 36°C during daytime and 34°C nighttime. However, the maximum relative humidity ranges from 47% to 64.5% with a minimum range

of 3% to 5% during daytime and nighttime with an average median equal to 10% during daytime and 16.5% during nighttime.

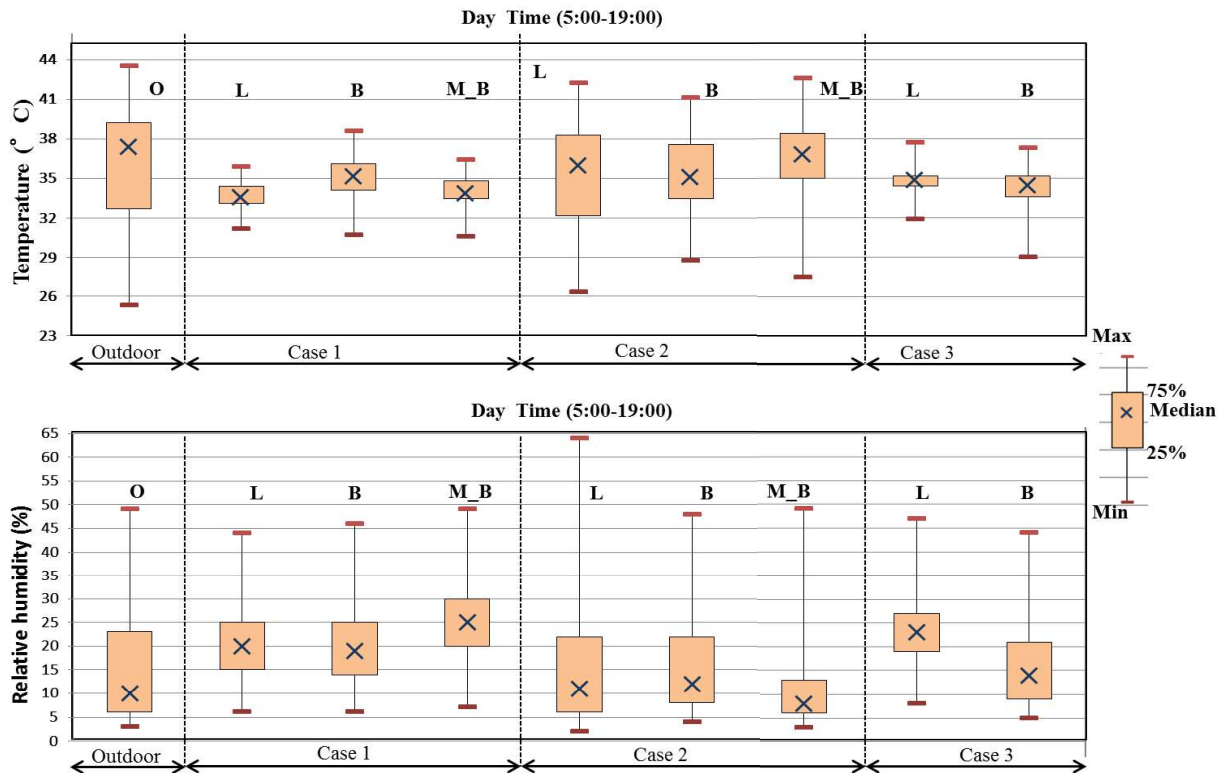


Figure (2-24): Temperature and humidity distribution during daytime for the three cases with outdoor condition for June 2012.

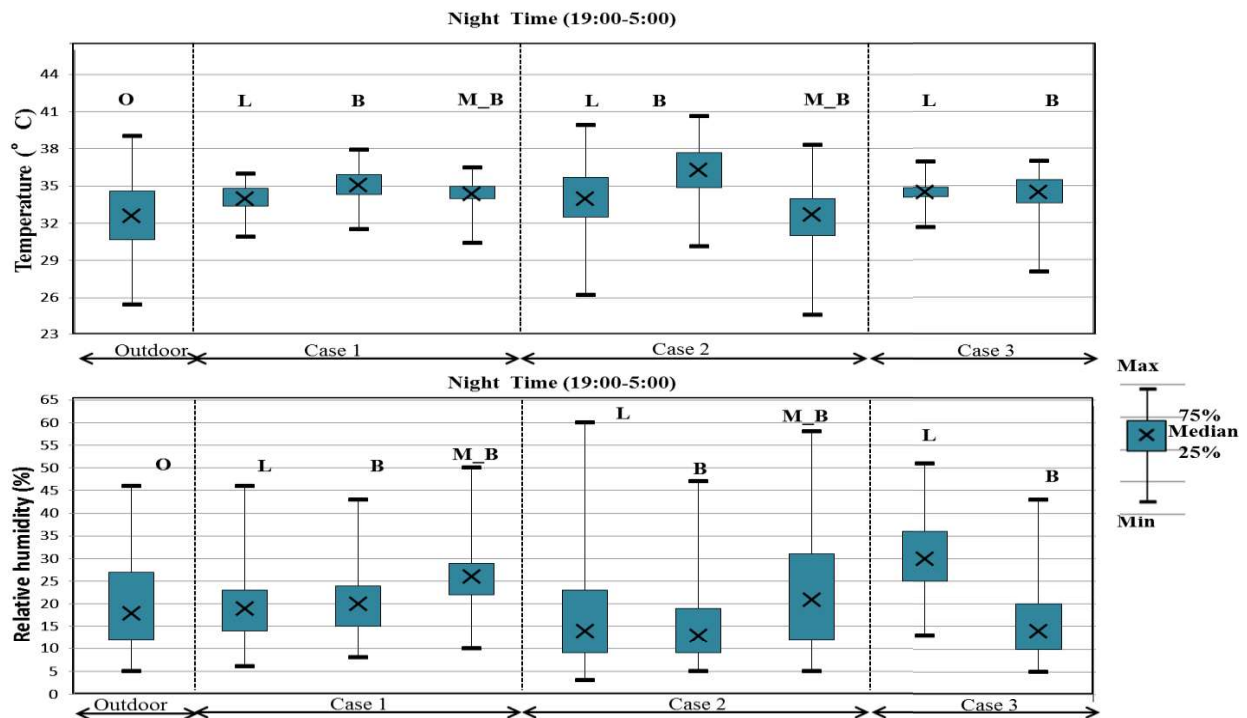


Figure (2-25): Temperature and humidity distribution during nighttime for the three cases with outdoor condition for June 2012.

three cases with outdoor condition for June 2012.

Case 3: the maximum temperature ranges from 37°C to 38°C and the minimum temperature ranges from 28°C to 32°C during daytime and nighttime with an average median equal to 34.5°C during daytime and nighttime. However, the maximum relative humidity ranges from 44% to 51% with a minimum range of 5% to 12.5% during daytime and nighttime with an average median equal to 18.5% during daytime and 22% during nighttime.

2.6.4 Evaluation of humidity environment according to ASHRAE 55, 2004 in June 2012

Figures (2-26, 27, 28 & 29) show the absolute humidity values for indoor environment in the three cases. In case 1, only 10% of the measured values exceeds the acceptable limit of the 12 g/kg' according to ASHRAE [24]. But most of the values were far from the comfort zone except when using air condition; the point becomes very near and starts to enter the comfort summer zone.

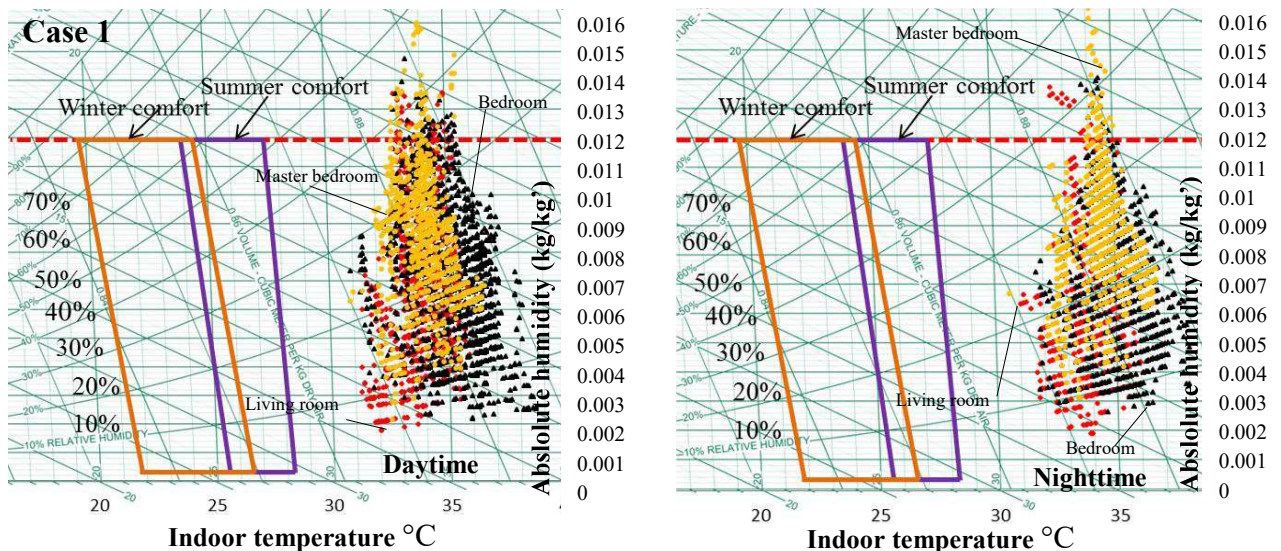


Figure (2-26): Temperature and humidity conditions in case 1 during daytime & nighttime.

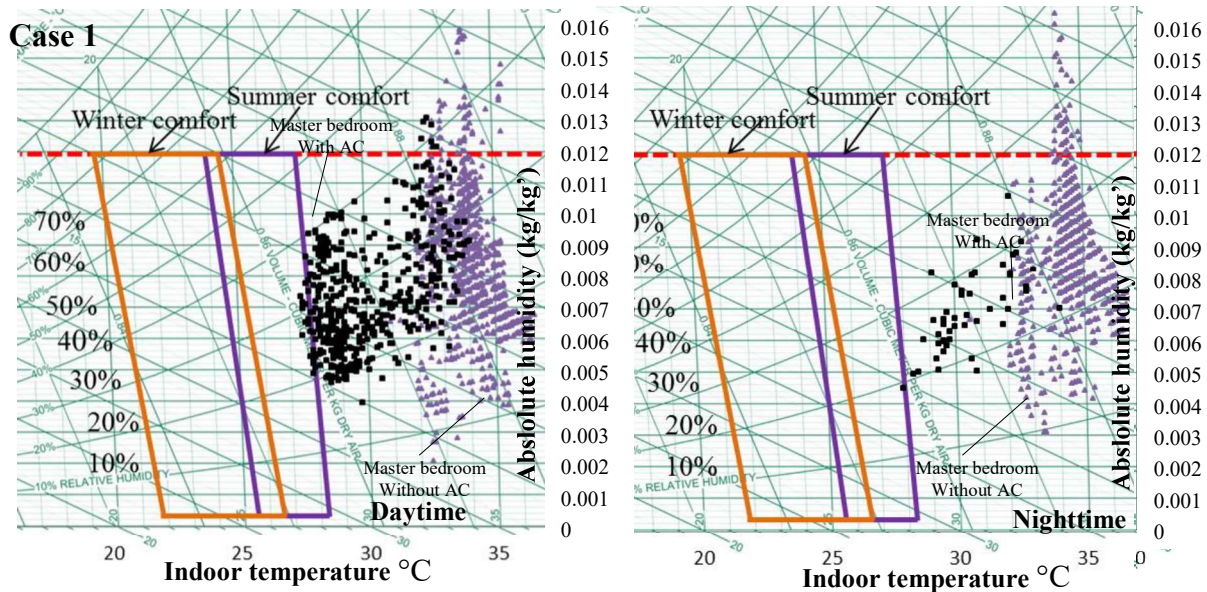


Figure (2-27): Temperature and humidity conditions in case 1 during daytime & nighttime with and without air conditioning.

While in case 2, there is a wide distribution for the measurement data. During nighttime, 3% of the values only enters the comfort zone which indicates discomfort with this type of ventilation. Also, only 8% of the measured values exceeds the acceptable limit of the 12 g/kg' according to ASHRAE [24]. However, in case 3; 20% of the humidity level in the living room exceeded the acceptable limit of 12g/kg' especially during nighttime. Also, all the measured values were far from the summer comfort zone.

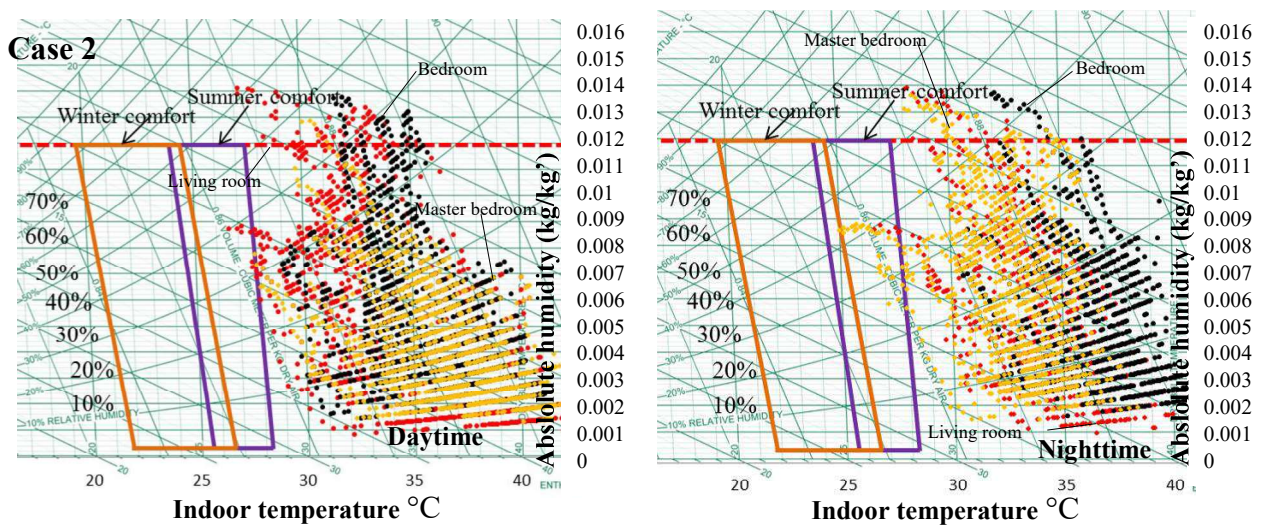


Figure (2-28): Temperature and humidity conditions in case 2 during daytime & nighttime.

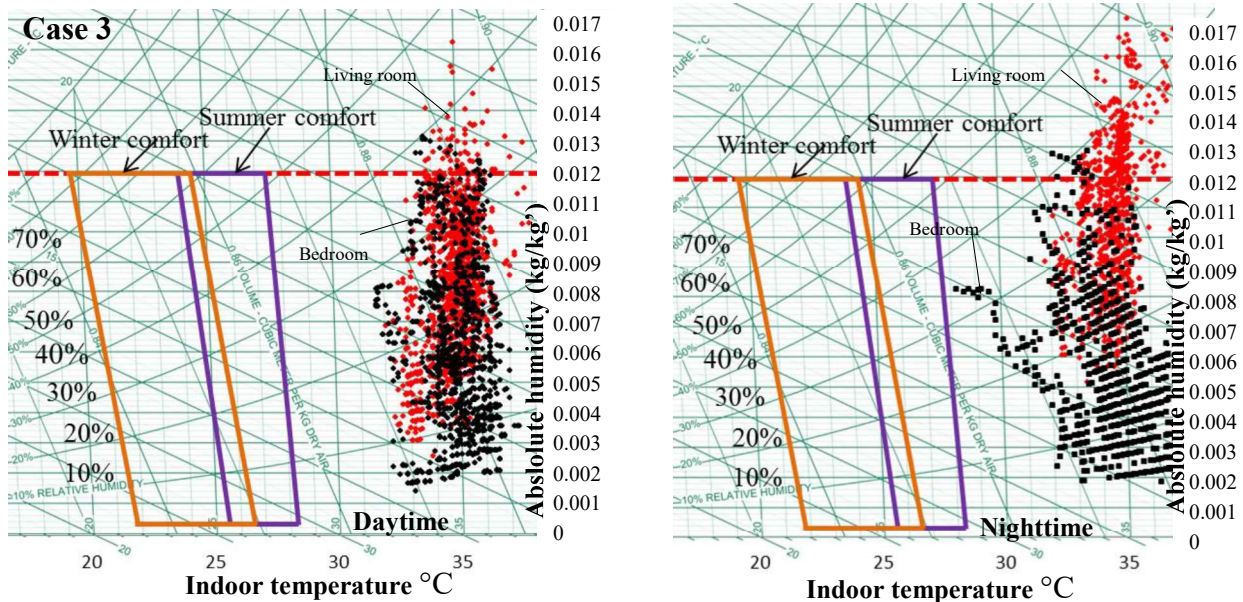


Figure (2-29): Temperature and humidity conditions in case 3 during daytime & nighttime.

2.6.5 The relationship between indoor and outdoor air temperatures (June 1st~June 4th, 2012)

Figure (2-30) shows the regression lines between daily outdoor temperature and indoor temperature in the three zones of different spaces during the period of June 1st~4th, 2012.

In case 1, the slopes of the regression line during the daytime and nighttime were very small with a correlation coefficient in the living room and master bedroom equal to 0.22 and 0.47 respectively in daytime, and 0.58 and 0.29 respectively in the nighttime. On the other hand, the correlation coefficient in the bedroom was 0.715 and 0.92; during daytime and nighttime, respectively. Therefore, it can be said that the indoor temperature of the living room and master bedroom was not influenced by outdoor air temperature.

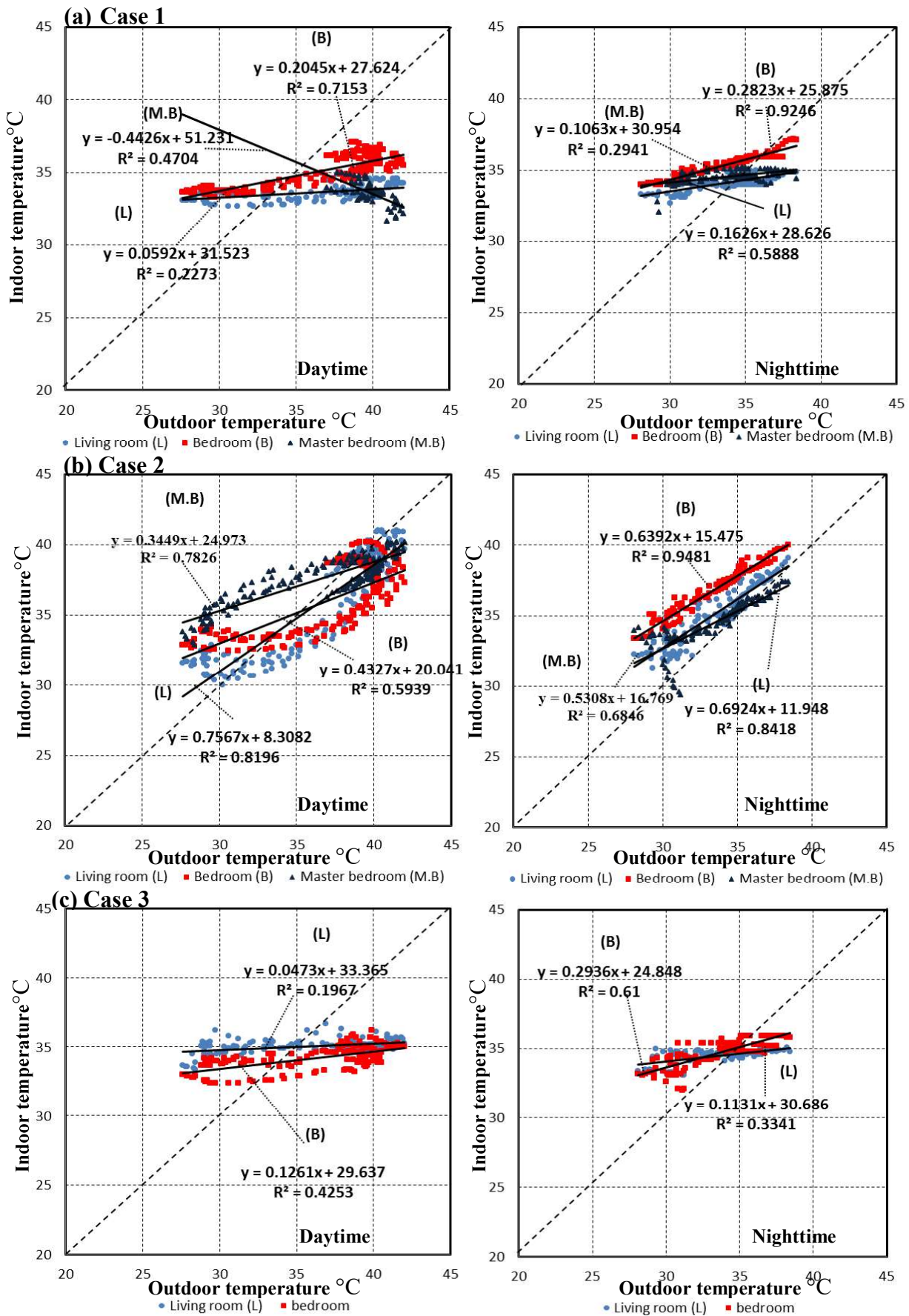


Figure (2-30): The regression lines between the daily outdoor temperature and

indoor temperature in the three different zones; living room, master bedroom, and bedroom June 2012; (a) the regression line in case 1, (b) the regression line in case 2, (c) the regression line in case 3.

On the contrary, the slope of the regression line in case 2 was relatively sharp with a high inclination in the living room, master bedroom and bedroom. The correlation coefficients in the living room, master bedroom and bedroom were high with values equal to 0.81, 0.78 & 0.59 during daytime and 0.84, 0.68 & 0.94 during nighttime, respectively. Therefore, outdoor air temperature greatly affects indoor air temperature of the living room, bedroom and master bedroom. In case 3, the slope of the regression line during the daytime and the nighttime was small especially in the living room with correlation coefficient 0.19 during daytime and 0.33 during nighttime.

Moreover, these graphs indicate that indoor houses in New Assiut city have indoor discomfort

2.7 Evaluation of July measurement

2.7.1 Temperature, humidity & absolute humidity profiles for one month measurements

Figures (2-31, 32 & 33) show the temperature and humidity patterns for indoor environment relative to the outdoor conditions in July. The maximum outdoor temperature was 43.7°C during the daytime with a low humidity level of 4%, and this is considered the hottest day (17July) in the measurement period. The minimum outdoor temperature was around 27.3°C with a humidity level of 40% on the 1st of July. While monitoring one month data for July, there was a great difference in the patterns of the three cases compared to the outdoors. The difference in ventilation strategies and building orientation influenced pattern strongly. When occupants used air conditioning, indoor temperature decreases to 26°C. This temperature falls within the 80% acceptable comfort range of ACS. While in the living room & the bedroom of case 1 & case 3, the indoor temperature had small fluctuation patterns. And, most of the measured values in

the living room & bedroom of cases 1 & 3 fall outside the Adaptive Comfort Standard of 80% acceptable range. On the contrary, the indoor temperature of case 2 nearly follows the pattern of outdoor temperature with a small difference of 1.5°C~3°C from the maximum outdoor temperature. However, a few hours at late night and early morning fell within in the comfort temperature zone of ACS, especially in the early and end of July. This happened as a direct effect of opening the windows during daytime and nighttime as shown in figure (2-32). Concerning the absolute humidity pattern, it increased in cases 1 & 3 especially in the living room due to practicing more activity. While in case 2, the indoor humidity pattern nearly follows the outdoor pattern, except during 16th, 17th July, and the second half of the month, when the humidity level significantly exceed that of the outdoors.

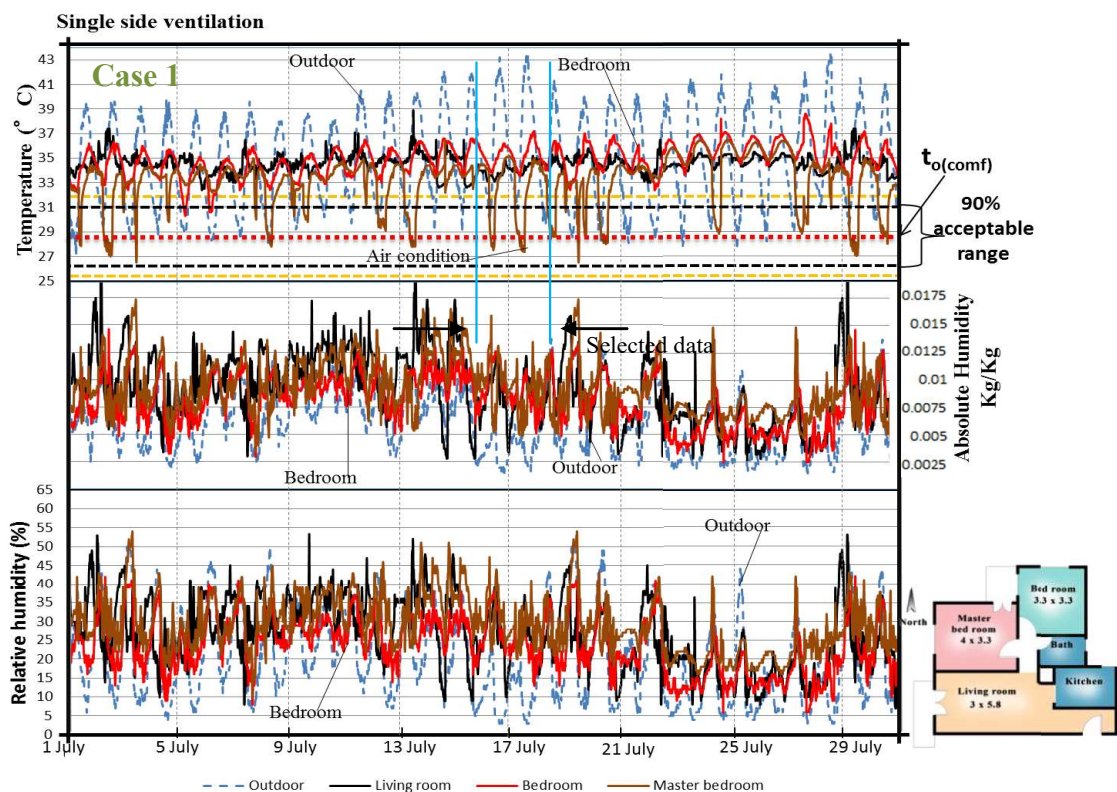


Figure (2-31): Temperature, humidity and absolute humidity patterns for indoor environment of July 2012 in case 1.

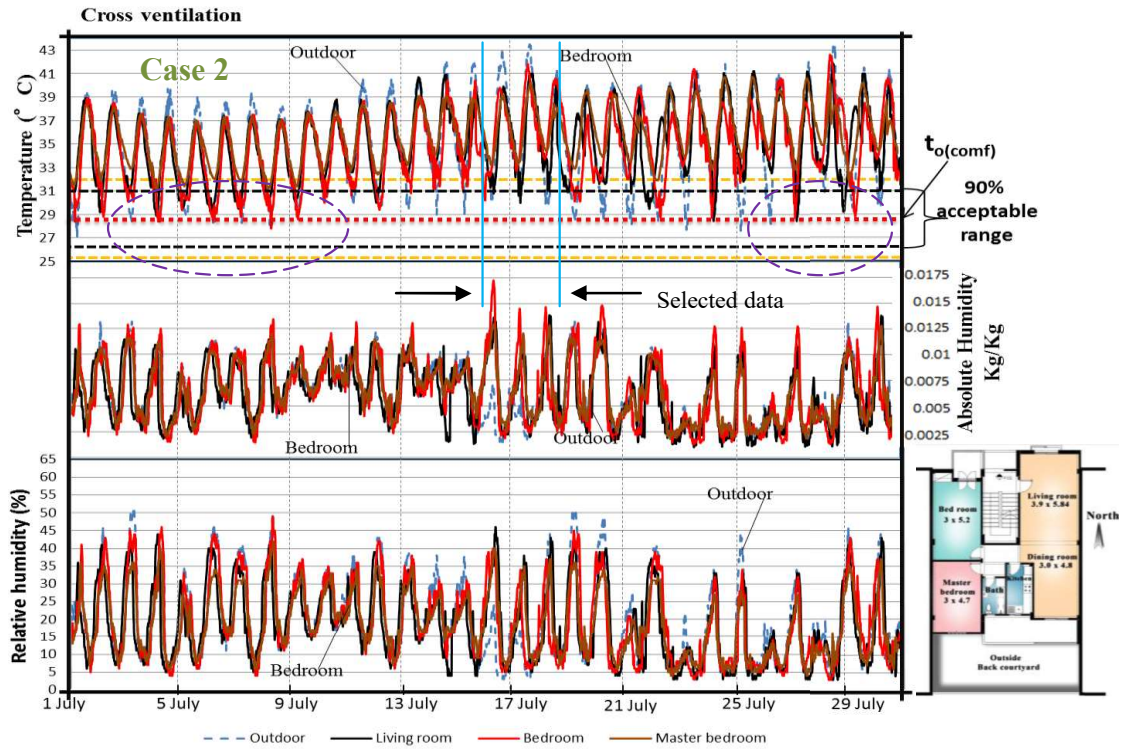


Figure (2-32): Temperature, humidity and absolute environment patterns for indoor environment of July 2012 in case 2.

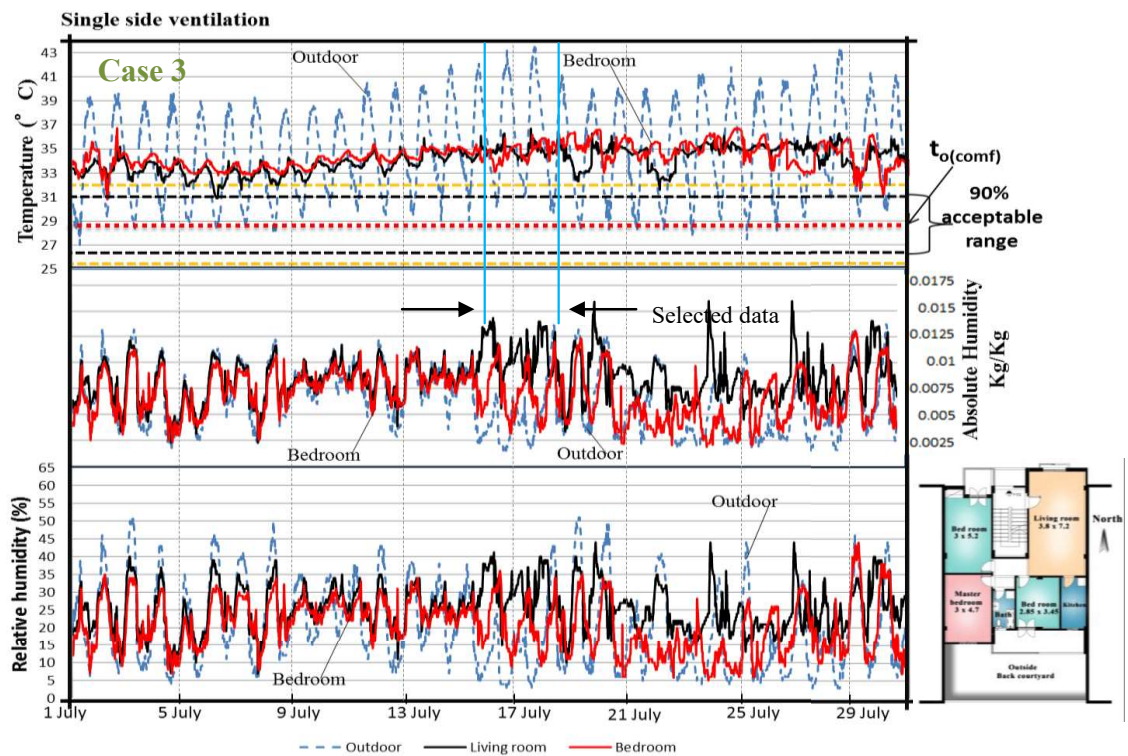


Figure (2-33): Temperature, humidity and absolute environment patterns for indoor environment of July 2012 in case 3.

2.7.2 Temperature, humidity & absolute humidity for 3 days data

Temperature and humidity profiles pattern for the three cases are shown in details for indoor environment for the selected data (July 16th~18th), figures (2-34, 35 & 36). It can be seen from the graphs that different ventilation strategies, single side and cross ventilation, have a significant effect on the occupants' thermal comfort. Case 1: there is a high heat gain in the three rooms; making an indoor temperature range from 33°C to 37°C, except when using the air conditioner. This is due to the orientation of the apartment to the west with high heat stored in the building facade. During daytime, occupants tend to close the windows due to higher outdoor temperatures and open them during the night to achieve single side ventilation. In terms of temperature, only air conditioner units in the master bedroom reduced and controlled the temperature to be within the 80% acceptable comfort range according to ACS. Based on this measurement, it was understood that the air conditioner was used at nighttime most probably from 10 pm until early morning in order to sleep comfortably in this period, as shown in figure (2-34).

Case 2: there is no air conditioner is installed in the house. Occupants use cross ventilation by opening the windows and doors of the rooms during the daytime and nighttime. This causes an increase in indoor temperatures during the daytime. The difference between the outdoor and indoor temperatures is 3°C during the daytime. But during the nighttime the temperatures are higher than the outdoor temperatures due to high thermal mass inside the house as shown in figure (2-35). Indoor environment in this house is far from the acceptable comfort range of ACS, except for some hours during nighttime.

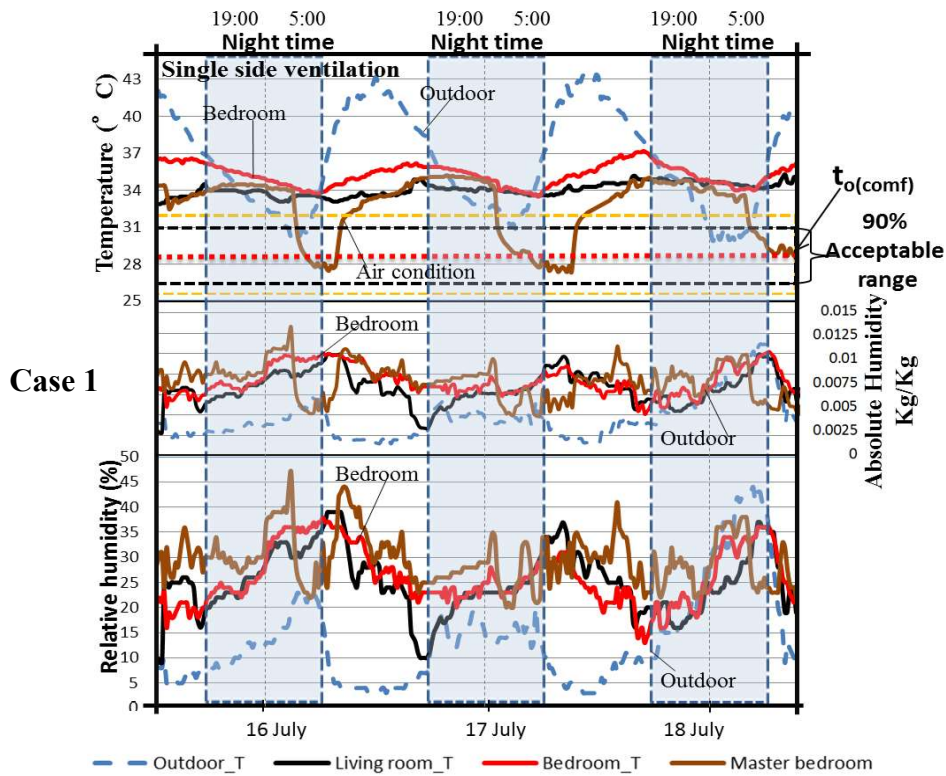


Figure (2-34): Temperature and humidity patterns for indoor environment on the hottest days of July 2012 in case 1.

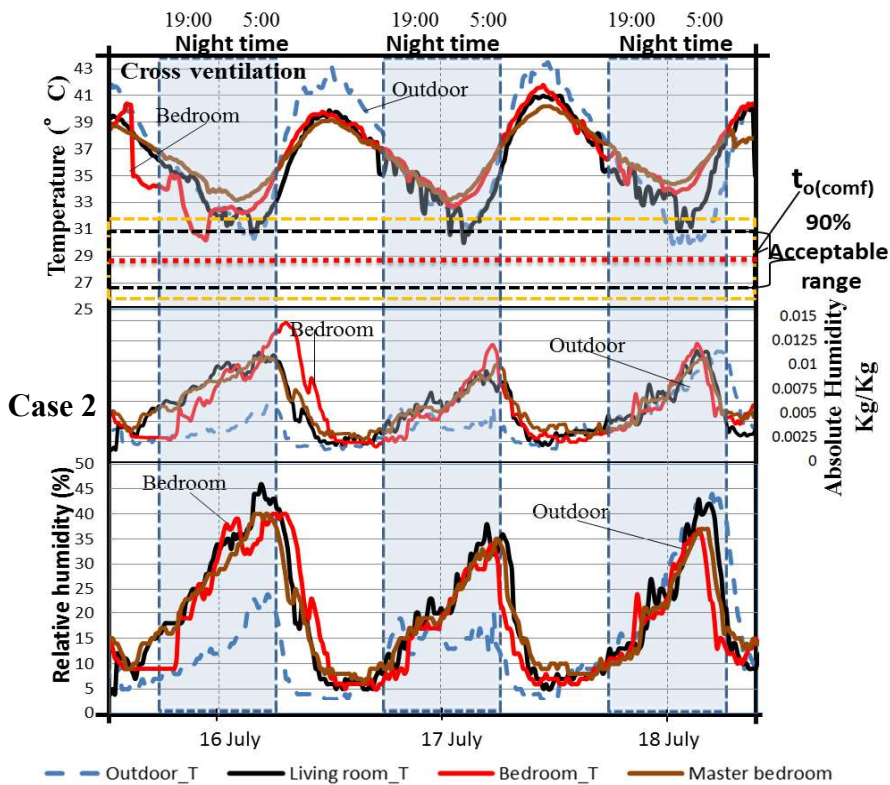


Figure (2-35): Temperature and humidity patterns for indoor environment in the hottest days of July 2012 in case 2.

Case 3: single side ventilation was used in this house without any cooling device (air conditioner). It can be seen that the temperature did not fluctuate; due to thermal mass. The measurement devices were placed in the top floor. Again, indoor temperature was quite far from the acceptable comfort range of ACS. Figure (2-37) shows the temperature and humidity patterns in July 16th~18th.

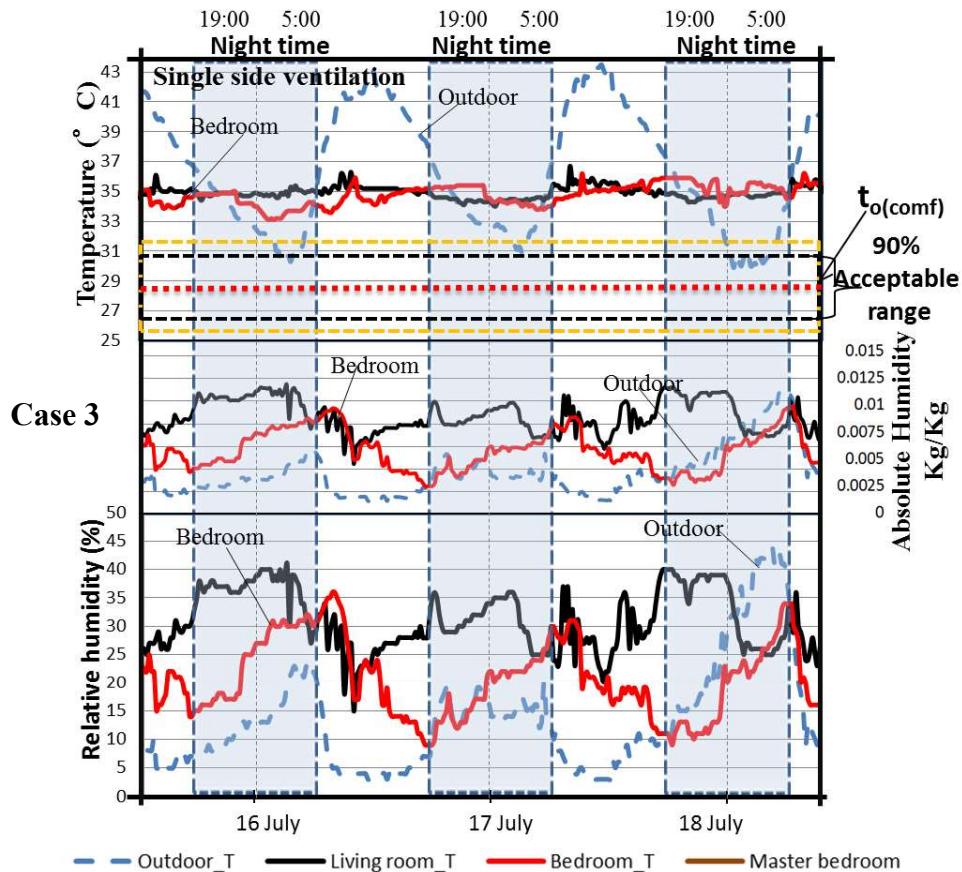


Figure (2-36): Temperature and humidity patterns for indoor environment from July 16th ~18th, 2012 in case 3.

In cases 1 & 3, the occupants tended to close the windows during the daytime due to high outdoor temperatures, and use mechanical fans which cause heat that was stored in the wall and the ceiling to circulate down. [Givoni](#) states that by increasing indoor air speed of internal fans this extends the indoor comfort range (comfort sensation), without elevating the indoor temperature [27].

As for the humidity level, there are huge fluctuations with higher humidity levels than outside. Concerning occupants' feeling, occupants of these houses

feel uncomfortable and very hot in the three cases except when using air conditioning (according to them).

2.7.3 Temperature & humidity distribution of the 3 cases

Figures (2-37 & 38) show the temperature & humidity distribution during daytime and nighttime for July. It is concluded that;

Case 1: the maximum indoor temperature ranges from 36.5°C to 39°C and the minimum temperature ranges from 29.5°C to 32.5°C with average median 34.5°C during daytime (5:00~19:00) and nighttime (19:00~5:00). But the difference between the maximum and the minimum relative humidity is slightly higher. The maximum relative humidity ranges from 41% to 54% and the minimum relative humidity ranges from 6% to 17% during daytime and nighttime with an average median 25% during daytime and 27% during nighttime.

Case 2: the maximum temperature ranges from 38.5°C to 43°C and the minimum temperature ranges from 28°C to 32°C during daytime and nighttime with an average median of 36°C during daytime & 34.5°C nighttime. The maximum relative humidity ranges from 35.5% to 49.5% during daytime and nighttime and the minimum relative humidity ranges from 3% to 6% with an average median of 14% during daytime and 20% during nighttime.

Case 3, the maximum temperature ranges from 36°C to 37°C and the minimum temperature ranges from 30.5°C to 31.5°C with an average median of 34°C during daytime and nighttime. The maximum relative humidity ranges from 40% to 44.5% and the minimum relative humidity ranges from 6% to 11% during daytime and nighttime with an average median of 24.5% during daytime and 25% during nighttime.

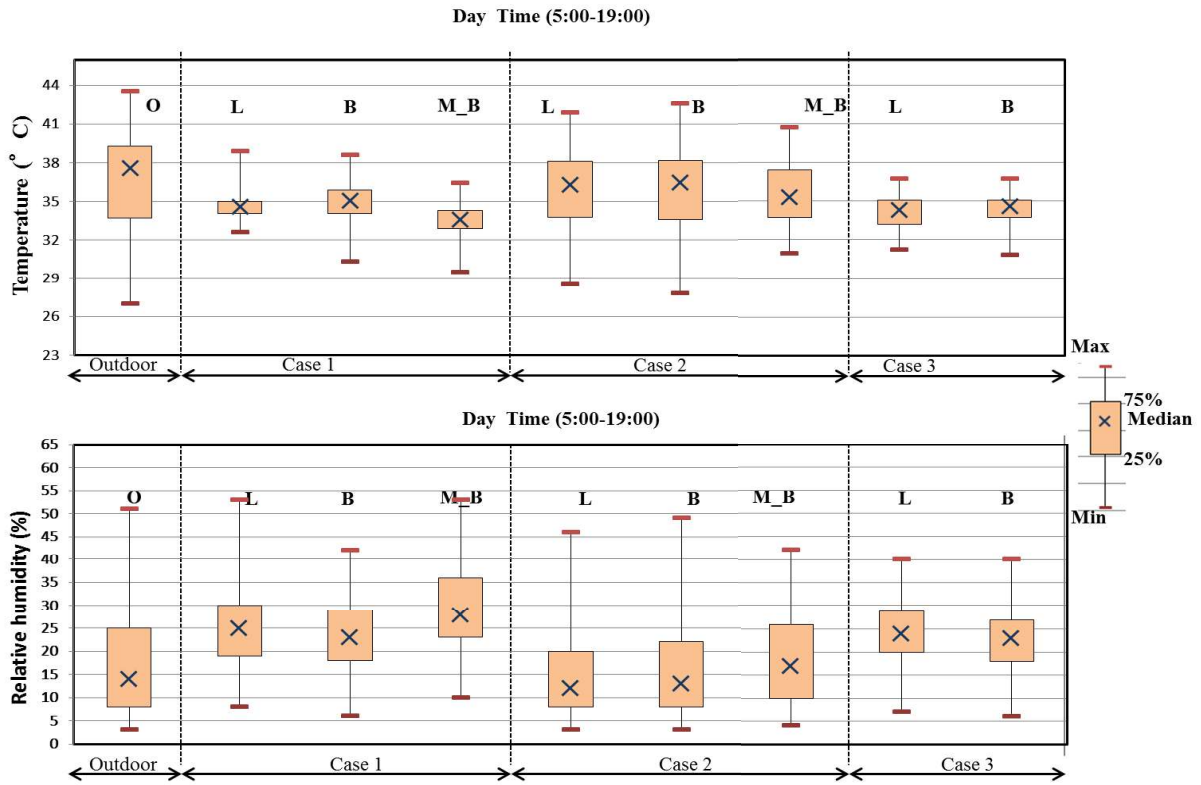


Figure (2-37): Temperature and humidity distribution during daytime for the three cases and outdoor condition for July 2012.

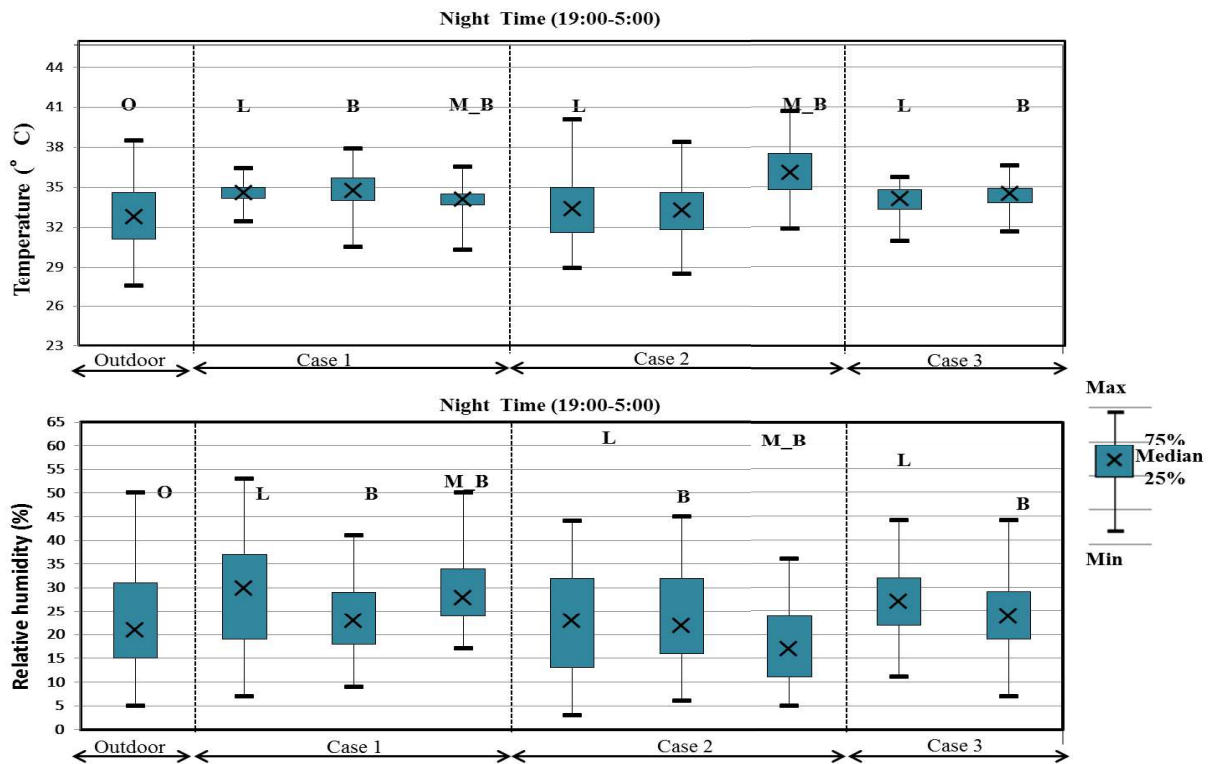


Figure (2-38): Temperature and humidity distribution during nighttime for the three cases and outdoor condition for July 2012.

2.7.4 Evaluation of humidity environment according to ASHRAE 55, 2004 in July 2012.

Figure (2-39, 40, 41 & 42) show the absolute humidity values for the three cases according to ASHRAE Psychrometric chart.

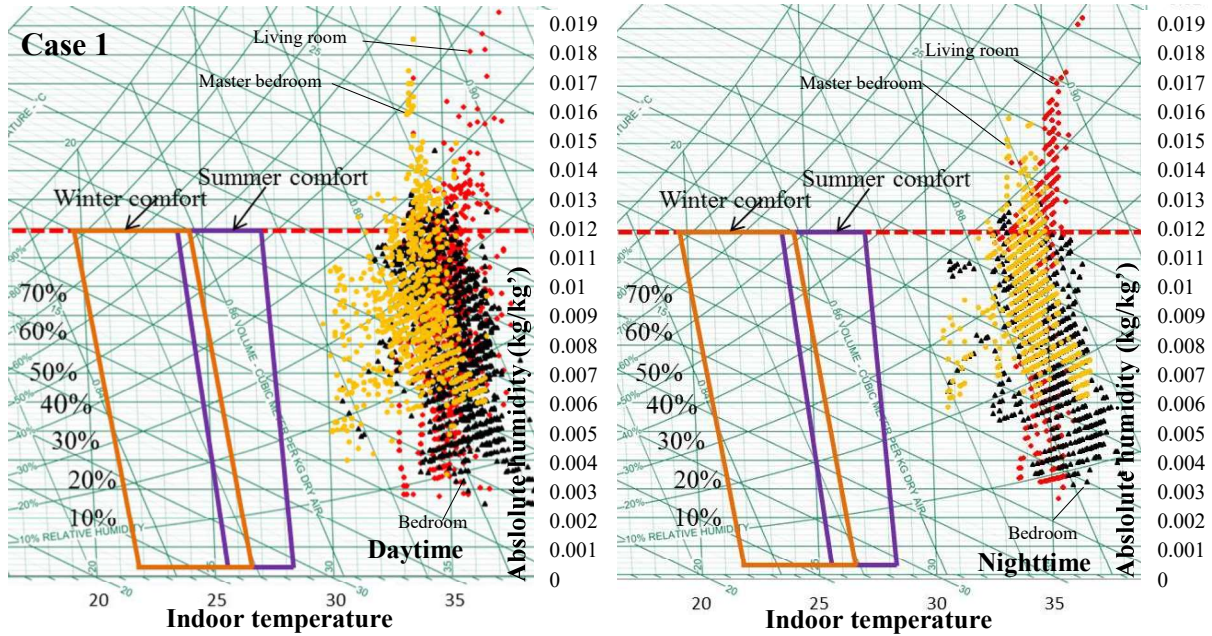


Figure (2-39): Temperature and humidity conditions in case 1 during daytime & nighttime of July, 2012.

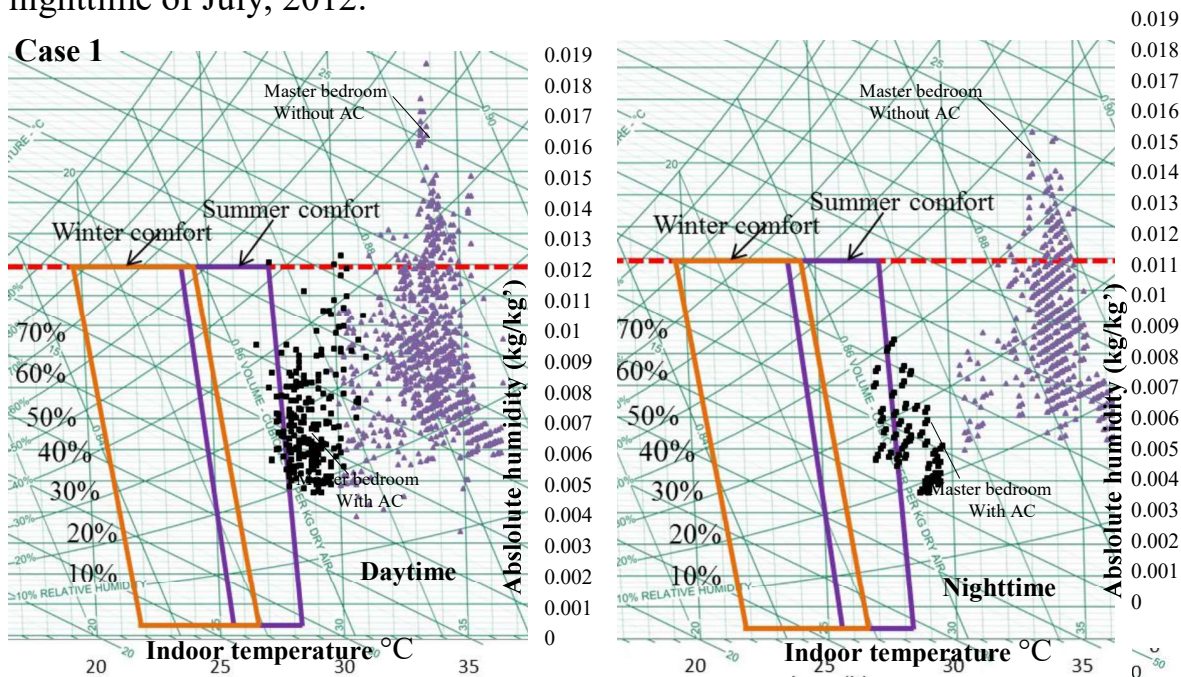


Figure (2-40): Temperature and humidity conditions in case 1 during daytime & nighttime with and without air condition (AC) of July, 2012.

It is clear that, the absolute humidity of the three cases of July located far from the summer comfort zone except for using air condition in the master bedroom of case 1.

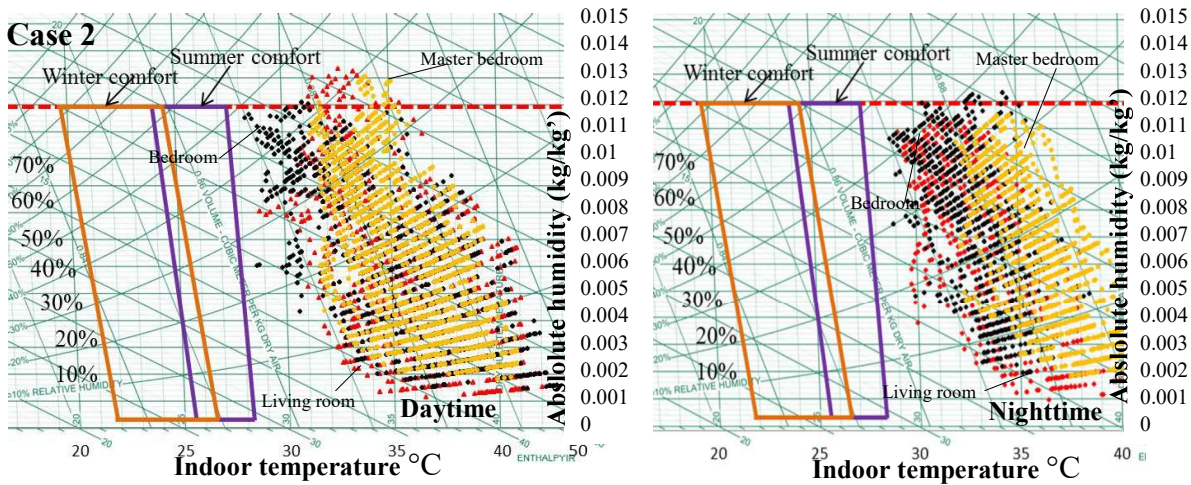


Figure (2-41): Temperature and humidity conditions in case 2 during daytime & nighttime of July, 2012.

In cases 1 & 3, the absolute humidity increased more than the acceptable humidity value of 12g/kg' during daytime and nighttime with a 20% increase in case 1 and 8% increase in case 3. It is clear that occupants used air condition during daytime before sunset more than nighttime due to high indoor temperature. However in case 2, there is a wide distribution of the measurement data with 5% only above the acceptable range 12g/kg' during daytime.

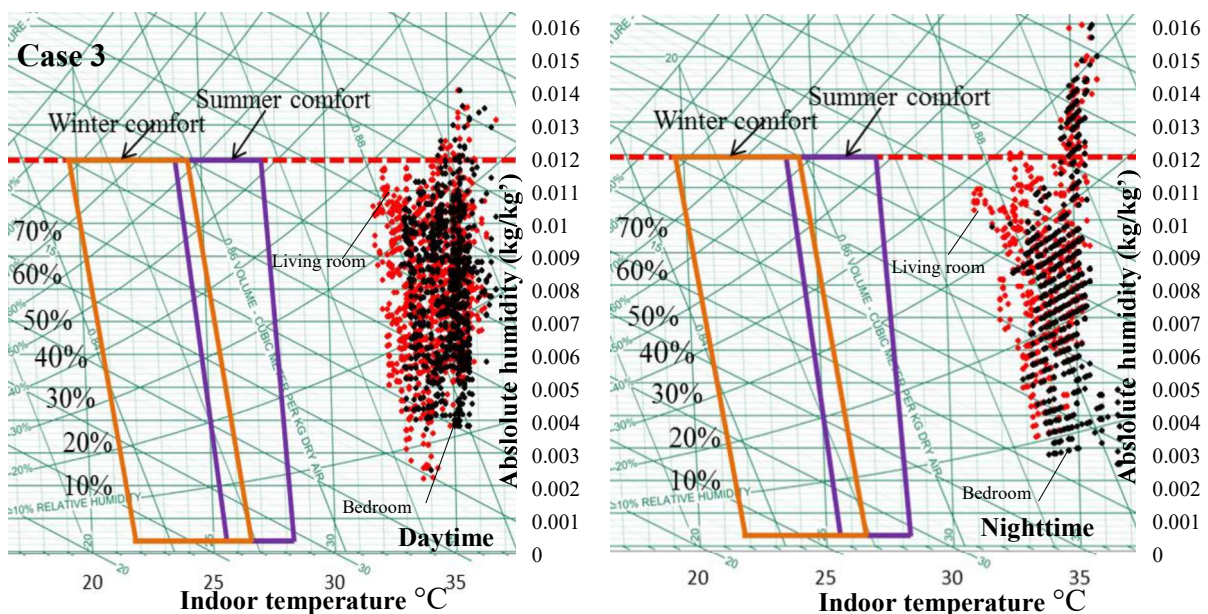


Figure (2-42): Temperature and humidity conditions in case 3 during daytime & nighttime of July, 2012.

nighttime of July, 2012.

2.7.5 Relationship between indoor and outdoor air temperature (16 July to 18 July, 2012)

Figure (2-43) shows the regression lines between daily outdoor temperature and indoor temperature in the three zones during the period of July 16th ~18th, 2012.

In case 1: the slope of the regression line during the daytime and nighttime for the living room and master bedroom are very small with small correlation coefficient (0.002 and 0.020) during daytime and (0.186 and 0.174) during nighttime respectively. This is because, in the living room and master bedroom the occupants closed the windows most of the day. While in the master bedroom the occupants tried to use air conditioning during some hours of the day. But, the correlation coefficient in the bedroom is high during daytime and nighttime with a high value of (0.83) during the nighttime. Therefore, it can be said that the indoor temperature of the living room and master bedroom is not influenced by outdoor air temperature.

On the contrary, the slope of the regression line in case 2 is relatively sharp in the living room, master bedroom and bedroom. The correlation coefficient of each space is greater in the order of the living room, master bedroom and bedroom during daytime with values of 0.85, 0.82 and 0.70 respectively during daytime and 0.81, 0.80 and 0.39 respectively during nighttime. Therefore, outdoor air temperature affects strongly indoor air temperature. This causes an increase in indoor temperature up to 42°C in the living room and bedroom during daytime.

In case 3: the slope of the regression line during the daytime and nighttime is small with a low correlation coefficient of 0.39 and 0.36 in the master bedroom and living room during daytime, and 0.002 and 0.04 during nighttime respectively. As a result of three cases, the outdoor air temperature affects strongly indoor air when using cross ventilation scenario (opening windows during daytime and nighttime), with high thermal mass.

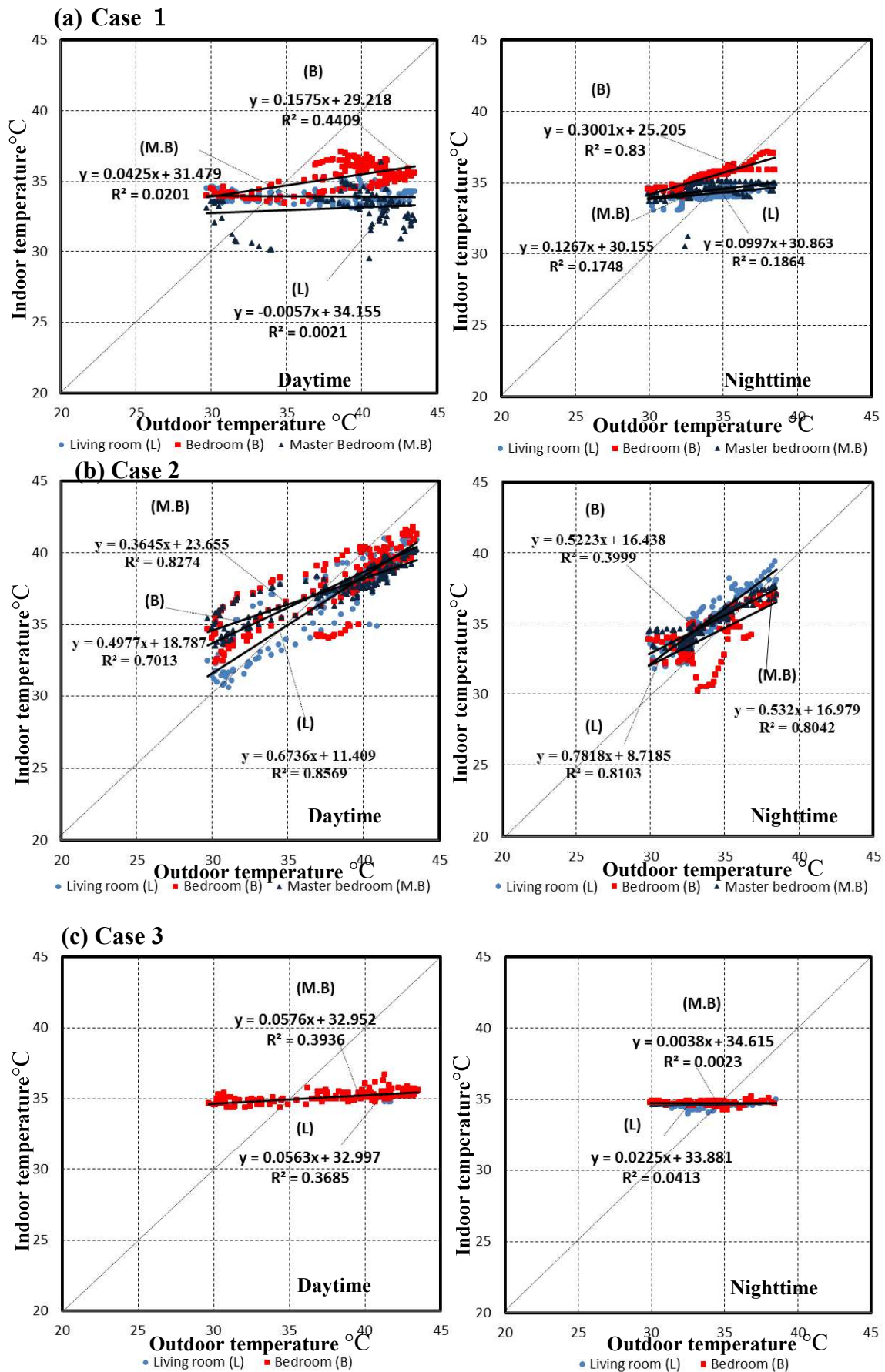


Figure (2-43): The regression line between the daily outdoor temperature and

indoor temperature in the three different zones; living room, master bedroom & bedroom from July 16th to July 18th, 2012; (a) the regression line in case 1, (b) the regression line in case 2, (c) the regression line in case 3.

2.8 Monitoring of indoor carbon dioxide concentration

Carbon dioxide is a normal constituent of exhaled breath. In recent years, more and more people have started to recognize the importance of the indoor air environment. CO₂ itself is not a pollutant at low concentrations. The main sources of indoor CO₂ are the exhalation of occupants, smoking and cooking. Therefore CO₂ can be a good indicator of bio-influence generated by human bodies. When the CO₂ concentration increases in room and become more than 1000 ppm¹, people will feel out of breath, headache and associated with increased prevalence of certain mucous membrane and lower respiratory sick building syndrome (SBS) symptoms with less indoor productivity. Carbon dioxide itself is not responsible for the complaints; however, a high level of carbon dioxide may indicate that other contaminants may also be present in the building at elevated levels and could be responsible for occupant complaints [28].

CO₂ can act as an indicator for ventilation efficiency, showing whether the supply of outside air is sufficient to dilute indoor air contaminants. Properly ventilated buildings should have carbon dioxide levels between 600 ppm and 1000 ppm [25, 26, 28]

Measuring of CO₂ concentration in the living room of the two cases of New Assiut city, helps to understand the effect of different type of ventilations scenario on carbon dioxide concentration in order to ensure indoor air quality (IAQ) and a safe living environment². IAQ is a comprehensive index, including room temperature, humidity, fresh air and a diverse range of low concentrations of air contaminants [29, 30].

¹The measurements of indoor airborne concentrations of substances.

²The same condition for case 1 and 2 is taken into account (for example; activity, cooking, average number of people, furniture, painting) in order to analyze ventilation efficiency only.

Figure (2-44) shows the CO₂ concentration in the living room of the two houses (cases 1 & 2) during June, 2012. It can be seen that in case 1, the concentration was very high all over the month except between June 21st to June 27th. This is because, occupants are outside the house in that period. There is no continuous ventilation in the living room of case 1. Thus, high CO₂ concentration reached 1780 ppm. But in the period between June 21st to 27th, the concentration appears to be in the steady state. On the contrary, the CO₂ concentrations didn't exceed 1000 ppm in case 2. This is because occupants tried to use the cross ventilation strategy during the daytime and nighttime, which affects indoor environments and dilutes CO₂ concentration.

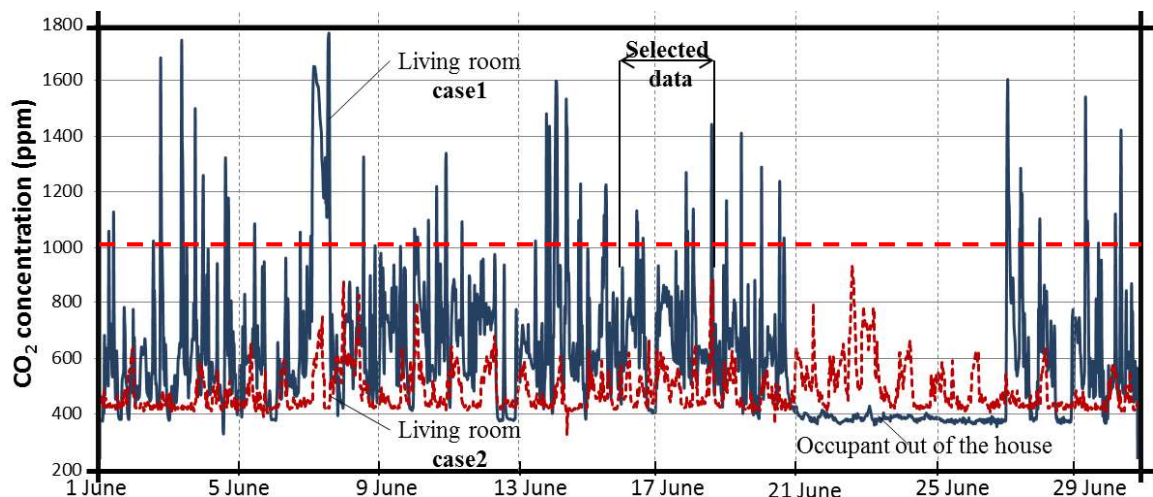


Figure (2-44): CO₂ concentration in the living room of cases 1 & 2 during June, 2012.

Figure (2-45) shows analysis of of CO₂ concentration for the selected data (June 16th~19th 2012). The maximum indoor CO₂ concentration was 1250 ppm to 1450 ppm in case 1, and from 600 ppm to 900 ppm in case 2. It can be seen during the daytime particularly in the morning, there was no increase in CO₂ concentration. This is because the few activities conducted in that period would not make the maximum concentration reach 800 ppm in case 1 and 450 ppm in case 2.

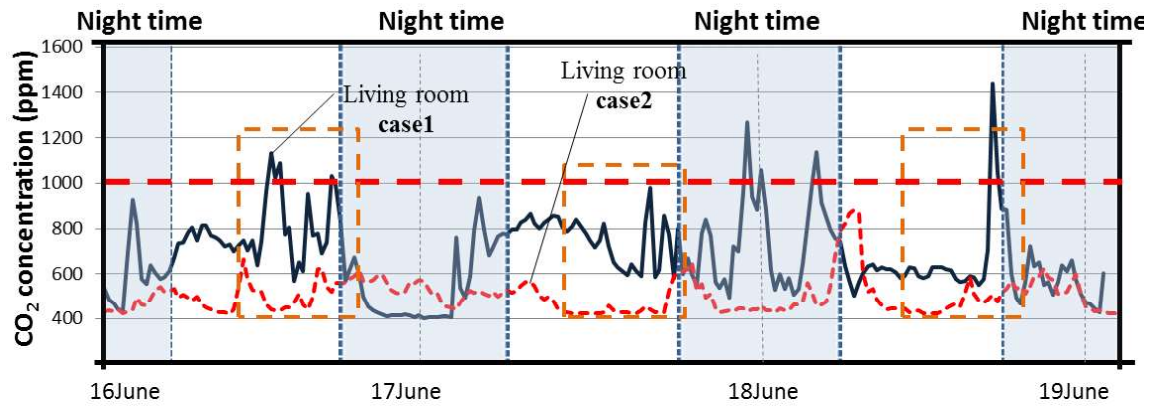


Figure (2-45): Three days measurements of CO₂ concentration in June, 2012.

Figure (2-46 & 47) show CO₂ concentration profile for indoor environment during July (16th~19th) and August (16th~19th), 2012. It is very interesting to see the increase of CO₂ concentration during the sun rise and sun set periods especially in case 1. This is due to the effect of different activities such as cooking.

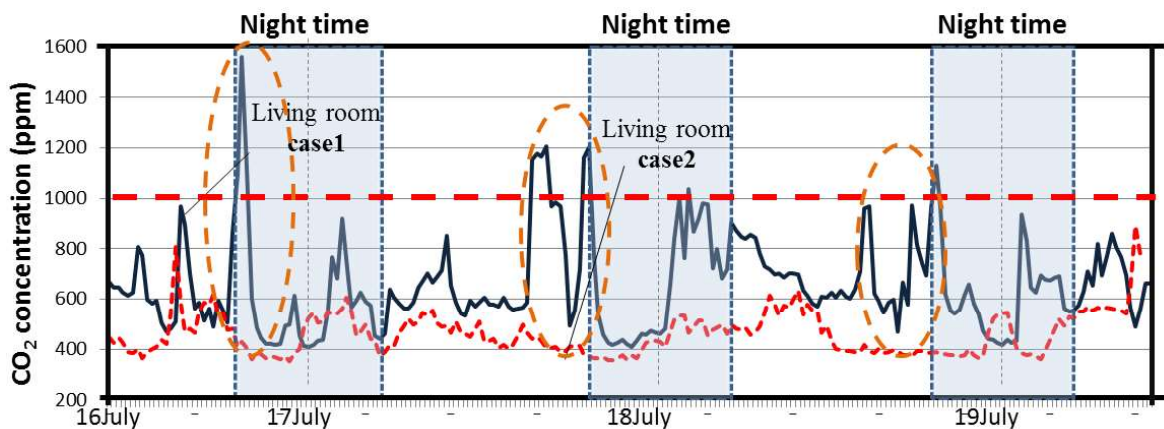


Figure (2-46): CO₂ concentration profiles for indoor environment during July 16th~19th, 2012.

Also, the occupants get together in month of the Muslim feast (Ramadan) and the maximum indoor concentration reaches 1600 ppm with outdoor concentration 380 ppm. This is due to closing the windows or sometimes opening the windows with single side ventilation only. On the contrary, in case 2, it can be observed that indoor concentrations are not so high with maximum

CO₂ concentration of 800 ppm. This is because, the occupants opened the windows during daytime and nighttime. Therefore, there was a continuous airflow from outdoor to indoor that resulted in low concentration and pollutants than case 1.

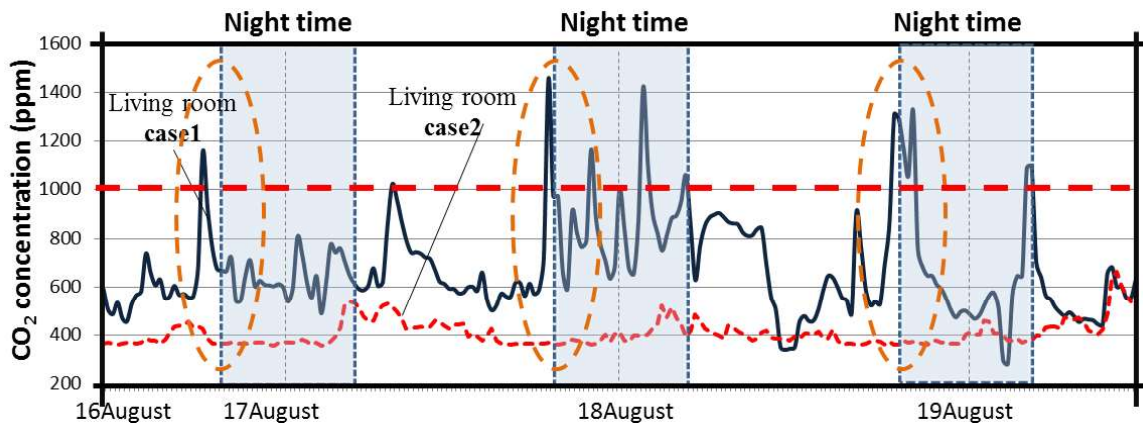


Figure (2-47): CO₂ concentration profiles for indoor environment during August 16th~19th, 2012.

By comparing the result with ASHRAE Standard “Ventilation for Acceptable Indoor Air Quality” [25, 26]. “Human occupants produce carbon dioxide, water vapor, particulates, biological aerosols, and other contaminants. Carbon dioxide concentration has been widely used as an indicator of indoor air quality. Comfort (odor) criteria are likely to be satisfied if the ventilation rate is set so that 1000 ppm CO₂ is not exceeded”. Therefore, case 1 is out of the comfort range. While in case 2, good indoor ventilation helps to achieve acceptable indoor air quality.

2.9 Research for the suitable strategy for climate of New Assiut city Assiut.

Based on the measurement conducted in the summer season (4 days of May, June & July), three important indices are studied to search for the suitable strategy for the climate of New Assiut city.

First index;

The bioclimatic chart is used to search for the suitable strategies that can be used for the buildings in that climate. This helps designers and architects to consider

climatic conditions when designing new buildings. A point of monthly average minimum outdoor temperature for one month with a monthly average maximum outdoor relative humidity is connected by a point with monthly average maximum temperature by minimum average outdoor relative humidity. The zones crossed by the lines plotted indicate the strategies that may be appropriate for that climate which helps to reduce the cost and energy consumption in such buildings [31]. Figure (2-48) shows the monthly average minimum and maximum points plotted for the three months of May, June & July, 2012 on the bioclimatic chart. This shows that the measurement data for the summer season of (May, June and July) fall within the boundaries of natural ventilation and evaporative cooling.

As a result, these strategies are suitable for indoor environments of buildings located in New Assiut city.

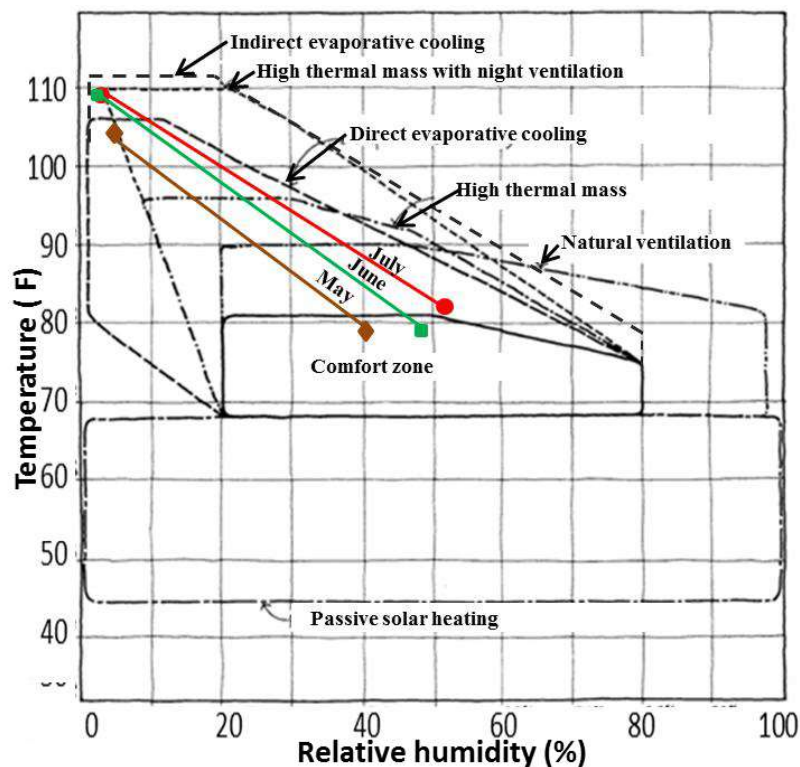


Figure (2-48): The bioclimatic chart for building design strategies with the measurement data for (May, June & July), 2012.

Second index;

Givoni suggested that direct evaporative cooling is advisable [32, 33] when the wet bulb temperature (WBT) in summer is not higher than 24°C and the dry bulb temperature (DBT) is not higher than 44°C in developing countries. Outdoor (WBT) is calculated based on outdoor (DBT) as shown in figure (2-49).

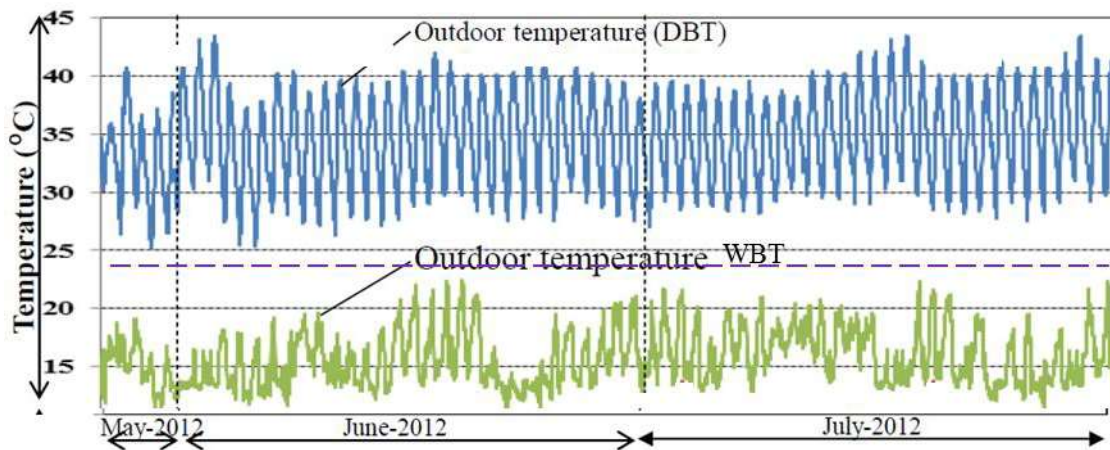


Figure (2-49): The outdoor DBT and WBT of the outdoor measurement data.

Third index;

Feasibility index (FI) is a method used to verify the viability of using evaporative cooling equipment for human thermal comfort and their application to several cities [34]. It is calculated based on this equation:

$$FI = T_{wb} - \Delta T$$

Where $\Delta T = (DBT - WBT)$ is the wet bulb depression. DBT and WBT are the dry bulb temperature and the wet bulb temperature of the outside air. According to evaporative air conditioning handbook [35, 36]. It is recommended that evaporative cooling is needed when the feasibility index is less than or equal to 10. Figure (2-50) shows the feasibility index pattern.

It is concluded from figure (2-50) that, 96.65% of the measured values fall located under 10 for the feasibility index. This indicates that evaporative cooling is needed.

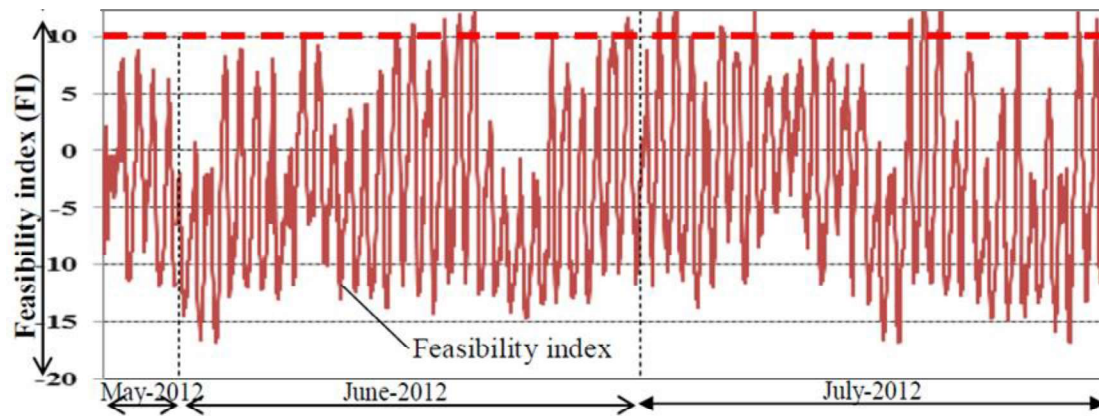


Figure (2-50): The feasibility index pattern based on the outdoor measurement data.

Conclusion

The most important outcome of this chapter is establishing an understanding the current situation of indoor environment concerning temperature, relative humidity & carbon dioxide concentration, in three houses in New Assiut city. Three ventilation strategies were studied in order to study the suitable strategy for that climate. The following are the key findings:

1. Using single side ventilation in cases one and three indicates; there was a small fluctuation in the temperature pattern, with high indoor temperature exceeding 38°C and high CO_2 concentration exceeding 1700ppm. As a result, discomfort occurs in these houses. The living room of the top floor indicates high internal heat gain with thermal mass
2. Using cross ventilation in case two; there was a high fluctuation in the temperature pattern with low CO_2 concentration (acceptable concentration of ASHRAE range 1000ppm [25, 26]). As a result, discomfort also occurs inside the house except during late hours at night.
3. Using air conditioning in the master bedroom of case one, causes the indoor temperature to be within the comfort range of ACS¹.

¹ The air condition is operating by users of this case during the hot hours of daytime and nighttime.

Therefore, the current situation indicated serious problems of discomfort in cases 1, 2 & 3; when using natural ventilation only. While, using cooling strategy (air condition) achieves the comfort range with high energy consumption. High internal heat gain occurs in the living room, where all the family member spend much time doing different activites.

Based on the three indices, the suitable strategy for that climate is natural ventilation with evaporative cooling strategies.

Finally, a new passive solution is needed to be studied using direct evaporative cooling and natural ventilation especially in the living room. In order to reduce the cost of building energy consumption, and achieve indoor thermal comfort & a high air flow rate (low CO₂) concentration; investigation of the suitable passive solutions that use natural ventilation with evaporative cooling strategy will be necessary.



Chapter 3

**Solutions and strategies for
indoor environmental problems**

Introduction

Indoor temperature is one of the most critical factors governing human comfort. Also, air movement plays a critical role in cooling down the body temperature in hot dry conditions. Therefore, understanding the related science of natural ventilation and evaporative cooling is crucial in order to increase occupants' satisfaction level in a space and make them thermally comfortable. Finally, the strategy and the technical levels of designing for natural ventilation and evaporative cooling are important to be studied with different passive techniques, in order to understand the limitations of the current system and search for a new system. In general, this chapter aims to understand the techniques for natural ventilation, evaporative cooling and search for new passive strategies based on the limitations of the conventional systems inside/outside Egypt.

3.1 The effect of traditional strategies for achieving indoor thermal comfort

Based on the results of three indices that discuss the suitable strategy for *hot dry* climate in chapter two, the mechanism of natural ventilation and evaporating cooling technique is needed to be studied;

3.1.1 Natural ventilation

Natural ventilation is one of the many passive design strategies that are considered when designing buildings in hot dry climates. It is very effective in maintaining acceptable internal thermal comfort in such climatic contexts especially when the building is oriented according to the prevailing winds [33, 37, 38, 39]. On the other hand, natural ventilation is expected to provide cooling and energy savings for indoor environment [40]. Therefore, it was emphasized that well designed natural ventilation systems can significantly reduce the energy consumption required for summer cooling [41].

Natural ventilation uses the natural forces of wind pressure and stack effect to aid and direct the movement of air through the building. So, when wind strikes a building it produce a positive pressure on the windward side and a relative negative pressure on the leeward side. This pressure difference, as well as the pressure difference inside the building, drives airflow [42]. As a result, the rate of natural ventilation varies according to the prevailing driving forces of wind and indoor/outdoor temperature difference [43].

a. Wind pressure;

When wind strikes a rectangular shaped building, it induces a positive pressure on the windward face and negative pressure on the opposing faces. This causes air to enter openings and pass through the building from the high pressure windward areas to low pressure downwind areas [43] as shown in figure (3-1).

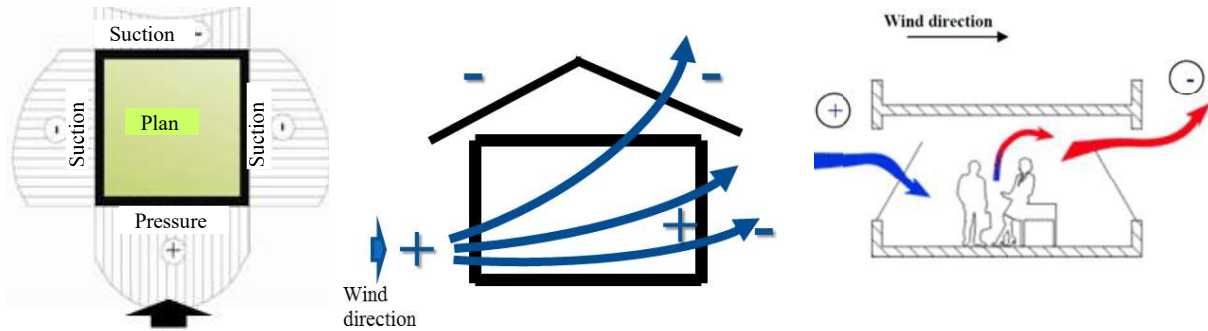


Figure (3-1): Schematic distribution of wind pressure around & inside a building exposed to perpendicular wind flow [43, 44].

Many factors can affect the pressure difference and consequently affect the magnitude of wind driven air movement through buildings. Among these factors are; the building geometry, the wind velocity, the wind direction, the building location in relation to its surroundings, the terrain context, the geographical location of the building and pressure coefficient on each façade of the building [43].

b. Stack effect (thermal buoyancy);

Stack effect is the difference in air temperature, and hence air density, between the inside and outside of the building. This produces an imbalance in the pressure gradients of the internal and external air masses which results in a vertical pressure difference. When the inside air temperature is greater than the outside air temperature, air enters through openings in the lower part of the building and escapes through openings at a higher level [43] as shown in figure (3-2).

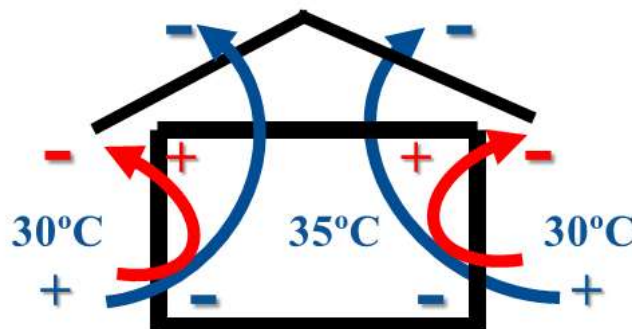


Figure (3-2): Natural driving mechanisms of stack pressure [43].

Also, the air flow due to thermal buoyancy occurs mainly in the vertical direction through air gaps within the building such as stairwells, elevators, atriums, and shafts [46]. Figure (3-3) shows the mechanism of the stack ventilation in a single room and inside an atrium. It is clear that air moves towards the upper part of the atrium and the room according to the temperature difference.

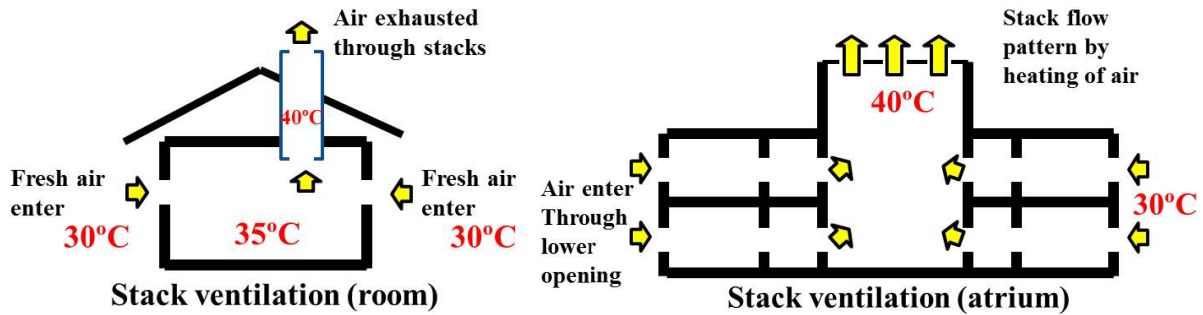


Figure (3-3): The mechanism of stack ventilation in a room & an atrium [43].

In most cases, the airflow through any building is the result of a combination of both wind pressure and stack effect [44].

Finally, an old traditional architecture in Egypt depended on natural ventilation (wind pressure and thermal buoyancy) to achieve comfort for users especially in old houses, mosques, pedestrian passes and compact forms. For example, in Cbshiry house, natural ventilation of "Ewan" depended on the existence of opposite windows and ventilation to achieve comfort. In this house, a large window in the first zone faces the northwest corner of the courtyard wall and faces the preferable wind. Meanwhile, small windows in the second zone, in its opposite direction, allow air to exit from "Ewan".

3.1.2 Evaporative cooling

Evaporative cooling is a physical phenomenon in which evaporation of a liquid, typically into the surrounding air as a result of latent heat¹, results in reducing air temperature and cools an object in contact with it as a result of sensible heat².

¹ **Latent heat** is the amount of heat that is needed to evaporate the liquid without a change in temperature (Change of state from water to vapor).

² **Sensible heat** is heat exchanged by a body or thermodynamic system that causes a change in temperature (the effect is only to raise or lower temperature).

When water evaporates into the air, its dry bulb temperature (DBT) is decreased and its water content is increased along a constant wet bulb temperature (WBT); the wet-bulb temperature compared to the air's dry-bulb temperature is a measure of the potential for evaporative cooling. The greater the difference between the two temperatures (DBT & WBT), the greater the evaporative cooling effect is [32, 47].

The appearance of evaporative cooling occurred at around 2500 B.C., during which the ancient Egyptians made use of water in a porous clay jar for the purpose of air cooling. This mechanism was applied in ancient Egyptian buildings and further spread across the Middle East regions where the climates are always in hot and arid state. Numerous strategies, similar to porous water pots, water ponds and pools, were integrated into the building construction in order to create the buildings' cooling effects [48].

There are many applications to lower indoor temperatures by passive evaporative cooling systems; two important methods [49] are direct and indirect evaporative cooling:-

Direct evaporative cooling; the temperature is reduced by increasing the humidity of the air.

Indirect evaporative cooling; the primary cooling is derived from evaporation but the building is cooled indirectly, without elevating the indoor humidity (lower air temperature without adding moisture into the air).

The most effective way for hot dry climate, such as that of Egypt, is direct evaporative cooling [32, 33, 47]. Figure (3-4) shows the mechanism of direct evaporative cooling psychrometrically with constant wet bulb temperature, where the decreasing in cooling temperature depends on the type of the wet medium used.

A: Entering air properties

$$T_{DB} = 43.3^{\circ}\text{C}$$

$$T_{WB} = 22.2^{\circ}\text{C}$$

B: Leaving air

$$T_{DB} = 25.6^{\circ}\text{C}$$

$$T_{WB} = 22.2^{\circ}\text{C}$$

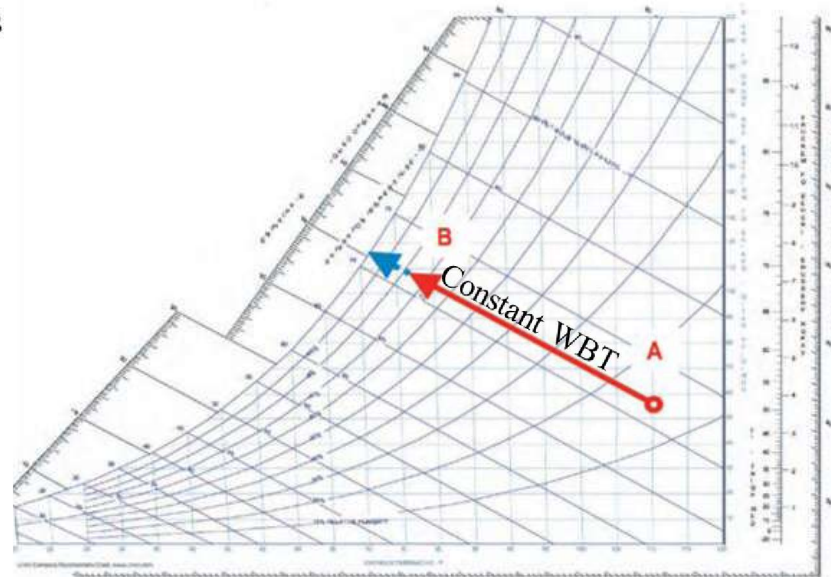


Figure (3-4): Direct evaporative cooling process shown psychrometrically [47].

Also it was concluded that one of the most common, and effective, applications of natural ventilation with evaporative cooling in old conventional Egyptian housing is a wind tower (Malqaf or wind catcher) [14, 16, 50].

3.1.3 Wind tower

Wind tower is a single duct to facilitate the supply and extraction of air. Their application in the hot arid regions of the middle east provides natural ventilation, passive cooling and hence thermal comfort, exploiting, particularly the night-time ventilation strategy [51, 52]. However, wind tower are also useful in reducing dust as the wind captured at a level carries less dust [38]. The primary attraction of wind towers is that they are passive strategy requiring no energy to operate. They work on the principles of natural ventilation, employing both wind driven and stack effect ventilation [42]. Numerous traditional houses in old Cairo, Egypt, used wind towers. The cooling capabilities depend on providing sufficient airflow and speed through proper design of the wind catcher. Also, it helps to provide good indoor conditions by passing the dry air through pottery jar filled with water, so indoor temperature decreased [53]. Several examples of using Malqaf in a traditional Egyptian building like Bayt al Suhaymi and Cbshiry houses provided a comfortable indoor environment [14].

Architect Hassan Fathy suggested wetted baffles which can help reduce the air temperature by evaporation of water inside the old wind tower. He also mentioned that baffles can reduce air flow which can be overcome by increasing the size of the Malqaf and suspending the wetted medium in its interior [53]. Figure (3-5) shows the wind tower designed by Architect Hassan Fathy.

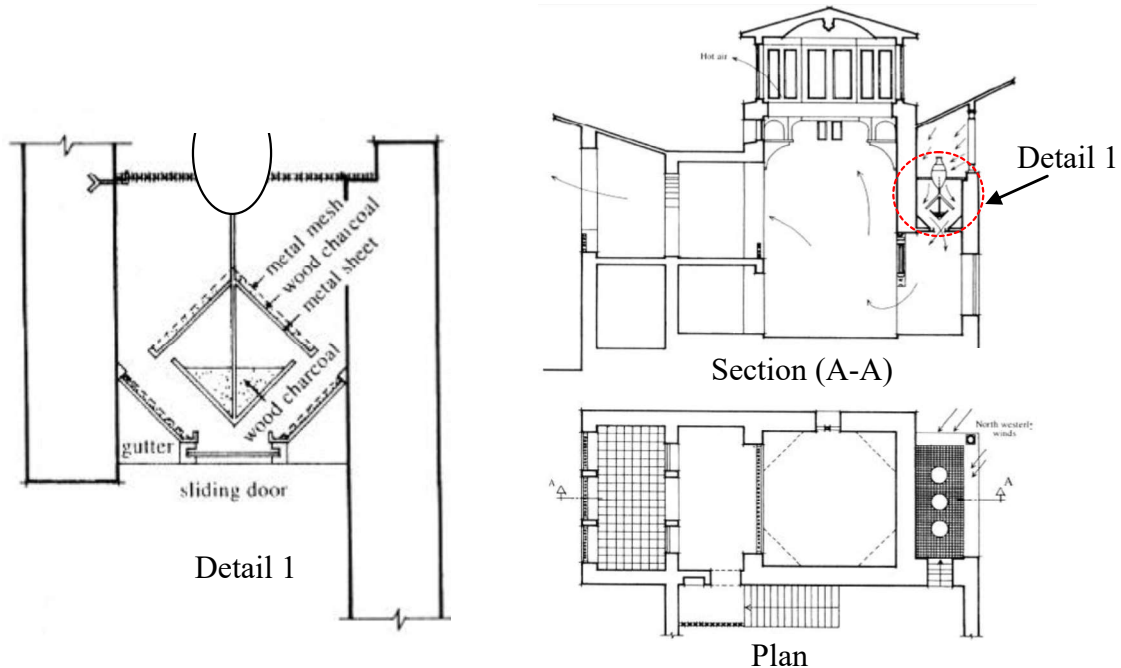


Figure (3-5): Wind tower with wetted baffles, design by Hassan Fathy [53].

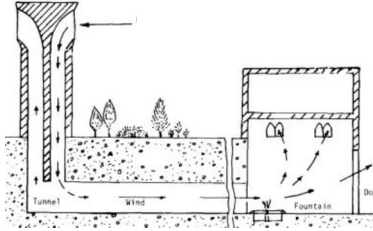
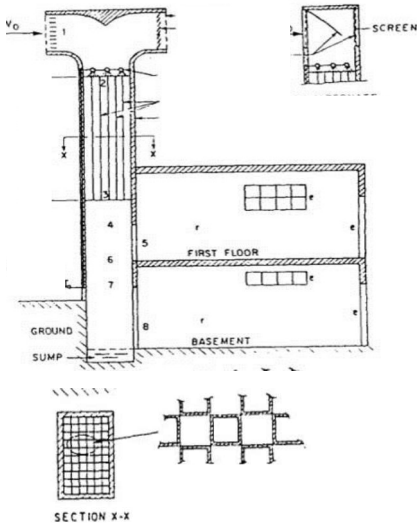
3.2 Search for solutions & strategies for providing thermal comfort

Many papers have been published on building and climate relationships, and studies to find passive cooling strategies for buildings in the hot dry climate country using natural ventilation. The first research solution is a wind tower concept.

3.2.1 Wind tower concept for providing thermal comfort

Many ideas and developing ways were applied for wind tower to increase its performance [16, 54, 55]. Important researches that studied this concept are shown in table (3-1).

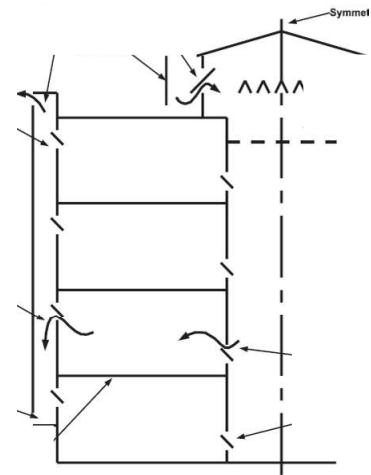
Table (3-1): Important researches that studied the wind tower concept.

No.	Research description	
1	<p>Wind towers acting as evaporative coolers are found in the Ancient Egyptian and Persian architectures. The old Egyptian tower had water pots in the lower parts of the tower [16].</p> <p>Result: The tower becomes more effective for indoor cooling. But, it has many problems like allowing dust, insects and small bird. Also, some of the air enters the tower normally lost through another opening that doesn't face the wind. This affects the pressure difference of the system.</p>	<p>Place: Egypt</p>
2	<p>Wind tower is studied with evaporative cooling pads placed at the tower entrance. Evaporative cooling surfaces are wetted manually or automatically, where a medium made from clay was proposed inside the wind tower for thermal energy storage that can be wetted uniformly by spraying (or pouring) water over them at the top of the column [17, 56].</p> <p>Result: Higher airflow rates with high evaporative cooling capability are achieved at nighttime in the summer. It helps to cool the building mass to a lower temperature. The decrease in temperature reaches 10°C lower than outdoor, when the outer temperature=35°C & wind speed=5m/s.</p>	

Place: Iran

- 3 An atrium located in the middle of the office building was used as a passive downdraught evaporative cooling PDEC to cool the rooms beside the atrium [57].

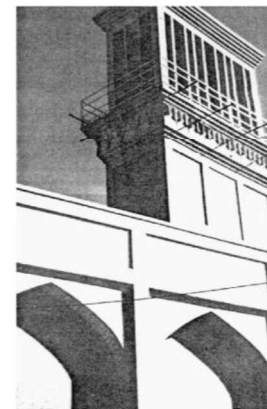
Result: Water is injected in the head of the atrium through wet medium. These droplets evaporate and the cold dense air descends into the capture zone. The dense air falls to the occupied spaces (rooms) to cool them. The temperature of indoor inside the room decreases by $10^{\circ}\text{C}\sim 12^{\circ}\text{C}$ less than the outdoor temperature.



Place: Spain

- 4 Measurement is conducted for high wind tower (11.7m) divided into three columns (one with wetted column consisting of wetted curtains hung in the tower column; the second one with wetted surfaces, consisting of wetted evaporative cooling pads mounted at its entrance, the last one is an empty column) [58].

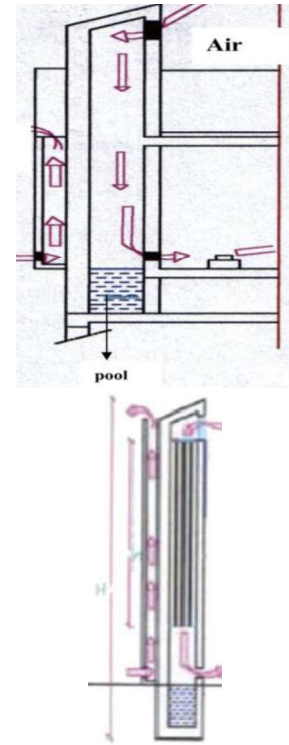
Result: It was found that the wind tower with wetted column performs better with high wind speeds whereas the tower with wetted surfaces performs better with low wind speeds. The temperature decrease to 19.2°C with $\text{RH}=73\%$ when the outside temperature= 34.2°C & $\text{RH}=10.7\%$ with wetted column & temperature decrease to 21.5°C and $\text{RH}=68\%$ with wetted surface.



Place: Iran

- 5 Thermal performance of wind tower with a wet medium made of brick with partition inside it and a pond down the tower is studied. [59].

Result: Indoor temperature decreased to 18.6°C with relative humidity 62.6%, when the outside temperature was 42.7°C and relative humidity was 14.1%. Indoor air temperature can be reduced by improving the two determinant factors of the wind tower: a higher height of a wetted column (h) and a smaller size of the conduits partition inside the tower by increasing the number of openings in the tower.



Place: Algeria

Therefore;

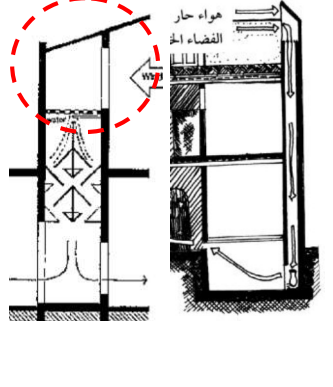
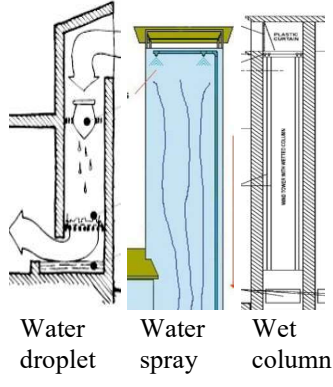
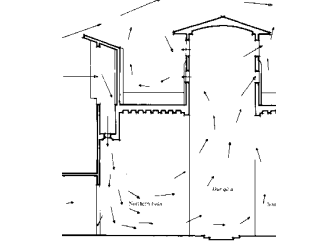
- Integration of wind catcher with different evaporating cooling strategies (wet medium, water spray, water droplet & wet column) could help decreasing indoor temperature.

Finally, the wind tower is an effective strategy for decreasing indoor temperature. But still there are some limitations for the conventional wind tower.

Limitations for the conventional wind tower.

There are some limitations of the conventional design that make it difficult to apply for any existing or new buildings regarding the design, evaporative cooling and air speed. Table (3-2) shows these limitations.

Table (3-2): The limitations for the conventional wind tower.

Items	Description	Figure
Design	<ul style="list-style-type: none"> • <u>It needs special design particularly for the upper part.</u> • It needs to be high enough to capture air from the upper layer of air. The height depends on the surrounding buildings. 	
Evaporative cooling	<ul style="list-style-type: none"> • <u>It consumed a lot of water particularly when using water droplet, water spray or wet column.</u> • It causes a significant reduction in indoor temperature (more cooling) with high humidity. 	
Air speed	<ul style="list-style-type: none"> • <u>It is not effective with low wind speed.</u> • It must be oriented to the preferable wind. 	

**Therefore, more techniques should to be studied;

- To move air continuously inside the tower without depending on wind speed or making it high with big structure.
- To consume less water consumption.
- Produce compact (small) designs easy to apply to the existing and new buildings.

As a result, a passive technique is needed to move air without depending on the wind or any mechanical means. Therefore, the concept of the solar chimney is needed to be studied.

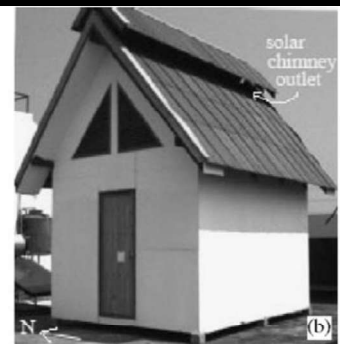
3.2.2 The solar chimney concept for providing thermal comfort

Solar chimney is a system that generates air movement by thermal buoyancy forces, in which hot air rises and exits from the chimney, drawing air through the building in a continuous cycle. This system relies upon heating part of the building fabric (material) by solar irradiation resulting in a greater temperature difference and, hence, larger air flow rates [60, 61, 62].

Egypt in general has rich sunny and clear skies [1]. Therefore, these conditions encourage to enhance solar chimney as a concept and save energy [63]. Many previous studies investigated the use of the solar chimney concept for improving room natural ventilation, which allows the amount of solar energy to be stored in its surface, then releases this energy to an adjacent column of air that raises as the temperature increases inside the chimney, and accordingly flows upward drawing air from the adjacent space [60, 62, 64, 65, 66]. Table (3-3) shows the important researches that studied the solar chimney concept for indoor thermal comfort.

Table (3-3): Important researches that studied the solar chimney concept.

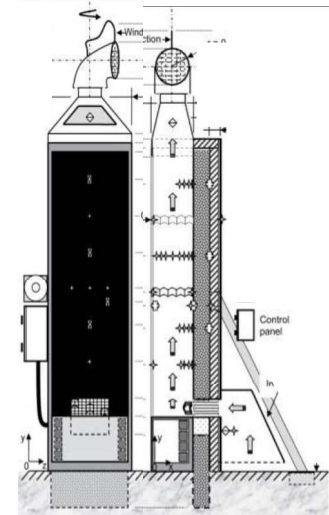
No.	Research description
1	<p>The effect of the solar chimney and/or water spraying over a roof on natural ventilation is experimentally studied [67].</p> <p>Result: When the ambient temperature was 40°C, they achieved a maximum of 3.5°C reduction in temperature was achieved for solar chimney only, and a maximum of 6.2°C reduction in temperature for the combined effect of solar and water spraying. This happened during high solar radiation.</p>



Place: Thailand

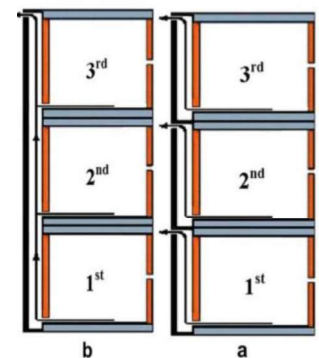
- 2 The thermal performance of a solar chimney under daylight and nighttime conditions is studied. A 4.5m high, 1.0m wide and 0.15m thick reinforced concrete wall was used as a solar absorber, whose southern surface was painted matt black with insulation on the side and back surfaces. The outer cover of the chimney is made of glass of 0.004m thickness [68].

Result: a high flow rate of 374m³/h occurred with solar intensity of 604W/m². The air flow rate through a solar chimney system is greatly affected by the pressure difference between openings caused by heat stored in the black absorber and by wind velocity.



Place: Spain

- 3 The use of solar chimney (SC) in the façade of high-rise building is investigated. Two small scale models of a three storey building were built. Solar chimneys were integrated into the south-faced walls of one unit. Two design configurations were considered. The first is a tall SC with an inlet opening at each floor and one outlet opening on the third floor (model b). While the second, an inlet and outlet openings were installed on each floor (model a). [69].



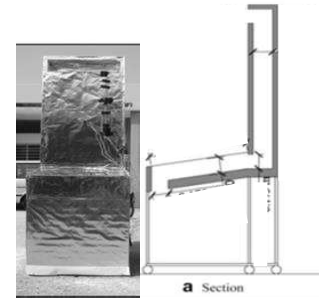
Place: Thailand

Result: First, room temperature of the model (a) was lower than the room temperature of the model b, depending on the floor level by up to 5°C.

Second, the best configuration is shown for temperature difference between the room and ambient. It was concluded that multi-storey solar

chimney could be an alternative for mechanical ventilation in high rise building in order to save energy with comfortable environment.

- 4 A combination of roof solar collector and a vertical stack is studied. The purpose of the roof solar collector was to capture as much solar radiation as possible, thus maximizing the air temperature inside the channel of the collector [61].



Results: This model creates a temperature difference of up to 9.9°C in semi- clear sky with solar radiation 877W/m² and 6.2°C in overcast sky condition with a solar radiation of 552W/m².

Place: Malaysia

Therefore;

- It is concluded that solar chimney can be used as an aid to promote stack effect ventilation in times or places of low wind speed [70].
- Solar chimney doubled the percentage of efficiency for improving the quality of life and reducing energy consumption [62].

But still there are some limitations to using solar chimney only for achieving indoor thermal comfort.

Limitations of the solar chimney concept.

Heat gain is still inside the room by using a solar chimney only. This is because, it helps to enter outside air without cooling it.

In order to achieve the desired natural cooling effect, it is very important to combine the solar chimneys with other passive cooling strategy [71].

As a result, integration of the solar chimney with the cooling wind tower is needed to achieve indoor cooling with continuous high flow rates (without depending on wind speed).

3.2.3 Integration of the solar chimney with an evaporative cooling concept for providing thermal comfort

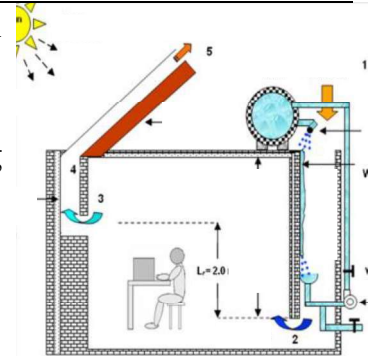
Several previous studies investigated the integration of the two systems for improving indoor environment [70, 72, 73]. Table (3-4) shows the important researches that studies this concept.

Table (3-4): Important researches that studied the integration concept.

No.	Research description	
1	<p><u>Big & high</u> wind tower coupled with multi solar chimney is studied. The system consisted of a uniform cross sectioned wind tower (without evaporative cooling) which connects to the rooms to be ventilated with natural ventilation, where the tower area is 2m^2 [74].</p> <p>Result: The system provides ventilation for variable wind speeds with a collector area of 3.0m^2. The wind tower is able to cool outdoor air by a 5°C reduction in temperature with 35 air change rates (ACH). Therefore, the system acts as a very good ventilation system.</p>	
	Place: India	
<p>2 Short <u>vertical chimney</u> made from steel integrated with <u>big & high cooling wind tower</u> and attached to a room of 93m^2 floor area made from wood. The chimney is located outside the room with a small opening located at the top of the room. The tower dimensions are $(1.8\text{m} \times 1.8\text{m})$ and 7.6m tall. [33, 49, 75].</p>		Place: Arizona-USA

Result: The result was analyzed by Givoni, 1994. The system was very effective, when the outdoor temperature was 40.6°C and the WBT was 21.6°C. The tower exit air temperature was 23.9°C. The corresponding speed of the exit air at that time was 0.75m/s.

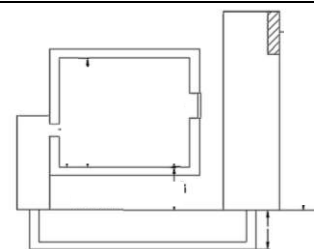
- 3 An inclined solar chimney, together with a small evaporative cooling cavity, is studied. The numerical study is done using falling water film without existing of occupants in the room [50].



Place: Iran

Result: When the ambient air temperature becomes 34°C at a solar radiation of 1000W/m² and relative humidity 40%, the resulting indoor temperature decreases to 26.26°C with high relative humidity 85.57%. The researchers suggested that a combination of the proposed system would help create a reasonable indoor environment for human thermal comfort, as well as being energy efficient and environmentally friendly.

- 4 A model of solar chimney and wind induced earth-cooling air tunnel (EAT) for both natural and hybrid ventilation systems, at the design stage, is developed. It focuses on the simulated performances and their impact on the comfort of occupants for the summer period [76].



Place: Australia

Result: The exit temperature from the EAT was below 26°C for the whole period; which shows its potential for precooling the outside air and providing passive cooling, when the outside temperature ranges between 14°C to 36°C.

Therefore;

- Employing natural or passive cooling systems can be an alternative way to maintain a house cooling or reduce air-conditioning load. A passive cooling system employs non-mechanical procedures to maintain suitable indoor temperature.

But still, there are some limitations, for the conventional integration systems.

Limitations for the conventional integration systems

- The advantage of the integration is not optimized yet. More work is needed for determining the optimum size.
- The structure of the current wind tower is big. This makes it difficult to integrate easily in the existing or new buildings.
- No inclined solar chimney (due to its high absorption of solar radiation) is integrated with evaporative cooling wind towers.

Figure (3-6) shows the problem of the conventional integration for the three important studies.

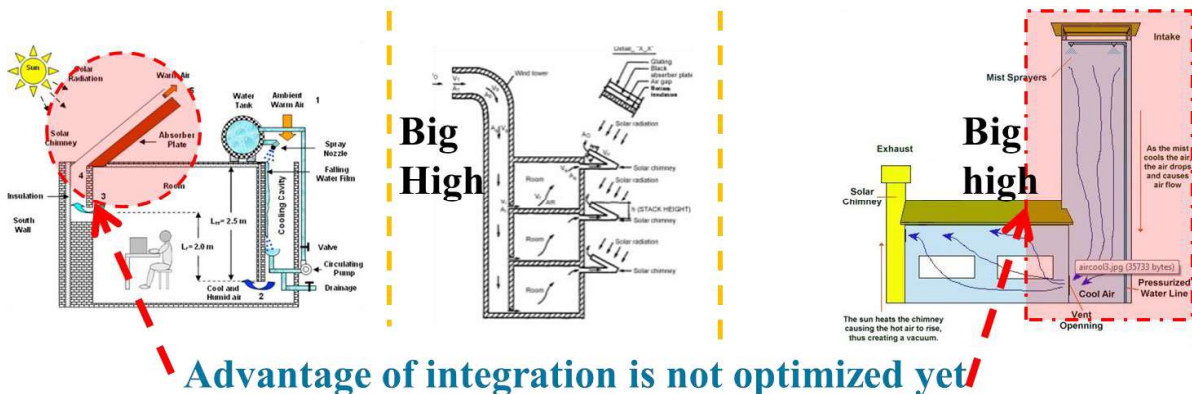


Figure (3-6): The problems of the conventional system integration.

3.3 Comfort ventilation

Comfort ventilation is the important factor that deals directly with the human body and depends on the strategy used. It is based on the theory that high air speed around the human body accelerates the skin's evaporation rate and, accordingly, improves accordingly the heat dissipation from the human body. This in turn shifts up the comfort upper level by providing by such direct physiological cooling effect and decreases human discomfort due to skin wetness and high humidity level [33, 77]. In comfort ventilation strategy, two different impacts of the air velocity of the human body were determined: first, the heat exchange of the body that happens with convection; second, the evaporative capacity of the air. According to ASHRAE standard 55 for naturally ventilated buildings, the acceptable thermal environment of indoor operative temperature¹ ranges between 22°C and 28°C and the comfort indoor air velocity of 1.6m/s can be beneficial for improving comfort at higher temperatures [24]. So, new residence must have the acceptable thermal environment for all occupants. According to ASHRAE 62-2001 standard, ventilation rates depend upon the floor area whereas the minimum ACH was 0.35, but no less than 15 CFM/person [25]. Also, passive natural ventilation standards require a minimum of 3 air changes for residential buildings [78]. Finally, The comfort ventilation can easily be enhanced by appropriate building design and the system used.

Conclusion

This chapter presented the mechanism of the natural ventilation and evaporating cooling. It is difficult to achieve thermal comfort with natural ventilation only. Also, the solar chimney is important to move indoor air flow continuously without depending on wind speed. Therefore, important findings are concluded according to:-

¹**Operative temperature**; is the acceptable internal conditions for indoor environment. It is due to the effect of air temperature and the influence of air velocity.

Design

Due to the limitations of the conventional integrated system (solar chimney (SC) & wind tower (WT)), new compact designs is needed to be studied for achieving indoor thermal comfort and applying easily to the existing and new buildings.

Indoor environment

New evaporative cooling wind towers with wet mediums need to be studied, in order to decrease water consumption - in the cooling process without increasing indoor relative humidity - and achieves acceptable indoor temperature.

Ventilation

As Egypt has a rich sunny and clear sky. Therefore, the solar chimney is important to be used and integrated with evaporative cooling to move air continuously without depending on wind speed force during daytime and nighttime.

Finally, it is important to use the advantages of the conventional and the traditional cooling concepts with new techniques and strategies for achieving compact, high advantage of integration of wind tower and solar chimney and high performance new designs.



Chapter 4

Integration of solar chimney with new cooling tower as a passive ventilation technique

Introduction

Buildings contribute more than 40% of the total global primary energy use corresponding to 24% of the world CO₂ [19]. Effective integration of passive features into the building design can significantly minimize the air-conditioning demand in buildings while maintaining thermal comfort [79]. Passive evaporative cooling is one of the most efficient and long recognized ways of inducing thermal comfort in predominantly hot arid climates [36, 80]. This chapter studied the effect of integration of inclined solar chimney (SC) with evaporative cooling short wind tower (ECWT) on the indoor environment. Based on the review of solar chimney with an evaporative cooling in chapter three, no research studied the integration of inclined chimney with short evaporative cooling wind tower and wet pad (compact design, easy to integrate with the building with high performance). Also, no research studied the performance of the integrated system in the Egyptian house. In general, this chapter aims to investigate the possibility of using natural ventilation with an evaporative cooling strategy using numerical modeling (simulation), in order to achieve zero energy consumption for cooling and indoor thermal comfort according to ACS and ASHRAE under the weather data of the New Assiut City. COMIS & TRNSYS simulation software are used in the developing stage.

4.1 Developing and description of the system

The new proposed system of inclined solar chimney (SC) with short wind tower (ECWT) was developed based on a reference system of solar chimney attached to a room with an evaporative cooling cavity (ECC) [50]. The reference model has some limitations in the system calculation; it assumes zero pressure boundaries at the inlet and outlet except the stack effect and therefore does not consider the various effects of building static pressure, from the atmospheric pressure, and the effect of wind pressure coefficient on buildings. Also, There are many reasons that make it very difficult to integrate in Egyptian houses. Some of these reasons are: ECC consumed a lot of water because of using water film, it occupies plenty of space in the room (it can't be attached to other room), it is difficult to maintain (because its width is 20 cm) and also the resulting humidity is very high, 93%, causing many health problems and discomfort (more than the maximum range of ASHRAE [24]. On the other hand, it is a very detailed calculation model for solar chimney and evaporative cooling to start developing from this reference model. Figure (4-1) shows the diagram of the new proposed system and the reference system.

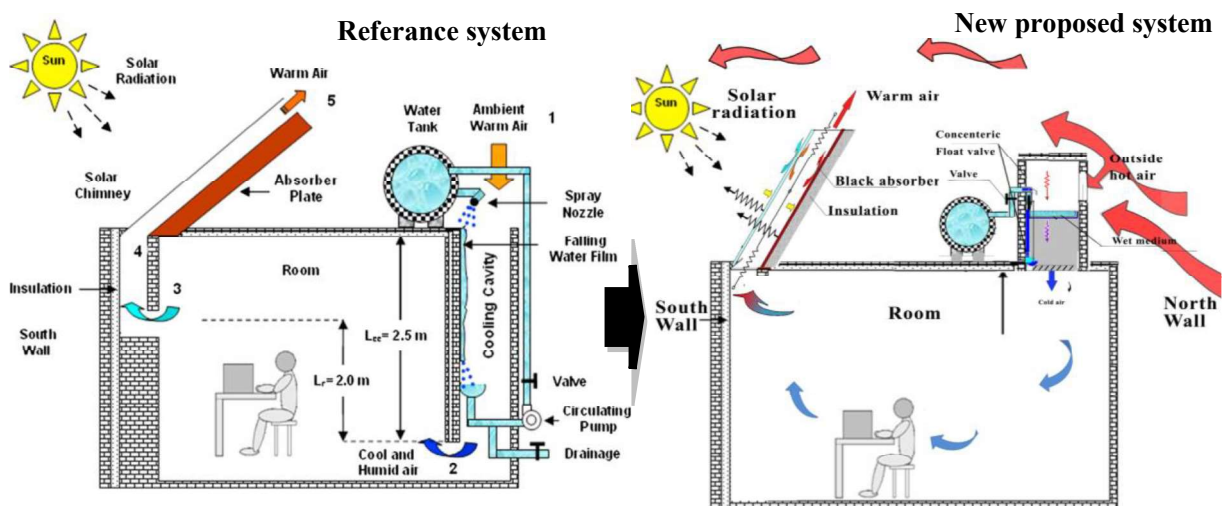


Figure (4-1): Schematic diagram of the new proposed system and the reference system.

The system is integrated for the living room of the upper floor without air exchange from other room. The living room of the upper floor is selected as a pilot base case, where all the family members spend much time doing different activities. Assuming the living room of the upper floor is located in a block of the building, with the same condition as the New Assiut City, where the front of the building is a 12m wide street and facing another block of the building as a big obstacle in the opposite direction with azimuth 180° . While from the back, there are private gardens back to back with another private garden for another building then there is a block of buildings as a big obstacle with the same height of the building in the opposite direction with azimuth 0° toward the north¹.

The following dimensions and specifications are applied to the proposed model: The room located in the New Assiut City, Egypt having 27.30°N latitude position and 31.15°E longitude position. The solar chimney is oriented towards the south. The calculations were carried out for a single zone (room) to study the integration of the new system in it. Room dimensions are $4.0\text{m}\times 4.0\text{m}\times 3.125\text{m}$ (L \times W \times H).

Nevertheless for the new system, the inclination length of the chimney was 2m on the inclined length in order not to extend the vertical height (1.5m) according to Egyptian Building Regulation Law [81], the height of the cooling tower was 1m. The chimney air gap was 0.2m & the inclination angle of the chimney was 50° based on the dimension of the reference system. Next, parametric studies for solar chimney and wind tower dimension are needed in the next chapter to choose the best dimension for the new proposed compact design. Figure (4-2) shows the location of the room and its dimensions with the integrated system according to north-south orientation.

¹See appendix (B)

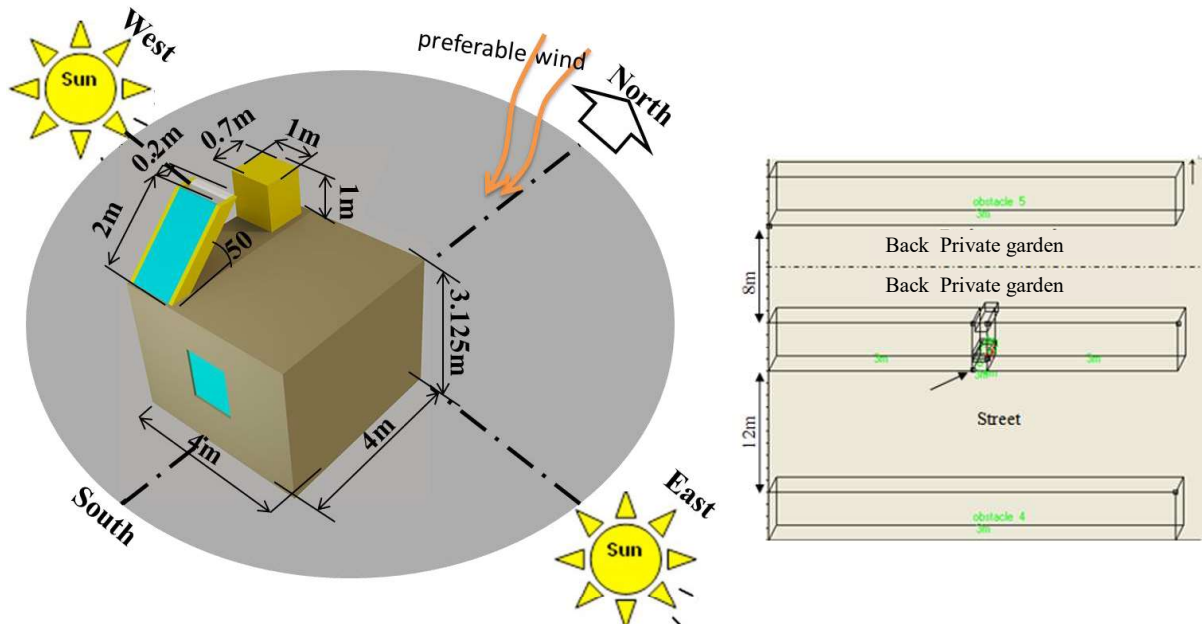


Figure (4-2): The location of the room with the new proposed system according to north-south orientation and its location in the building block as a pilot base case.

The function of the system is to provide desired comfort conditions and the suitable rate of ventilation depends on several parameters such as (temperature difference between indoor and outdoor, solar intensity, relative humidity, wind speed & pressure coefficient). In addition, experimentation is time-consuming and very expensive. Therefore, the numerical model is made and developed for the new proposed system.

4.2 TRNSYS and COMIS simulation programs

The new proposed model is implemented in COMIS-TRNSYS programs;

a. COMIS program

Calculates air exchange and contaminant migration within the rooms of the building and between a building and the outdoors [82]. These models typically represent the rooms of the building as zones (multizone model) with homogeneous air properties. Airflows are driven by pressure difference or temperature difference and interconnect with each other and have the user define leakage characteristics. Multizone models in COMIS have been used to represent many types of buildings with acceptable accuracy and it was compared

with over fifty test cases with either an analytical or a numerical solution to ensure that the code didn't contain numerical errors. Also, the program was checked against 14 other simulation programs performed by 15 different laboratories and against 9 experimental studies conducted within Annex 23 and supported by the International Energy Agency (IEA) [83, 84]. Multizone airflow network models deal with the complexity of flows in a building by recognizing the effects of internal flow restrictions. They require extensive information about flow characteristics and pressure distributions [85].

b. TRNSYS program;

Calculates the building thermal model under the effects of internal heat load, solar load, occupant & heat transfer through ventilation, walls, windows, roof and ground. It is currently maintained by an international collaboration with the United States (Thermal Energy System Specialists and the University of Wisconsin-Solar Energy Laboratory), France (Centre Scientifique et Technique du Bâtiment), and Germany (TRANSSOLAR Energietechnik). It is programmed in Fortran [86].

TRNSYS is a simulation program (Transient Simulation Program) which is widely used around the world [87, 88, 89, 90]. The calculation model used in the program was verified, both practically and theoretically, in many experiments and research projects [91, 92].

c. Couple concept of TRNSYS & COMIS programs;

The indoor air temperatures calculated by the building thermal model (TRNSYS) strongly depends on the exchange of air between the zones (COMIS) as well as the outside. To make links between the two models, the exchange of data between the thermal and the air flow model is required by inputs and outputs as in figure (4-3). TRNSYS Solver can be used for the iteration process between the two models with continuous feeding of air flow in the thermal model so that an optimum of stability and convergence is achieved [86, 93].

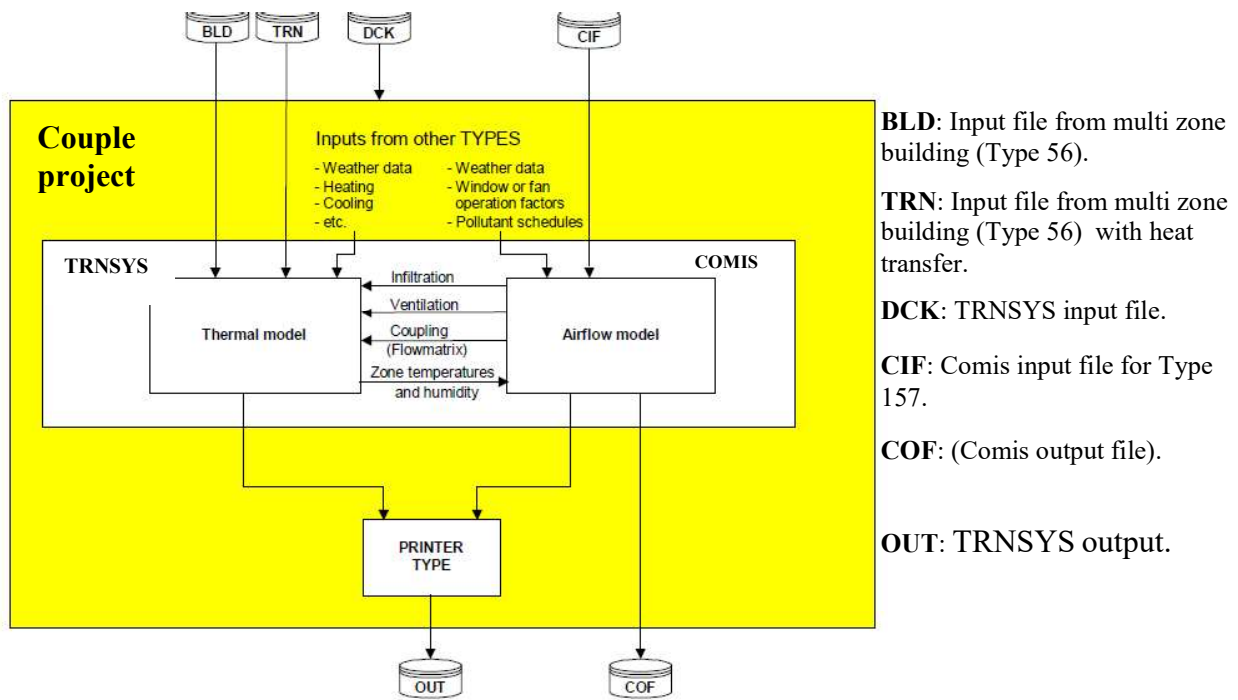


Figure (4-3): The concept of the couple project between TRNSYS & COMIS programs [93].

4.3 Multi-zone thermal ventilation model

The proposed models of solar chimney (SC) with short evaporative cooling wind tower (ECWT) are built in COMIS-TRNSYS programs. This direct evaporative cooling tower uses a component “506d- TESS” library which uses wet medium at the top, and this component is created and validated by Thermal Energy System Specialists-USA; it was modified in 2004. The present model includes airflow components which need simultaneous prediction of temperature and airflow rates in the components. In the multi-zone ventilation model, the model is created as a system of zones, openings & ducts linked together by the airflow path connection. Zones are represented by nodes. Chimney and evaporative cooling channel are represented by ducts for resistance & pressure drop calculations¹. A hydrostatic condition is assumed in zones and the flow rate in each link is defined as a function of zone pressure, which results in a system of nonlinear equations, defined by the mass conservation² for each zone [94].

¹See appendix B.

²**Mass conservation: principle of mass conservation**, states that the mass of the system must remain constant over time, as the system mass cannot change its quantity. Hence, the quantity of mass is "conserved" over time [86].

Figure (4-4) shows the flow chart solving procedure of TRNSYS-COMIS and the connection between the two programs.

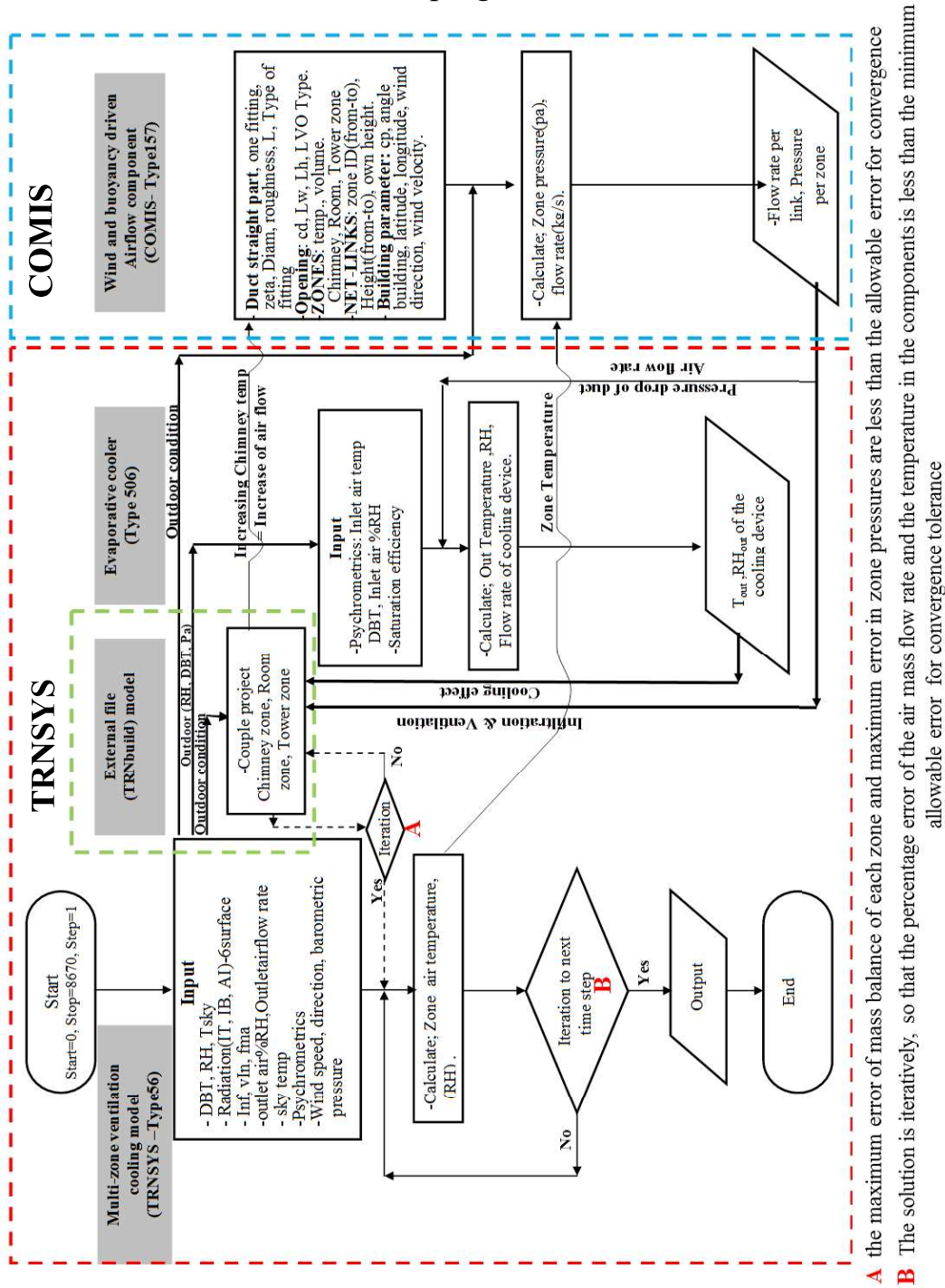


Figure (4-4): Flow chart solving procedure of TRNSYS-COMIS (Author)¹.

¹**Convergence Tolerances:** is a control statement used to specify the error tolerances to be used during a TRNSYS simulation. Specifying a relative tolerance indicates that TRNSYS should not move on to the next time step until all connected outputs are changing by less than (100 εa) percent of their absolute value. The error tolerances is set to 0.01.

The equations are solved numerically to predict zone pressures and zone pressures are back substituted in the flow equations to predict the airflow rate at each link [94]. The detailed equations used for large openings and ducts are presented in the fundamentals of the multizone airflow model-COMIS [95, 96]. A description of the mathematical models used in each component (Types 109, 69, 33, 65d & 25a)¹ can be found in the TRNSYS 16 manual handbook. The pressures calculated in the previous step was used as an initial guess for pressures in the next step. Initial zone densities are based on the pressures found in the last step. The solver update zone densities as it updates zone pressures [94]. The simultaneous set of mass balance equations is typically solved using the Newton-Raphson method² [86] to correct the zone reference pressures until the simultaneous mass balance of all flows is achieved with stable convergence.

4.4 System mechanism

Solar radiation passes through the glazing and is absorbed into the absorber surface (black aluminium). The air in the chimney is then heated by convection from the absorber. The decrease in density experienced by the air causes it to rise, whereupon it is replaced by air from below, i.e. from the attached room. The rate at which air is drawn through the room depends upon the buoyancy-force experienced, i.e. depending upon the temperature differential, the resistance to flow through the chimney and the resistance to the entry of fresh air from the room. While in the wind tower the opening of the tower faces the north wind. This compact design with dimensions $1\text{m}\times 0.7\text{m}^3$ & height 1m depends on solar intensity and solar chimney effect that absorb air from the room. Figure (4-5) shows the mechanism cycle of the system.

¹ See appendix (B).

²**Newton-Raphson method:** is the most common tool used to solve the set of non-linear equations required to model complex air flows. The idea of the method is as follows: one starts with an initial guess which is reasonably close to the true root and the method can be iterated.

³**Tower dimension** ($1\text{m}\times 0.7\text{m}$): is considered as initial dimension and then parametric investigation will be studied in chapter five.

While evaporative cooling with a wet medium (EC), is a device that cools air by passing it across a wet medium. As hot air passes over the wet media, some of its energy goes to evaporate water from the media. The air comes out of the other side of the device having given up some of its energy and consequently, exits at a lower temperature, higher humidity, and constant enthalpy¹. The minimum temperature that can be reached is the wet bulb temperature (WBT) of the incoming air [98]. Figure (4-6) shows the concept of evaporative cooling.

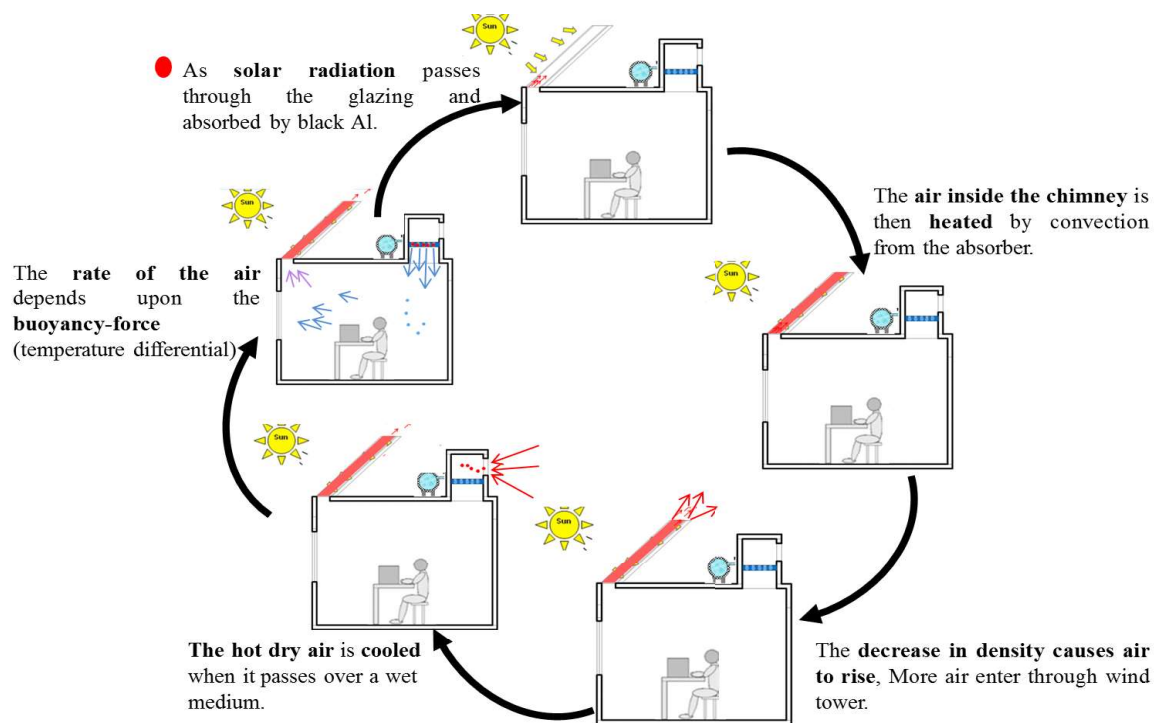


Figure (4-5): The mechanism of the system during daytime.

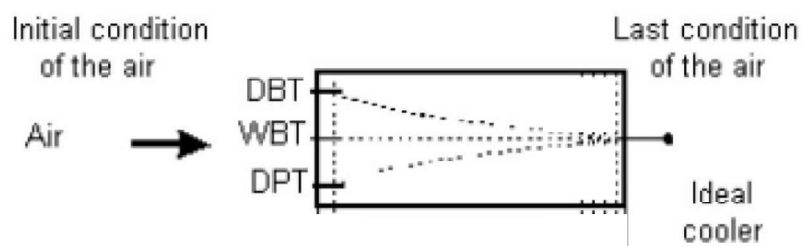


Figure (4-6): Evaporative cooling with constant water flow [34].

¹**Enthalpy:** It is the preferred expression of system energy changes, is a measure of the total energy of a thermodynamic system (energy inlet equal energy outlet) [97].

4.5 Mathematical modeling of the integrated system

The proposed model (the room with the integrated system) is built into COMIS-TRNSYS programs according to detailed input in Appendix (B) and based on the mathematical model of every part of the integrated system which is described as follows:

4.5.1 Pressure calculation and mass flow rate through openings (COMIS model)

To estimate the amount of air flow through an opening, it is necessary to know the pressure difference across the opening and its effective flow area. The pressure at an opening can be due to wind, as well as buoyancy. Therefore, it is determined by the location of the opening, as well as the internal and external environmental parameters such as wind velocity, wind pressure coefficient (C_p)¹ and inside and outside temperatures. Figure (4-7) shows the location of different pressure points solved from eq. 1 to eq.2.

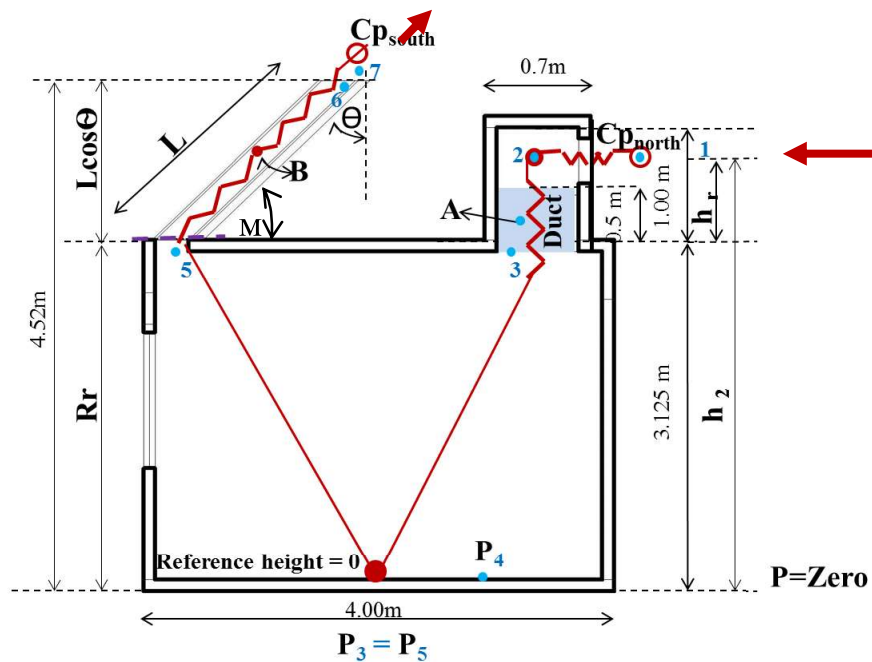


Figure (4-7): The location of different pressure points taking into account base pressure on the ground (Author).²

¹**Wind pressure coefficient;** The portion of the dynamic wind pressure, which acts on the specific façade or roof at a certain wind direction [95].

² M; is the inclination angle of the chimney with the horizontal.

The ventilation rate inside the system is calculated according to six variable (P_2 , P_3 , P_4 , P_5 , P_6 , P_7) which is solved from the eq.1 to eq.6 taking into account base pressure on the ground ($P=0$) as shown in figure (4-7). Appendix (C) shows the nomenclatures (scientific symbols) of these equations.

$$P_2 = (-\rho g h_2 + 0.5 \rho_1 C p_{north} v^2) - \frac{\rho_2}{2} \left(\frac{Q}{\alpha_1 A_1} \right)^2 \quad (1)$$

Where $P_1 = (-\rho g h_2 + 0.5 \rho_1 C p_{north} v^2)$ is the pressure at point 1 (N/m^2), α is the discharge coefficient of the opening in the wind tower & A_1 is the area of the opening 1 (m^2).

$$P_3 = P_2 - (\zeta_{WetMediumInlet} + \zeta_{DuctOutlet} + \zeta_{DuctFriction}) \frac{\rho_3}{2} v_A^2 + \rho_A g h_r \quad (2)$$

Where the local pressure losses in the inlet $\zeta_{WetMediumInlet}$ of evaporative cooling (wet medium), the friction of duct $\zeta_{DuctFriction}$ & local losses of the duct outlet $\zeta_{DuctOutlet}$ can be calculated according to dynamic dimensions of Lamda fitting, Re (Reynolds number), roughness, duct dimention and lamda (λ). It can be determined in details from [94]. Also, the indoor velocity equals $v_A = \frac{Q}{A}$ (m/s).

$$P_4 = P_3 - \rho_4 g R_r \quad (3)$$

$$P_5 = P_4 + \rho_4 g R_r \quad (4)$$

$$P_6 = P_5 - (\zeta_{ChimneyInlet} + \zeta_{ChimneyOutlet} + \zeta_{ChimneyFriction}) \frac{\rho_B}{2} v_B^2 + \rho_B g (L \cos \theta) \quad (5)$$

Where the local pressure losses $\zeta_{ChimneyInlet}$ in the inlet of a solar chimney, the friction of chimney $\zeta_{ChimneyFriction}$ & local losses of the chimney outlet $\zeta_{ChimneyOutlet}$ can be calculated using an approach similar to that of evaporative cooling.

$$P_7 = P_6 - \frac{\rho_6}{2} \left(\frac{Q}{\alpha_6 A_6} \right)^2 \quad (6)$$

¹ θ : is the inclination angle of the solar chimney from vertical (for considering the vertical height)

Where $P7 = -\rho g(R_r + L \cos \theta) + 0.5 \rho_1 C p_{south} v^2$ and $\rho = \frac{353.25}{T} = \frac{353.25}{t + 273.15}$ [97] is the air density (kg/m^3). Then the pressure differences across the opening due to buoyancy and wind is required and solved with each others in order to predict pressure of the room and ventilation rate Q (m^3/s).

4.5.2 Temperature prediction in solar chimney

The average air density in the chimney channel ρ_6 is predicted using the thermal resistance network model in TRNbuild-TRNSYS, based on the heat balances of each element of the solar chimney. The model used by Ramadan and Ong [63, 99] and modified by Alemu et al. [76] for solar chimney is adopted with some assumptions to enable solving the mathematical model. The chimney inlet area and exit areas are equal. The thermal network for the physical model considered is shown in Figure (4-8) [94].

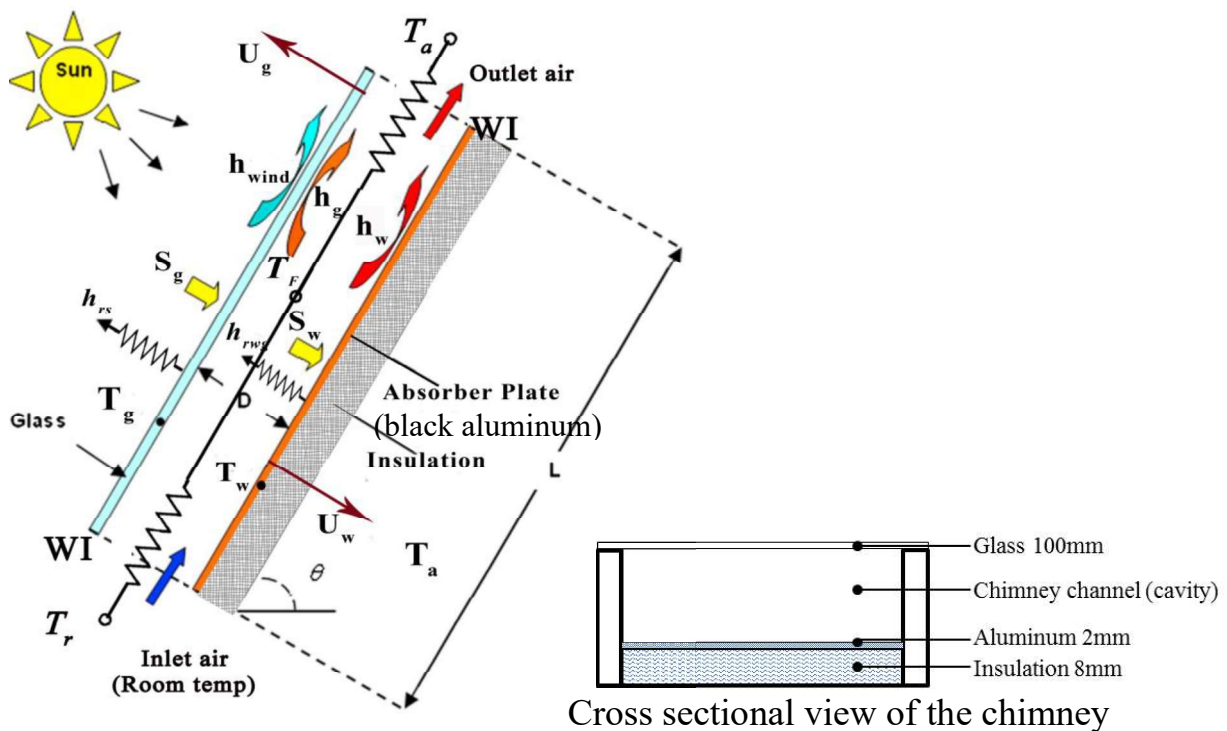


Figure (4-8): Thermal network for solar chimney with air flow.

Where the heat balance equations from the thermal network at each element of the solar chimney:

$$T_{g(\text{glass cover})}: S_g + h_{rwg}(T_w - T_g) + h_g(T_f - T_g) = U_g(T_g - T_a) \quad (7)$$

$$T_{f(\text{Air})} : h_w(T_w - T_f) = h_g(T_f - T_g) + q'' \quad (8)$$

$$T_{w(\text{absorber})}: S_w = h_w(T_w - T_f) + h_{rwg}(T_w - T_g) + U_w(T_w - T_a) \quad (9)$$

The heat transfer to the air stream in the chimney q'' with a length L and the width of the air channel is:

$$q''_{wl} = \dot{m} C_f (T_{airout} - T_{airin}) \quad (10)$$

where \dot{m} is the mass flow rate of the air component

The mean air temperature T_f is given by:

$$T_{f(\text{air})} = \gamma T_{airout} + (1 - \gamma) T_{airin} \quad (11)$$

Where assumed γ (mean temperature weighting factor) = 0.75 [64].

Considering that air inlet to the chimney has a temperature equal to the room average temperature, and substituting in the above equation of q''_{wl}

$$q''_{wl} = \dot{m} C_f \frac{T_{f(\text{air})} - T_{airin}}{\gamma} \quad (12)$$

The heat transfer coefficient from glass to atmospheric air

$$U_g = h_{rs} + h_{wind} \quad (13)$$

The radiation heat transfer coefficient between the glass and the sky is:

$$h_{rs} = \frac{\sigma_g \varepsilon_g g (T_g + T_{sky}) (T_g^2 + T_{sky}^2) (T_g - T_{sky})}{T_g - T_a} \quad (14)$$

where σ = solar absorptance, ε = emissivity, g = gravitational acceleration 9.81,

$$T_{sky} = 0.0552 T_a^{1.5}$$

The convective heat transfer outside the glass due to the wind is

$$h_{wind} = 5.7 + 3.8 V \quad (15)$$

(wind speed at reference height)

The radiation heat transfer coefficient between absorber and glass h_{rwg} is:

$$h_{rwg} = \frac{\sigma_w (T_g + T_w) (T_g^2 + T_w^2)}{1/\varepsilon_g + 1/\varepsilon_w - 1} \quad (16)$$

The heat transfer coefficient between the absorber and outside air

$$U_w = \frac{1}{1/h_w + th_{insulation}/k_{insulation}} \quad (17)$$

Where $th_{insulation}$ is the thickness, $k_{insulation}$ is the thermal conductivity

The convective heat transfer coefficient between air and absorber plate or glass

($h_{air. absorber}$, $h_{air. glass}$)

$$h_x = \frac{Nu_{air.x} k_{air}}{d_{chimney.gap}} \quad (18)$$

where x refers to absorber plate or glass, d is the chimney gap.

The Nusselt number (Nu)¹ correlation for a constant heat flux on one side of the channel [100] is:

$$Nu_{air.x} = 0.9282 Ra_{air.X}^{0.2035} \left(\frac{d_{ChimneyGap}}{L} \right)^{0.8972} \quad (19)$$

Where $Ra_{air.x}$ is Rayleigh number² for constant heat flux .

L: inclined length of the chimney

Solar energy absorbed by the glass

$$S_g = \sigma_g I_{incident\ radiation} \quad (20)$$

Solar energy absorbed by the absorber (black aluminum)

$$S_w = \sigma_w \tau_g I_{incident\ radiation} \quad (21)$$

Substituting the above equations into Eq.(7,8,9) and solving three equations solved simultaneously to give the $T_{g(glass\ cover)}$, $T_{f(Air)}$, $T_{w(absorber)}$.

The mean air temperature $T_{(Air)}$ in the solar chimney channel is used to determine the average air density ρ_B which is then substituted in eq.5 then the flow rate in the solar chimney is a function of the chimney temperature.

4.5.3 Temperature predictions in evaporative cooling wind tower

Evaporative cooling wind tower (ECWT) is used to cool hot dry air from outside after passing over a wet medium. When air passes through the evaporative cooler, the component calls the TRNSYS Psychrometrics to fully determine the

¹**Nusselt number:** It is the ratio of convection to conductive heat transfer across the boundary.

²**Rayleigh number:** is the bouyancy driven flow.

state of the inlet air. The psychrometrics component in TRNSYS returns the inlet air wet bulb temperature and enthalpy backs the inlet temperature, pressure, relative humidity and humidity ratio. Figure (4-9) shows the evaporative cooler of the schematic diagram.

The energy balance equation expressing the heat removed from the air to evaporate the water is expressed as:

$$m_1 a h_1 \text{enthalpy.AirIn} = m_2 a h_2 \text{enthalpy.Airout} + m_{2\text{vapour}} h_{2\text{vapour}} \quad (23)$$

The rate of heat transfer from air to water in the wet panel surface, Q sensible (the heat exchange by temperature difference), is given by Δy

$$Q_s = h A \Delta T_{LM} = m c_p (T_r - T_a) \quad (24)$$

And the heat gain of latent heat of air (heat exchange by humidity ratio) can be expressed as:

$$Q_L = m_L h_L (\Delta w) \quad (25)$$

Where w is the humidity ratio

ΔT_{LM} is the log mean temperature difference [98, 101] which is given by:

$$\Delta T_{LM} = \frac{(T_r - T_a)}{\ln(T_r - T_{wb}) / (T_a - T_{wb})} \quad (26)$$

The performance of the systems with different flow type can be assessed on the saturation efficiency as:

$$\eta_{\text{Saturation}} = \frac{T_a - T_r}{T_a - T_{wb}} \quad (27)$$

The air temperature leaving the cooling device can be calculated from eq. (27)

$$T_r = T_a - \eta_{\text{Saturation}} (T_a - T_{wb}) \quad (28)$$

The wet bulb temperature of the air entering and exiting the device is assumed to be constant

Where the minimum outlet temperature equals the inlet wet bulb temperature

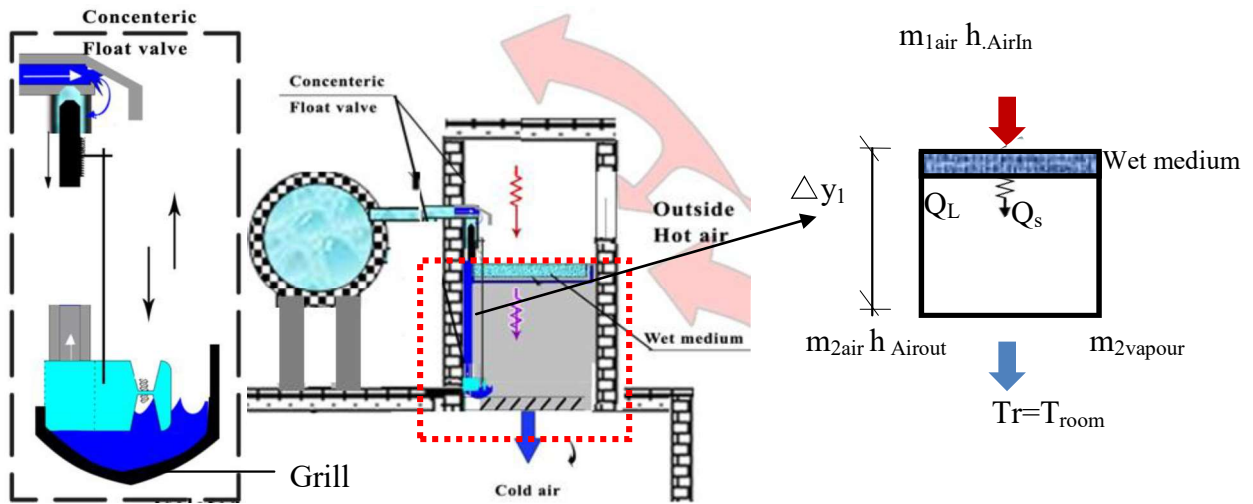


Figure (4-9): Evaporative cooler schematic.

Since the performance in the evaporative cooler is an adiabatic process¹.

$$Q_{Latent} = Q_{Sensible} \quad (29)$$

The humidity ratio of the air outlet of the device [102]:

$$RH_{out} = \frac{X_{inlet} p_{outside}}{(0.622 + X_{inlet}) p_{saturated vapour pressure}} \quad (30)$$

The saturate vapor pressure (atm) [59]:

$$P_{saturated.vapour.pressure} = 10^{\left(\frac{17.443 - \frac{2795}{T-273}}{T-273} - 3.868 \log_{10}(T-273) \right)} \quad (31)$$

The corresponding energy removed from the air stream to evaporate water under these conditions is given by:

$$Q_{air} = \dot{m}_{cooler} (h_{AirIn} - h_{AirOut}) \quad (32)$$

where $h_{enthalpy} = C_p T + x(r + C_{p.vapour} T)$ kJ/kg(dry) [97]

$$1.005 T + x(2501.1 + 1.846T) \quad (33)$$

$C_{p.air}$ = the specific heat of air kJ/kg.K.

x = humidity ratio kg/kg (dry).

r = The amount of heat to evaporate water kJ/kg.

$C_{p.vapour}$ = the specific heat of vapour kJ/kg.K.

T = temperature °K.

¹Adiabatic process: No heat added or removed from the system.

The wet pad in the evaporative cooling is always wet. The saturation efficiency of the system is based on the standard options for direct evaporative cooling in hot climate published by the California Energy Commission. This standard value ranges from 45 to-61% for the wet pad with no water droplet [103], where the wet pad (medium) is made from expanded paper.

The pad is wetted by dripping water onto its upper surface using a concentric floating valve as in figure (4-9). It opens when the level of water decreases in the grill below the wet medium. As a result, less water is consumed and zero energy consumption for, cooling due to passive system used, is reached.

4.6 Air flow network & building thermal model of the integrated system in COMIS-TRNSYS programs

The ventilation model is integrated in the conventional building thermal model with a strong influence on the system performance as shown in figure (4-4).

4.6.1 Building thermal model (TRNSYS model)

The internal heat load, solar load and the heat transfer through walls, windows, roof, ground and opening are considered and shown in figure (4-10), where Q is the heat transfer. Also, the temperature of the ground at a depth of 0.5m is used in calculating for heat transfer from the ground and derived from Egyptian Typical Meteorological Year (ETMY) for periods of 12 years from 1991 until 2003 [23]. Also, the internal load of occupants is used in the calculation. There are four occupants inside the single zone doing light work and seating with light load. Each occupant is assumed to have a sensible gain 75W and latent gain 75W¹ according to ISO 7730 [86]. The occupants are assumed to be staying in the room for the whole day to apply the maximum load inside. The room light heat is 13W/m². It is an energy saving lamp with a convective part (visible) 20%. And, one 140W device is used [86].

¹Occupants emit heat from their activities through breathing and perspiration. Total occupant heat gain consists of sensible gain and latent load gain. The sensible load affects dry bulb air temperature, while the latent load affects relative humidity.

TRNSYS

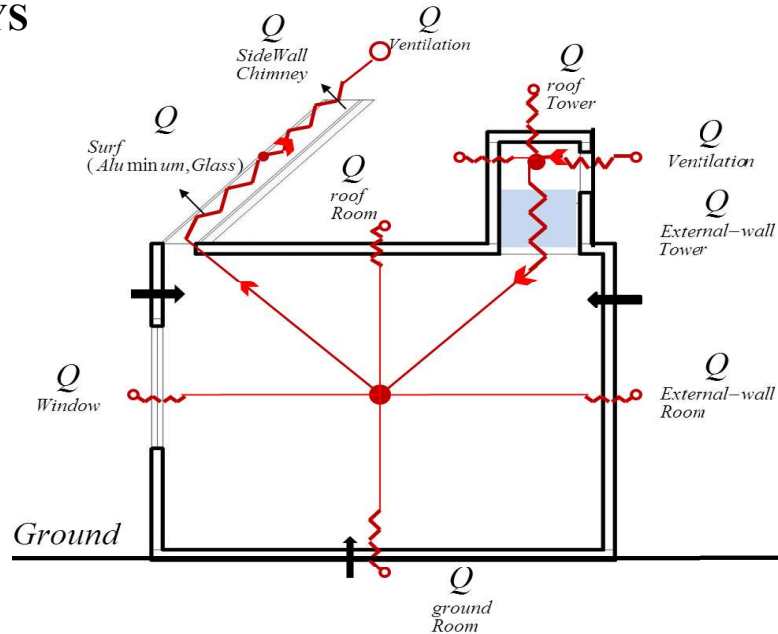


Figure (4-10): The building thermal model with the heat flows in the ECWT, Room & the solar chimney with the combination of ventilation rate in the TRNSYS model (Author).

Table (4-1) shows the building construction material description based on the ideal thermophysical properties [104] used in TRNSYS (Type 56).

Table (4-1): Description of building material used in the calculation.

Building part	Material	Conductivity kJ/h m K	U-Value ¹ (W/m ² K)	Thickness (m)
Glass windows	Single glass	-	5.68	0.004
External walls	Common plaster (coating)	1.26		0.02
	Brick	3.60	2.60	0.10
	Common plaster (coating)	1.26		0.02
Roof	Insulation	0.2		0.05
	Concrete slab	4.2	0.443	0.12
	Cement plaster (coating)	4.50		0.01
Ground	Floor	-		0.10
	Insulation	0.2	0.797	0.02
	Concrete	4.2		0.10

¹**U-Value:** The flow of heat through an insulating or building material. It measures how well parts of a building transfer heat. This means that the higher the U-value the worse the thermal performance of the building envelope. A low U-value usually indicates high levels of insulation. $U = 1 / (\text{sum of } R \text{ value})$ [105].

Where the overall heat transfer coefficient of the windows, is based on the convective and radiative heat transfer coefficients in the two sides boundaries (outdoor & indoor).

Table (4-2) shows the properties of the materials used in the model.

Table (4-2): Material properties in the model [86, 104].

Material name	Capacity kJ/kg K	Density kg/m ³
Brick	0.84	1800
Concrete	1.0	1400
Common plaster (coating)	0.84	1200
Cement plaster	0.84	2000
Insulation	1.88	120
Aluminum	0.88	2700

Table (4-3) shows the parameters used for solar chimney calculation based on the reference model parameters.

Table (4-3): The parameters used in the solar chimney calculation (dimensionless).

Parameters	Value	Parameters	Value
Transmissivity of glass	0.84	Absorptivity of absorber wall	0.95
Absorptivity of glass	0.06	Emissivity ¹ of the absorber surface	0.95
Emissivity of glass	0.90		

4.6.2 Air flow network (COMIS model)

In the air flow network, the zones (ECWT, Room, SC) are linked to its ambiance (outside) via external nodes for outside and to north and south facades. Wind pressure data, wind speed, wind velocity profile for the building, Meteo & orientation are defined. Wind pressure coefficient values for a specific building are calculated according to terrain roughness, the orientation of the

¹**Emissivity:** the ratio of the radiation emitted by a black body (the relative ability of its surface to emit energy by radiation).

room, the obstacles of the building, and Cp position¹. Figure (4-11) shows the air flow network in COMIS.

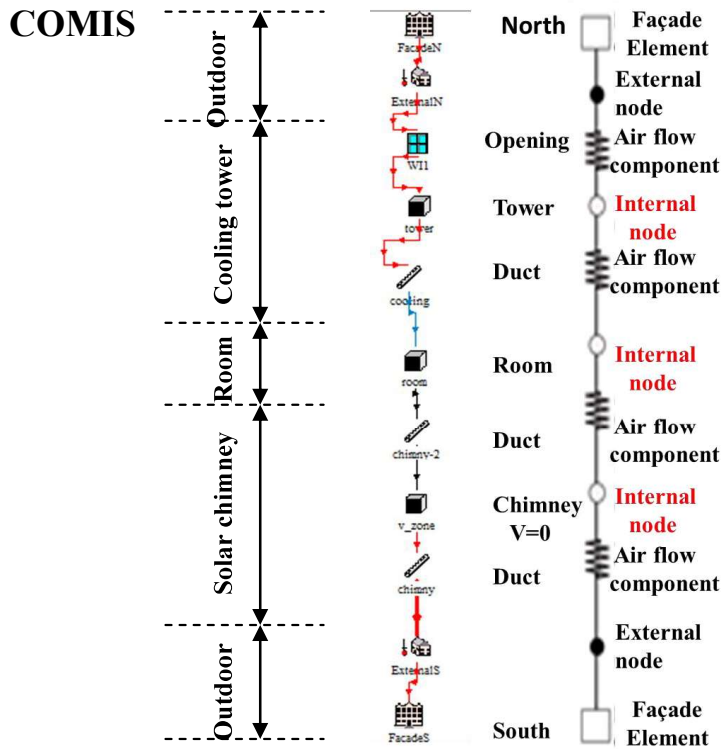


Figure (4-11): The air flow network of the integrated model with a description of the internal node, external node & airflow component (Author).

Also, the solar chimney is treated as rectangular duct connected to the room from one side and a node with volume equal zero from the other side to transfer the calculated temperature of the chimney from TRNSYS and then another rectangular duct connected from the zone with volume zero to outside. The pressure losses; in the inlet, outlet & the friction of the chimney and cooling ducts are taken into account².

4.6.3 Mathematical calculation of the building thermal model

Heat transfer through external walls (and roof) for room zone & tower zone is predicted in figure (4-10):

¹See appendix (B)

²See appendix B.

$$\sum_{external} Q = \sum^{ne} \frac{A_z (T_{star} - T_z)}{R} \quad (34)$$

Where ne is the number of external walls attached to the zone, T_{star} is star temperature which can be used to calculate a net radiative and convective heat from the wall surface, R is the overall thermal resistance value including convective heat transfer resistance on both sides of the surface, and z is the zone [86].

The total gain to chimney zone from all surfaces is the sum of the combined heat transfers

$$\sum_{\substack{Surface \\ Chimney}} Q = \sum A_s \dot{Q}_{Comb_z} + S_{\substack{outside \\ surface}} \quad (35)$$

Where, A_s is the inside area of the surface

$S_{outside\ surface}$ is the solar radiation for outside surface (W/m^2).

\dot{Q} is the total heat transfer of convective and radiative ($W/m^2\text{°C}$).

The heat transfer across the windows is:

$$\sum_{Window} Q = \sum A_z U_w (T_a - T_{star}) + I(SHGF) \quad (36)$$

Where U_w is the overall heat transfer coefficient across the window (the rate of heat transfer through the window from outside to inside ($W/m^2\text{°C}$), $SHGF^1$ is the window's Solar Heat Gain Factor; its calculations are presented in details in [107].

For external surfaces the long wave radiation is considered using a fictive sky temperature² T_{sky} [86].

$$\dot{Q}_{Comb} = \dot{Q}_{convective} + \dot{Q}_{radiative} \quad (37a)$$

$$\dot{Q}_{convective} = h_{ConvOutside} (T_{AdjSurface} - T_{outsideSurface}) \quad (37b)$$

¹**SHGF:** represents the fractional amount of the solar energy that strikes the window and cause warming the house [107].

²**Fictive sky temperature:** is used to considered the long-wave radiation exchange at the outside surface (T_{sky}) [86].

$$\dot{Q}_{Radiative} = \beta \varepsilon_{outside} (T_{OutsideSurface}^4 - T_{fsky}^4) \quad (37c)$$

$$T_{fsky} = (1 - f_{sky}) T_{AdjSurface} + f_{sky} T_{sky} \quad (37d)$$

Where f_{sky} is the view factor¹ to the sky, ε is the long wave emissivity of outside surface= 0.9 for walls

The sky model is used to calculate diffuse radiation on inclined surface for the solar chimney by Perez model², which is considered the best available model [86]. Heat transfer due to ventilation in a zone is:

$$\sum_{Ventilation} \dot{Q} = \sum_{Infiltration} \dot{m} c_p T_{outside} - \sum_{FromZone} \dot{m} c_p T_{zone} + \sum_{ToZone} \dot{m} c_p T_{zoneAdjacent} \quad (38)$$

Then the total heat load, required maintain the zone at a specific temperature, can be calculated as

$$Q_{load} = \sum_{Ventilation} Q_{Out} + \sum_{External_wall} Q_{Tower} + \sum_{External_wall} Q_{Room} + \sum_{ground} Q_{Room} + \sum_{Window} Q_{Room} + \sum_{Roof} Q_{Tower} + \sum_{Roof} Q_{Room} + \sum_{Side_wall} Q_{Chimney} + \sum_{Surface} Q_{Chimney} + \sum_{People} Q_{Light} \quad (39)$$

Then, zone temperatures are iteratively predicted in the calculation based on the temperature prediction of the room, ECWT, SC from equation 7, 8, 9, 28, 34.

4.7 The impact of the integrated system on indoor environment

The model in COMIS-TRNSYS software was built according to the mathematical equation and inputs were checked. The performance of the integrated system has been numerically studied.

4.7.1 Indoor temperature investigation

The performance of the system was studied in two stages; the steady state condition and the actual weather data.

¹**View factor:** is defined as the fraction of radiation leaving surface [86].

²**Perez model:** This model determined the sky radiation striking the surface using hourly values (from the NSRDB) of diffuse horizontal and direct beam solar radiation. Other inputs to the model included the sun's incident angle to the surface, the surface tilt angle from horizontal, and the sun's zenith angle. Also, this model was recommended by the International Energy Agency for calculating diffuse radiation for tilted surfaces [108].

4.7.1.1 The steady state condition

This stage helps to understand the performance of the integrated system in the indoor environment. This was done under the effect of low/high radiation with/without wind. So, that, the effect of the system was studied during daytime and nighttime (low/high radiation). Also, the effect of the system was studied in the case of very low wind speed (with/without wind). This is due to low wind speed during nighttime.

The effect of wind pressure coefficient on ACH and system performance was studied with different solar radiation intensity. The wind pressure coefficients were taken (0.081) for the northern façade and (-0.040) for the southern façade according to the calculation of C_p^1 at wind direction 360° from the north and zero when there is no wind. The main results showed the increase of ACH with the increase of solar radiation & pressure coefficient as shown in figure (4-12 & 13). Also, indoor ACH is zero in case of no wind and no solar radiation.

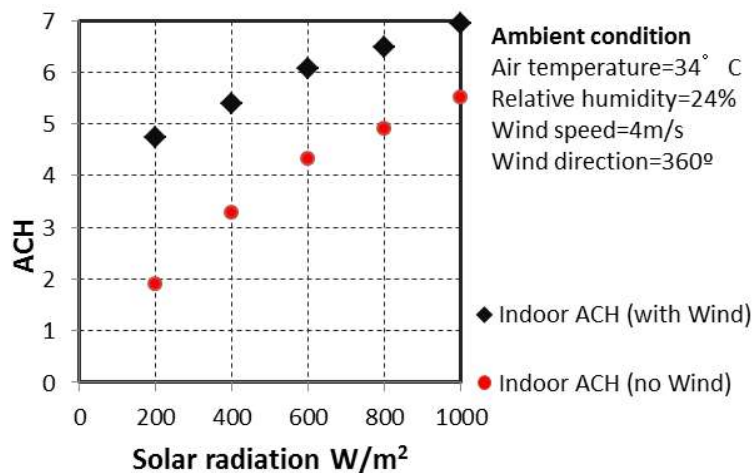


Figure (4-12): The variation of indoor ACH with different solar radiation.

¹See appendix (B).

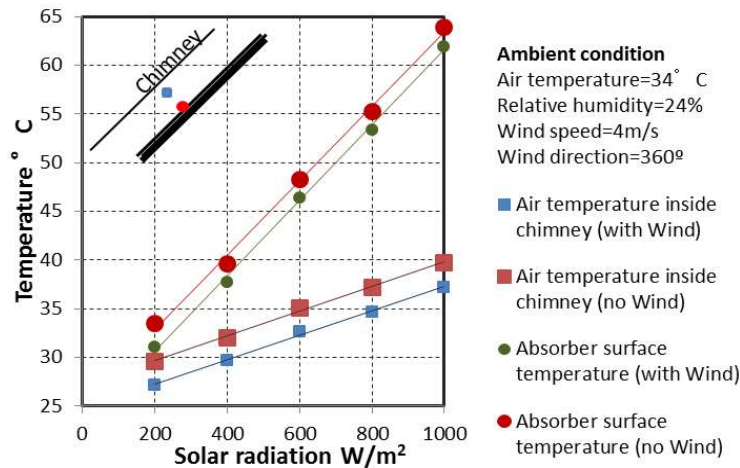


Figure (4-13): The variation of the absorber & chimney temperature with different solar radiation and with/without wind.

It can be seen that the chimney cavity temperature is higher than ambient temperature with high temperature of the aluminum surface (black absorber) that reach 64°C at the radiation level of 1000W/m². Then, the surface temperature of the aluminum decreased to 40°C at the radiation of 400W/m². It can be also seen that the black absorber (Aluminum) has a high temperature value compared to air temperatures of the chimney. This was due to capturing more radiation and storing high thermal energy. This absorbed energy in the chimney accelerates the air through the chimney cavity during daytime and nighttime. As a result, this exit air flow helped entraining more fresh air to the space from the opening of the wind tower.

Also, the effect of different combinations of three values of solar radiation and temperature and two values of relative humidity on indoor environment was studied as a reference value in the steady state condition. The investigation was done at constant wind speed 4m/s (at Meteo), wind direction 360° & wind pressure coefficient (C_p) of (0.081) for the northern facade and (-0.040) for southern facade. The results are shown in table (4-4).

It was concluded that the system was capable to generate 130.5m³/h ventilation rates for a collector area of 2.4m² under the effect of solar radiation only. The

values of these induced air flows depend on the geometry of the air collector and the performance parameters of the solar collector.

Table (4-4): The results of the steady state condition with different combination of solar radiation, temperature & relative humidity.

With wind effect

	Ambient Temp	Solar Radiation w/m2	Ambient Relative Humidity	Indoor room Temp_cooling	Indoor room RH_cooling	Indoor ACH	Indoor m3/h
High radiation	34	1016	17	24.38	52.23	6.93	346.8
			25	25.64	58.65	6.95	347.7
	38		17	27.45	51.39	6.8	340.3
			25	28.91	57.97	6.82	341.2
	42		17	30.52	50.63	6.68	334
			25	32.13	57.53	6.7	335
Moderate radiation	34	425	17	24.33	52.36	5.45	272.9
			25	25.59	58.82	5.48	274.3
	38		17	27.41	51.51	5.34	267
			25	28.83	58.22	5.37	268.5
	42		17	30.48	50.74	5.22	261.3
			25	32.08	57.69	5.25	262.9
No radiation	34	0	17	24.2	52.78	4.28	214.1
			25	25.45	59.31	4.31	215.8
	38		17	27.28	51.91	4.17	208.7
			25	28.7	58.69	4.21	210.5
	42		17	30.36	51.11	4.07	203.5
			25	31.95	58.14	4.1	205.4

4.7.1.2 Actual weather data

In this stage a study was conducted to evaluate the performance of the integrated system during the summer season using real weather data of the New Assiut City. The real weather data were applied in TRNSYS model. It was taken from the typical meteorological year (TMY2)¹ data sets which derived from the 1961-1990 National Solar Radiation Data Base (NSRDB). Investigation of this system in the New Assiut City is needed, because of high solar radiation and high

¹TMY2: are data sets of hourly values of solar radiation and meteorological elements for a 1-year period. It was produced by the National Renewable Energy Laboratory's (NREL's).

average solar brightness up to 12.125 hours per day [10]. Investigation is done in two stages.

First, the performance of single rooms under the effect of solar radiation and occupants was investigated without indoor air flow or applied cooling system. Five day data during June is chosen between June 19th to June 24th, because 20 June is the hottest day in the summer season of the weather data file. Figure (4-14) shows the indoor air temperature of single room without any cooling system. It is clear that there is a difference in time lag between the maximum peak of outdoor and indoor temperature. This is due to high indoor thermal mass with no internal ventilation.

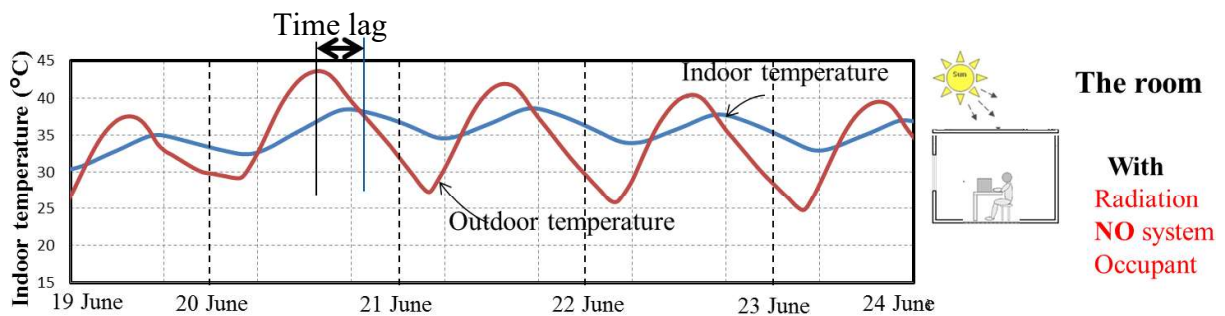


Figure (4-14): Indoor temperature of single room without any cooling system.

Second, the integration of the inclined solar chimney with a short wind tower in the room was studied according to the input parameters and the previous mathematical calculation. The performance of the system on indoor environment was studied during the same five days of June as shown in figure (4-15).

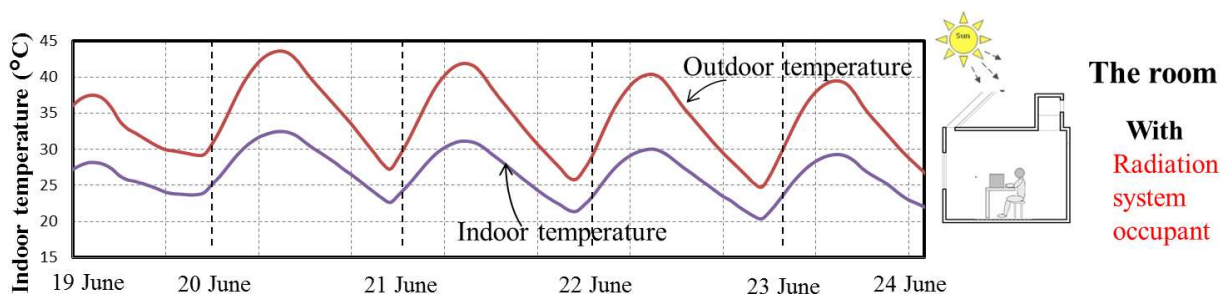


Figure (4-15): The influence of the integrated system on indoor temperature.

It is clear that, indoor temperature decreases with high ventilation rates without any time lag between outdoor and indoor after installing the system. Theoretically speaking, this is because outdoor air that flows through the pads is cooled to a temperature close to the WBT and sinks down [49]. Then, indoor air of the building, cooled by an evaporative cooling system, is further heated by about 1°C to 3°C above the output air from the evaporative cooling system, depending on the air flow rate of evaporative cooling and indoor heat gained by the building [33]. Figure (4-16) shows the general concept of the cooling in the system.

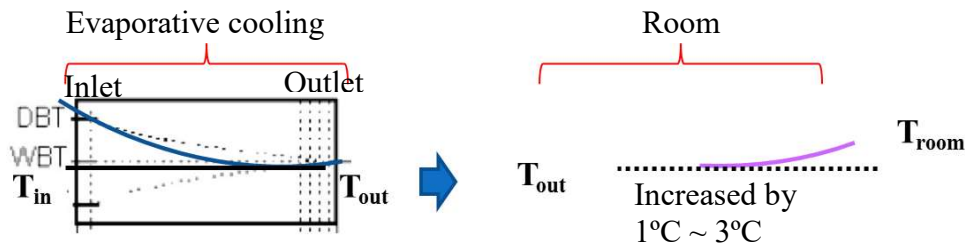


Figure (4-16): The general concept of the system performance.

The performance of the system during the three months of summer (21-May~21-August) was studied. The resulting data are analyzed in relation to ACS. Figure (4-17) shows indoor temperature after applying the integrated system.

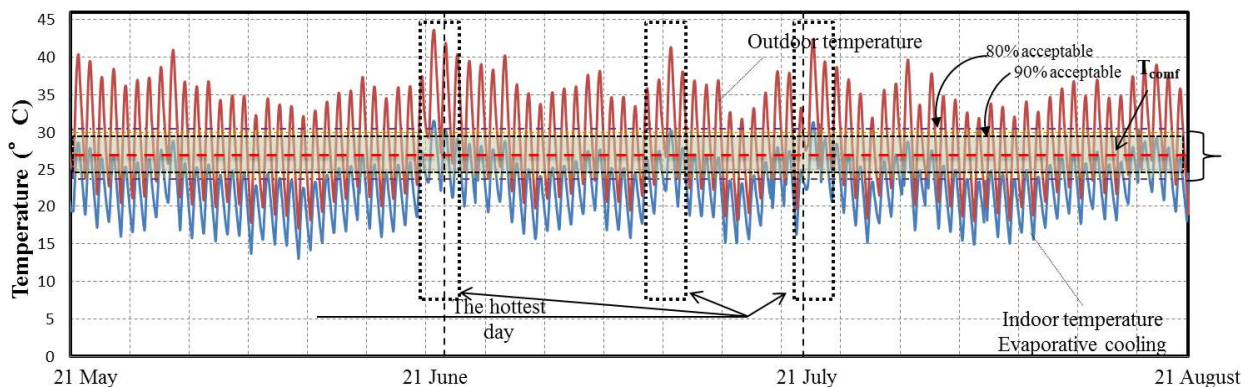


Figure (4-17): The performance of the system during the three months of summer (21-May until 21-August).

It is clear that the system achieves indoor thermal comfort. Only 5% of the resulting data exceeds the upper limit of 80% acceptable range of ACS especially for the hottest days. On the other hand, the system can be controlled or closed during nighttime when the outdoors is less than or equal to 24°C. Figure (4-18) shows indoor temperature of the hottest day in June.

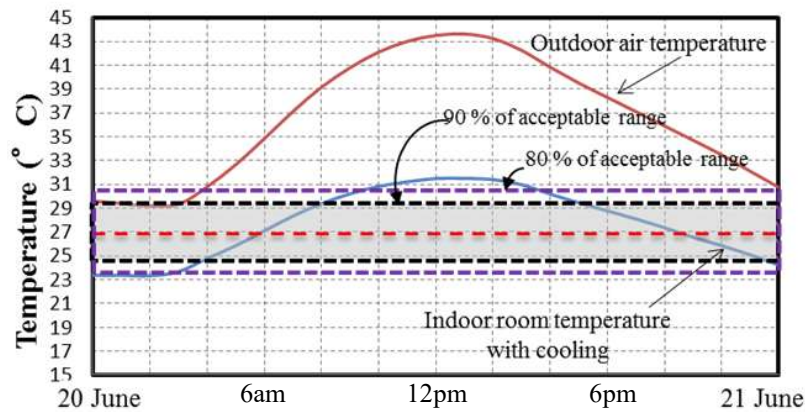


Figure (4-18): The performance of the system for the hottest day of the summer season (20 June).

4.7.2 Evaluation of the humidity environment

Temperature and humidity conditions of the hottest day (20 June) for indoor and outdoor temperature and absolute humidity are plotted in the psychrometric chart of ASHRAE as shown in figure (4-19).

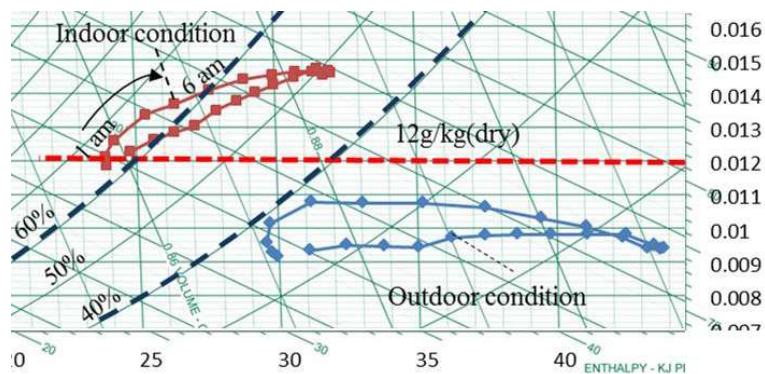


Figure (4-19): The temperature and humidity condition of the system on 20 June.

Arundel et al proposed that low or high humidity strongly affects the health. The optimum humidity level is between 40% and 60% [109]. It is clear from figure

(4-19) that most of the simulation values fall between 40% and 60% of the humidity level except before the sun rise between 12am and 5am. This is due to high outdoor relative humidity that enters the system during that period.

4.7.3 Evaluation of CO₂ concentration in the room

This stage helps to investigate the performance of the integrated system to achieve the acceptable CO₂ with acceptable air flow rate according to the acceptable ASHRAE standard [110].

Carbon dioxide concentration can be calculated based on this equation [97];

$$Q = \frac{K}{(P_i - P_o)} \quad (40)$$

Where,

Q Flow rate (m³/h) = that is generated from the system in simulation.

K CO₂ generation rate per person=23.89 (l/h/person) according to Egyptian body surface area 1.84m² [111] with metabolic rate =1.2 met (69.84W/m²).

P_i The indoor CO₂ concentration needs to be calculated

P_o Outdoor CO₂ concentration=380ppm

Based on the calculation of CO₂ concentration from the resulting air change rate, indoor concentration doesn't exceed 1000 ppm during daytime at a high solar radiation (high system performance) and maximum occupant load. While sometimes before the sunrise especially between 12am and 5am, indoor concentration exceeds 1000ppm especially when indoor air flow rate falls below than 2.3ACH (lower limit) as shown in figure (4-20). This is because, the Aluminum plate of the chimney releases less heat with less surface temperatures. This occurs during the five hours before the sunrise when the wind speeds less than 1.7m/s at Meteo.

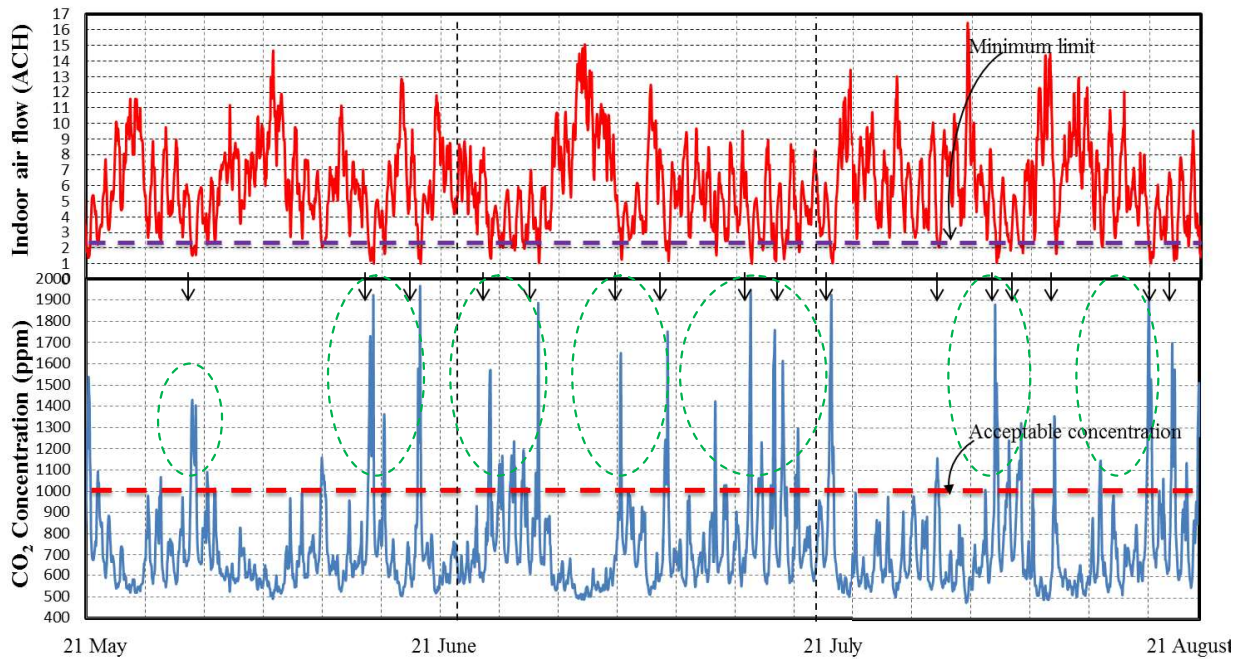


Figure (4-20): Indoor carbon dioxide concentration relative indoor air change rate in the room between May 21th to August 21th.

Conclusion

The present study aims to investigate the effect of inclined solar chimney integrated with short wind tower parameters on indoor ventilation rate and summer thermal comfort of the living room under the climate of the New Assiut City. The temperature of the black absorber affects strongly indoor air change rate with strong relation to outdoor solar radiation. Its temperature reached 64°C with high solar radiation (1000W/m²).

Important conclusions are drawn from the numerical operations for the a new proposal integrated system according to;

Indoor environment

- The system achieves comfort during the hottest days with 95% of indoor temperature below the upper range of 80% acceptable comfort according to ACS with dimensions 1m(width) × 0.2(gap) for solar chimney and 1m(width) × 0.7(depth) for the wind tower.
- Indoor temperature decreased by 10°C~11.5°C compared to the outdoor temperature.

- Most of the humidity levels fall between 40% and 60% of the humidity level except before the sun rise between 12am~5am due to increase of inlet outdoor relative humidity.

Ventilation

- The system is capable of generating 130.5m³/h ventilation rates for a collector area of 2.4m² under the effect of solar radiation only.
- The system achieves the acceptable air change rate with lower CO₂ concentration during daytime (lower than the acceptable concentration 1000ppm).
- While sometimes indoor air flow falls below the lower limit (2.3ACH). This causes an increase of indoor concentration especially during five hours before the sun rise, when the outdoor wind speed is $\leq 1.7\text{m/s}$. This happens when the temperature of Aluminum plate decrease.

The priority of the system is to apply for the hottest period. So, the system can be applied during daytime and nighttime for the summer season. It can be controlled and limited its use during nighttime when indoor temperature becomes very low, especially when the inlet outdoor is $\leq 30.5^{\circ}\text{C}$. These results are for the integrated system in the living room with occupant as a single zone.

Based on these results, parametric investigation and optimization of the important operating parameter needs to be studied in the next chapter. This helps to improve the system performance according to match the climate of the New Assiut city and achieves compact small designs which are easy to integrate into the buildings.



Chapter 5

**Optimization and parametric investigation
for the new proposed system**

Introduction

The proposed system was proposed and its effect on the indoor environment were investigated. System optimization and parametric investigation are so important for the improvement of the system performance, especially for the hot period. A number of factors influence the design of the chimney and its efficiency. These factors are: inclination angle, air gap, length of the chimney, and the height of the chimney. Also, the performance of the wind tower area has a strong effect on ventilation rate and indoor temperature. Several researchers are being conducted in studying optimization and parametric investigation for the solar chimney with passive cooling; Ramadan B. et al. studied some geometrical parameters such as chimney inlet size and width to predict the flow pattern in the room as well as in the chimney. It can be concluded that increasing the inlet size three times only improved the ACH by almost 11%. However, increasing the chimney width by a factor of three improved the ACH by almost 25%. This is happening while keeping the inlet size fixed [62]. Sudaporn and Bundit experimentally investigated the effect of using a vertical chimney with and without a wetted roof to enhance indoor ventilation. They reported that the solar chimney can reduce the indoor temperature by 1–3.5°C depending on the ambient temperature and solar intensity. In addition, spraying water on a roof along with solar chimney can further reduce indoor temperature by 2–6.2°C [67]. The effect of roof solar chimney under different inclination angle on natural ventilation was studied by Mathur et al. The authors found that, the optimum inclination angle of the chimney varies from 40° to 60° with latitude ranges from 20° to 30°. Further, they reported that the air flow rate was 10% higher at an angle of 45° compared to 30° and 60°. In their results, they found that the highest flow rate (190 kg/h) was obtained for inclination angles equal 45° at noon time and an air gap of 0.3 m. Moreover, the optimum inclination angle at any place varies between 40° to 60°, depending upon its latitude [112].

Tawit and Pornsawan studied, a transparent roof used, with an attic room underneath, to create the driving force that induces natural ventilation in the building. They studied different chimney inclination angles and heights for a two floor building. They analyzed the flow streamlines inside the space as well as in the attic room and the vertical chimney. The results showed that, increasing the inclination angle of the roof from 15° to 60° improved the air change per hour (ACH) [113]. Harris and Helwig computationally analyzed the effect of inclination angle on the induced ventilation rate. They reported that the optimum angle for a maximum flow rate was 67.58° from the horizontal. This gives an increase in the ventilation rate by almost 11% compared to the vertical chimney [114].

As a result, there are limitations for the past literatures that studied the effect of different solar chimney parameters on wind tower parameters. Also, the advantage of integrating the two systems are not optimized yet, especially the system dimension. Therefore, parametric investigation and optimization of the integrated system is needed, in order to achieve new compact design and indoor thermal comfort close to 80% acceptable comfort range.

5.1 Optimization methodology

The aim for the system performance is to provide the desired comfortable conditions and a suitable rate of ventilation, depending on several parameters such as (Temperature, solar radiation, relative humidity, wind speed & wind pressure coefficient). Figure (5-1) shows the schematic diagram for the proposed system.

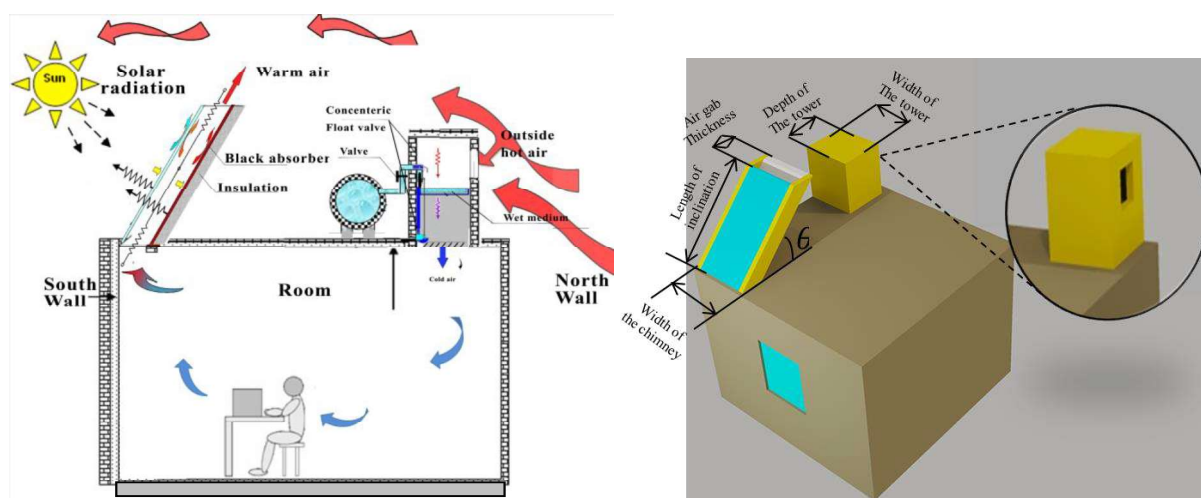


Figure (5-1): Schematic diagram of the solar chimney with evaporative cooler wind tower.

Figure (5-2) shows the flow chart of the optimization procedure.

Parametric investigation is started (in the 1st & 2nd stages) by understanding the effect of each parameter of solar chimney and wind tower on the sensitivity of the system performance under the steady state conditions.

The optimization used the critical outdoor condition¹ for summer season to study the parametric investigation under the steady state conditions. The outdoor input temperature is 38°C, relative humidity is 17% & solar radiation is 600W/m². Then, important parameters from the steady state of the 1st & 2nd stage are chosen to be studied in the third stage using real weather data of the New Assiut city in TRNSYS-COMIS model [86, 94]. So, the third stage aims to study the combination of different parameters that achieves compact and high

¹This condition is chosen to examine the moderate condition on the system performance.

performance system. Real weather data were taken from the typical meteorological year (TMY) data sets [86].

Then, the results of the final stage of optimization were analyzed and compared with the proposed system before optimization according to the comfort range of ACS and ASHRAE psychrometric chart.

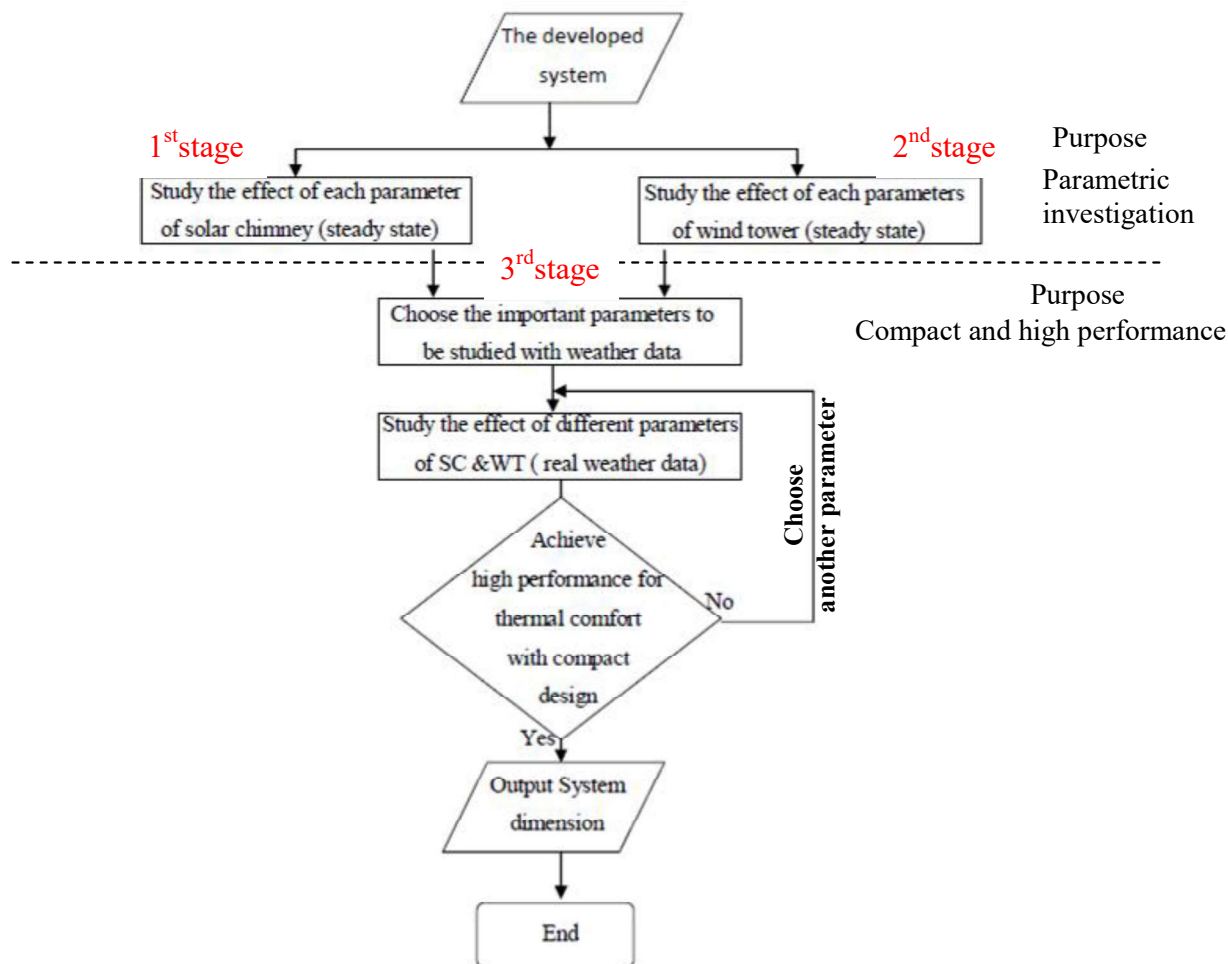


Figure (5-2): Flow chart of the optimization procedure.

Optimization was done for the important dimension parameters of solar chimney and wind tower. While other performance parameters like (absorptance-transmittance of the absorber, discharged coefficient, length between inlet and outlet, $L\cos\Theta$, heat transfer coefficient,... etc.) were kept constant. Also, the inclination length of the chimney was 2m in order not to extend the vertical height (1.5m) according to The Egyptian Building

Regulation Law [81] and the height of the cooling tower was 1m. It was assumed that 1m is the maximum width of the chimney and the tower to be easily integrated into the building. Therefore, the optimization was done under these assumptions and range.

Table (5-1) shows the optimization cases which need to be simulated in the first and second stages of the solar chimney and the wind tower.

Table (5-1): The optimization cases of the first and the second stage.

	Solar chimney	Wind tower	
7 Cases	Inclination angle	Tower width ×	9 Cases
8 Cases	Air gap	tower depth	
12Cases	Width × air gap		

Calculation results are based **on choosing the optimum** parameter. Then, the optimum case can **be used in the next step**.

The optimization process is based on the system operating in the first stage of development (mathematical calculation).

5.2 Parametric studies and optimization

5.2.1 Investigation of solar chimney parameters only under steady state:

a. Effect of solar chimney inclination angle on indoor ventilation rate.

This parameter helps to study the room air flow rate at different chimney inclination angles under the effect of solar radiation. The variation of the air flow in the room depends on the absorber inclination angle. This parameter is studied in two stages according to the optimization structure in figure (5-3);

First stage: The inner flow pattern was predicted as a result of variation of different inclinations with a wide range of angles: 10°, 20°, 30°, 40°, 50°, 60° and 70°.

Second stage: Inclination of the solar chimney is calculated from the equation of the daily optimum angle [115] for the summer season; May, June, July &

August; according to the New Assiut city latitude as shown in table (5-2) and the estimation of the optimum angle is based on this equation;

$$\beta^{opt} = 54.01 + 0.39 \sin(n+10) + 10.04 \cos(n+10) \quad (41)$$

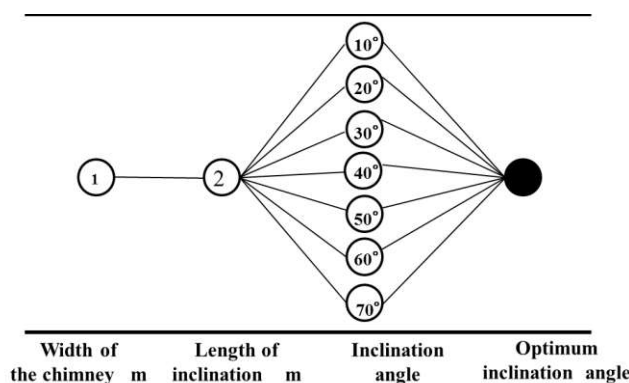
Where n= the day of the year starting from 1 January

Table (5-2): The optimum angle estimation during different months according to Morcos equation.

Month	n	Optimum angle°
1 May	121	59.55893°
1 June	152	55.70149°
1 July	182	44.48528°
1 August	213	44.00483°
1 September	244	45.23041°

Based on the simulation results of the first stage, simulation of detail angle is needed to be studied to check the optimum angle.

Wide range angle
First stage



Calculated angle
Second stage

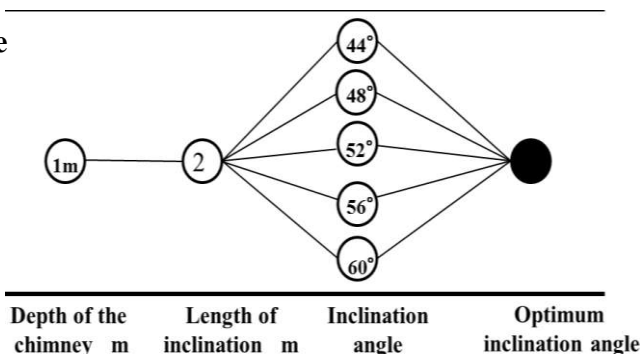


Figure (5-3): Optimization structure of the inclination angle.

Figure (5-4) shows the result of ACH according to different inclination angle. As a result, there is a significant effect of the chimney inclination angle on the

space air flow pattern. These variations of air flow rates depend on the intensity of solar radiation, surface azimuth angle of the chimney & surface tilt with the horizontal. Figure (5-5) shows the effect of different inclination angle on indoor ACH.

It is clear that a small inclination angle of 10° has a high flow resistance and weak flow with low absorption of solar energy. This reduction in stack height doesn't allow the air flow rate to increase. Once the chimney inclination angle increases to 40°, the flow speed increases in the room and the chimney. The optimum flow pattern can be seen for inclination angle 40°. On the other hand, as the chimney inclination angle increases upto 70°, the indoor air flow decreases again. This is due to less absorption of solar energy as shown in figure (5-5).

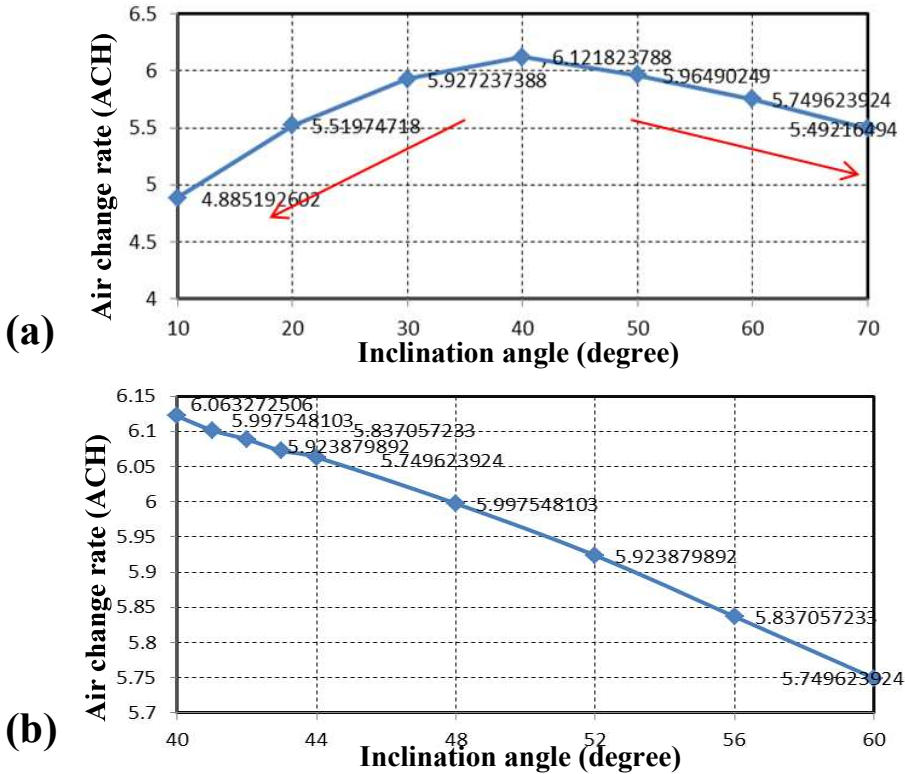


Figure (5-4): The result of ACH according to different inclination angle: (a) wide range of inclination angle in the first stage; (b) angle estimation in the second stage [115].

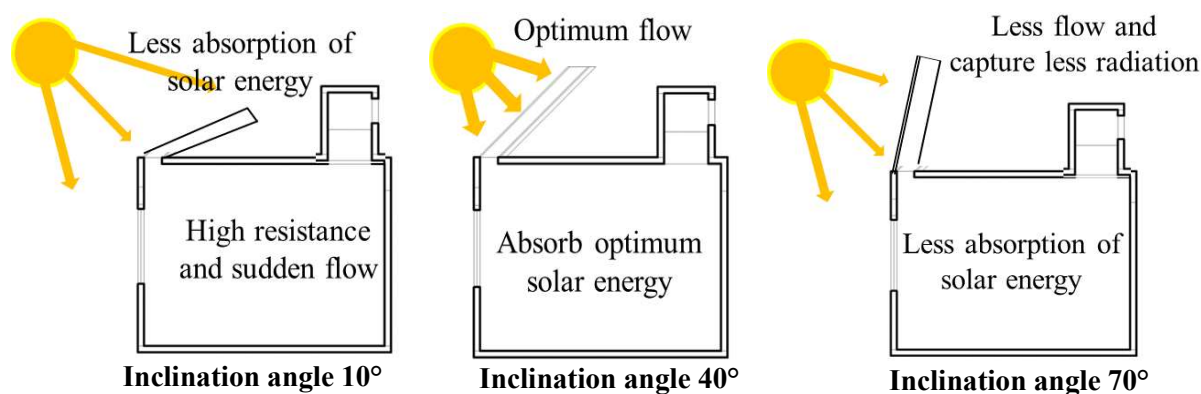


Figure (5-5): The effect of different inclination angles on indoor ACH and chimney solar absorption.

b. Effect of chimney air gap dimension on ventilation rate

The air gap between the absorber (black aluminum plate) and the glass cover plays an important role in chimney ventilation rate. Figure (5-6) shows the optimization structure of the air gap. A wide range of air gap dimensions from 0.1m to 0.8m is investigated.

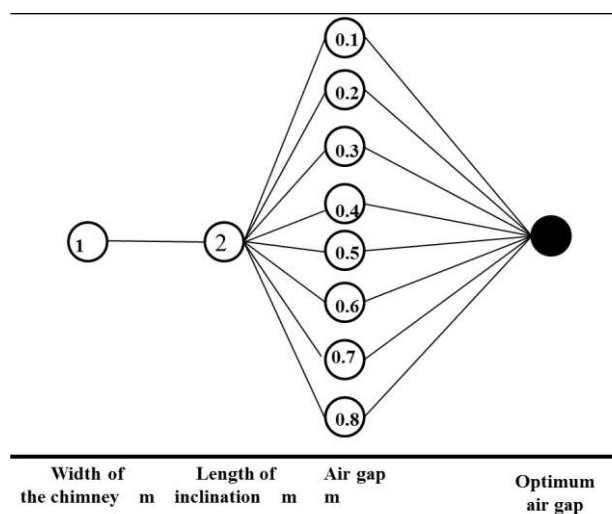


Figure (5-6): The optimization structure of the air gap of the solar chimney.

The variation of chimney air gap on indoor temperature and air change rate is shown in figure (5-7). The results show increasing indoor air change rate with increasing air gap thickness from 0.1m to 0.4m; while the indoor temperature has continued to decrease to 0.4m with a big difference between 0.1m and 0.2m. On the contrary, increasing the air gap thickness over 0.4m has no effect on indoor cooling temperature and air change rate. This is because when the air

gap increases, the convective heat transfer coefficient decreases. According to the calculation of temperature prediction in the solar chimney, the convective heat transfer coefficient¹ is inversely proportional to the air gap thickness as shown in figure (5-8). With the air gap equal to 0.1m, the chimney has high resistance that decreases the flow. Therefore, increasing the chimney air gap would increase the ventilation rate to a certain value.

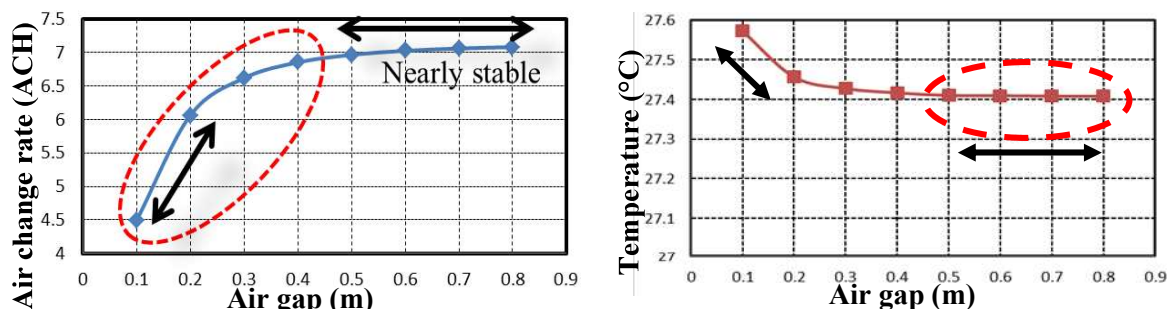


Figure (5-7): The effects of different air gap on indoor air change rate and chimney air temperature.

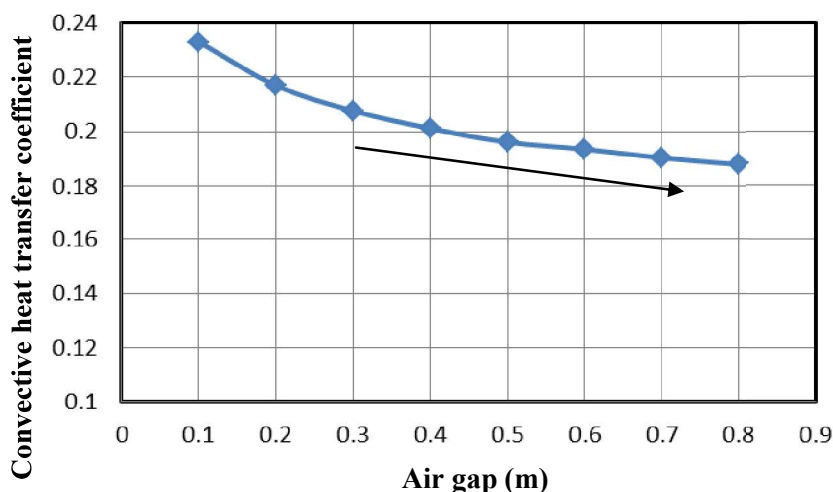


Figure (5-8): The relation between the convective heat transfer coefficient and the chimney air gap

c. Effect of chimney area on ventilation rate

Investigation of big chimney dimension (2, 3, and 4m) as a reference is shown in figure (5-10). Less chimney widths relative to air gap width are required to be investigated in order to study the effect of a combination of different parameters on indoor ACH & indoor temperature. The optimization structure of the

¹According to equation no. 18, 19 in chapter 4.

chimney width with the important parameters of air gap (0.1, 0.2, 0.3, and 0.4m) and chimney width (1, 0.75, and 0.5m) are shown in figure (5-9).

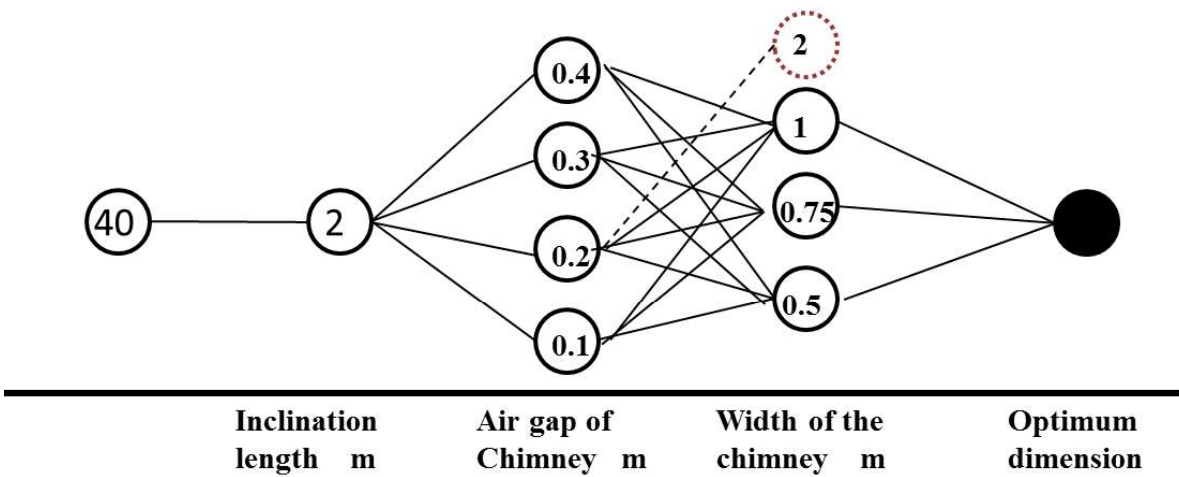


Figure (5-9): The optimization structure of the chimney width and airgap.

Figures (5-10&11) show the effect of the chimney width with different air gap dimensions on indoor air change rates and chimney temperatures.

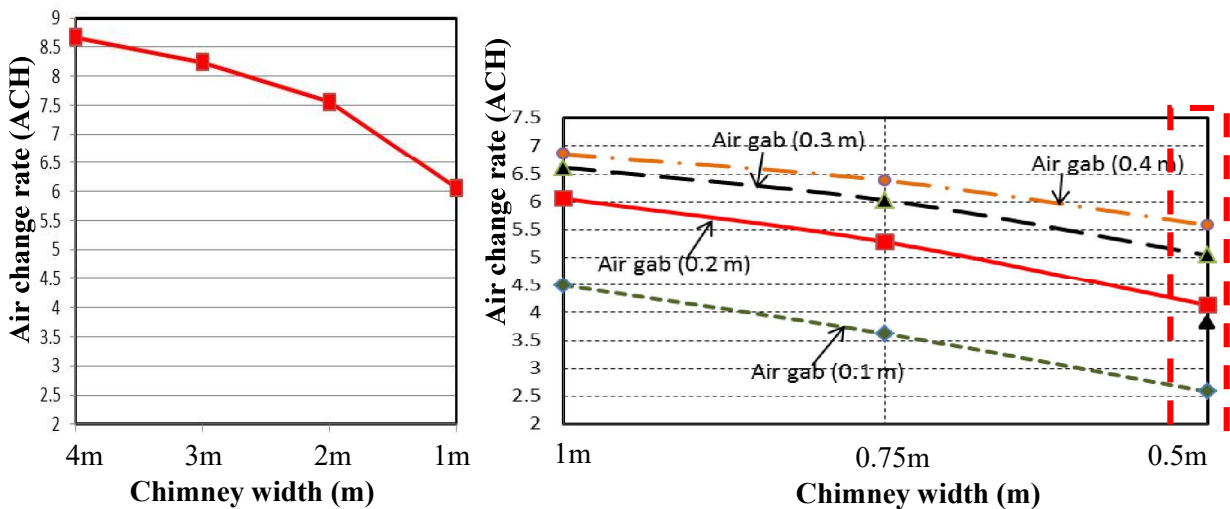


Figure (5-10): The change in ACH under the effect of Chimney width and air gap.

It is clear that indoor air temperature increases when chimney decreases with different air gaps. This happens most for chimney width equal to 0.5m. In addition, an air gap with dimension equal to 0.1m causes high resistance in the chimney which affects air flow through the chimney and indoor air temperature.

Therefore, a chimney width with dimension equal to 0.5m is not advisable in the system. Also, there is no need for extending the chimney width and magnifying the amount of natural ventilation in the room; leading to increasing the cost of the chimney. This is because increasing chimney width causes an increase in indoor temperature with small differences between 1m & 4m.

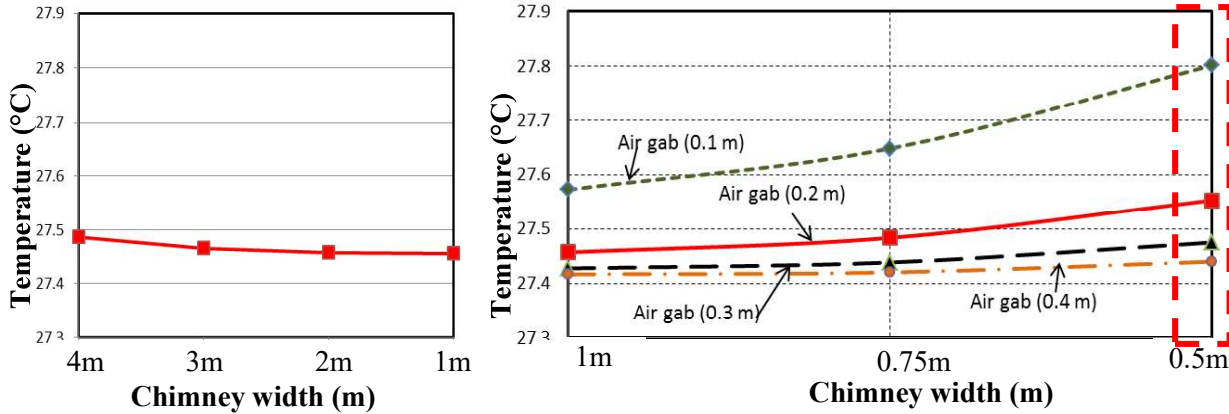


Figure (5-11): The change of indoor temperature under the effect of Chimney width and air gap.

5.2.2 Investigation of tower parameters only under steady state.

It is important to understand the effect of tower depth and width on indoor temperature and the air flow rate, taking into account tower width facing the north preferable wind. The optimization structure of the tower dimension is shown in figure (5-12). Figure (5-13) shows the effect of tower depth and width on indoor air flow rate and indoor temperature.

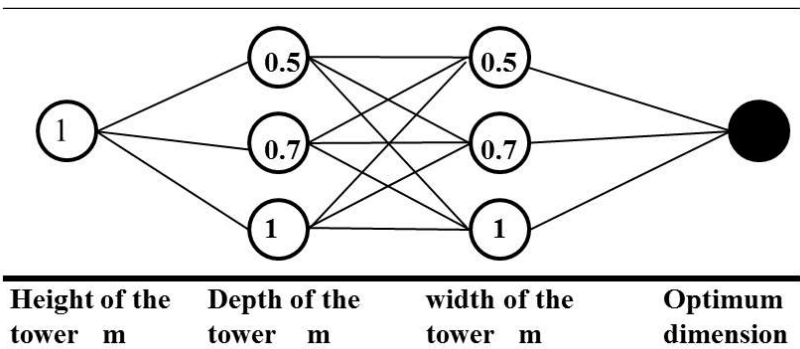


Figure (5-12): The optimization structure of the tower dimension.

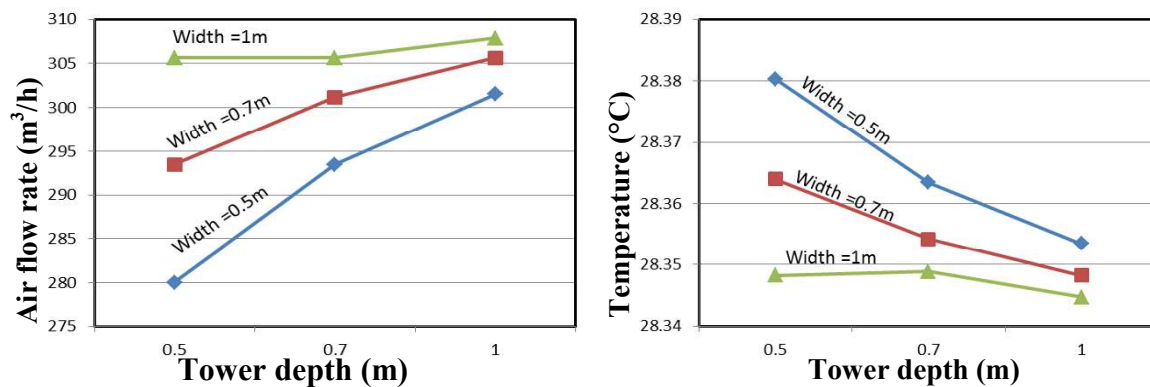


Figure (5-13): The change of ACH & chimney air temperature under the effect of wind tower width and depth.

When the dimension of the tower decreases, low outside air enters the tower with a few layers of air having contact with the wetted pad surface and this decreases the evaporation rate. Therefore, indoor air temperature increases especially for tower depth and width =0.5m. On the other hand, the performance of the system is improved with dimension equal to 1 m for tower width and depth. This causes a decrease in indoor air temperature with more cooling achieved. Moreover, a small increase is achieved for indoor air change rate when the width equals 1m and the depth equals 0.75m & 1m.

Finally, based on the investigation of each parameter of solar chimney and wind tower on indoor temperature and air change rate in 1st and 2nd stages, important parameters will be chosen in the next stage to optimize the system using real weather data. This helps to achieve compact and high performance design.

5.2.3 Selection of important optimization parameters

It is important to understand the criteria for choosing the important parameters of width of the chimney, air gap, and tower width and depth;

a. Width of the chimney

Based on the chimney width investigation, more than 1m increases indoor air temperature (without supporting thermal comfort), and increases the cost of the system. Also for a chimney width equal to 0.5m, indoor air temperature

increases with less air flow rate. Therefore, two important parameters need to be optimized. These parameters are 1m & 0.75m as shown in figure (5-14).

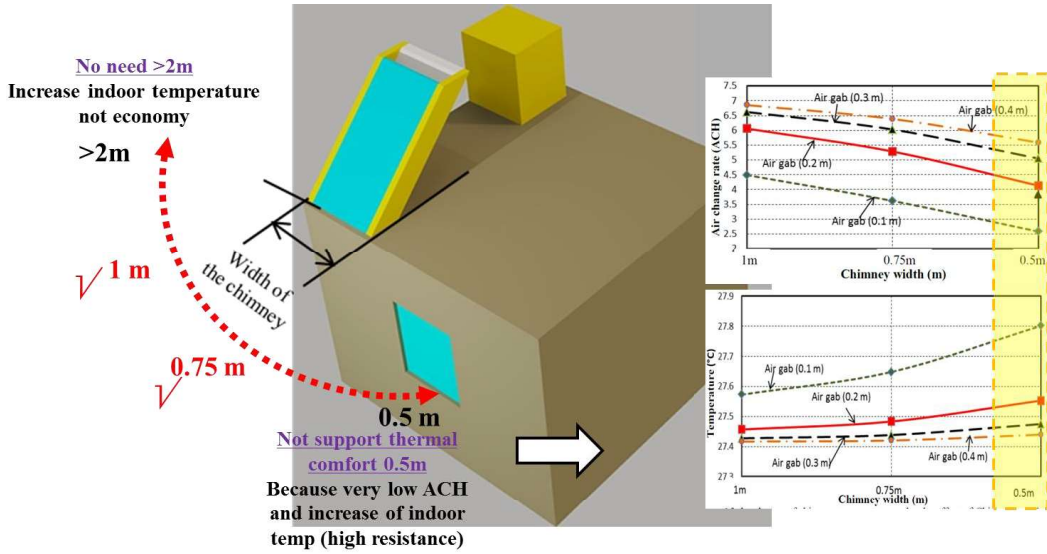


Figure (5-14): The criteria for choosing chimney width parameters.

b. Air gap thickness

Based on the air gap investigation, 0.1m causes a decrease in the air change rate and increases indoor temperature. Also increasing the air gap more than 0.4 has no effect on indoor air temperatures and ACH. Therefore, different air gaps with dimensions (0.2, 0.3, and 0.4m) need to be optimized as shown in figure (5-15).

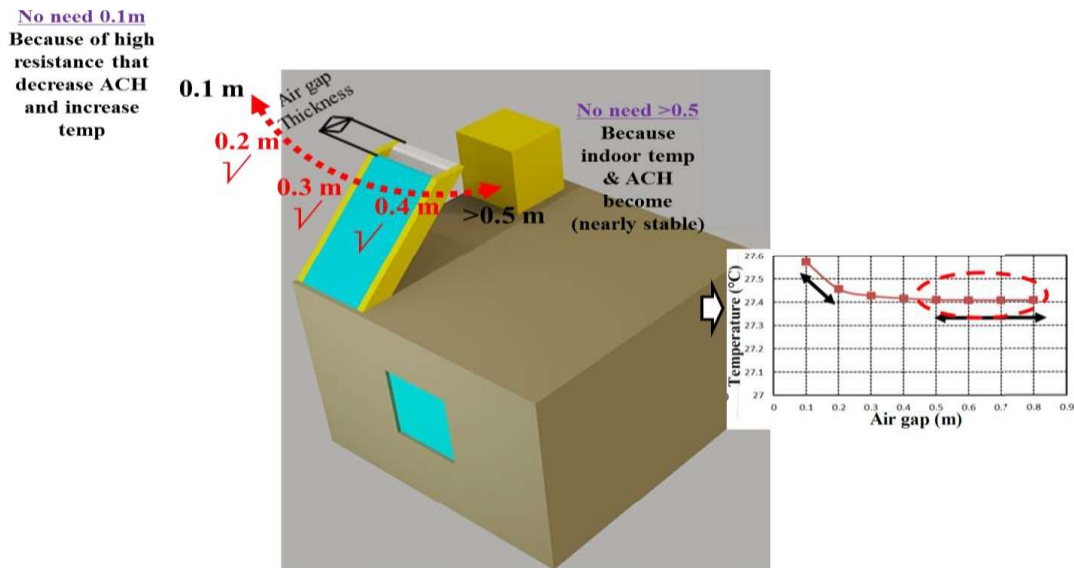


Figure (5-15): The criteria for choosing air gap parameters.

c. Wind tower dimension

Based on the tower dimension investigation, it is concluded that dimension less than 1m for tower width increase indoor air temperature.

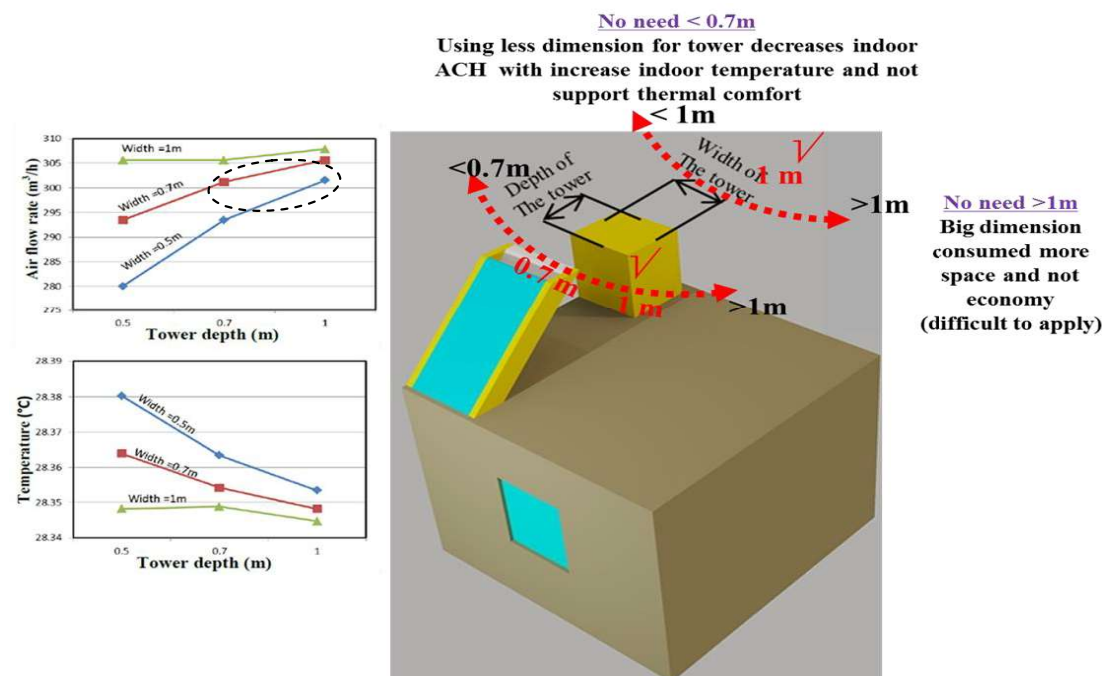


Figure (5-16): The criteria for choosing wind tower parameters.

Thus, this decreases the possibility of achieving indoor thermal comfort. Investigation of 1m for tower width and (1m & 0.7) for tower depth need to be optimized as shown in figure (5-16).

Finally based on the selection of the important parameters, eleven cases need to be investigated using real weather data (typical) for the hottest days in the summer season from 19 June until end of 23 June.

5.3 Optimization of solar chimney and wind tower using real weather data

Two groups in the optimization structure will be investigated using weather data: group A for chimney width equal to 1m with different air gaps 0.2, 0.3, and 0.4m and tower widths equal to 1m and tower depths equal to 1 & 0.7m, and group B for chimney width equal to 0.75m with different air gaps equal to 0.2, 0.3, and 0.4m and tower widths equal to 1m and tower depths equal 1 & 0.7m as shown in figure (5-17).

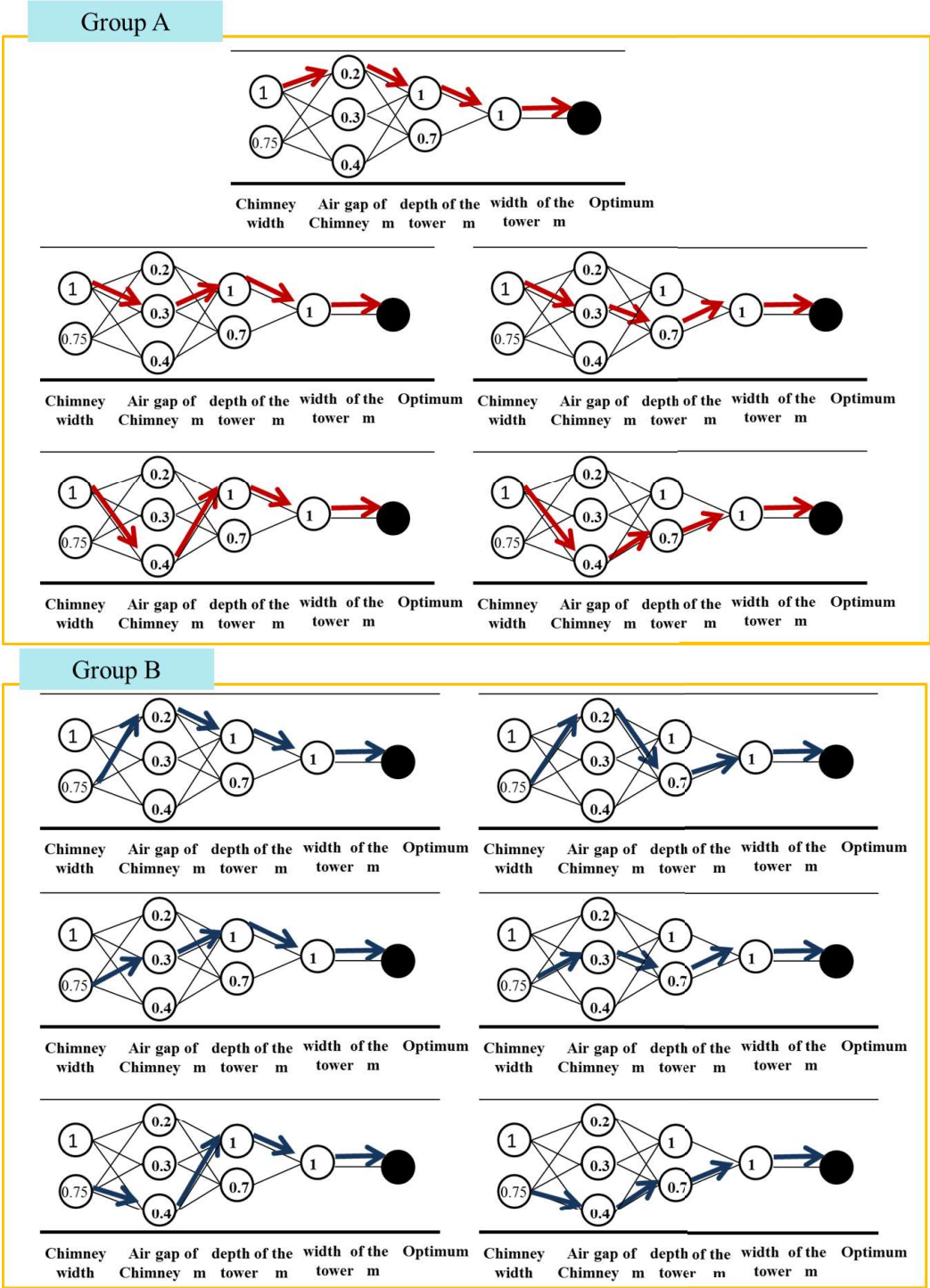


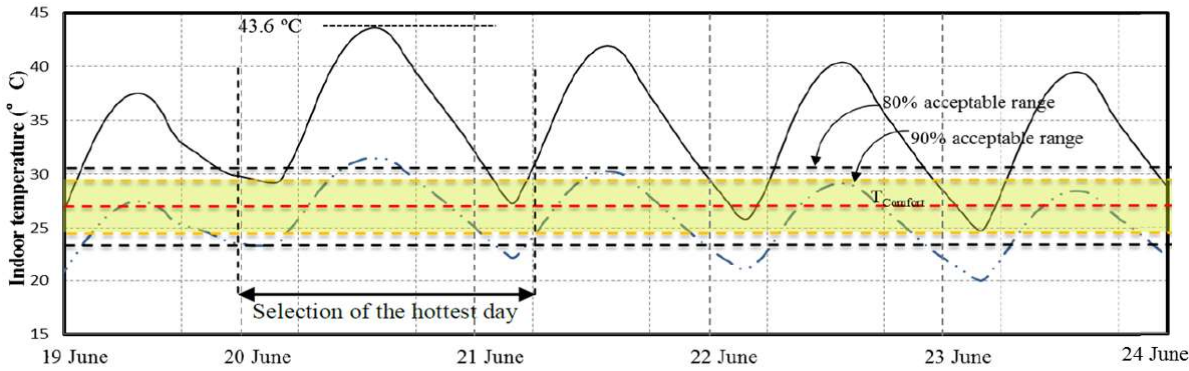
Figure (5-17): The optimization structure for group A & B.

5.3.1 Indoor temperature and air flow rate investigation.

Eleven cases are simulated using real weather data between June 19th and June 23rd. Temperature and air flow rates is monitored. Figure (5-18) shows the proposed system before optimization and the optimum case relative to other 10 cases after the optimization process. The result shows, only one optimum case

with dimension (0.75m × 0.4m) for solar chimney and (1m × 1m) for wind tower achieves a minimum close to the upper range of 80% acceptable comfort range. By selecting the hottest day (June 20th) and comparing the simulation result before and after optimization, the difference between before and after optimization is nearly 1.5°C. Figure (5-19) shows the pattern for the hottest day (20 June).

The proposed system before optimization



The optimum case with relative to other 10 cases

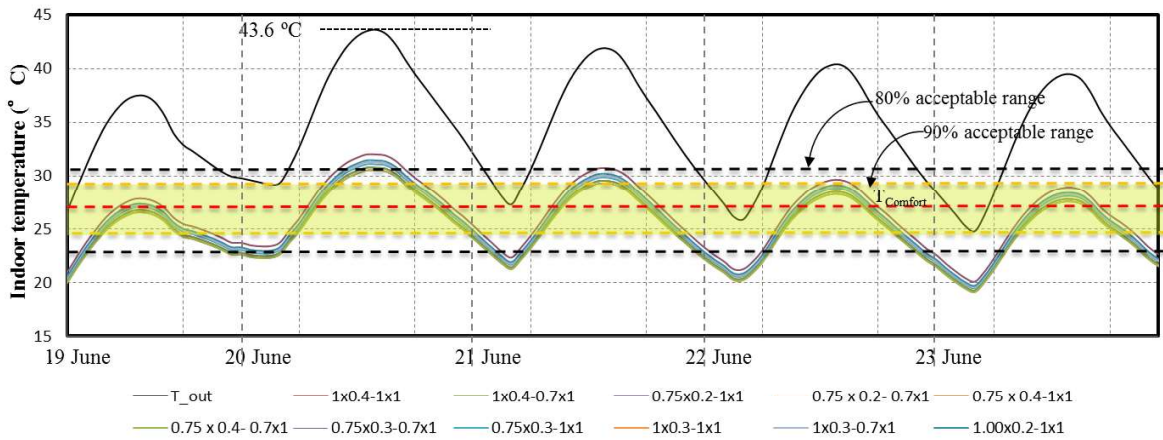


Figure (5-18): Indoor air temperature for the system before optimization and the optimum case after optimization with relation to other 10 cases.

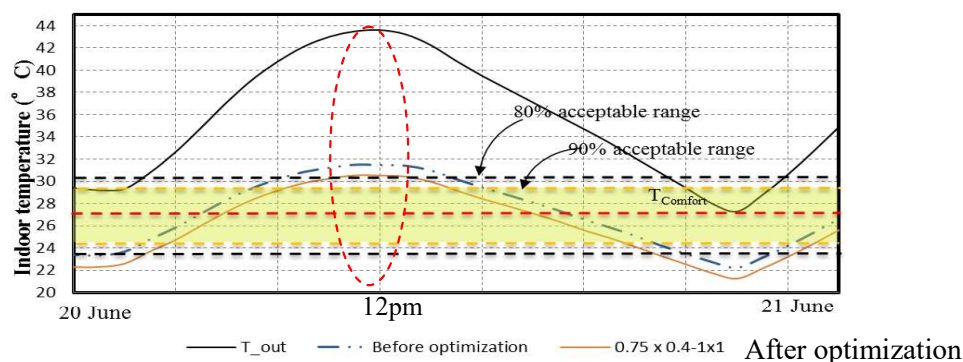


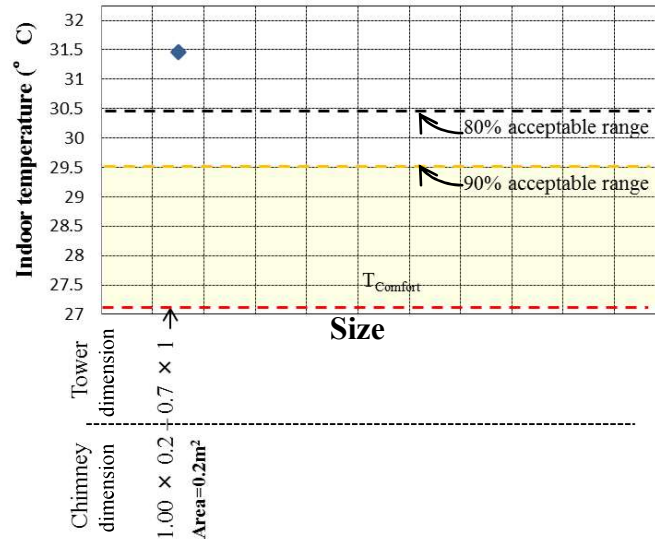
Figure (5-19): Indoor air temperature for the system before and after optimization on 20 June.

Then the results focus on the hottest hour on 20 June, the performance is studied and investigated. Figure (5-20) shows the performance of the system in the hot hour of 20 June for the eleven cases.

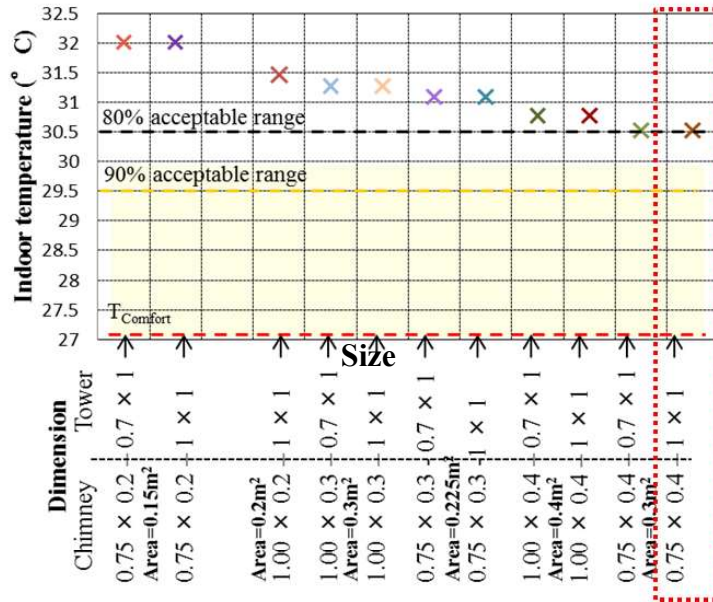
Based on the result in the figure (5-20), only one case nearly achieved the upper 80% acceptable range of ACS.

In order to understand the reason for choosing the optimum case and mechanism, effective ventilation rates need to be studied relative to indoor air temperatures. Figure (5-21) shows the relation between indoor air temperature and indoor ventilation rate (m^3/h). It is clear that increasing the ventilation rate ($>414m^3/h$) inside the room causes indoor air temperature to increase. Also, low ventilation rates ($<414m^3/h$) cause indoor air temperatures to increase. Therefore, the optimum ventilation rate is $414m^3/h$; which achieved the optimum indoor air temperature.

The proposed system before optimization



The optimum case with relative to the other 10 cases.



The system before and after optimization

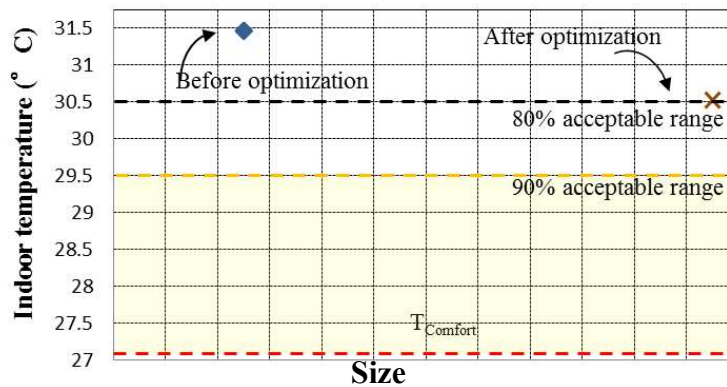


Figure (5-20): The performance of the system in the hot hour during daytime.

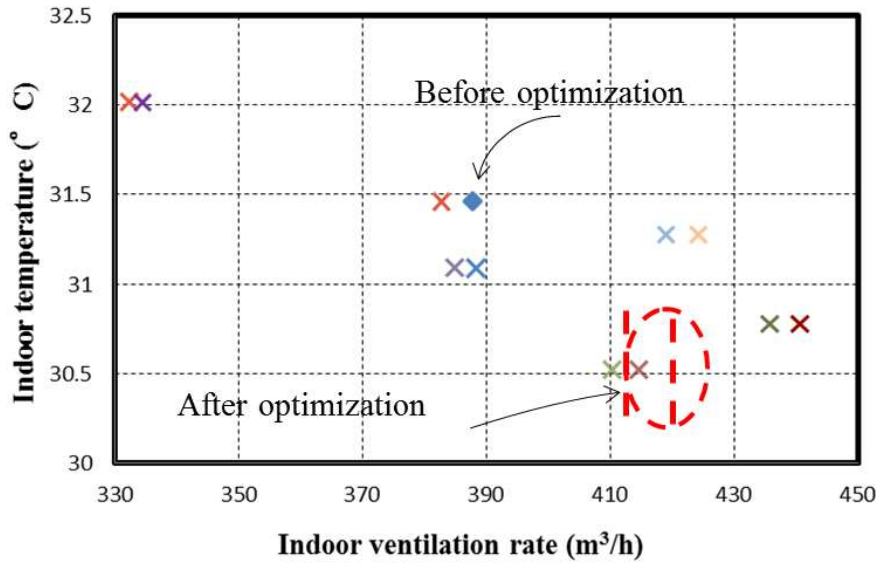


Figure (5-21): The effective ventilation rate in the system after optimization.

Then, indoor air temperature pattern for the system with the optimal dimension from May 21th ~ August 21th was studied. It is clear from figure (5-22) that pattern is located below the upper 80% acceptable comfort range; particularly for the hottest days .

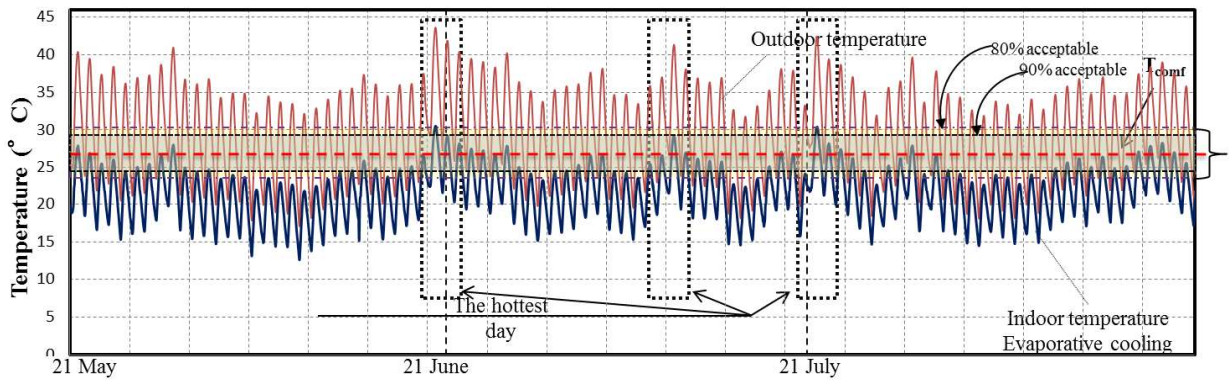


Figure (5-22): Indoor air temperature pattern for the proposed system after optimization between May 21th ~ August 21th.

5.3.2 Evaluation of the humidity environment after optimization.

Based on the summer comfort range of ASHRAE 55 [24] for the acceptable humidity value (12g/kg') and the optimum humidity level for minimizing adverse health effects [109], the absolute humidity of the system after optimization is lower than the system before the system optimization as shown

in figure (5-23). This is because the indoor air temperature decreases with increasing the relative humidity. So, the absolute humidity decreased. All the simulated data fall between the optimum humidity level (40%-60%) except before the sunrise between (1am-5am).

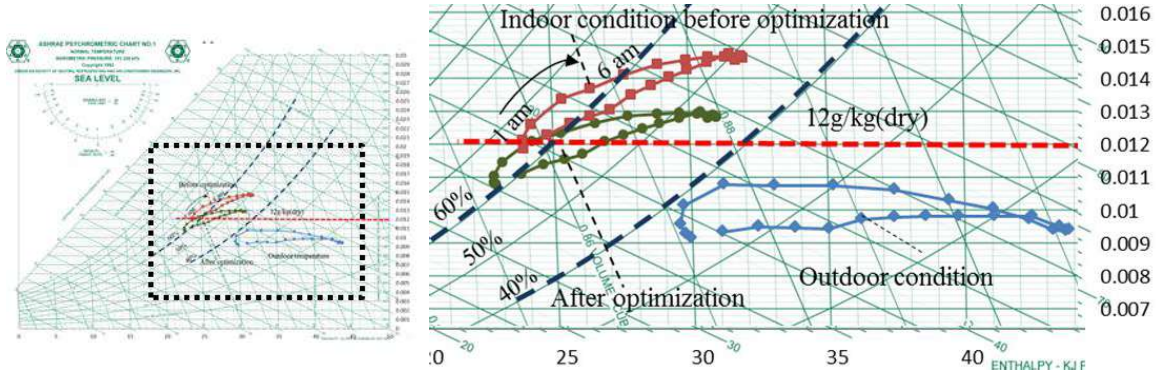


Figure (5-23): The temperature and humidity conditions for the system before and after optimization.

Figure (5-24) shows the pattern of the humidity environment between May 21th ~ August 21th.

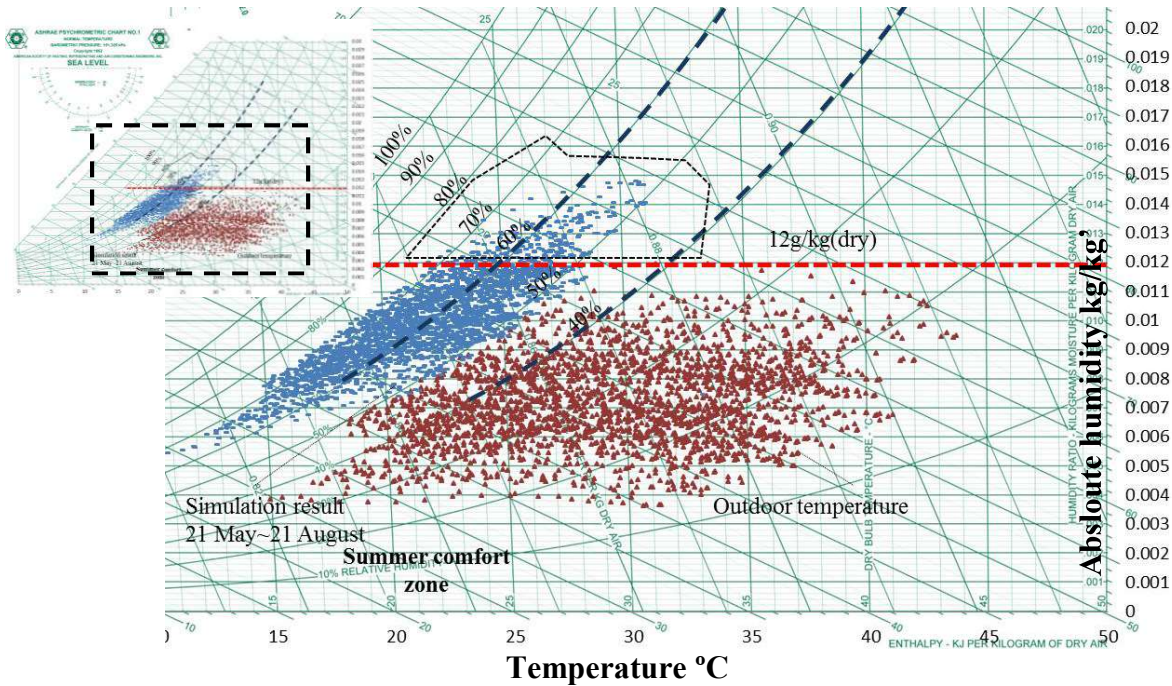


Figure (5-24): Temperature and humidity levels for the system after optimization between May 21st~August 21st.

5.3.3 Evaluation of CO₂ concentration in the room.

Carbon dioxide concentration is calculated in the room from the resulting air change rate. The calculation is based on the equation in the Japanese text book [97]. It is clear that CO₂ concentration doesn't exceed 1000 ppm according to ASHRAE comfort criteria [110], especially during daytime. On the other hand, CO₂ is increased during nighttime, when the indoor air flow rate falls below 2.45ACH (lower limit) as shown in figure (5-25).

Selected data are analyzed and compared with the proposed system before optimization. Also, ACH & the CO₂ percentage difference were calculated between June 19th ~ June 23rd in figure (5-26).

It is clear that the maximum difference (%) in CO₂ concentration before and after optimization is 7.8% to average 3.1% for the selected data. This helps understand the performance of the integrated system on one single zone assuming maximum occupant load (before and after optimization).

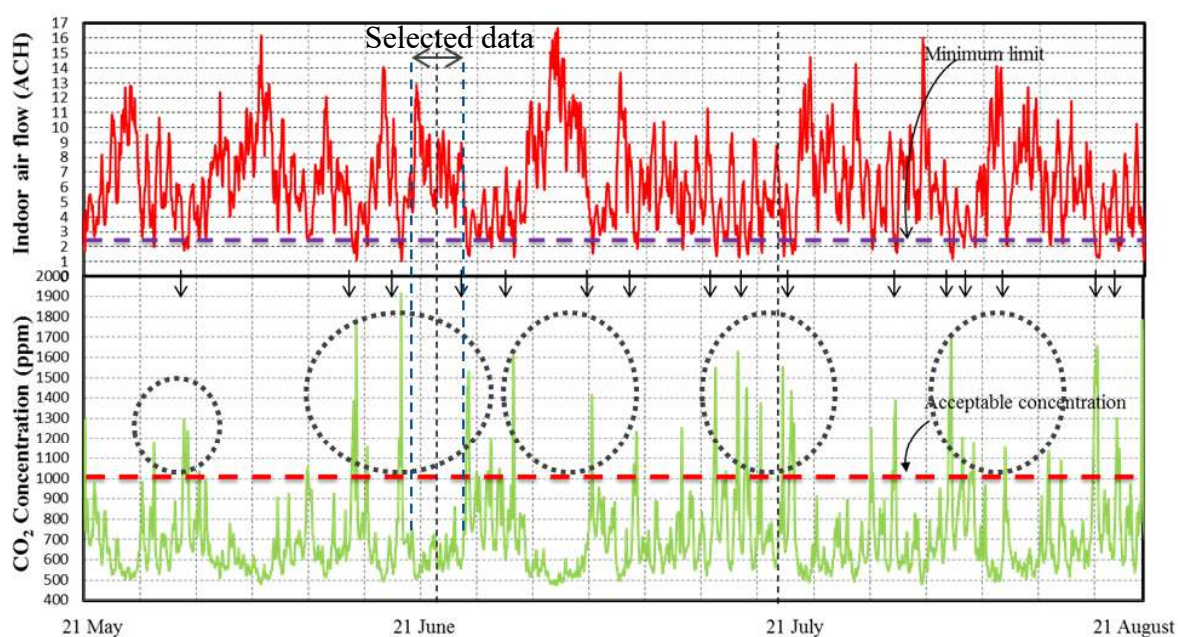


Figure (5-25): The CO₂ concentration pattern and indoor ACH between 21st May~ August 21st.

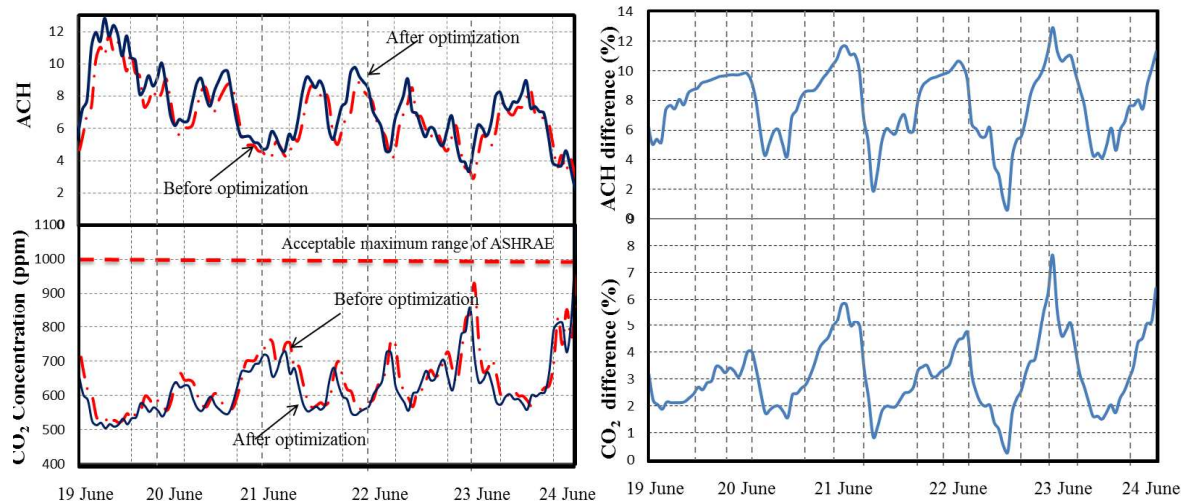


Figure (5-26): The CO₂ concentration and ACH for the proposed system before and after optimization between June 19th ~ June 23rd with the percentage difference.

5.4 The performance of the integrated system.

The performance of the proposed system can be realized from the four cases;

	Case 1	Case 2	Case 3	Case 4
	High solar radiation + Strong wind (Day time)	High solar radiation + Weak wind (≤ 1.7) (Day time)	No solar radiation + Strong wind (Night time)	No solar radiation + Weak wind (≤ 1.7) (Night time)
Cause	↓	↓	↓	↓
	Very high flow rate	High flow rate	Moderate flow rate	Weak flow rate

After optimization, the system achieves high performance during daytime with and without wind as in cases 1 & 2. Also, no effect for indoor environment is achieved in case 3. On the other hand, the performance of the system is weak in case 4 especially during the late hours of the nighttime (before sunrise). This is due to decreasing for Aluminum surface temperature which affects chimney air temperature. This causes weak air movement in the chimney and in the room. Figure (5-27) shows the performance of the system when the wind speed is very low. Thus, the system depends only on the effect of the solar radiation.

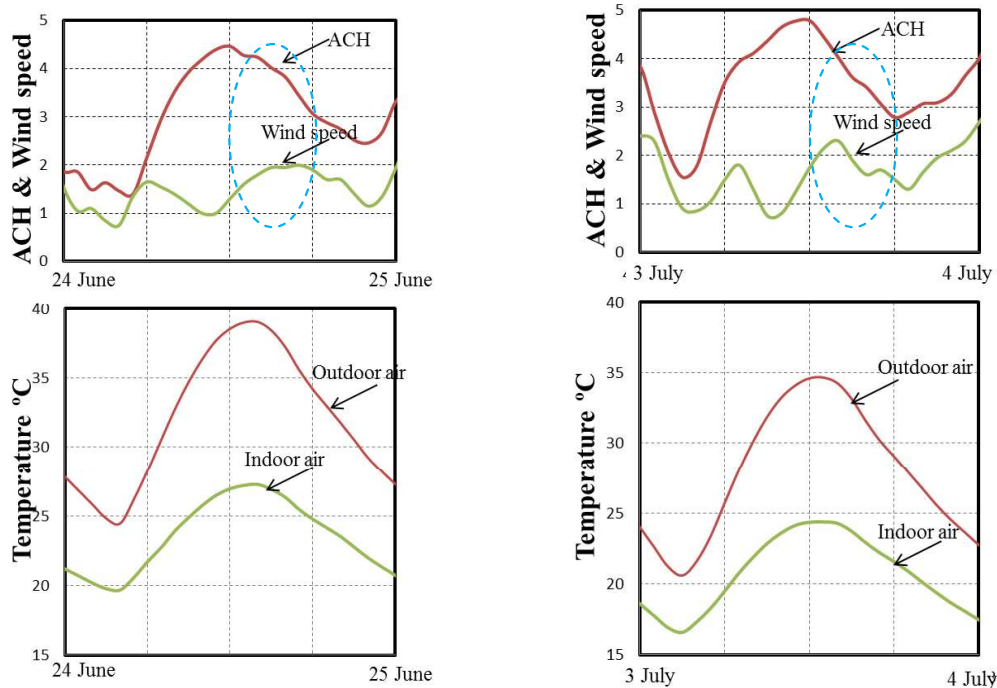


Figure (5-27): The performance of the system under the effect of solar radiation only.

The graph shows, outdoor wind speed affects indoor ventilation rate when it exceeds 1.7m/s during daytime at Meteo, while the indoor ventilation rate increases with increase solar radiation.

Conclusion

This chapter aims to optimize the integrated system, in order to achieve compact and high performance design. Important conclusions are drawn from the numerical operations of the system optimization according to:

Design

- The system achieves compact design (small) with dimension 0.75m (width) × 0.4m (gap) for the solar chimney and 1m (width) × 1m (depth) for the wind tower.

Indoor environment

- The system achieves the upper range of 80% acceptable range during the hottest days with the effective ventilation rate equal to 414m³/h for a room of volume 50m³.

- The absolute humidity decreases after optimization than before optimization. Most of the results are located between 40% -60% optimum humidity level except before the sun rise between 1am and 5am.

Ventilation

- The system could achieve the acceptable CO₂ concentration during daytime due to high air change rate. On the other hand, CO₂ exceeds the acceptable range when the air change rate is less than 2.45ACH, particularly between 1am and 5am.
- System limitation appears for low wind speed (less than 1.7m/s) with no solar radiation during nighttime. This lasts for four hours before sunrise.



Chapter 6

Conclusion and future work

6.1 Conclusion

This research studied environmental application to improve indoor air temperature and indoor ventilation rate and CO₂ concentration for houses of low income people, using natural ventilation with a passive cooling system. The research is concluded with a numbers of results:

6.1.1 Understand indoor environment:

The current situation of indoor environment concerning temperature, relative humidity and carbon dioxide concentration in the three houses in the New Assiut City was monitored during the summer season. Three ventilation strategies were investigated. The following conclusions could be drawn:

1. Using natural ventilation with single side ventilation strategy (from case 1 investigation) caused high indoor temperature reached 38°C with small fluctuation in the temperature pattern and high CO₂ concentration reached 1780ppm. This caused thermal discomfort according to ACS and ASHRAE standard.
2. Using natural ventilation with cross ventilation (from case 2 investigation) caused high indoor temperature more than 40°C with high fluctuation in the temperature pattern during daytime and nighttime and low CO₂ concentration less than the acceptable ASHRAE range (1000ppm). This caused high thermal discomfort especially in the living room.
3. The current situation of the three investigated houses (case 1, 2, & 3) in the New Assiut City indicated that a serious problem of discomfort exists when using natural ventilation only. While, using cooling strategy (air-condition) achieved indoor comfort of 80% acceptable range according to ACS but with high energy consumption.

6.1.2 Concerning search for the suitable strategy for that climate

Based on the measurement of outdoor air temperature in the New Assiut City in chapter 2, outdoor dry temperature was analyzed for the suitable strategy for

that climate according to the bioclimatic chart for building design strategies and the feasibility index.

1. It was concluded that the suitable passive strategies for that climate are natural ventilation and direct evaporative cooling.
2. It was suggested that direct evaporative cooling was advisable, when the wet bulb temperature fell below 24°C and the dry bulb temperature fell below 44°C according to outdoor measurement data of New Assiut City (May, June, and July).
3. Due to the limitations of the conventional systems of the past researchers that used natural ventilation and evaporative cooling techniques inside and outside Egypt in chapter three, integration of inclined solar chimney with evaporative cooling wind tower with wet pad (medium) is studied in order to achieve a high advantage of integration, high performance, easy to integrate and compact design especially in the living room of the final floor of New Assiut City.

6.1.3 Investigating for the possibility of achieving indoor comfort using natural ventilation and evaporative cooling.

Numerical modeling of the proposed system in the living room of the top floor was studied using COMIS-TRNSYS software. The inclined solar chimney was integrated into the proposed system to drive air to move continuously without depending on wind speed force only, and depending on strong solar radiation effect. This is due to the rich sunny and clear sky of Egypt. Simulation was done using the real weather data of New Assiut City.

1. The system was capable of generating 130.5m³/h ventilation rate for a collector area of 2.4m² under the effect of solar radiation only.
2. The proposed system decreased indoor temperature by 10°C~11.5°C compared to the outdoor temperature during the period of May 21th and August 21th (summer season).

3. The system achieved comfort during the hottest days with 95% of the indoor air temperature pattern below the upper range of 80% acceptable comfort according to ACS with dimension 1m (width) \times 0.2 (gap) for solar chimney and 1m (width) \times 0.7 (depth) for the wind tower.
4. Optimization of the proposed system was studied to achieve compact and high performance design. The system achieved the upper range of 80% acceptable comfort range during the hottest days of the real weather data. The effective ventilation rate was 414m³/h for a room volume of 50m³ and system dimensions 0.75m (width) \times 0.4m (gap) for the solar chimney and 1m (width) \times 1m (depth) for wind tower.
5. Most of the humidity level (after optimization) during the period of May 21th and August 21th (summer season) located between 40% to 60% of the optimum humidity level except before the sunrise between 1am~5am. This was due to increase of inlet outdoor relative humidity.
6. The proposed optimized system achieved the acceptable air change rate with lower CO₂ concentration during daytime (lower than the acceptable concentration 1000ppm according to ASHRAE standard).
7. In some conditions, indoor CO₂ concentration increased during nighttime especially four hours before the sunrise. This happened, when the indoor air flow fell below the lower limit (2.45ACH) and the outdoor wind speed was \leq 1.7m/s. This was due to decreasing for the Aluminum surface temperature which affects chimney air temperature and air movement in the chimney, especially four hours before the sunrise.

Finally, these results are for the integrated system in the living room of the top floor. They can't be extended to another stage without further simulation.

Based on the outdoor temperature of the real weather data, the total number of hours that need cooling (to reach the 80% acceptable comfort range) are 967h during the three months (Summer season). If air condition is installed in the room with the same condition, energy consumption will be 1701.92

kWh/summer season. While using the new proposed system in the same room without using air condition consumed zero energy for cooling.

6.2 Guidelines for the efficient optimization process

Based on the study of the integrated system on one case of the living room (according to some circumstance), important procedures will be taken into account in the simulation process to apply the integrated system on different living room with different area and different numbers of occupants according to;

1. Defining the objectives:

- a. Achieving the minimum amount of natural ventilation and acceptable CO₂ concentration (1000 ppm of ASHRAE) needed for the zone according to number of occupants. The minimum ventilation rate is based on the equation:

$$Q = \frac{K}{(P_i - P_o)} \quad (42)$$

Where P_i =1000 ppm (maximum acceptable CO₂ concentration)

$$P_o = 380 \text{ ppm.}$$

$$K = \text{CO}_2 \text{ generation} \times \text{number of occupants.}$$

- b. Achieving the acceptable indoor thermal comfort according to 80% acceptable comfort range of ACS.
- c. Achieving the acceptable humidity value of 12g/kg' according to ASHRAE.

2. Defining the variables:

- a. Estimating the pressure coefficient according to different zone dimensions and location based on different wind direction (300°-360°). Then, the result is fed back to COMIS model.
- b. Optimization of the system parameters according to:

Air gap variables ($\geq 0.2\text{m}$)¹, Width of the chimney ($\geq 0.75\text{ m}$)¹, Width of the tower ($\geq 0.5\text{m}$)² and depth of the tower ($\geq 0.5\text{m}$) using real weather data. These parameters will be changed in Type 56 (TRNSYS model) and COMIS model.

- c. Calculating the CO₂ generation (k) of the body surface area multiplied by the number of occupants according to occupant activity (met).

3. Performing the simulation for the created solution according to:

- a. The same sequence of the input parameters for COMIS and TRNSYS in appendix (B). Input parameters are based on the flow chart of the solving procedure. These COMIS input parameters are duct properties, opening parameters, zone parameters, environment building parameters, and wind pressure coefficient. While TRNSYS input parameters are weather data, sky temperature, psychrometric, evaporative cooling, TRNbuild, and online parameters.

- b. Changing the important parameters for each case of optimization process:

For the solar chimney; chimney volume, area of collector, east & west area, and massless (inlet & outlet opening area of the chimney).

For the wind tower; width and depth of the tower, height of the tower, volume of the tower, area of the opening of the tower, and the net area of the tower opening to the room.

- c. Selection for some range of cases based on combination of the important parameters that affect strongly ACH and air temperature in order to save time and cost. Solar chimney width and tower width³ will

¹Less than 0.2m for air gap and 0.75m for chimney width have high resistance that decreases the flow.

²Due to the cooling mechanism of the tower; Tower dimension less than 0.5m decreases the evaporation rate of air due to few layers of air having contact with the wetted pad surface. Therefore, the tower can't provide much cooling.

³Chimney width is important for the solar chimney, in order to capture more solar radiation that influence Ach and ventilation. While the tower width faces north wind.

be chosen in the initial stage. Then, selection for the big, medium, and small range for air gap and tower depth.

4. Making design decisions:

Choosing the optimum system dimension based on the important output parameters (air change rate, indoor air temperature, indoor relative humidity). One optimum parameter will be achieved for the integrated system based on the above objective.

So, a rough estimation for the optimum value will be done to help designers to optimize different living room. Therefore, this research produced optimization process for not only one special case but also guideline for efficient optimization for other cases (living rooms).

6.3 Further work

- Further research is required to integrate heat storage materials (PCM)¹ with black aluminum in the solar chimney. This helps to increase heat stored during daytime with low heat released during nighttime. Thus, high ventilation rate is achieved during nighttime in order to overcome the limitations of the system, particularly for CO₂ concentration in the late four hours the sunrise.
- Economical studies for the integrated system are needed.
- Further investigation is required to examine the effectiveness of the proposed system to be integrated on the top floor of an apartment using experimental studies in a test building.
- Also, investigation using simulation is required to multi floor building (high rise building) occupied by low income people to achieve indoor

¹ It is a substance with a high heat of fusion which, melting and solidifying at a certain temperature, It is capable of storing and releasing large amounts of energy. It has many applications for building integration that improve indoor environment, reduce energy consumption, reduce pollutant emissions,...etc.

thermal comfort with acceptable ventilation rates. Hence, experimental studies will be conducted in a test building.

This research could provide an economical and potential passive alternative to the conventional air conditioning systems in hot & dry climates with no energy consumed for cooling. It can be an alternative solution for indoor thermal comfort for the living room of the top floor apartment.

References are arranged according to their appearance in the manuscript.

1. The central agency for public mobilization and statistics, (2012),: “*Statistical year book*”, (cited March 2013), Available from: <http://capmas.gov.eg/pdf>
2. World maps of Köppen-Geiger climate classification, (cited June 2012), Available from: <http://koeppen-geiger.vu-wien.ac.at/>
3. Medhat M. A. Osman, (2011),: “*Evaluating and enhancing design for natural ventilation in walk-up public housing blocks in the Egyptian desert climatic design region*”, Ph.D Thesis (unpublished work style), Dundee School of Architecture, university of Dundee.
4. HBRC. Code: ECP 306-2005, (2006),: “*The Egyptian Code for enhancing energy use in buildings*”, Housing and Building Research Center (HBRC), Cairo, Egypt.
5. Ayman Hassaan A. Mahmoud, (2011),: “*An analysis of bioclimatic zones and implications for design of outdoor built environments in Egypt*”, Building and environment, Vol. 46, P. 605-620.
6. National Oceanic and Atmospheric Administration [NOAA], (cited November 2011), Available from: www.climate-charts.com
7. Amr Sayed, (2009),: “*An Evaluation of land allotment policies for low-income housing in the New Egyptian*”, Master Thesis (unpublished work style), Department of Architecture, Faculty of Engineering, Assiut University, Egypt.
8. New Urban Communities Authority [NUCA],: “*New cities*”, (cited 2008), Available from: www.urban-comm.gov/cities.asp
9. New Urban Communities Authority Portal [NUCAP],: “*The National Housing Project*”, (cited April 2013), Available from: http://www.newcities.gov.eg/english/aboutUs/Authority_projects/Housing_projects/National_Housing/default.aspx
10. Riyadh El-Shamery, (2006),: “*The impact of climatic conditions on the urban desert communities in Upper Egypt Assiut city as an example of the*

- new Applied*”, Master Thesis (unpublished work style), Department of Architecture, Faculty of Engineering, Assiut University, Egypt.
11. Wael Sheta, Steve sharples, (2010),: “*A building simulation sustainability analysis to assess dwelling in a new cairo development*”, Fourth National Conference of IBPSA-USA, New York, P. 94-101.
 12. Abdeen MO., (2008),: “*Renewable building energy systems and passive human comfort solutions*”, Renewable and Sustainable Energy Reviews, Vol. 12, No.6, P. 1562-1587.
 13. Etzion Y, Pearlmutter D, Erell E, Meir IA., (1997),: “*Adaptive architecture: integrating low-energy technologies for climate control in the desert*”, Automation in Construction, Vol.6, P. 417-425.
 14. Abd El-Monteleb M. Ali, (2001),: “*The desert climate and architecture*” (book style), 1st Edition, New El-Ofest, Assiut, Egypt.
 15. Shady Attia, (2006),: “*The role of landscape design in improving the microclimate in traditional courtyard-buildings in hot arid climates*”, PLEA2006, Geneva, Switzerland.
 16. M. A. Yaghoubi, A. Sabzevari, and A. A. Golneshan, (1991),: “*Wind towers-Measurement and performance*”, Solar Energy, Vol. 47, No. 2, P. 97-106.
 17. Mehdi N. Bahadori (1994),: “*Viability of wind towers in achieving summer comfort in the hot arid regions of the middle east*”, Renewable energy, Vol.5, P. 879-892.
 18. M. Zimmermann, H.-J. Althaus, A. Haas, (2005),: “*Benchmarks for sustainable construction: A contribution to develop a standard*”, Energy and Buildings, Vol. 37, P. 1147-1157.
 19. IEA, (2011),: “*Promoting Energy Efficiency Investments*”, (cited April 2012), Available from:
http://www.iea.org/publications/freepublications/publication/25recom_2011.pdf
 20. S.M. Robaa, (2003),: “*Thermal human comfort in Egypt*”, Journal of Meteorology, Vol. 28, No. 283, P. 359-371.

21. Google satellite map, New Assiut city (27.267295,31.291723), (cited June 2012), Available from: <https://maps.google.com.eg/maps?hl=en>
22. Development authority of New Assiut city, (December 2008).
23. U.S Department of energy, Building Energy Software Tools Directory, (cited August 2012), Available from: http://apps1.eere.energy.gov/buildings/tools_directory/subjects_sub.cfm
24. ASHRAE Standard 55, (2004),: “*Thermal Environmental Conditions for Human Occupancy*”, America Society of Heating Refrigerating and Air-Conditioning Engineers, Inc , Atlanta, USA.
25. ASHRAE standard 62, (2001),: “*Ventilation for Acceptable Indoor Air Quality*”, America Society of Heating Refrigerating and Air-Conditioning Engineers, Inc, Atlanta, USA.
26. ANSI/ASHRAE 62, (1989),: “*Ventilation for Acceptable Indoor Air Quality*”, America Society of Heating Refrigerating and Air-Conditioning Engineers, Inc, Atlanta, USA.
27. B. Givoni, (1992),: “*Comfort, climate analysis and building design guidelines*”, Energy and building, Vol. 18, P.11-23.
28. Pat Quinn, (2011),: “*Environmental Health-Fact sheet*”, Illinois Department of Public Health Guidelines for Indoor Air Quality, (cited August 2012), Available from: http://www.idph.state.il.us/envhealth/factsheets/indoorairqualityguide_fs.htm
29. Yan You, Can Niu, Jian Zhou, Yating Liu, Zhipeng Bai, Jiefeng Zhang, Fei He, Nan Zhang, (2012),: “*Measurement of air exchange rates in different indoor environments using continuous CO₂ sensors*”, Journal of Environmental Sciences, Vol. 24, No. 4, P. 657-664.
30. Indoor Air Quality Management Group, (2003),: “*Guidance Notes for the Management of Indoor Air Quality in Offices and Public Places*”, (cited March 2013), Available from: <http://www.iaq.gov.hk/cert/doc/GN-eng.pdf>

31. G.Z. Brown and M. Dekay, (2001),: “*Sun, Wind & Light: Architectural design strategies*” (book style), ISBN 0-471-346877-5, Second edition, John Wiley & sons, Inc, USA, P. 54-55.
32. B. Givoni, (1991),: “*Performance and applicability of passive and low-energy cooling systems*”, Energy and Buildings, Vol. 17, P. 177-199.
33. B. Givoni, (1994),: “*Passive low energy cooling of buildings*” (book style), ISBN: 0471284734, Wiley, 1st edition, Ch.5.
34. G. Heidarinejad et al., (2007),: “*Heat and mass transfer modeling of two stage indirect/direct evaporative air coolers*”, ASHRAE journal, Thailand.
35. J. R. Camargo, C. D. Ebinuma, and S. Cardoso, (2006),: “*Three methods to evaluate the use of evaporative cooling for human thermal comfort*”, Journal of thermal engineering, Vol. 5, No. 2, P. 9-15.
36. Watt J. R., (1986),: “*Evaporative air conditioning handbook*” (book style), ISBN 0-412-011514, 2nd edition, Chapman and Hall Publishers,.
37. Capeluto, I.G., (2004),: “*A methodology for the qualitative analysis of winds: Natural ventilation as a strategy for improving the thermal comfort in open spaces*”, Building and Environment, Vol. 40, No.2, P. 175-181.
38. Allard F., Santamouris M., Alvarez S., (1998),: “*Natural ventilation in buildings a design handbook*” (book style), ISBN 1-873936-729, James & James, London.
39. Hans Rosenlund, (2000),: “*Climatic design of buildings using passive techniques*”, Building issues, Vol.10, No.1, P.1-26.
40. Pow Chew Wong, (2008),: “*Natural ventilation in double-skin façade design for office building in hot and humid climate*”, Ph.D thesis (unpublished work style), University of new south wales, Australia.
41. Cardinale N., M. Micucci, F. Ruggiero, (2002),: “*Analysis of energy saving using natural ventilation in a traditional Italian building*”. Energy and buildings, Vol.35, P. 153-159.
42. Naghman Khan, Yuehong Su, Saffa B. Riffat, (2008),: “*A review on wind driven ventilation techniques*”, Energy and Buildings, Vol.40, P.1586–1604.

43. Martin W. Liddament, (1996),: “*A guide to energy efficient ventilation*” (book style), ISBN 0946075-85-9, Annex V, Air infiltration and ventilation center, Ch.5.
44. B. Givoni, (1976),: “*Man, Climate and Architecture*” (book style), 2nd edition, Applied science publishers LTD, London. P.483.
45. Hazem B. Awbi, (2003),: “*Ventilation of buildings*” (book style), 2nd edition, ISBN 0-415-27056-1[pbk], Spon Press, London.
46. U.S. Army corps of engineers, (2004),: “*Cooling buildings by natural ventilation -Military handbook*” (book style), UFC 3-440-06N ed. Unified Facilities Criteria (UFC), Department of defense, USA.
47. U.S Department of Energy, (2006),: “*Technology installation review*”, (cited December 2012), Available from: www.eere.energy.gov/femp/
48. Zhiyin Duana, Changhong Zhan, Xingxing Zhang et al., (2012),: “*Indirect evaporative cooling: Past, present and future potentials*”, Renewable and Sustainable Energy Reviews, Vol. 16, P. 6823–6850.
49. B. Givoni, (2011),: “*Indoor temperature reduction by passive cooling systems*”, Solar Energy, Vol. 85, P.1692-1726.
50. M. Maerefat, A.P. Haghighi, (2010),: “*Natural cooling of stand-alone houses using solar chimney and evaporative cooling cavity*”, Renewable Energy, Vol.35, P. 2040–2052.
51. Abbas Ali Elmualim, (2006),: “*Effect of damper and heat source on wind catcher natural ventilation performance*”, Energy and Buildings, Vol. 38, P. 939–948.
52. Yuehong Su, Saffa B. Riffat, Yen-Liang Lin, Naghman Khan, (2008),: “*Experimental and CFD study of ventilation flow rate of a Monodraught TM windcatcher*”, Energy and Buildings, Vol.40, P. 1110–1116.
53. Fathy Hassan, (1986),: “*Natural energy and vernacular architecture: Principles and examples with reference to hot arid climates*” (book style), ISBN: 978-0226239170, University of Chicago, Chicago, P. 59, 124, 125.

54. Liu Lia, C.M. Mak, (2007),: “*The assessment of the performance of a windcatcher system using computational fluid dynamics*”, Building and Environment, Vol. 42, P. 1135–1141.
55. Bakr Gomaa, Mark Gillott, (2010),: “*Wind ceiling a novel passive ventilation system for deep plan high rise buildings*”, IAQVE, Syracuse, P. 115-123.
56. Mehdi N. Bahadori, (1985),: “*An improved design of wind towers for natural ventilation and passive cooling*”, solar energy, Vol.35, No.2, P.119-129.
57. K.J. Lomas, D. Fiala, M.J. Cook, P.C. Cropper, (2004),: “*Building bioclimatic charts for non-domestic buildings and passive draught evaporative cooling*”, Building and Environment, Vol. 39, P. 661–676.
58. M.N. Bahadoria, M. Mazidib, A.R. Dehghani, (2008),: “*Experimental investigation of new designs of wind towers*”, Renewable Energy, Vol. 33, P. 2273–2281.
59. Yasmina B., Fatiha B., Azeddine B., (2011),: “*Performance analysis and improvement of the use of wind tower in hot dry climate*”, Renewable Energy, Vol. 36, P. 898-906.
60. N. K. Bansal, Rajesh Mathur, M. S. Bhadari, (1993),: “*Solar Chimney for Enhanced Stack Ventilation*”, Built and environment, Vol.28, No. 3, P. 377-377.
61. W. F. M. Yusoff, Elias Salleh, N. M. Adamb, A. Sopian, M. Y. Sulaiman, (2010),: “*Enhancement of stack ventilation in hot and humid climate using a combination of roof solar collector and vertical stack*”, Building and Environment, Vol.45, P. 2296-2308.
62. Ramadan Bassiouny , Nader S.A. Korah, (2009),: “*Effect of solar chimney inclination angle on space flow pattern and ventilation rate*”, Energy and Buildings, Vol.41, P. 190–196.
63. Ramadan Bassiouny, Nader S.A. Koura, (2008),: “*An analytical and numerical study of solar chimney use for room natural ventilation*”, Energy and Buildings, Vol. 40, P. 865–873.

64. J Hirunlabh, W Kongduang, P Namprakai, J Khedari, (1999),: “*Study of natural ventilation of houses by a metallic solar wall under tropical climate*”, Renewable Energy, Vol. 18, P. 109-119.
65. Z.D. Chen, P. Bandopadhyay, J. Halldorsson, C. Byrjalsen, P. Heiselberg, Y. Li, (2003),: “*An experimental investigation of a solar chimney model with uniform wall heat flux*”, Building and Environment, Vol. 38, P. 893–906.
66. Kwang Ho Lee, Richard K. Strand, (2009),: “*Enhancement of natural ventilation in buildings using a thermal chimney*”, Energy and Buildings, Vol. 41, P. 615–621.
67. Sudaporn Chungloo, Bundit Limmeechokchai, (2007),: “*Application of passive cooling systems in the hot and humid climate: The case study of solar chimney and wetted roof in Thailand*”, Building and Environment, Vol. 42, P. 3341–3351.
68. J. Arce, M.J. Jimenez, J.D. Guzman, M.R. Heras, G. Alvarez, J. Xaman, (2009),: “*Experimental study for natural ventilation on a solar chimney*”, Renewable Energy, Vol. 34, P. 2928–2934.
69. Sompop Punyasompun, Jongjit Hirunlabh, Joseph Khedari, Belkacem Zeghami, (2009),: “*Investigation on the application of solar chimney for multi-storey buildings*”, Renewable Energy, Vol. 34, No. 12, P. 2545–2561.
70. C. Karakatsanist, M. N. Bahadori, B. J. Vicker, (1986),: “*Evaluation of pressure coefficient and valuation of pressure coefficients and estimation of air flow rates in buildings employing wind towers*”, Solar Energy, Vol.37, No. 5, P. 363-374.
71. X.Q. Zhai, Z.P. Song, R.Z. Wang, (2011),: “*A review for the applications of solar chimneys in buildings*”, Renewable and Sustainable Energy Reviews, Vol.15, P. 3757– 3767.
72. M. Macias, J.A. Gaona, J.M. Luxan, Gloria Gomez, (2009),: “*Low cost passive cooling system for social housing in dry hot climate*”, Energy and Buildings, Vol. 41, P. 915–921.

73. Rajeev Kathpalia, Jyotirmay Mathur, (2008),: “*Design of passive cooling system for a building in composite climatic conditions in India*”, International journal of sustainable design, Vol. 1, No. 1, P. 110-126.
74. N. K. Bansal, Rajesh Mathur, M. S. Bhadari, (1994),: “*A Study of Solar Chimney Assisted Wind Tower System for Natural Ventilation in Buildings*”, Built and environment, Vol.28, No. 3, P. 495-500.
75. B. Givoni, (1993),: “*Semiempirical model of a building with a passive evaporative cool tower*”, Solar Energy, Vol. 50, No. 5, P. 425-434.
76. Alemu, T. A., Saman, W. & Belusko, M., (2012),: “*A model for integrating passive and low energy airflow components into low rise buildings*”, Energy and Buildings, Vol. 49, P.148-157.
77. M. Santamouris, D. Asimakopoulos, (1996),: “*Passive cooling of buildings*” (book style), ISBN 1 873936 478, James & James (science publishers) Ltd.
78. Bureau of Indian Standards, (1987),: “*Handbook on functional requirements of buildings*” (book style), ISBN 81-7061-011-7, BIS, Indian.
79. M. Santamouris, (2007),: “*Advances in Passive Cooling*” (book style), ISBN-13: 978-1844072637, Earth scan. London.
80. MN. Bahadori, (1978),: “*Passive cooling systems in Iranian architecture*”, Scientific American, Vol. 238, No.2, P. 144-154.
81. Construction Law, (2008),: “*Urban Planning and coordination of civilization (Unified Construction Law)*”, No. 119.
82. Schaelin A., Dorer V. et al., (1993),: “*Improvement of Multizone model predictions by detailed flow path values from CFD calculation*”, ASHRAE Transactions, Vol. 93, P. 709-720.
83. Furbringer J., Roulet C., Borchiellini R, (1996),: “*Evaluation of Comis: Final report*”, IEA annex 23.
84. Helmut E. Feustel, (1999),: “*COMIS-an international multizone air-flow and contaminant transport model*”, Energy and buildings, Vol. 30, P. 3-18.

85. ASHRAE, (1985),: “*Handbook of Fundamentals*”, American Society of Heating, Refrigerating and Air-Conditioning Engineers, Atlanta, GA, Chapter 22.
86. Klein S. A. et al., (2006),: “*TRNSYS version 16, A transient system simulation program+Mathematical equation*”, Solar Energy Laboratory, University of Wisconsin, USA.
87. Al-Homoud MS, (2001),: “*Computer-aided building energy analysis techniques*”, Building and Environment, Vol. 36, No. 4, P. 421-433.
88. Gouda MM., Underwood CP., Danaher S., (2002),: “*Modeling the robustness properties of HVAC plant under feedback control*”, 6th International Conference of System Simulation in Buildings, Liege, Belgium, P. 16-18.
89. Kalogirou SA., Florides G., Tassou S., (2002),: “*Energy analysis of buildings employing thermal mass in Cyprus*”, Renewable Energy, Vol. 27, No. 3, P. 353-368.
90. Lebrun J., Strengart M., (1986),: “*Simulation of residential heating systems*”, Proceedings of the International Conference System Simulation in Buildings, Liège, Belgium, P. 316-334.
91. Adam Ch., André Ph., (2006),: “*Validation Exercise Applied to Some TRNSYS Components in the Context of IEA34/43*”, AIVC 27th conference - EPIC2006AIVC, Technologies & sustainable policies for a radical decrease of the energy consumption in buildings, Lyon.
92. Kummert M., Bradley D. E., McDowell T. P., (2004),: “*Combining different validation techniques for continuous software improvement – implication in the development of TRNSYS 16.*” The Bi-Annual Conference on IBPSA-Canada, eSIM, Vancouver.
93. M. Hiller, S. Holst , T. Welfonder, A. Weber, M. Koschenz, (2006),: “*TRNFLOW: Integration of the airflow model COMIS into the multizone building model of TRNSYS- Report*”, TRANSSOLAR Energietechnik GmbH, (cited December 2011), Available from: <http://www.trnsys.de>

94. COMIS software version 3.2, (2005),: “*Conjunction of Multizone Infiltration Specialists. Energy Performance of Buildings Group*”, Lawrence Berkeley Laboratory’s, Applied Science Division, USA.
95. Feustel H E, Raynor A H, (1990),: “*Fundamentals of the multizone airflow model-COMIS*”, Annex V Air infiltration and ventilation center. ISBN 0946075441, Berkeley, California.
96. Feustel H E, Dieries J., (1992),: “*A survey of airflow models for multizone structures*”, Energy and buildings, Vol. 18, P. 79-100.
97. Tanaka, T. Iwate, Th. Terao, (2006),: “*Kenchiku kankyo kougaku*” (book style), 3rd edition, ISBN 978-4-7530-1742-3C, Japan, P. 55-60. (Japaness).
98. Elmetenania S., Yousfia M. L., Merabetia L., Belgrouna Z., Chikouche A., (2011),: “*Investigation of an evaporative air cooler using solar energy under Algerian climate*”, Energy Procedia, Vol. 6, P. 573–582.
99. Ong K. S., (2003),: “*A mathematical model of a solar chimney*”. Renewable Energy, Vol. 28, P. 1047-1060.
100. Pica Rodon G., Volpes R., (2004),: “*An experimental investigation on natural convection of air in a vertical channel*”, International Journal of heat and mass transfer, Vol. 36, P. 193-208.
101. Bellorio M. B., & Pimenta J. M. D., (2005),: “*Theoretical analysis of air conditioning by evaporative cooling influence on gas turbine cycles performance*”, 18th International congress of mechanical engineering . Ouro preto.
102. Kulkarni R. K., Rajput S. P. S., (2011),: “*Theoretical Performance Analysis of Indirect-Direct Evaporative Cooler in Hot and Dry Climates*”, International Journal of Engineering Science and Technology (IJEST), Vol. 3, No.2, P. 1239-1251.
103. Davis Energy group (Energy solution), (2005),: “*Analysis of standards options for evaporative coolers*”, (cited March 2013), Available from: <http://www.energy.ca.gov/appliances>

104. H. Asan, Y.S. Sancakter, (1998),: “*Effects of Wall’s thermophysical properties on time lag and decrement factor*”, Energy and Building, Vol. 28, P. 159-166.
105. John Brennan, “U-Values”, Edinburgh School of Architecture and Landscape Architecture, (cited January 2013), Available from:
[http://www.architecture.com/SustainabilityHub/Designstrategies/Earth/1-1-1-10-Uvalues\(INCOMPLETE\).aspx](http://www.architecture.com/SustainabilityHub/Designstrategies/Earth/1-1-1-10-Uvalues(INCOMPLETE).aspx)
106. ASHRAE, (2009),: “*Handbook of Fundamentals*” (book style), American Society of Heating, Refrigerating and Air-Conditioning Engineers, Atlanta, GA, Chapter 9.
107. Danny H.W. Li., Joseph C. L., (2000),: “*Solar heat gain factors and the implications to building designs in subtropical regions*” Energy and Buildings, Vol. 32, P. 47-55.
108. R. Perez, R. Stewart C. Arbogast, R. Seals, J. Scott, (1986),: “*An anisotropic hourly diffuse radiation model for sloping surfaces: description, performance validation, site dependency evaluation*”, Solar Energy, Vol. 36, No. 6, P. 481-497.
109. AV. Arundel, EM. Sterling, JH. Biggin, TD., (1986),: “*Sterling, Indirect health effects of relative humidity indoor environments*”, Environmental health perspectives, Vol. 65, P. 351-61.
110. ASHRAE standard 62-1, (2010),: “*Ventilation for Acceptable Indoor Air Quality -Technical FAQ*”, America Society of Heating Refrigerating and Air-Conditioning Engineers, Inc., Atlanta, USA, No. 35.
111. Fatma Elzanaty, Ann Way, (2008),: “*Egypt demographic and health survey*”, (cited February 2013), Available from:
www.measuredhs.com/pubs/pdf/fr220/fr220.pdf
112. J. Mathur, S. Mathur, Anupma, (2006),: “*Summer-performance of inclined roof solar chimney for natural ventilation*”, Energy and Buildings, Vol. 38, P. 1156–1163.
113. C. Tawit, T. Pornsawan, (2004),: “*Natural ventilation in building using attic and solar chimney*”, The Joint International Conference on Sustainable Energy and Environment (SEE), Hua Hin, Thailand, P. 45–48.

114. D.J. Harris, N. Helwig, (2007),: “*Solar chimney and building ventilation*”, Applied Energy, Vol. 84, P. 135–146.
115. Morcos V. H., (1994),: “*Optimum tile angle and orientation for solar collectors in Assiut, Egypt*”, Renewable Energy, Vol. 4, No. 3, P. 291- 298.
116. ASHRAE Standard 55, (2008),: “*Thermal environmental conditions for human occupancy*”, 1st public review, American society of heating, refrigerating and air conditioning engineers, INC.
117. ISO 7730, (2005),: “*Ergonomics of the thermal environment -- Analytical determination and interpretation of thermal comfort using calculation of the PMV and PPD indices and local thermal comfort criteria*”, International Organization for Standardization, 3rd edition, Switzerland.
118. Fanger P. O., (1970),: “*Thermal Comfort: Analysis and Applications in Environmental Engineering*”, ISBN: 0898744466, Danish Technical Press, Copenhagen.
119. ISO 8996, (2004),: “*Ergonomics of the thermal environment -- Determination of metabolic rate*”, International Organization for Standardization, Switzerland.
120. ISO 9920, (2007),: “*Ergonomics of the thermal environment- Estimation of thermal insulation and water vapour resistance of a clothing ensemble*”, International Organization for Standardization, Switzerland.
121. ISO 7726, (1998),: “*Ergonomics of the thermal environment - Instruments for measuring physical quantities*”, International Organization for Standardization, Switzerland.
122. P C Wong, D Prasad, M Behnia, (2005),: “*Methodology for natural ventilation design for high-rise buildings in hot and humid climate*”, World sustainable building conference [SB05], Tokyo, japan, P. 284-292.
123. ASHRAE Standard 55, (2004),: “*A Standard for Natural Ventilation*”, American society of heating, refrigerating and air conditioning engineers, INC.

124. R.J. de Dear, G.S. Brager, (2002),: “*Thermal comfort in naturally ventilated buildings - revisions to ASHRAE Standard 55*”, Energy and Buildings, Vol. 34, P. 549-561.
125. Hazim B. Awbi, (1998),: “*Chapter 7- Ventilation*”, Renewable and sustainable energy reviews, Vol. 2, P. 157-188.
126. Viktor dorer, Andreas Weber, (1995),: “*Output options for COMIS*”, IEA-ECB Annex23, Multizone air flow modeling, EMPA 175, Dubendorf.
127. J.C. Phaff, B. Knoll, W.F. Gids,: “*Cp-Generator - pressure simulation program*”, (cited February 2012), Available from:
<http://cpgen.bouw.tno.nl/cp>



Ap

A.1 Thermal comfort standards

Thermal comfort is defined as ‘the condition of the mind which expresses satisfaction with the thermal environment and is assessed by subjective evaluation’. It also defines thermal sensation as a conscious feeling, commonly graded into categories of cold to neutral to hot [116].

There is a number of international thermal comfort standards that have made a substantial contribution to the knowledge of thermal comfort; the most important are:

ISO 7730: which is based upon the predicted mean vote (PMV) and predicted percentage of dissatisfied (PPD) [117].

Indices (Fanger, 1970): which provides methods for assessing the local discomfort caused by draughts, asymmetric radiation and temperature gradients [118].

ISO 8996: which describes six methods for estimating the metabolic heat production and it is an important requirement in the use of ISO 7730 and the assessment of thermal comfort [119].

ISO 9920: provides a database of the thermal properties of clothing and garments based upon measurements on heated manikins [120].

ISO 7726; supports thermal comfort assessment with measuring instruments [121].

ASHRAE Standard 55, “Thermal Environmental Conditions for Human Occupancy” was first established in 1966. Since then, there had been some revisions to incorporate the latest understanding and findings of thermal comfort. It derived its results from laboratory experiments using a thermal-balance model of the human body. Six key variables were identified as affecting the perception of thermal comfort, namely air temperature, radiation, relative humidity, air movement, clothing and metabolic rate. This standard attempted to provide an objective criterion for thermal comfort by specifying personal and

environmental factors that would produce an acceptable interior thermal environment for at least 80% of a building's occupants [24, 40, 122].

A.2 Adaptive comfort standard (ACS)

ASHRAE recognized that the conditions required for thermal comfort in spaces, which are naturally conditioned, are not necessarily the same as those required for other indoor spaces. Then, a new ACS for naturally ventilated buildings has been proposed to be integrated within ASHRAE Standard 55 [123]. The ACS is based on a number of experimental studies (measurement) conducted globally. This comfort could be applicable to buildings in which occupants control operable windows and where activity level <1.2 Met and Clo factor range between 0.66 to 0.93.

In the ACS, the mean monthly outdoor air temperature determines the acceptable indoor operative temperature. This relationship is expressed by the following formula [124]:

$$T_{o(Comf)} = 0.31T_{a(out)} + 17.8$$

Where $T_{o(Comf)}$ is the optimum comfort operative temperature in °C and $T_{a(out)}$ is the mean monthly outdoor air temperature in °C. Further, the 80% and 90% acceptability limits of indoor operative temperature were calculated as follows:

$$80\% \text{ acceptability limits} = T_{o(Comf)} \pm 3.5^\circ\text{C}$$

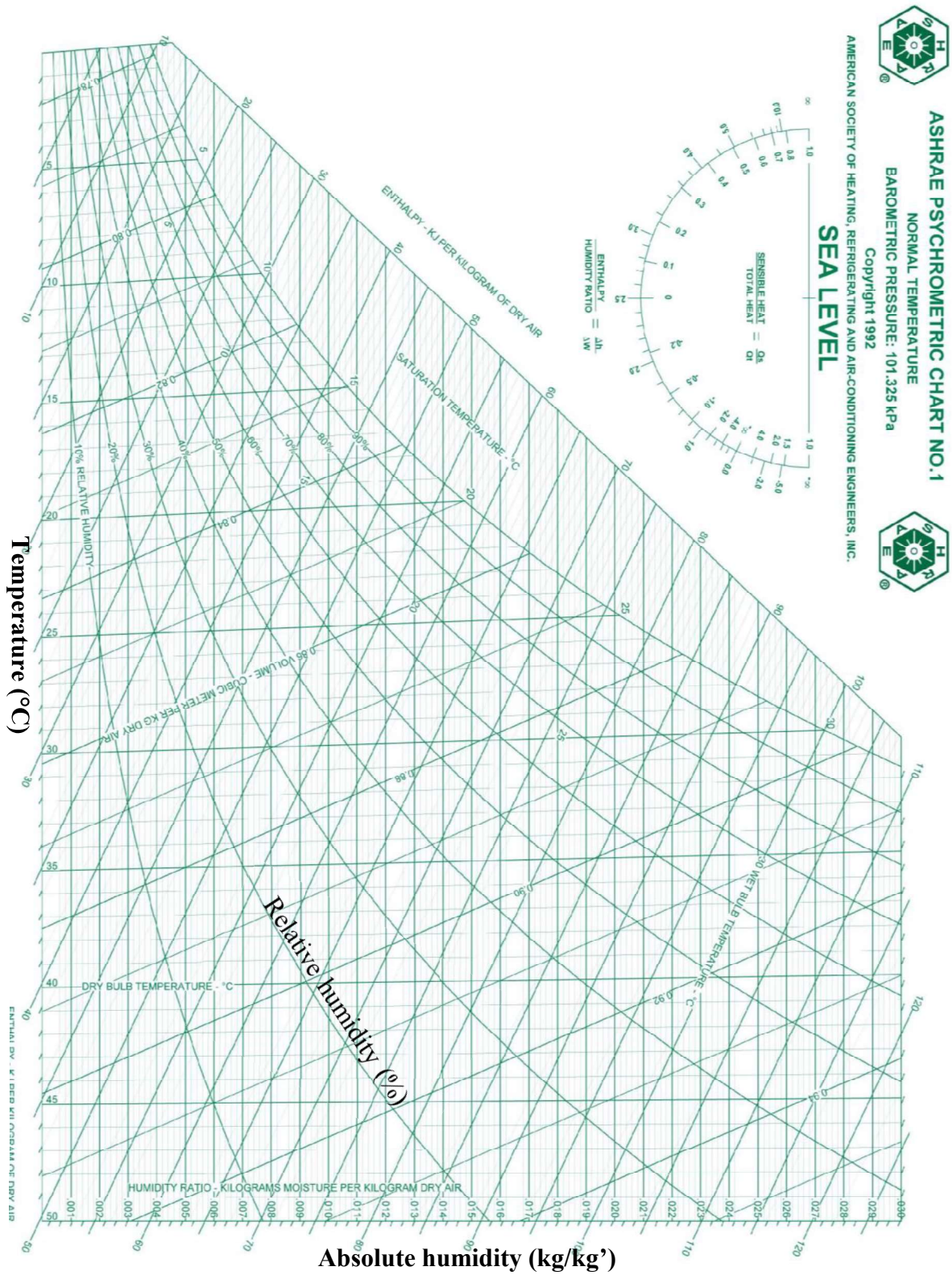
$$90\% \text{ acceptability limits} = T_{o(Comf)} \pm 2.5^\circ\text{C}.$$

In this research, ASHRAE & ACS will be used in the evaluation of acceptable indoor environment.

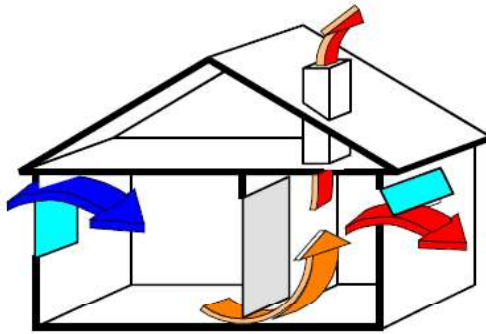
Figure (A-1) shows the ASHRAE psychrometric chart.

Appendix (A): Thermal comfort standard.

Figure (A-1): ASHRAE psychrometric chart.



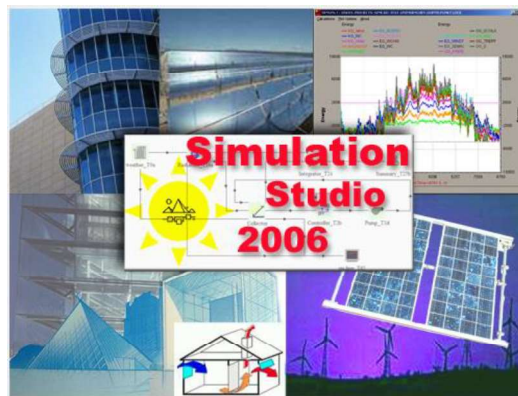
Appendix (B): (COMIS and TRNSYS input)



Eidgenössische Materialprüfungs- und Forschungsanstalt
Laboratoire fédéral d'essai des matériaux et de recherche
Laboratorio federale di prova dei materiali e di ricerca
Institut fédéral da controlla da material e da retschergas
Swiss Federal Laboratories for Materials Testing and Research

Empa
Überlandstrasse 129
CH-8600 Dübendorf
Tel. +41-1-823 55 11
Fax +41-1-821 62 44

EMPA 
Energiesysteme / Haustechnik
Energieforschungsgruppe



B.1 COMIS simulation inputs

Inputs for COMIS simulation software of chapter 4 are discussed according to: Duct (D) properties, Opening (WI), Zones parameters & Environment building parameters (ENV). Figure (B-1) shows the solving procedure flow chart for the model. Figure (B-2) shows the schematic of the system with the description of COMIS parameter.

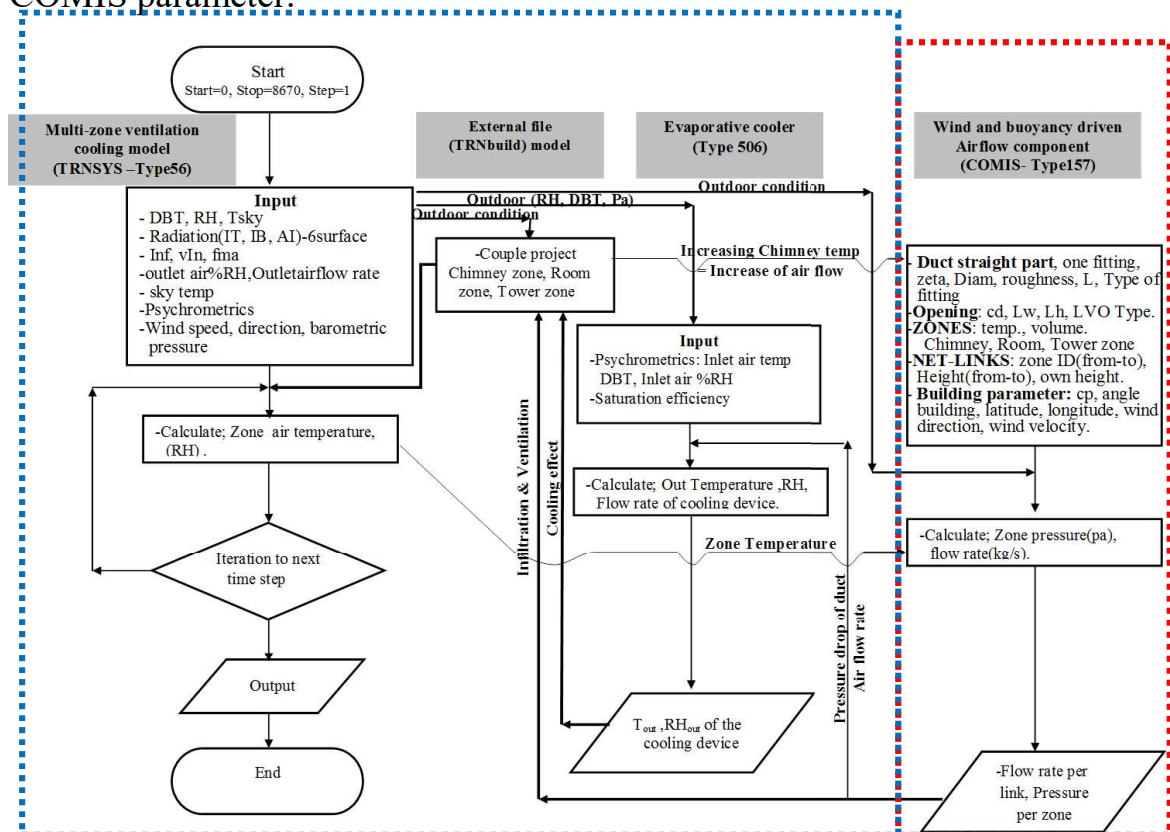


Figure (B-1): Flow chart of solving procedure.

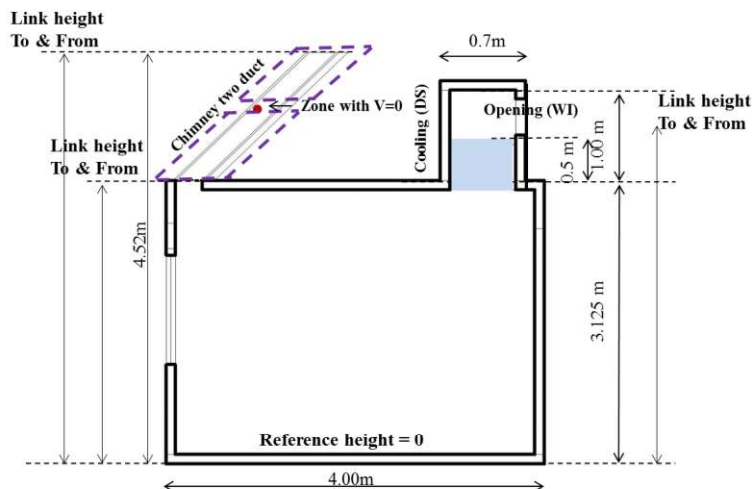


Figure (B-2): The schematic of the system with the description of COMIS parameters.

B.1.1 Duct properties

a. Straight duct (DS) for cooling

The evaporative cooling is treated as a straight duct with pressure loss in the inlet, outlet, and the flow pass resistance are calculated in the model.

```

-----
|1.| Prefix and Name | Description |
|__|          (-)   |   [-]     |
-----

|2.| Ducts straight part |           |           |           |           |           |           |           |           |
|__|          |           |           |           |           |           |           |           |           |
| Diam1 | Diam2 | Rough | Lduct | Zeta1 | Type | Param1 | Param2 | Zeta2 |
| (m)   | (m)   | (mm)  | (m)   | [-]   | [-]  | [?]    | [?]    | [-]   |
-----

|3.| Filter 1 | Filter 2 | Filter 3 | Filter 4 | Filter 5 |
|__|          | [-]     | [-]     | [-]     | [-]     |
-----
    
```

Cooling DS

```

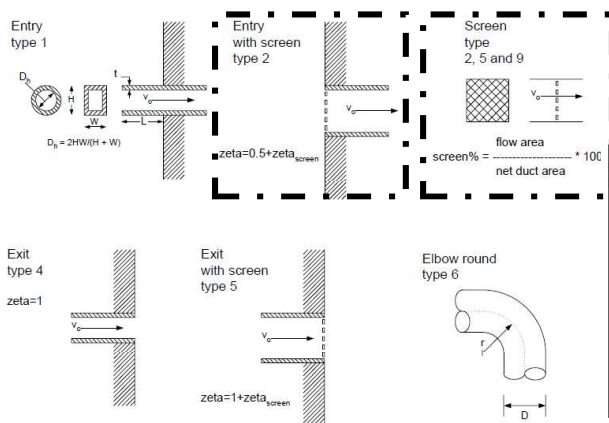
▶ 0.7   1.0   0.03   0.5   1.5   2   50   0   0.5
▶ 0.0
    
```

Where

- Duct fittings given here will result in an extra dynamic pressure.
- Zeta1 is the Dynamic loss coefficient of duct, Zeta2 is the dynamic loss coefficient of reverse flow; = 0.5 according to COMIS reference .

Typically, the entrance loss is equal 0.5 and the exit loss is 1 (zeta). So the input Zeta is 1.5.

Fittings are not available as separate components. Type 2 is used with a screen on the top to simulate the pressure drop in the wet medium as in figure (B-3).



Type	Name	No of Param	Parameter 1	Description	Parameter 2	Validity, range
1	Entry	2	t/D_h	L/D_h		no limits
2	Entry with screen	1	screen%	screen%		screen% < 100%; L=0
3	Round	2	Type	angle		no limits
4	Type 1: round Type 2: rectangular Exit	0	-	-	-	-
5	Exit with screen	1	screen%	-	-	screen% < 100%
6	Elbow round	1	r/D	-	-	$0 < r/D < 5$
7	Diffuser round	2	A_1/A_2	β	-	$A1/A2 < 1, \beta < 180^\circ$
8	Contraction round	2	A_2/A_1	β	-	$A2/A1 < 1, 15^\circ < \beta < 45^\circ$
9	Obstruction Screen	1	screen%	-	-	screen% < 100%
10	Perforated plate	2	T/d	screen%/100	-	$0.015 < T/d < 0.8$ $0.0 < \text{screen\%/}100 < 1.0$
11	Orifice A ^a	1	A_1/A_2	-	-	$A1/A2 < 1$
12	DIN orifice ^b	-	-	-	-	-
13	Damper round	1	β_d	-	-	$\beta_d < 75^\circ$

^a Routine according to Feustel [12]

^b This duct fitting is not available

Available fittings of the duct

The parameter describe for every type

Figure (B-3): The parameters used for the cooling duct.

b. Straight duct (DS) for chimney

The solar chimney is treated as two straight ducts with pressure loss in the inlet, outlet, and flow pass resistance calculated in COMIS and a zone with volume equal zero between the two ducts, in order to send the temperature of the thermal model from TRNSYS to COMIS.

```

-----
|1.| Prefix and Name | Description |
|__|          (-)  | [-]      |
-----

|2.| Ducts straight part |           |           |           |           |           |           |           |           |
|__|          |           |           |           |           |           |           |           |           |
| Diam1 | Diam2 | Rough | Lduct | Zeta1 | Type | Param1 | Param2 | Zeta2 |
| (m)   | (m)   | (mm)  | (m)   | [-]   | [-]  | [?]   | [?]   | [-]   |
-----

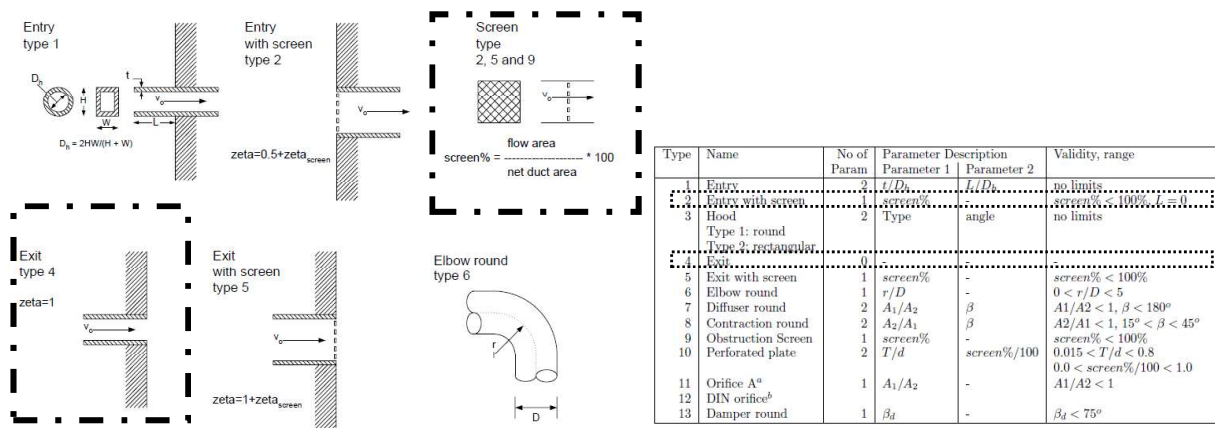
|3.| Filter 1 | Filter 2 | Filter 3 | Filter 4 | Filter 5 |
|__|          | [-]      | [-]      | [-]      | [-]      |
-----

First duct attached to the room
▶ 0.2   1.0   0.01  1   1   2   100   0   0.51
▶ 0.0

Second duct attached to the zone with volume equal zero to outside.
0.2   1.0   0.01  1   1   4   0   0   0.51
0.0
    
```

Where

- Zeta1 is the Dynamic loss coefficient of duct, Zeta2 is the dynamic loss coefficient of reverse flow. Open inlet is treated as type 2 with 100% screen. Also, type 4 is treated for the outlet as in figure (B-4).



^a Routine according to Fenstel [12]
^b This duct fitting is not available

Figure (B-4): The parameters used for the two chimney ducts.

¹ COMIS manual, 2005

B.1.2 Opening (WI) properties

It is the opening in the north façade through which outside air enters the tower. Height differences between openings (links) in a ventilation network together with temperature differences, may be an important driving factor for ventilation. The reference height of the opening in the zone (the 'from' and 'to' height of a link) as in figure (B-2) is taken into account.

WI (opening)

1.	Prefix and Name	Description				
---	(-)	[-]				

2.	Closed:	Expn	LVO Type	Lwmax	Lhmax	Type specific
---	Cs	(-)	(-)	[m]	[m]	Length
	(airl/m)					[m]

3.	Open.	Cd	Width	Height	Start Height
---	Fact.		Factor	Factor	Factor
	(-)	[-]	[-]	[-]	[-]

4.	Filter 1	Filter 2	Filter 3	Filter 4	Filter 5
---	(-)	[-]	[-]	[-]	[-]

The opening from external node to opening of the wind tower;

→	0.0001	0.5	1	1	0.4	0
→	1	0.6	1	1	0	
→	0					

Height From & To = 3.825m

Height factor =1 (vertical opening) is the cosine of the angle between opening plane and vertical plane.

Where

- Cs; is used only for closed window,
- Expn; (Flow exponent) is turbulent flow¹,
- LVO is Type of Large Vertical Opening

1 = Rectangular LVO

¹ **Turbulent flow**; It is the normal airflow in nature and inside architectural spaces. The air moves randomly in chaotic flow and its molecules cross over other molecules path forming eddies and difference in speed

2 & 3 = Horizontal Pivoting Axis LVO

4 & 5 = Triangular LVO

- L_{wmax} = width of the window
- L_{hmax} = height of the window

Type specific length = Extra crack length for LVOs with multiple openable parts
 = 0 for Type 1

- $C_d = 0.6$ is the discharge coefficient which depends on the sharpness of the opening [125].

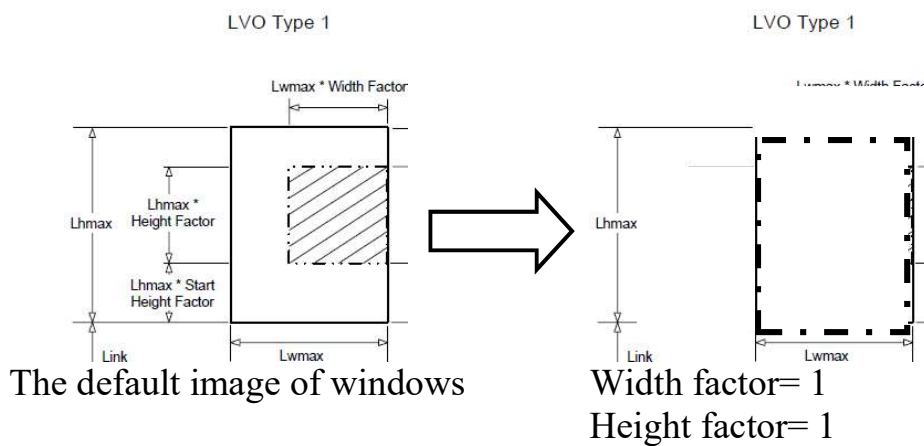


Figure (B-5): The description for the opening in the north façade of the tower.

B.1.3 Zones parameters

NET-ZONES (Zones Definition)

Zone ID	Name	Temp	Ref. Height	Volume H/D/W	Humid.	Schedule
(-)	(-)	[temp]	[m]	[m ³ /m/m]	[humi]	(-)
	Tower	--	--	0.5/0.7/1	--	--
	Room	--	--	2.875/3.75/3.75	--	--
	Chimney	--	--	volume=zero	--	--

Where,

- Temp; is connected in TRNbuild (Type 56).
- Humid; in zone=0 as H₂O is not used as a pollutant in the model is not taken into account.

- Ref. Height; is kept for all zones at the reference equal 0m. Then all heights for the links have to be the absolute height (referred to the surrounding ground level).

For calculation of air change rate, zones with a volume of $V > 0^1$ are considered in order to consider the temperature of the chimney in COMIS transferred from TRNSYS [126].

B.1.4 Environment building parameters (ENV)

a. ENV-BUILDING (Building Related Parameters)

The information of the building location and its angle is taken into account

1.	Altitude	Angle Building	Geographic Position	
		North to Axis	Latitude +=N	Longitude +=E
	(m)	(deg)	[deg] --S	[deg] --W
	69	0	27.30	31.15

b. ENV-WIND (Wind and Meteo Related Parameters)

The information of the Meteorological station and its surrounding according to the weather data file in TRNSYS

1.	Ref. Height	Altitude	Wind Velocity
	for Wind Speed	Meteo Station	Profile Exponent
	(m)	(m)	Meteo Station
			(prof)
	10	69	0.149
	360	0.218	

2.	Wind Direction	Wind Velocity
	Angle	Profile Exponent
	(deg)	Building Location
		(prof)
	10	0.149
	360	0.218

Where

- Wind velocity profile exponent of Meteo station (α) = 0.149¹ for open--low crops, low hedges, few trees, very few height.

¹For zone which shall not be considered in calculation (e.g. Just for moving the air in a virtual zone under the effect of temperature difference, the volume must be set to $V=0$).

- Wind velocity profile exponent of building location (α) = 0.218¹ for rough—high and low crops, large obstacles at distances.

The wind speed is measured at a 10m height above the ground level at the meteorological station with roughness length ($z_0=0.03$) and denoted as reference wind speed in the form of a power law as follows [125]:

$$v_z = v_m K h^\alpha = C h^\alpha$$

Where

v_z = the air speed at building height (m/s)

v_m = the wind speed at the weather station (reference wind speed)

h = the building height

K, α = factors depend on surface roughness and terrain.

$$C = v_m K$$

COMIS software uses wind speed at the Meteo site in reference height to calculate the speed above the boundary layer using the wind velocity profile² of the Meteo station, where the boundary layer is 60 m high for smooth terrain as shown in figure (B-6) [86, 94].

¹Related to the weather data file (*.Tm2) of new city of Assiut city.

²**Wind velocity profile;** A series of wind direction and wind speed measurements taken at various levels in the atmosphere that show the wind structure of the atmosphere over a specific location.

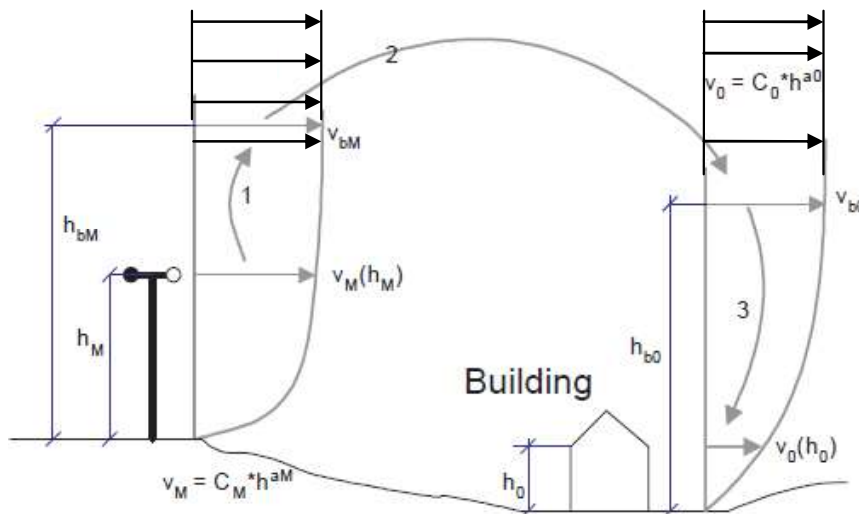


Figure (B-6): Wind velocity profile: relations at Meteo and on building site [94, 125].

Where: (M) Meteo station, (0) building site, (b) boundary. (h_0) Building reference height, (h_M) Reference height at Meteo station.

c. NET-EXTeRnal (External Node Data)

The building is linked to its ambiance (outside) via external nodes. Two important inputs must be used:

Cp value input; which is calculated from CPgenerator.

Wind direction; which is connected with weather data in TRNSYS.

d. SCH-METeo Data (Meteo Data Schedule)

It is used for input parameters of temperature, humidity at the steady state condition or the weather data condition.

[1.] Dataset Name					
[2.]					
Time	Wind		Temperature	Humidity	Barometric
	Speed	Direction			Pressure
(-)	(velo)	(deg)	(temp)	[humi]	Absolute [kPa]

The Meteo data can be stored under the keyword &-SCH¹-MET in the CIF²-file as input data in COMIS or in a separate weather file in TRNSYS.

e. CP-VALues

Wind pressure coefficients (Cp values) belonging to a certain facade element can be given in several wind directions. The angle of the wind direction is measured clockwise from the north. Two angles of Cp- values are given in the north and the south façades in the steady state condition.

```

-----
|1.|Dataset Name |
|_|-----|

-----
|2.| *          | Wind Direction with respect to Building Axis (first line ) | | | | | | | | |
|_| Facade    | Cp Values (second and following lines) |
| Elem.Name  | | | | | | | | | | |
| (-)       | (-) | [-] | [-] | [-] | [-] | [-] | [-] | [-] | [-] |
|-----|-----|-----|-----|-----|-----|-----|-----|-----|-----|

```

North Façade Cp = 0.081 for angle 360°
 South Façade Cp=-0.040 for angle 360°

B.1.5 Calculation of wind pressure coefficient on buildings

Cp is defined as the portion of the dynamic wind pressure, which acts on the specific façade or roof at a certain wind direction. As wind is a major actuator for natural ventilation, Cp-values are calculated from natural ventilation simulation programs (www. cpgen.bouw.tno.nl) [127]. The pressure coefficient at a specific point on the building façade could be obtained from: “Cp-Generator”³ which was developed at TNO applied research organization.

The input for Cp Generator is based on existence of the building and obstacle coordinates, terrain roughness and orientations. Also, coordinates of Cp positions on the building have to be defined.

¹ SCH; schedule

² CIF; Comis Input File

³The pressure coefficient at a specific point on the building façade could be obtained from computer simulation program “CP-Generator” using databases (examples) of calculated Cp values based on systematic performed wind tunnel tests and on published results of on-site tests of different research organizations [127].

Input data for Cp-Generator

The estimation is done using a data set of FORTRAN in CP-Generator program [127] according to;

a. North arrow:

The direction of the room is towards the north with an angle equal to 0° , where façade 1 with a solar chimney is facing the south and façade 3 with wind tower is facing the north as in figure (B-7).

b. Wind Z_0 :

It is the terrain roughness for different wind flow directions. It defines the changes at which terrain roughness occurs, where $Z_0=3^1$ for all wind direction.

c. Obstacles:

Assuming the living room of the final floor is located in a block of the building, where the front of the building is a 12m wide street and facing another block of the building as a big obstacle in the opposite direction with azimuth 180° . While from the back, there are private gardens back to back with another private garden for another building then there is a block of buildings as a big obstacle with the same height of the building in the opposite direction with azimuth 0° toward the north. Figure (B-7) shows the angle of the four façades according to their location with the reference to the north counterclockwise. Also, figure (B-8) shows the location of the building (living room) with the integrated system with the obstacles.

¹ $Z_0 = 3$ for normal sub-urban, industrial estate or village. The obstacles are of mutual varying heights like: suburbs with one to four storey buildings, industrial estates with varying industrial and commercial buildings up to four storeys, and a village center with higher buildings, like a church or a mall (the same condition of the New Assiut City).

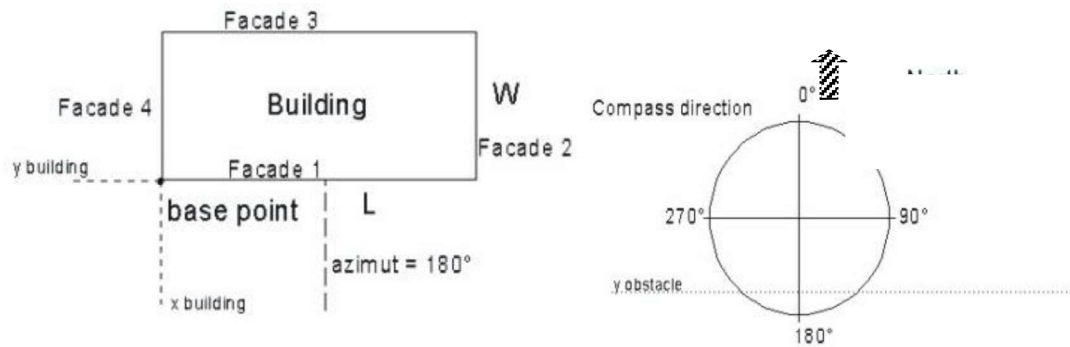


Figure (B-7): The base point of the building and the name of the façade according to the FORTRAN data set.

d. Cp-positions

These are the points on the north façade (opening of the tower) and the top of the chimney (outlet of the solar chimney) which need to be calculated.

Point (A) on façade 3 (opening of wind tower); with coordinates $X, Y = (0.6, 3.88)$ with the base reference point $X, Y = 0, 0$ for the building corner.

Point (B) on façade 5 on the roof (outlet of the chimney); with coordinates $X, Y = (0.6, 1.52)$ ¹.

After running the simulation and checking all the inputs, the results of the Cp-value according to different orientations are directly pasted into 'Comis-Cp.txt' from the simulation program in the 'CP-VALues' section of COMIS input file (*.CIF). This is needed when the real weather data is connected to Type 157-COMIS. Table (B-1) shows the results of Cp of point (A & B).

¹The Y coordinate values depend on the inclination angle of the chimney.

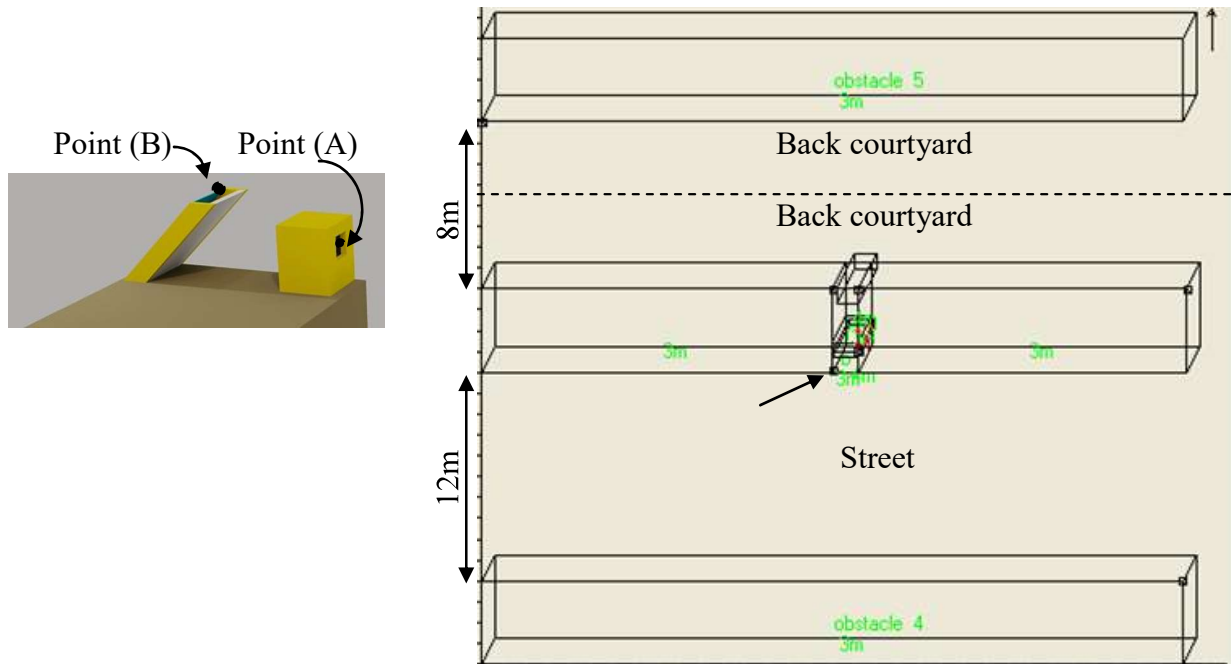


Figure (B-8): The location of Cp points and the location of the living room with the surrounding obstacles.

Table (B-1): The results of the Cp values¹.

Angle°	Cp of points (A)-North	Cp of points (B)-South
300°	-0.097	-0.058
305°	-0.061	-0.057
310°	-0.028	-0.059
315°	0.001	-0.064
320°	0.025	-0.070
325°	0.043	-0.079
330°	0.057	-0.087
335°	0.067	-0.088
340°	0.073	-0.084
345°	0.077	-0.073
350°	0.079	-0.060
355°	0.080	-0.047
360° (0°)	0.081	-0.040

¹The results of wind directions from 300° to 360° only were discussed. This is due to the majority of the wind directions in the summer season is north and north west according to outdoor real weather data analyzed in chapter 2 of The New Assiut city.

B.2 TRNSYS simulation inputs

Six different components are used in the calculation of TRNSYS as shown in figure (B-9). These components are;

Weather data (Type 109), Sky temperature (Type 69), Psychrometric (Type 33), Air flow-COMIS (Type 157), Evaporative cooling (Type 506d), TRNBuild (Type 56), Output-online printer without file) (Type 65d) & TRNSYS supplied unit (Type 25a).

a. Weather data (Type 109)

This component is connected;

To the building (Type 56), air flow (Type 157), psychrometric (Type 33), sky temp (Type 69) & 2output printer (Type 65d & Type 25a).

The most important input that must be considered in type (109) are;

- Total radiation on horizontal (connected to the six surfaces of type 56)¹.
- Beam radiation on horizontal (connected to the six surfaces of type 56).
- Angle of incidence for title surface (connected to the six surfaces of type 56).
- Slope of the surface (Six surfaces including inclinations faces of the chimney of type 56).
- The azimuth of the surface (Six surfaces including inclinations of type 56), it can be calculated according to the façade orientation as in figure (B-7).
- Also, the temperature, relative humidity, wind speed, atmospheric pressure, and wind direction are connected to another component according to solving procedure chart of figure (B-1)

¹**Six surfaces:** These are the surfaces that faced the north, south, east & west orientations. Also, two faces of the chimney inclination surface that faced the south (with inclination) & the north (with inclination).

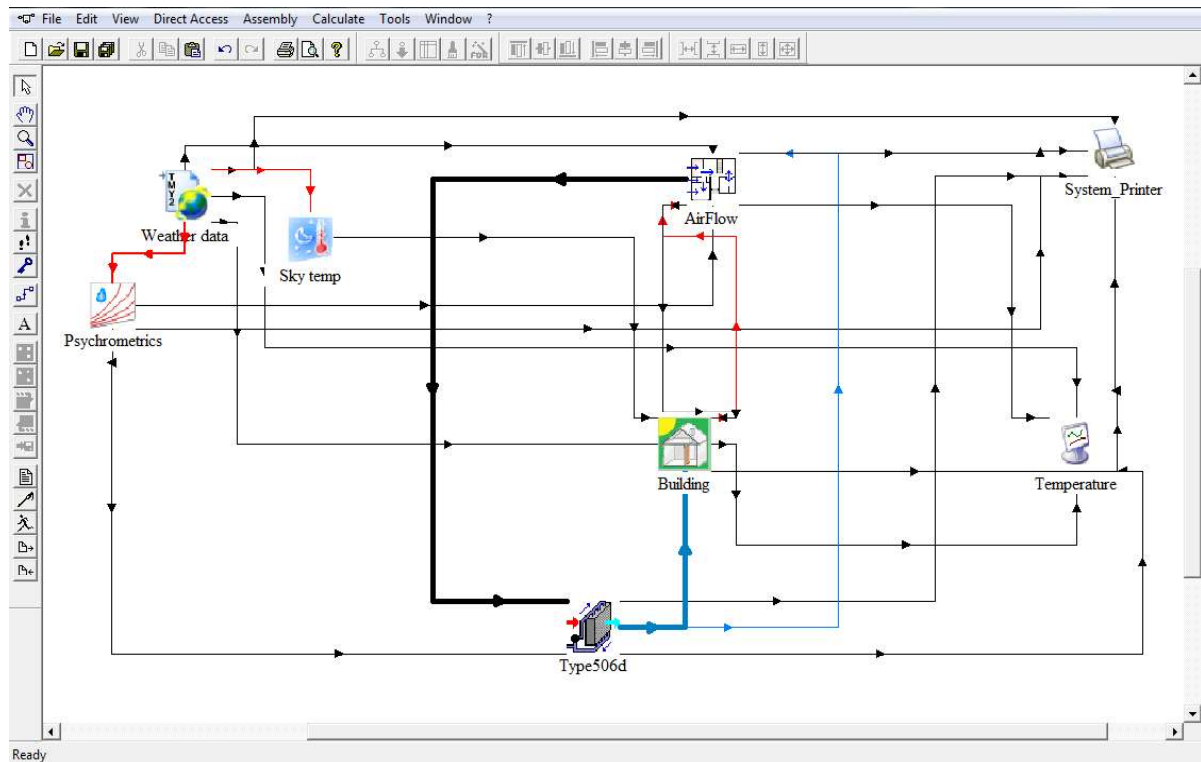


Figure (B-9): The TRNSYS file program façade.

b. Sky temperature (Type 69)

This component is connected;

To the building (Type 56)

From the weather date (Type 109).

The parameters that must be considered in this component are;

- Ambient temperature (connects from weather data file to Type 69).
- Beam radiation on horizontal (connects from weather data file to Type 69).
- Diffuse radiation on horizontal (connects from weather data file to Type 69).
- Fictive sky temperature (connects from Type 69 to Type 56).

c. Psychrometric (Type 33)

This component is connected;

To the air flow (Type 157), evaporative cooling (Type 506 d), output printer (Type 65d & 25a).

From the weather date (Type 109).

The parameters that must be considered in this component are;

- Dry bulb temperature (connects from the weather data file to Type 33).
- Percent relative humidity (connects from the weather data file to Type 33).
- Humidity ratio (connects to type 157).
- Dry bulb temperature and percent relative humidity (connects to type 506d).

d. Air flow-COMIS (Type 157)

It is the components that represents the link and the ventilation network of COMIS calculation connected to the building (Type 56) as initial values. Then, the calculation of the temperature from TRNSYS is fed back to COMIS again. Therefore, continuous iterations are done for the mathematical equations until convergence. This component is connected;

To evaporative cooling (Type 506d), 2 output printer (Type 65d, 25a), building (Type 56).

From the weather data (Type 109), psychrometric (Type 33), evaporative cooling (Type 506d), building (Type 56).

The parameters that must be considered are;

- Wind speed (connects from the weather data file to Type157).
- Wind direction (connects from the weather data file to Type 157).
- Ambient temperature (connects from the weather data file to Type 157).
- Absolute humidity (connects from the weather data file to Type 157).
- Ambient Pressure (connects from the weather data file to Type 157).
- Zones air temperatures (connect from Type 56 to Type 157).
- Couple air flow¹ (connects from Type 157 to Type 56).
- Couple air flow (connects from Type 157to evaporative cooling Type 506d)
- Outlet air temperature after cooling (connects from evaporative cooling (Type 506 d to Type 157).

¹**Couple air flow:** It is the flow of air between zones according to different parameters (temperature difference, wind pressure).

e. Evaporative cooling (Type 506d) -Tess library

This component is connected;

To the airflow (Type 157), building (Type 56), 2 output printer (Type 65d & 25a).

From the air flow (Type 157), psychrometric (Type 33).

The parameters that must be considered in this component are;

- Inlet air temperature (Connects from Type 33 to Type 506d).
- Inlet air relative humidity (Connects from Type 33 to Type 506d).
- Inlet air flow rate (connects to Type 157 to Type 506d).
- Inlet air pressure (connects from Type 33 to Type 506d).
- Air side pressure drop¹ (connects from Type 506d to Type 157).
- Outlet air temperature after cooling (connects from Type 506d to Type 157).
- Couple air flow (connects from air flow to inlet air temp of evaporative cooling).
- Saturation efficiency is based on the standard options for direct evaporative cooling in hot climate published *by the California Energy Eommission*. This standard is ranging from 45-61% for the wet pad with no water droplet [103].

f. TRNbuild (Type 56)

It is used to describe the building thermal zone. The inputs indicate the building description (*.BLD) and the ASHRAE transfer function for walls (*.TRN). All data entered are saved in a building file (*.BUI). So, the link between other components and this component helps to simulate the real situation of the building with the same wall properties and weather data and other parameters in the mathematical equation as in chapter four. This component is connected;

To the airflow (Type 157), 2 output printer (Type 65d & 25a).

¹**Pressure drop:** Pressure drop occurs with the frictional forces, caused by the resistance for the flow from the inlet, outlet and through the duct.

From the weather data (Type 109, sky temp (Type 69), air flow (Type 157), evaporative cooling (Type 506d).

g. Output (online printer without file) (Type 65d) & TRNSYS supplied unit (Type 25a)

Type 65d helps to plot the output results as a graph to see them after running the simulation (without external files).

Type 25a helps to plot the results as an excel file.

Nomenclature

Symbol	Description	Unit
C_p	Specific heat at constant pressure	$\text{kJ/kg}^\circ\text{C}$
$C_{p_{\text{south, north}}}$	Wind pressure coefficient	--
C_f	Specific heat of air	J /kg K
g	Gravitational constant= 9.8	m/s^2
h_{AirIn}	Enthalpy of air entering the device	J/kg
h_{AirOut}	Enthalpy of air exiting the device	J/kg
h_{rwg}	Radiative heat transfer between absorber and the glass	$\text{W/m}^2 \text{K}$
h_{rs}	Radiative heat transfer between the glass and the sky	$\text{W/m}^2 \text{K}$
h_g	Convective heat transfer between glass and sky	$\text{W/m}^2 \text{K}$
h_{wind}	Convective heat transfer outside glass due to wind	$\text{W/m}^2 \text{K}$
h_w	Convective heat transfer between the absorber and the air	$\text{W/m}^2 \text{K}$
h	Heat transfer from air	W
I	Incident solar radiation	W/m^2
k	Thermal conductivity	W/m.K
\dot{m}_{coolere}	Mass flow rate of the air through the cooling device	kJ/hr
\dot{m}	Mass flow rate of the air	kg/s
Q	volume flow	m^3/s
Q_{air}	Energy transferred to or removed from the air stream	kJ/hr
\dot{Q}	Total heat transfer	$\text{W/m}^2\text{K}$
q''	Heat transfer to the air stream in the chimney	w/m^2
S_g	Solar radiation absorbed by glass	W/m^2
S_w	Solar radiation absorbed by absorber	W/m^2
T	temperature	K
t	temperature	$^\circ\text{C}$
U	Overall convective heat transfer coefficient	$\text{W/m}^2 \text{K}$
v	air velocity	m/s
V	Wind speed at reference height	m/s
Δw	Humidity ratio	---

Dimensionless terms

Nu	Nusselts number ($h_f d / k_{air}$)
Ra	Rayleigh number

Greek symbols

ε	Emissivity of glass =0.9,Emissivity of absorber= 0.95
γ	temperature weighting factor= 0.75
$\eta_{\text{Saturation}}$	Saturation efficiency of the evaporative cooling
ρ	air density (kg/m^3)
τ	Transmissivity
β	Stefan Boltzmann constant ($=5.67 \times 10^{-8} \text{W}/(\text{m}^2 \text{K}^4)$)

Subscripts

a	Ambient
g	Glass
L	Latent
r	Room
S	Sensible
W	Absorber
Wb	Wet bulb temperature

Abbreviations

ABBREVIATION	DESCRIPTION
ACS	Adaptive comfort standard
ASHRAE	American Society of Heating, Refrigerating and Air-Conditioning Engineers
ACH	Air change rate per hour
AC	Air condition
CFM	Cubic feet per minute
COMIS	Conjunction of multizone infiltration specialists program
Cp	Wind
DBT	Dry bulb temperature (DB)
DPT	Dew point temperature
EAT	Earth cooling air tunnel
ECWT	Evaporative cooling short wind tower
ECC	Evaporative cooling cavity
IAQ	Indoor air quality
PPM	Part per million (1000ppm= 0.1%)
PCM	Phase change material
RH	Relative humidity
SC	Solar chimney
TRNSYS	Transient systems simulation program
TESS	Thermal Energy System Specialist library of TRNSYS 16
WBT	Wet bulb Temperature (WB)
WT	Wind tower

- 1 Amr Sayed H, Hiroshi Yoshino, Tomonobu Goto, Napoleon Enteria, Magdy M. Radwan, M. Abdelsamei Eid, (2013),: “*Integration of evaporative cooling technique with solar chimney to improve indoor thermal environment in the new city of Assiut, Egypt*”. International Journal of Energy and Environmental Engineering.2013, 4:45. DOI: 10.1186/10.1186/2251-6832-4-45

Abstract— Cooling buildings in summer is one of the main environmental problems for architects and occupants in many hot dry countries. The summer temperature during these countries reaches peaks of more than 40°C in some. Mechanical air conditioners can solve the problem but they put a heavy strain on the electricity consumption. Egypt in general has rich sunny and clear skies. Therefore, these conditions encourage to enhance evaporating with natural ventilation and save energy. This paper develops an integration of direct evaporative cooling tower with a solar chimney multi-zone thermal ventilation model. Simulation is done using commercial couple multi-zone airflow under COMIS-TRNSYS software to assess natural ventilation and indoor thermal comfort. The results show that the system generates 130.5m³/h under the effect of solar radiation only and minimum 2 ACH without pressure coefficient which is considered the minimum requirement of ACH .The findings show that the new integrated system interacts with the building envelope and weather conditions to achieve a decrease in indoor temperatures that reach to 10°C~ 11.5°C compared to outdoor temperatures.

- 2 Amr Sayed H, Hiroshi Yoshino, Tomonobu Goto, Napoleon Enteria, Magdy M. Radwan & M. Abdelsamei Eid, (2013),: “*The Impact of Natural Cooling Design on Indoor Environment Using Solar Chimney with New Cooling Tower under New City of Assiut, Egypt Climate*”, 7th CLIMAMED Mediterranean Congress of Climatization- Net-Zero Energy Use in Buildings, Turkey, P.19-27.

Abstract— In Egypt's hot-dry climate, new housing is poorly adapted to the climate because architects lack of knowledge and adequate design tools. As a result, there has been a vast expansion in the use of air conditioning to cool buildings which expected to continue for sometime yet. Also, the production of CO₂ encourages designers to apply more passive means for controlling the indoor environment. Therefore, these conditions encourage such a concept to enhance evaporating natural ventilation and save energy. This paper studies integration of direct evaporative cooler with a solar chimney to ventilate and provide thermal need for the occupants in the buildings & indoor air quality. Simulation is done using commercial couple multi-zone airflow under COMIS-TRNSYS software to assess natural ventilation. The dependence on the new city of Assiut outdoor air temperature has been studied to determine the thermal comfort criteria and indoor air quality. The temperature and airflow rates are predicted iteratively taking into account the zone pressure and the pressure drop in the evaporative cooler component. The simultaneous set of mass balance equations is typically solved using the Newton - Raphson method to correct the zone reference pressures until the simultaneous mass balance of all flows is achieved. The result shows that room air temperature can be decreased to 10°C~11.5°C compare to outdoor temperatures with an acceptable humidity ratio between 40%~60%. The system generates 205-345 (m³/h) with acceptable carbon dioxide concentration according to ASHRAE standards. The findings show that natural ventilation with evaporative cooler can be a potential alternative to air conditioning systems in the new city of Assiut, Egypt with zero energy for cooling in the building.

- 3 Amr Sayed H., Yoshino H., Goto T., Enteria N., Abdelsamei Eid M., Radwan M. M., (2013),: “*Analysis of thermal comfort for indoor environment of the new Assiut housing in Egypt*”. World Academy of Science Engineering and Technology, Issue 77, P. 1191-1197.

Abstract— Climate considerations are essential dimensions in the assessment of thermal comfort and indoor environments inside Egyptian housing. The primary aim of this paper is to analyze the indoor environment of new housing in the new city of Assiut in the Southern Upper Egypt zone, in order to evaluate its thermal environment and determine the acceptable indoor operative temperatures. The psychrometric charts for ASHRAE Standard 55 and ACS used in this study would facilitate an overall representation of the climate in one of the hottest months in the summer season. This study helps to understand and deal with this problem and work on a passive cooling ventilation strategy in these contexts in future studies. The results that demonstrated the indoor temperature is too high, a ranges between 31°C to 40°C in different natural ventilation strategies. This causes the indoor environment to be far from the optimum comfort operative temperature of ACS except when using air conditioners. Finally, this study is considered a base for developing a new system using natural ventilation with passive cooling strategies.

- 4 Amr Sayed H., Yoshino H., Abdelsamei Eid M., Radwan M. M., (2012), : “*Indoor natural ventilation using evaporative cooling strategies in the Egyptian housing: A review and new approach*”, International Journal of Engineering and Technology, Vol. 4 (3), P. 229–233.

Abstract—Houses in Egypt are often designed without sufficiently taking the climate into account. Factors such as the urban environment, site characteristics, orientation and architectural design of the building, choice of building materials, etc. are not emphasized. Consequently, buildings often have a poor indoor climate, which affects comfort, health and building efficiency. One reason why

buildings are poorly adapted to the climate is lack of knowledge among architects, planners and engineers. This review focuses on two main areas of research: First, the housing problem in terms of thermal comfort, indoor environment problem. Second, present solutions, strategies and the future research. Moreover, this review found that the problem of achieving thermal comfort is not fully understood but there are new integrated strategies that can be developed which use low cost passive cooling strategies to reduce the heating loads. Besides, it is suggested to further study the optimization and the control strategy of such integrated system in Egypt.

ملخص الدراسة:

تصمم المساكن المصرية غالبا دون وضع المناخ في الاعتبار بجدية، حيث أن كثيرا ما تهمل عوامل مثل: البيئة الحضرية وخصائص الموقع وتوجيه المبنى وتصميمه المعماري واختيار مواد البناء وغيرها. قام كثير من الباحثين بدراسة الراحة الحرارية بمشروعات الإسكان المصرية – وخاصة مدينة أسيوط الجديدة – و تم إجراء قياسات عديدة أوضحت نتائجها أن هناك مشاكل كبيرة بشأن عدم الراحة الحرارية في مشروعات الإسكان الجديدة، بالإضافة إلى انخفاض جودة الهواء الداخلي. وبناء على هذه النتائج، فإن الاستراتيجيات التي قد تكون ملائمة للمباني في ذلك المناخ هي التبريد بالبخار والتهوية الطبيعية – وذلك طبقا للخريطة البيومناخية لاستراتيجيات البناء وكذلك المؤشرات الأخرى. وقد ظهر توسع كبير في استخدام مكيفات الهواء لتبريد المباني. ولكن استهلاكها الكبير للطاقة الكهربائية أصبح يفوق القدرات المالية لذوي الدخل والموارد المالية المحدودة. ولذلك، فإن هذه الظروف تشجع على تعزيز استخدام استراتيجية التهوية الطبيعية السلبية لمدينة أسيوط الجديدة بما تعنيه من خفض استهلاك الطاقة للتبريد.

ولتحقيق ذلك الهدف، فإن البحث يستخدم أربع أساليب بما يتناسب مع هدف كل فصل فيه فاستخدام الأسلوب الوصفي (للفصل الأول)، والأسلوب التحليلي (للفصل الثاني)، والأسلوب الاستقرائي (للفصل الثالث)، والأسلوب التطبيقي (للفصلين الرابع والخامس). وأخيرا، ينتهي البحث بالنتائج وإرشادات حول الاستخدام الأمثل لهذه النظم.

الفصل الأول: سياق البحث وخلفيته ومشكلته وأهدافه

هو فصل تمهيدي يقدم عرضا عاما لجميع محتويات البحث والظروف الجغرافية والمناخية للمكان الذي أجري عليه البحث، وخلفية البحث، ومشكلة البحث، ومدى البحث، وطبيعته، وهدف البحث الرئيسي والأهداف الفرعية له. وأخيرا، يتم عرض المنهجية العامة التي إتبعها البحث.

الفصل الثاني: القياسات المناخية بمبنى حالة الدراسة وتقييم البيئة الداخلية به (مدينة أسيوط الجديدة)

في هذا الفصل يتم دراسة البيئة الداخلية لمشروعات الإسكان بمدينة أسيوط الجديدة، وذلك بمراقبة درجة حرارة الهواء الداخلي والرطوبة وتركيز ثاني أكسيد الكربون في فصل الصيف، وذلك للوقوف على حقيقة الظروف المناخية داخل أمثلة من المساكن بمدينة أسيوط الجديدة و من ثم البحث عن استراتيجيات "سلبية" جديدة ملائمة لحل مشكلة الراحة الحرارية لشاغلي المبنى. وقد تم إجراء تحليل مفصل لحالة الدراسة المختارة وذلك بإلقاء الضوء على تركيز ثاني أكسيد الكربون داخل المبنى والراحة الحرارية وأثرها على جودة الهواء الداخلي (IAQ) في مختلف سيناريوهات التهوية.

الفصل الثالث: الحلول والاستراتيجيات لمشاكل البيئة الداخلية

يقدم هذا الفصل المعلومات المرتبطة بالتهوية الطبيعية (أثر المدخنة & ضغط الرياح) والتبريد بالبحر. أيضا، كما يقدم الفصل عرضا نقديا للأدبيات الخاصة بمختلف التقنيات السلبية (برج الرياح، المدخنة الشمسية، وإدماج المدخنة الشمسية في مفهوم التبريد بالبحر) وذلك لفهم قيود النظام الحالي والبحث عن نظام جديد أكثر كفاءة. وبشكل عام فإن هذا الفصل يهدف إلى فهم تقنيات التهوية الطبيعية، والتبريد بالبحر، والبحث عن استراتيجيات جديدة تتخطى على قيود النظم التقليدية داخل/ خارج مصر وذلك للوصول الي تصميم مدمج بكفاءة عالية.

الفصل الرابع: إدماج المدخنة الشمسية مع برج التبريد الجديد كتقنية تهوية سلبية

يهدف هذا الفصل بشكل عام إلى دراسة إمكانية استخدام التهوية الطبيعية في الاستفادة من تقنية التبريد بالبحر وذلك عن طريق النمذجة الرقمية (المحاكاة)، من أجل الوصول إلى صفرية استهلاك الطاقة للتبريد وتوفير الراحة الحرارية الداخلية، حسب كل من مواصفات ACS و ASHRAE وبيانات الطقس لمدينة أسبوت الجديدة. تم أولا عمل النمذجة الرياضية للنظام المدمج. وبعد ذلك تم بناء النظام المقترح في برامج محاكاة COMIS و TRNSYS. وأخيرا، جرى تقييم لدرجات الحرارة الداخلية ونسبة الرطوبة وتركيز ثاني أكسيد الكربون.

الفصل الخامس: تحسين كفاءة النظام المقترح للوصول الي اداء أفضل

ركز هذا الفصل على دراسة المعاملات الهامة لمكونات النظام لتحسينه والوصول الي أقل حجم للتصميم مع الحصول على أكبر كفاءة للنظام. تم تحليل درجة حرارة الهواء الداخلي، والرطوبة ومعدل سريران الهواء للنظام المقترح، ومقارنتها بالنظام قبل التحسين. ثم الوصول لنتائج حول أداء النظام المدمج تتوافق مع متطلبات الراحة الحرارية المطلوبة، مع إلقاء الضوء على قيود النظام.

الفصل السادس: الخاتمة والأبحاث المستقبلية

توصل البحث إلى نتائج خاصة بحالة الدراسة في مدينة أسبوت الجديدة ومن ثم التوصل الي استراتيجية مناسبة لذلك المناخ، وكذلك أداء النظام المقترح بناء على النمذجة الرقمية. وبالتالي، فقد قدمت إرشادات لعملية التحسين الفعالة لتطبيقها على النظام المعدل في مختلف غرف المعيشة وتحت مختلف الظروف. وأخيرا، قدم البحث مقترحات للأبحاث المستقبلية.



كلية الهندسة
قسم العمارة

التصميم المستدام للبيئة المبنية بالتجمعات السكنية الجديدة -تكاملاً تقنية التبريد التبخيري مع المدخنة الشمسية- (مدينة أسيوط الجديدة - مصر)

رسالة مقدمة للحصول على درجة الدكتوراه في العمارة
من كلية الهندسة - جامعة أسيوط

إعداد:

م/ عمرو سيد حسن عبد الله

مدرس مساعد بقسم الهندسة المعمارية - كلية الهندسة - جامعة أسيوط
عضو بعثة إشراف مشترك - جامعة توهوكو - اليابان

لجنة التحكيم:

الأستاذ الدكتور/مراد عبد القادر عبد المحسن
استاذ بقسم العمارة- كلية الهندسة - جامعة
عين شمس - مصر
الأستاذ الدكتور/محمد مؤمن عفيفي
استاذ بقسم العمارة- كلية الهندسة- جامعة
القاهرة - مصر
الأستاذ الدكتور/مجدى محمد رضوان
الأستاذ الدكتور/ محمد عبدالسميع عيد
استاذ بقسم العمارة- كلية الهندسة- جامعة
أسيوط - مصر

لجنة الإشراف:

الأستاذ الدكتور/مجدى محمد رضوان
استاذ بقسم العمارة- كلية الهندسة -
جامعة أسيوط - مصر
الأستاذ الدكتور/محمد عبدالسميع عيد
استاذ بقسم العمارة- كلية الهندسة-
رئيس جامعة أسيوط - مصر
الأستاذ الدكتور/هيروشي يوشينو
استاذ بقسم العمارة وفيزيائيات
المباني- كلية الهندسة- جامعة
توهوكو - اليابان